UNIVERSITY OF NEWCASTLE-UPON-TYNE
CIVIL ENGINEERING DEPARTMENT

COMPUTER MODELLING OF WATER SUPPLY DISTRIBUTION NETWORKS USING THE GRADIENT METHOD.

by

Rubén O. Salgado-Castro

VOLUME ONE
****

Thesis submitted in fulfilment of the requirements for the degree of Doctor of Philosophy in Civil Engineering.

November, 1988.

ACKNOWLEDGEMENTS

I would like to acknowledge the constant and enthusiastic support given to this work by Professor P. E. O'Connell, Head of the Water Resources Division of the Civil Engineering Department, University of Newcastle-upon-Tyne (United Kingdom). He supervised this thesis and contributed with many discussions and ideas; his permanent encouragement has been invaluable through all this time.

I am indebted to Professor E. Todini, Head of the Institute of Hydraulic Constructions of the University of Bologna (Italy). He created the gradient method and contributed with his advice for its further improvement.

It has been a privilege and a pleasure to work with Professors O'Connell and Todini.

Some institutions made possible my stay in Newcastle University and I am most grateful to them: The Overseas Development Administration provided the funds for a three years scholarship; The British Council managed this scholarship and also provided extra support for attending Conferences and courses. I am particularly grateful for the support provided by the chilean office of The British Council and of that received from the staff of Newcastle Regional Office. The University of La Serena (Chile), granted me with a leave of absence which I fully appreciate and my colleagues at the Civil Engineering Department have shared the extra burden due to my absence.

The Civil Engineering Department of the University of Newcastle-upon-Tyne provided a stimulating environment and the facilities for carrying out this work and I am grateful for that too. Mr. R. Mackay, lecturer in Hydrology, kindly allowed me to use his Kriging suite of programs.

My family and friends from Chile constantly supported me and I truly appreciate their encouragement.

ABSTRACT

A water distribution network analysis method known as the gradient method, due to Todini (1979), has been generalised and subjected to an extensive program of testing and evaluation. The method has been extended to include pumps and some pressure regulating valves, and an original physically-based method has been proposed for modelling the latter devices. Also, a generalised version of the algorithm which considers the nodal demands as a linear function of the pressures has been introduced. The gradient method has been tested with numerous examples, showing remarkable robustness and convergence speed when compared with the most efficient traditional methods. The gradient algorithm does not break down with disconnected networks.

The performance of the gradient algorithm when using seven different linear solvers, including direct and iterative methods, has been investigated. A multifrontal linear solver has been identified as the most efficient method when enough computer memory is available (routine MA27 of the Harwell Library); if storage is limited, a preconditioned (modified) conjugate gradient method is the recommended linear solver. A good compromise between memory and speed is represented by the one-way dissection method of George and Liu (1981).

An automatic calibration algorithm has been proposed which estimates the true pipe resistance parameters, based on the estimation of the unmeasured piezometric heads and unmeasured flows. For the piezometric head estimation, three different

methods have been proposed and compared: one based on Kriging, another based on bi-cubic splines and a third based on an original deterministic one-dimensional interpolation procedure. The latter producing the closest estimates with respect to the true values. For the estimation of the unmeasured flows, the raw (un-calibrated) network model itself is used, based on initial estimates of the pipe roughnesses, leading to an iterative procedure. The results of using the proposed calibration algorithm with a set of test examples show that the unmeasured flow estimation needs further work and an alternative approach has been suggested, which, hopefully, would lead to improvements both in the flow estimation and in the estimation of the true roughnesses.

TABLE OF CONTENTS

CHAPTER FOUR

EXTENSION OF THE GRADIENT METHOD TO INCLUDE REGULATING VALVES: A NEW PHYSICALLY-BASED APPROACH 143

CHAPTER FIVE

EFFICIENT COMPUTER PROGRAM IMPLEMENTATION OF THE GRADIENT METHOD FOR WATER SUPPLY DISTRIBUTION NETWORKS 196

CHAPTER SIX

CALIBRATION OF WATER SUPPLY DISTRIBUTION SYSTEMS:

A NEW COMPUTER-BASED EXPLICIT METHOD 217

VOLUME TWO
****

APPENDIX A

EFFICIENT SOLUTION OF LINEAR SYSTEMS OF EQUATIONS IN THE CONTEXT OF THE GRADIENT METHOD FOR THE ANALYSIS OF WATER SUPPLY DISTRIBUTION NETWORKS

APPENDIX B

DERIVATION OF THE KRIGING ESTIMATOR EQUATIONS

APPENDIX C

DERIVATION OF THE BI-CUBIC SPLINES APPROXIMATION EQUATIONS

APPENDIX D

LIST OF FIGURES

VOLUME ONE
****

VOLUME TWO
****

LIST OF TABLES

VOLUME ONE
****

VOLUME TWO
****

LIST OF MAIN SYMBOLS

NETWORK ANALYSIS

Symbol	Description
NN	Total number of nodes in the network.
NP	Number of links in the network (pipes, pumps, valves, etc.).
NL	Number of loops in the network (natural loops).
NS	Number of sources in the network (known piezometric head nodes), typically reservoirs.
$\underline{Q}$	Flowrate, (NP*1) column vector.
Q_i	Flow corresponding to link "i", i-th component of vector $\underline{Q}$.
Q_{ij}	Flow in link joining nodes "i" and "j".
δQ_{ij}	Flow correction in pipe joining nodes "i" and "j".
δQ_i	Flow correction in loop "i". Also used as flow (mass) imbalance at node "i".
$d\underline{Q}$	Pipe flow differential, (NP*1) column vector.
$\underline{H}$	Nodal piezometric head, ((NN-NS)*1) column vector.
H_i	Piezometric head corresponding to node "i", i-th component of vector $\underline{H}$.
δH_i	Piezometric head correction at node "i" (in nodal approach).
$\underline{H_O}$	(NS*1) column vector of fixed (known) piezometric heads for the source nodes.
$d\underline{H}$	Nodal piezometric head differential, ((NN-NS)*1) column vector.
$\underline{h}$	Head loss, (NP*1) column vector.

Symbol	Description
h_i	Head loss corresponding to link "i", i-th component of vector $\underline{h}$.
h_{ij}	Head loss in link joining nodes "i" and "j": $\boxed{h_{ij} = H_i - H_j}$
$\underline{q}$	Nodal consumption (demand), ((NN-NS)*1) column vector.
q_i	Nodal consumption corresponding to node "i", i-th component of vector $\underline{q}$.
$\delta\underline{q}$	Flow (mass) nodal imbalance, ((NN-NS)*1) column vector.
n	Flow exponent in head loss/flow relationship.
$\underline{K}$	Pipe resistance (NP*1) column vector.
K_{ij}	Resistance corresponding to pipe joining nodes "i" and "j". $\boxed{h_{ij} = K_{ij}\, Q_{ij}^{n}}$
$\underline{R}$	Pipe conductance, (NP*1) column vector.
R_{ij}	Conductance corresponding to pipe joining nodes "i" and "j". $\boxed{Q_{ij} = R_{ij}\, h_{ij}^{1/n}}$
$(.)^{(k)}$	Refers to the value of a variable corresponding to the k-th step within an iterative procedure.
$\underline{\alpha}$	Resistance parameter in head loss/flow relationship, (NP*1) column vector.
α_i	Resistance parameter corresponding to link "i", i-th component of vector $\underline{\alpha}$.
α_{ij}	Resistance parameter corresponding to link joining nodes "i" and "j".

Symbol	Description
$\underline{\beta}$	Resistance characteristic parameter in head loss/flow relationship, (NP*1) column vector (it has head units).
β_i	Resistance parameter corresponding to link "i", i-th component of vector $\underline{\beta}$.
β_{ij}	Resistance parameter corresponding to link joining nodes "i" and "j".

$$h_{ij} = \alpha_{ij} Q_{ij}^{n} + \beta_{ij}$$

Note that β_{ij} has units of piezometric head.

A_{12}	Branch to node (NP*(NN-NS)) connectivity (incidence) matrix, corresponding to unknown head nodes (non-source nodes).
A_{10}	Branch to node (NP*NS) connectivity matrix, corresponding to source nodes.
A_{21}	Transpose of matrix A_{12}: $A_{21} = A_{12}^{T}$.
A_{01}	Transpose of matrix A_{10}.
A_{11}	Diagonal (NP*NP) matrix, defined as:

$$A_{11} = \text{diag.}(\alpha_{ij} |Q_{ij}|^{n-1} + \beta_{ij}/Q_{ij})$$

N	Diagonal (NP*NP) matrix with the flow exponents "n" corresponding to each link. N = diag.(n_i), where n_i is the i-th component of a vector $\underline{n}$ of flow exponents (if the exponents change from one link to another).
A_{11}^{*}	Diagonal (NP*NP) matrix defined as:

$$A_{11}^{*} = \text{diag.}(\alpha_{ij} |Q_{ij}|^{n-1}), \text{ i.e.:}$$
$$A_{11}^{*} = A_{11} - \text{diag.}(\beta_{ij}/Q_{ij})$$

G	(NP*NP) diagonal matrix of the derivatives of the head loss vector with respect to the flows: G = N A_{11}^{*}

Symbol	Description
$\delta \underline{E}$	Head loss imbalance per pipe, a (NP*1) column vector.
B_{11}, B_{12}, B_{21}, B_{22}	Block partitioned matrix used to compute the inverse of the system matrix: $\left[\begin{array}{c\|c} A_{11} & A_{12} \\ \hline A_{21} & 0 \end{array}\right]^{-1} = \left[\begin{array}{c\|c} B_{11} & B_{12} \\ \hline B_{21} & B_{22} \end{array}\right]$
A_{31}	Loop to branch (NL*NP) incidence matrix.
$\underline{Q}_2$	(NN-NS) flow vector, corresponding to the flows in the tree of the network (dependent flows).
$\underline{Q}_3$	NP-(NN-NS) flow vector, corresponding to the flows in the co-tree of the network (independent flows).
A_{22}, A_{32}	Partitioned matrices of the incidence matrix $A_{12} = \left[\begin{array}{c} A_{22} \\ \hline A_{32} \end{array}\right]$; A_{22}: (NN-NS)*(NN-NS) matrix associated to the dependent flows. A_{32}: (NP-(NN-NS))*(NN-NS) matrix associated to the independent flows.
$\underline{p}$	(NN*1) column vector of nodal pressures.
p_i	pressure at node "i", i-th component of vector $\underline{p}$.
$\underline{z}$	(NN*1) column vector of nodal ground levels.

$$\underline{p} = \underline{H} - \underline{z}$$

p_s	Service pressure: pressure at which nodal demands are assumed to be satisfied.
$p_{min.}$	Minimum allowable pressure within the network.
$p_{max.}$	Maximum allowable pressure within the network.
A_{22}	Has also been used to describe the sensitivity of nodal consumption with respect to the pressures: diagonal (NN-NS)*(NN-NS) matrix defined as:

Symbol	Description

$$A_{22} = \text{diag.}(-\partial q_i / \partial p_i).$$

q_s Nodal consumption at service pressure.

q_o auxiliary nodal consumption variable:

$$q_o = q_s + A_{22}\, z + A_{22}\, p_s$$

$(.)^*$ Refers to the estimated value of the variable (piezometric head, resistance parameter, flow, etc.).

$(.)^t$ Refers to the true value of the variable.

$E[.]$ Refers to the mathematical expectation of a random variable.

Symbol	Description
A, B	A capital letter denotes a matrix, particularly:
L	Denotes a lower triangular matrix.
U	Denotes an upper triangular matrix.
D	Denotes a diagonal matrix.
a, $\underline{A}$, $\underline{a}$	A lower case letter, or a capital (or lower case) underlined letter denotes a vector.
α, μ	A greek letter denotes a scalar.
a_i	A lower case subindexed letter denotes a scalar, normally the i-th component of a vector.
a_{ij}	A lower case doubly subindexed letter denotes a scalar, normally the coefficient of a matrix A, located at the intersection of row "i" and column "j".
A_i	A capital subindexed letter denotes either a matrix in a sequence of matrices or a block-partitioned matrix.
$(.)^T$	Denotes transposition, either of a vector or matrix.
A^{-1}	Denotes matrix inversion.
$(.)^{(k)}$	Refers to the k-th value of the variable (scalar, vector or matrix) within an iterative procedure.
$\|\|x\|\|$	Denotes the norm of a variable (vector or matrix).
$\|x\|$	Denotes the absolute value of a scalar.
λ_i	Denotes a particular eigenvalue of a matrix.
$\rho(A)$	Spectral radius of matrix A.
$\langle x,y \rangle$	Inner (scalar) product of vectors "x" and "y": $\langle x,y \rangle = x^T y = y^T x = \sum_{i=1}^{n} x_i y_i$

Symbol	Description
$(\underline{x}, H)$	State variable representing the piezometric head at any point $\underline{x}$ of the domain: $(\underline{x},H) = (x_1, x_2, H)^T$ in a two-dimensional space.
$Z(\underline{x}, H)$	Random function representing the value of the state variable H at a location $\underline{x}$ (in general).
$Z(\underline{x}_o, H)$	Random variable (at the particular location $\underline{x}=\underline{x}_o$. Simplified notation: $Z(x_i, H) \iff Z_{\underline{x}_i} \iff Z_i$
$E[Z(\underline{x}_1, H)]$	expected value of the random variable at $\underline{x}=\underline{x}_1$.
$\Gamma(\underline{x}_1, \underline{x}_2)$	Semi-variogram: $\Gamma(\underline{x}_1, \underline{x}_2) \equiv \frac{1}{2} E[\{Z(\underline{x}_1,H)Z(\underline{x}_2,H)\}^2]$
$Cov(Z(\underline{x}_1,H),Z(\underline{x}_2,H))$	Covariance: $Cov(Z(\underline{x}_1,H),Z(\underline{x}_2,H)) = E[Z(\underline{x}_1,H)Z(\underline{x}_2,H)]$
$Var(Z(\underline{x},H))$	Variance of the random variable: $Var(Z(\underline{x},H)) = E[Z(\underline{x}, H)^2] - \{E[Z(\underline{x}, H)]\}^2 = \sigma^2$
$\lambda_o{}^i$	Unknown weight of the Kriging estimator, where"i" refers to the measurement Y_i and "o" to the point being estimated $\underline{x}_o$, i.e.: $Y_o{}^* = Y_o{}^*(\underline{x}_o) = \sum_{i=1}^{n} \lambda_o{}^i Y_i$

Symbol	Description

One dimensional splines:

$s(x)$ General spline polynomial function.

λ_i Set of knots associated to the spline.

h Number of knots (λ_i , $i=1,2,..,h$)

$(x_r, f(x_r))$, $r=1,2,..,m$ set of data points.

$M_i(x)$ Cubic Basic (or fundamental) spline (B-spline).

$M_{n,i}(x)$ General B-spline of degree (n-1). For a cubic spline $n=4$, i.e.: $M_{4,i}(x) = M_i(x)$ (simplified notation).

Γ_i Linear (unknown) weights, combining the cubic B-splines into a general cubic spline polynomial:

$$s(x) = \sum_{i=1}^{h+4} \Gamma_i \, M_i(x)$$

$\underline{\Gamma}$ (h+4)*1) column vector of linear weights Γ_i.

A Matrix of observation equations (observation matrix), of order m*(h+4) in a cubic spline: $A_{r,i} = M_i(x)$.

$A\,\underline{\Gamma} = \underline{f}$ Observation equations, overdetermined system.

$\underline{f}$ (m*1) column vector with the value of the spline polynomial at each data point:

$$f_i = f(x_i) = s(x_i) \quad i=1,2,\ldots,m$$

$A^T A\underline{\Gamma}=A^T\underline{f}$ Normal equations. Linear system of (h+4)*(h+4) equations (determined system).

Bi-cubic splines:

$s(x,y)$ General spline polynomial function.

λ_i Set of knots associated to the independent variable x.

μ_j Set of knots associated to the dependent variable y.

Symbol	Description
h	Number of knots in the x-axis (λ_i , i=1,2,..,h)
k	Number of knots in the y-axis (μ_j , j=1,2,..,k)
R_{ij}	Set of (h+1)*(k+1) panels in which the x-y space is sub-divided.
$(x_r, y_r, f(x_r, y_r))$, r=1,2,..,m	set of data points.
$M_i(x)$	Cubic B-spline related to the independent variable x.
$N_j(y)$	Cubic B-spline related to the dependent variable y.
Γ_{ij}	Linear (unknown) weights, combining the cubic B-splines into a general cubic spline polynomial: $$s(x,y) = \sum_{i=1}^{h+4} \sum_{j=1}^{k+4} \Gamma_{ij} M_i(x) N_j(y)$$
$\underline{\Gamma}$	((h+4)(k+4)*1) column vector of linear weights Γ_{ij}.
A	Matrix of observation equations (observation matrix), of order m*(h+4)(k+4).
$A\,\underline{\Gamma} = \underline{f}$	Observation equations, overdetermined system.
$\underline{f}$	(m*1) column vector with the value of the spline polynomial at each data point: $f_i = f(x_i) = s(x_i)$ i=1,2,...,m
$A^T A\underline{\Gamma} = A^T\underline{f}$	Normal equations. Linear system of (h+4)(k+4)*(h+4)(k+4) equations (determined system).

CHAPTER ONE

INTRODUCTION

1.1. Computer modelling of water distribution systems.

The increasing complexity of water supply distribution systems on the one hand, and the pressing need for the efficient management of the resources involved in those systems on the other hand, have led to the need for simplified representations of the real systems, which can make it easier to take adequate decisions on the operation and design of such systems. The answer to this need is a model, which although being a simplified representation of a more complex reality, encapsulates its main features and reproduces the response of the reality to a certain stimulus, within a certain degree of accuracy. A model enables the predicted behaviour of the real system to be assessed beforehand, in a simpler, cheaper and quicker way, without having to involve the real system in that process. Thus, different alternative operating policies, or different alternative designs can be evaluated with the help of a model, and only the most efficient alternative can be implemented in the real system.

Future conditions can be anticipated and simulated in the model, in order to assess the performance of the real system under a different scenario. This is typically the design case, where increased consumptions are fed into the model to study the need for future reinforcements in the system, or to improve the

quality of the service. Clearly this is something that is impossible to do in the real system itself.

In general, the process of building and operating a model helps us to get a better understanding of the reality, something which is beneficial in itself, apart from the benefits deriving to design and operation.

Different kinds of models have been used to represent water supply distribution systems. In the past, analogue models, exploiting the known analogy between electric and hydraulic networks, have been used for that purpose. The advent of digital computers, and the availability of powerful numerical methods to solve complex mathematical problems, has allowed the development of more versatile, cheaper and easier-to-use computer-based models, constituting nowadays the main field for model development.

Even though a model is meant to be a simplified representation of a reality, this does not mean that the model itself is simple. A computer-based model of a water supply distribution system involves a number of separate components, which only when linked together can be used effectively for practical purposes; some of these components are described below:

a) Physical component.

Any real water distribution network is made up of a number of physical devices, joined together in some particular way: reservoirs, pipes, pumps, valves, etc. are some of the typical devices which can be found in any distribution network. Each

device has some physical characteristics which must be explicitly considered: dimensions (pipe lengths, diameters), characteristic parameters (pipe roughness, pump and valve characteristic curves), etc. Any network model has to include some or all of these devices as the basic components of the network, with their corresponding physical characteristics. Additionally, the topography, geometry and connectivity of the water distribution system are also important parts of the physical component.

Depending on the model objectives, existing physical devices (for operational purposes for example) or future ones (new pipes or pumps in a design-oriented model) may be represented within the model.

b) Demand component.

The purpose of any real distribution network is to satisfy the water consumption requirements of the population being served by it, at a pre-specified minimum service level. In fact, the demands can be seen as the driving force in the behaviour of a water supply distribution system; in general, unless there is some transfer of water between reservoirs or leakage, the absence of demands will imply no flows in the network, while higher demands will produce higher flows.

Due to the fact that the demands are spatially distributed alongside the pipes, a simplifying assumption is made in order to render the problem mathematically tractable by concentrating the demands in the nodes.

Furthermore, depending on the model objectives, interest may be focused on the consumptions either at a particular time (for design purposes we are normally interested in the demands at peak time), or during a certain period of time (for operational purposes we may be interested in the demands throughout a day, a week, etc.).

c) Operational component.

Each model, according to its particular objectives, will have a set of operating rules, establishing the way the system is to be managed. These rules follow closely the real operation of the system: pumps switched on and off, valve movements, reservoir levels, pressure reducing valve settings (P.R.V.'s), etc.

In design applications the operating rules are assumed to be known, although in optimum operation modelling the set of rules itself is the main unknown.

d) Measurement component.

Real water distribution networks have data measurement systems with varying degree of sophistication, ranging from manually operated systems to fully automated telemetry systems.

As far as the network model is concerned, measurements are a key factor, since they enable us to determine how close our model is representing the real network. This information can be fed back into the model, in order to improve its predictions. The measurements are then the bridge between the model and reality.

Typical field network measurements are: pressures, water levels, and flows, whereas the characteristic parameters of pumps and valves are normally the subject of laboratory measurements.

Together with the basic data gathering system, bad-data detection and missing data replacement mechanisms (both normally computer programs), and parameter estimation routines to estimate unmeasured data are needed.

e) Hydraulic component.

The hydraulic component in the model is mainly related to the kind of hydraulic regime in which the real network is operating. We may be interested either in the steady state behaviour of the network, or in the unsteady state (slow or fast transient); in each case different physical processes are involved, and a different approach is needed for modelling purposes.

Another aspect of the influence of the hydraulic component on the overall modelling deals with the head loss/flow relationship for each physical device in the network. In this sense we have to decide, based on our hydraulics knowledge, on the formula which best represents the real behaviour of a pipe, or which values should be assigned to initial estimates of roughness, minor losses coefficients, maximum/minimum pressures and velocities, etc.

f) Mathematical component.

Depending on whether the network is under steady state or unsteady state regimes, the problem of representing

mathematically the behaviour of the real system leads either to a set of non-linear equations, or to a set of hyperbolic partial differential equations, respectively; each case demands completely different numerical techniques to be applied to find a solution to the problem.

Additionally, different ways of setting up the physical conditions for the solution lead to different ways of assembling the sets of equations and, indeed, to different analysis methods. Each method has its advantages and disadvantages, which should be recognised by the modeller, since the amount of work demanded by their solution, or their stability properties, might be quite different.

Since the systems of equations, either in the steady or unsteady state case, cannot be solved analytically, we need to find a suitable numerical scheme to solve the mathematical problem. Because the amount of computation involved in most of the solution schemes is generally high, except for relatively small and simple problems, this leads to the need for a digital computer.

g) Computational component.

In a computer-based model there are two computer-related components: hardware and software.

On the hardware side we have the machine itself, with its central processing unit and a vast variety of peripherals, which handle the input/output of information: video display units, printers, plotters, digitizers, etc. It is indeed the

availability of powerful and cheaper hardware, which has made it possible to expand the use of computer-based water distribution models, into the operation and design of medium and small networks. In particular, the availability of microcomputers and personal computers is revolutionising this and, indeed, other sectors of the water industry.

On the software side, apart from the system-related software (operating system, utilities, compilers, etc.), there are a number of items of specially dedicated software which work in connection with the different components already mentioned, for example:

* Network analysis programs: for solving the steady (or unsteady) state of the networks. They incorporate the hydraulic and the mathematical components of the model.
* Demand forecasting programs: for the efficient storage, retrieval and prediction of consumption data.
* Data management programs: providing input/output facilities for data and results, data updating, etc.
* Data measurement management programs: including bad data detection, missing data replacement routines, storage and retrieval of measurement data.
* Unmeasured data estimation programs: estimation of unmeasured nodal piezometric heads and pipe flows.
* Automatic model calibration programs: responsible for guaranteeing agreement between model and reality.
* Extended period simulation programs: for studying the behaviour of the water distribution system during a certain

period of time and under particular operating conditions.

* Optimum design programs: to determine the best physical configuration of the system in order to meet certain objectives (cost, reliability, service level, etc.)
* Optimum operation programs: for determining the operational rules which optimise the performance of the system.

Hence, the computational component interacts with many of the other components of the model, and it might be better seen as playing a support role, perhaps at a different level in comparison with the rest of the components. Figure 1.1 shows schematically the interaction of the different model components, where we distinguish between a raw model and a calibrated model; the latter incorporates the measurement information, thus resulting in a better representation of the reality. In principle, only calibrated models should be used for practical purposes, though there are some cases where a calibrated model is not possible, for example when studying the behaviour of a system in meeting future demands.

Another important point illustrated in Fig. 1.1, is that a computer-based water distribution model incorporates not only computer-related elements, but also physical, operational, mathematical, hydraulic and customer-related aspects. The network analysis program is only one component of the whole model, although it may be used a posteriori in tandem with simulation and optimisation programs.

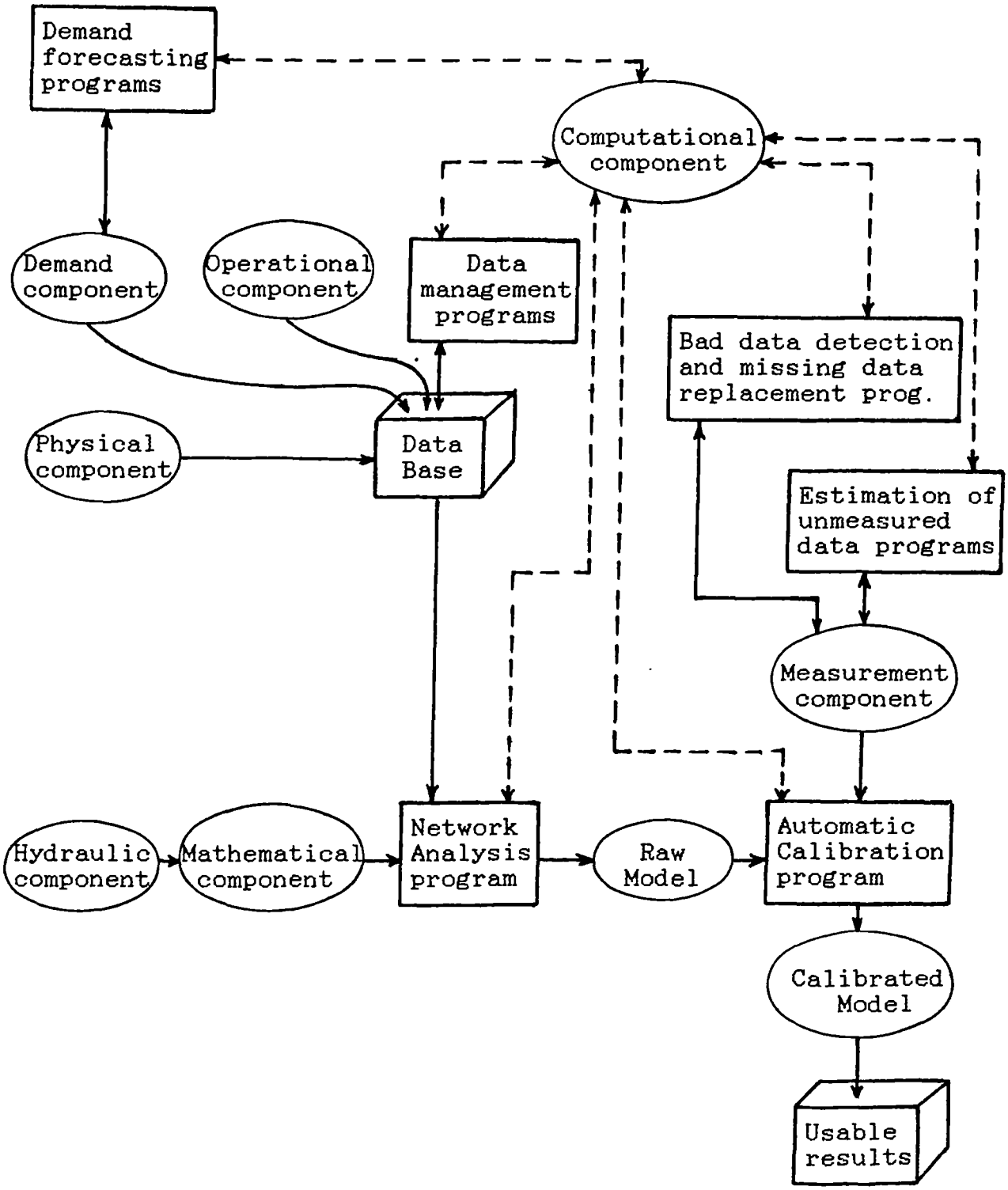

Fig. 1.1. The water distribution network model and its main components.

The work presented in this thesis, contributes to some key aspects of the computational component of water distribution systems modelling. Specifically, we shall concentrate on the following problems:

* Network analysis for the steady state condition.
* Automatic calibration of the network and estimation of unmeasured variables.
* Extended period simulation.

1.2. Network analysis: need for a reliable algorithm for design and operational purposes.

It is a well-known fact that most of the traditional methods for water distribution network analysis do have stability problems [Wood (1981a)]. Indeed, problems related to slow convergence, or lack of convergence, have been documented since the earliest stages of the development of network analysis algorithms.

Because the network analysis program is used intensively in many simulation and optimisation applications (design and operation), it becomes clear that an efficient and reliable network solver is highly desirable. Traditionally, the solution to many convergence problems has been via manual intervention and via the application of problem-dependent relaxation coefficients, tuned in each case to produce a stable trajectory towards the solution. Since, in simulation and optimisation applications, convergence problems would certainly lead to the break-down of

the main algorithm, an unreliable network analysis routine is not acceptable. Finally, the possibility of using a network analysis program in a real-time application is simply unthinkable, without having a priori a fully reliable and stable method of analysis.

On the other hand, the increasing availability and use of micro and personal computers in the water industry, has made it highly desirable that any network analysis program should be able to be implemented on such machines. This adds storage and speed as important requirements for the development of network solvers, apart from the stability problem already mentioned.

Here, a non-traditional method of network analysis has been used as a starting point, which, in theory should not present most of the convergence problems reported in the application of traditional methods. This method of analysis is known as the gradient method and was introduced by Todini (1979).

Todini's gradient method [Todini (1979), Pilati and Todini (1984)] was initially formulated to incorporate pipes only, and the initial aim of this work has been to expand the method to incorporate pumps, valves and pressure regulating valves.

From the numerical point of view, Todini's original gradient method was implemented with a standard conjugate gradient scheme for the solution of the linear systems of equations generated in the network analysis problem. A further aim of this work has been to investigate the feasibility of alternative numerical schemes for the solution of the linear systems of equations, since the performance of the overall analysis program (and consequently

that of its simulation and optimisation applications) relies heavily on the efficient solution of the linear systems. In investigating these numerical schemes the need for microcomputer implementation has been kept in mind.

1.3. Need for an automatic calibration algorithm for the network model.

As already noted, if a model is to be used for operational purposes, it is a necessary condition for this model to represent the reality as closely as possible. To ease this task an automatic calibration algorithm is highly desirable. At the present time, no satisfactory explicit automatic model calibration algorithm is available, and many users are still calibrating network models by hand, on a trial-and-error basis, and with considerable manpower expenditure. Some existing calibration algorithms just automate the trial-and-error approach, without a proper understanding of the underlying problem. On top of that, calibration techniques based on non-linear programming techniques lead to solutions which are extremely expensive from the computational standpoint.

In this work, a further aim has been to produce a calibration algorithm which can use the raw model (see Fig. 1.1.), the limited amount of measurements normally available in water distribution networks to solve the problem of matching reality and model in an automatic and computationally efficient way.

1.4. Simulation of water distribution networks.

Most practical applications of the calibrated network model can be regarded as simulations of the water distribution system, carried out at different time horizons. Thus, for operational purposes we shall be especially interested in short term simulations, say 24 or 48 hours in advance, in order to anticipate the expected behaviour of the system, and take adequate measures to cope with the forecasted demands in an efficient way, guaranteeing minimum service levels. Medium term simulations can be carried out, for example one week in advance, prior to predicted extreme weather conditions. Short and medium term simulations basically deal with a fixed physical system and aiming at the efficient management of the storage within the system in order to satisfy customers demands.

Design optimisation problems can be considered as long term simulations (say a few years in advance), and they are geared towards the determination of major changes in the physical structure of the system, to comply with predicted future demands and different operating conditions.

The gradient method for network analysis has been used in the development of an extended period simulation program, which can handle short term simulations. The basic structure of the extended period simulation program is shown in Fig. 1.2.

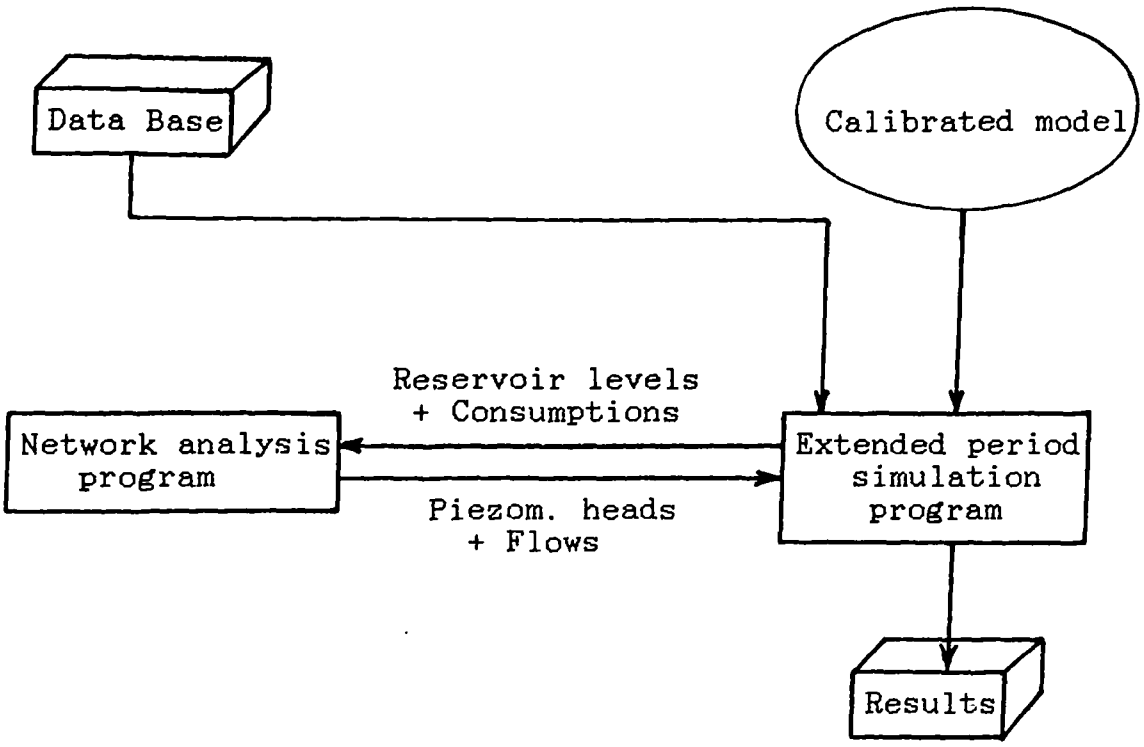

Fig. 1.2. Structure of the extended period simulation program.

1.5. Thesis structure.

In Chapter Two a review of the existing network analysis algorithms is presented, identifying their advantages and disadvantages, particularly from the convergence point of view.

In Chapter Three Todini's gradient network analysis algorithm is extended to include pumps. Also a comparison with other similar techniques is included in this chapter.

Chapter Four deals with the modelling of pressure regulating devices introducing a new physically-based algorithm.

In Chapter Five some aspects related to the efficient computer implementation of the gradient method are dealt with, particularly, the efficient solution of the symmetric positive

definite linear systems of equations generated by the gradient method.

Chapter Six deals with the development of an automatic calibration algorithm. A review of the existing calibration methods is presented and a new computer-based explicit calibration algorithm is introduced. Because the calibration algorithm relies on estimates of the piezometric heads, three alternative methods for estimating unmeasured piezometric heads are proposed and compared.

In Chapter Seven further extensions of the gradient method are introduced. An extended period simulation version of the gradient method is presented. Also, a generalised version of the network analysis algorithm is introduced, able to handle explicitly the influence of the pressures in the nodal demands.

Finally, in Chapter Eight some conclusions are drawn and areas of further work are identified.

Four appendices are also included. Appendix A presents a complete review of the existing direct and iterative methods for solving the linear systems of equations generated in the gradient network analysis method. Appendix B summarises the theory and derivation of the equations used in the application of Kriging as an unmeasured piezometric head estimator, while Appendix C serves the same purpose for the case of the estimation using bi-cubic splines. Finally, Appendix D presents the numerical results of using the proposed calibration algorithm for solving some test examples.

1.6. Summary of main achievements.

In pursuing the extension of the gradient method for the analysis of water distribution systems, and in looking for an automatic algorithm for the calibration of a network model, the following original contributions have been made:

a) Todini's original formulation of the gradient method has been extended using a general head loss/flow model which allows the inclusion of pumps and valves into the algorithm, and which provides a general framework for the future incorporation of additional devices. The corresponding algorithm equations have been modified accordingly. The implemented computer program has demonstrated that the extended formulation does work, and that it is stable and computationally efficient when compared with some of the best traditional algorithms available.

b) An exhaustive investigation has been carried out, covering the widest possible range of sparse linear solvers, and the most efficient methods have been identified and implemented at microcomputer level, in the context of the gradient method.

c) An original method for modelling pressure reducing and sustaining valves has been proposed, implemented and tested. The method follows closely the physical behaviour of these devices, and has proved to be robust and able to detect problems in the solutions given by alternative methods. Due to its physically-based characteristics, the method can be used as an adequate framework for the modelling of other regulating devices in the future.

d) A new algorithm for the automatic calibration of network models has been proposed and tested with synthetic data. The results show that the algorithm is able to replicate piezometric head and flow measurements.

e) In the context of the measurement component of a network model, three alternative nodal piezometric head estimators have been proposed, implemented and compared. The methods are based on the application of Kriging, bi-cubic splines and a one-dimensional deterministic interpolation method. The results of the tested examples indicate that the deterministic interpolation method performs best.

f) An extended period simulation program based on the gradient method has been implemented.

g) Finally, a generalised version of the gradient method, able to consider explicitly the variation of nodal consumptions with the pressures has been proposed.

CHAPTER TWO

REVIEW OF THE MAIN EXISTING METHODS OF NETWORK ANALYSIS

2.1. Introduction.

Given the network geometry, its physical properties and the demands to be satisfied, the network analysis problem consists in finding the flow in each pipe and the piezometric head in each node corresponding to the steady-state conditions.

Some assumptions are usually made in order to simplify the solution to the analysis problem:

a) the kinetic heads (velocity component of the total head) are much smaller than the friction head losses, and they can be neglected without loss of accuracy;

b) minor head losses at the junctions of pipes and fittings are smaller than the friction losses, and they can also be neglected;

c) the consumptions derived from the use of water by the customers are assumed to be concentrated in the nodes of the network, and not along the pipes, as happens in the real world;

d) the demands are constant and do not change with pressure variations in the network. A particular time instant is considered; consequently the demands are "instantaneous demands";

e) all the pipes are working under positive pressure;

f) a non-linear mathematical relationship between head loss and flowrate is accepted as an adequate representation of the flow of water through the pipe.

The analysis problem is mostly concerned with looped networks, since in branched networks with only one source, the solution is directly obtainable from the nodal demands and the network connectivity. In looped networks, the flow distribution depends not only on the resistance of one particular pipe, but on the resistances of the rest of the pipes in the network as well. Nevertheless, most of the real networks are a mix of partly branched and partly looped networks.

It must be pointed out that, under the previous assumptions, the flow distribution does not depend on the ground level. Only the pressures are affected by the ground level. To avoid confusion and misunderstandings, we shall work in terms of nodal piezometric heads as state variables, instead of pressure; note that the flow is always produced from a higher piezometric head node into a lower one, but the same is not generally true when dealing with pressures.

We shall review in this chapter most of the network analysis methods, in chronological order, starting with the early solutions of Cross (1936), one of which was the standard solution for hand computation and early computer programs. Next, we shall review the methods made possible by digital computers, where the capability of the computer in solving large linear systems of

simultaneous equations is fully exploited; most of these methods are based on the explicit application of the Newton-Raphson technique for the solution of non-linear systems of equations. The linear theory method is also reviewed, both in its original formulation [Wood and Charles (1972)] and its gradient-based formulation [Wood (1981a)]. We shall refer to a network analysis method as a "gradient-based" algorithm, if the algorithm itself produces the linearization, which is usually done applying the gradient operator to the non-linear functions, without having to pass the non-linear problem to an independent Newton-Raphson algorithm. A set of non-traditional methods is reviewed, some of them based on the explicit application of optimisation theory, while others are based in the application of the unsteady state equations. Finally, the gradient method of Todini (1979) is introduced.

Published numerical comparisons of some of the existing network analysis methods are reviewed and some preliminary conclusions are drawn. Particular attention will be paid to the convergence properties of the methods, as well as their storage requirements and the amount of work involved in their application.

2.2. Hardy Cross (1936) methods.

Hardy Cross (1936) developed two methods based on systematic successive approximations, or "successive corrections" in Cross' words, for the solution of the network analysis problem. Mainly due to their simplicity, Cross' methods became widely used, and they are invariably considered the starting point for network analysis.

H. Cross stated that two conditions for the steady state solution of the flow in a network are:

a) Flow continuity: at any node of the network, the total inflow must be exactly equal to the total outflow.

b) Potential continuity: the total (algebraic) change in potential (piezometric head) around any closed loop of the network is zero.

These two conditions, together with the non-linear head loss/flow relationship for each pipe, must be fulfilled simultaneously in a network under steady state conditions, thus generating a system of non-linear equations, which Cross managed to transform into a succession of (linear) scalar problems.

As will be seen later on, these two "conditions", which have been elevated to the category of "laws" by some authors (especially in the case of the second condition), are in fact the necessary conditions, but not sufficient conditions for the steady state flow.

There are two H. Cross methods, each one starting from the fulfilment of a different condition (flow continuity or potential continuity). In the first method, known as "loop flow method", an initial flow distribution satisfying flow continuity (but not potential continuity), is successively improved until potential continuity is met, within some pre-specified accuracy. In the second method, an initial solution which fulfils potential continuity is improved until flow continuity is accomplished,

within some accuracy limits. We shall review both methods in the next paragraphs.

2.2.1. Method of balancing heads.

This is the most widely known Cross' method, sometimes thought to be the Cross method, and its success can be attributable to the fact that it is suitable for hand computation. The method is also known under such names as: the "head balance" method, loop method or "loop-flow method".

Starting from an initial flow distribution, supplied by the user, the method allows the calculation of corrective loop flow equations. Earlier computer programs were based on this method.

This method can only be used for looped networks with a single source, though the addition of some "imaginary" pipes allows us to include more than one reservoir.

Traditionally, the loop-flow method has been derived in the following way:

Let the head loss/flow relationship for the pipe joining nodes "i" and "j" be expressed as:

$$h_{ij} = K_{ij} Q_{ij}^2 \qquad (1)$$

where:

K_{ij} is the resistance characteristic parameter, which depends on the roughness, length, diameter and units used.

Q_{ij} represents the flow from node "i" to "j", which initially satisfies the flow continuity (or node balance) condition.

The second condition establishes that, under steady state conditions, these flows must produce pipe head losses which are balanced round any loop, i.e. the algebraic summation of the head losses around any loop must be zero:

$$\sum_{loop} h_{ij} = 0 \quad \forall \text{ loop} \tag{2}$$

Suppose that the steady state equilibrium conditions have not been reached yet, but we are close enough; then a loop-flow correction δQ_k can be calculated for each loop "k", so that the new corrected flows $Q_{ij} + \delta Q_k$ are a better approximation to the equilibrium conditions. Note that a flow correction applied over all the pipes in a loop does maintain flow continuity. The new head loss in the pipe joining nodes "i" and "j" will be:

$$h_{ij} = K_{ij} (Q_{ij} + \delta Q_k)^2 \tag{3}$$

or, expanding the binomial:

$$h_{ij} = K_{ij} (Q_{ij}^2 + 2 Q_{ij} \delta Q_k + \delta Q_k^2) \tag{4}$$

In the vicinity of the equilibrium conditions, the corrective terms δQ_k^2 will be small enough to be neglected, leading to:

$$h_{ij} \approx K_{ij} Q_{ij}^2 + 2 K_{ij} Q_{ij} \delta Q_k \tag{5}$$

and imposing the loop condition $\sum h_{ij} = 0$:

$$\sum h_{ij} \approx \sum K_{ij} Q_{ij}^2 + 2 \delta Q_k \sum K_{ij} Q_{ij} = 0 \tag{6}$$

which allows us to compute the corrective term:

$$\delta Q_k = \frac{- \sum K_{ij} Q_{ij}^2}{2 \sum K_{ij} Q_{ij}} \tag{7}$$

i.e.

$$\delta Q_k = \frac{- \sum h_{ij}}{2 \sum (h_{ij}/Q_{ij})} \tag{8}$$

The process can be easily tabulated to facilitate hand-computation, and it can be programmed in a computer or even in a

programmable calculator.

In general, for a head loss/flow relationship of the form:

$$h_{ij} = K_{ij}\, Q_{ij}^{n} \qquad (9)$$

the correction formula becomes:

$$\boxed{\delta Q_k = \frac{-\Sigma\, h_{ij}}{n\, \Sigma\, (h_{ij}/Q_{ij})}} \qquad (10)$$

The original Cross' method was subsequently improved by different authors, in order to reduce the amount of computation involved and improve its convergence.

Dubin (1947) developed a slide-rule-like device to ease the hand computation, and suggested some improvements to the original Cross loop method. He recognised that the convergence of the method depended on the way the loops are chosen, suggesting that the loops should be chosen in such a way that the common pipes are those having the minimum resistance.

Voyles and Wilke (1962) insisted in choosing the loops having the minimum resistance in their common pipes, they gave a correlation between the number of iterations and the "common flow resistance".

Barlow and Markland (1969) suggested that retaining the quadratic term in the binomial expansion (4) should improve the convergence of the method. They also found that an over-relaxation factor of 1.25 affecting their loop-flow correction δQ_k [computed from the full binomial expansion (4)], reduced the number of iterations by about a half in some small test networks

(10 nodes and 13 pipes).

Williams (1973) demonstrated that taking second order terms (or higher) for the computation of loop-flow corrections, does not improve the convergence. He adhered to the use of acceleration factors, applied directly to the correction formula:

$$\delta Q_k = \frac{- A \sum h_{ij}}{n \sum (h_{ij}/Q_{ij})} \qquad (11)$$

where A is a constant acceleration factor, empirically determined by Williams, which depends mainly on the number of pipes in the network. Improvements of as much as 80% were reported by Williams in networks of 100-250 loops (120-290 nodes).

By the early 1970's, new methods had emerged which proved to have better convergence properties than the Cross loop method, they are discussed later.

For the application of the Cross loop-flow method, or any of its improved versions mentioned so far, a balanced initial flow distribution is needed as input data.

In the case of mixed (looped and branched) networks, the method requires the isolation of the looped part, as a pre-requisite for the application of this algorithm. More than one fixed-head source can be handled via the introduction of "pseudo-loops", made of imaginary pipes.

Because loop corrections do not affect flow continuity at the nodes, the accuracy in the computation of the correction factor

is not critical in the initial iterations. This was important in hand calculations.

From a topological point of view this method requires the specification of the loops (i.e. pipe belonging to each loop, following a certain order). Epp and Fowler (1970) described a method for the automatic generation of the loops within the computer; these loops are the natural set of loops, i.e. those which do not contain other loops inside themselves.

The application of the Darcy-Weisbach relationship, with Colebrook-White formula for the calculation of the friction factor, requires an iterative procedure, since this formula is implicit in the friction factor.

As it will be seen later on, the Cross loop method can also be interpreted as the application of Newton's method for the solution of the non-linear steady state flow problem.

2.2.2. Method of balancing flows.

This is the second method proposed by H. Cross (1936) and is usually referred to as the nodal method or "head-equations" method.

Starting with some assumed heads (any set of heads fulfils automatically the potential continuity condition), successive head corrections lead to the fulfilment of the flow continuity. H. Cross proposed that at any stage when flow continuity has not been achieved, the imbalance at a node can be computed and spread to the pipes connected with this node "in inverse proportion to

their resistances".

Cross himself (1936), on solving a number of examples, pointed out that the convergence of this method can be "slow and not very satisfactory".

Cornish (1939-1940) published a development of Cross' balancing flows method, which is known as the "quantity balance method". The derivation of the Cross-Cornish method is as follows.

Starting with an estimated piezometric head at each node (given by the user), let us assume that the node (flow) balance is not fulfilled. This means that:

i) there is a difference between the inflows and outflows at a node that is greater than a maximum tolerance value. Let us denote this difference by δQ_i (for node "i"), i.e.:

$$\delta Q_i = \sum_j Q_{ij} - q_i \qquad (12)$$

where:

Q_{ij}: flow through the pipe joining nodes "i" and "j".

q_i : consumption at node "i"

ii) If,

$$h_{ij} = K_{ij}\, Q_{ij}^{n} \qquad (13)$$

is the head loss/flow relationship, and if the situation is such that the nodal balance is not fulfilled, the previously assumed piezometric head is either underestimating or overestimating the head losses in any pipe connected to this node, by a quantity that is denoted by δH_i. It is possible to calculate that correction (δH_i), based on the flow imbalance δQ_i,

from the following relationship:

$$h_{ij} + \delta H_i = K_{ij} (Q_{ij} + \delta Q_{ij})^n \qquad (14)$$

where δQ_{ij} is the imbalanced flow contributed by the pipe connecting nodes "i" and "j". δH_i is the error in the assumed piezometric head, which is exactly the correction needed at node "i". We can re-write this expression as:

$$h_{ij} + \delta H_i = K_{ij} Q_{ij}^n \left[1 + \frac{\delta Q_{ij}}{Q_{ij}} \right]^n \qquad (15)$$

or,

$$h_{ij} + \delta H_i = h_{ij} \left[1 + \frac{\delta Q_{ij}}{Q_{ij}} \right]^n \qquad (16)$$

but, as a first approximation:

$$\left[1 + \frac{\delta Q_{ij}}{Q_{ij}} \right]^n \approx \left[1 + n \frac{\delta Q_{ij}}{Q_{ij}} \right] \qquad (17)$$

this is, if: $\delta Q_{ij}/Q_{ij}$ is small.

Hence,

$$h_{ij} + \delta H_i = h_{ij} \left[1 + n \frac{\delta Q_{ij}}{Q_{ij}} \right] \qquad (18)$$

then,

$$h_{ij} + \delta H_i = h_{ij} + n\, h_{ij} \frac{\delta Q_{ij}}{Q_{ij}} \qquad (19)$$

and the piezometric head correction can be computed as:

$$\delta H_i = n\, h_{ij} \frac{\delta Q_{ij}}{Q_{ij}} \qquad (20)$$

which is reordered to give:

$$\delta H_i \frac{Q_{ij}}{n\, h_{ij}} = \delta Q_{ij} \qquad (21)$$

We do not know the value of δQ_{ij} for each pipe, but we do know their summation (ΣQ_{ij}) for any node "i", which is exactly the imbalance existing at this node:

$$\sum_j \delta Q_{ij} = \sum_j Q_{ij} - q_i \qquad (22)$$

then, on applying the summation operator on (21) we get:

$$\sum_j \delta H_i \frac{Q_{ij}}{n\, h_{ij}} = \sum_j \delta Q_{ij} \qquad (23)$$

By introducing (22) into (23), and factorizing by δH_i, which is constant for node "i", we obtain:

$$\delta H_i \sum_j \frac{Q_{ij}}{n\, h_{ij}} = \sum_j Q_{ij} - q_i \qquad (24)$$

which results in:

$$\delta H_i = \frac{\sum_j Q_{ij} - q_i}{\sum_j \frac{Q_{ij}}{n\, h_{ij}}} \qquad (25)$$

Note that the correction formula (25) collapses if the head loss in a pipe is exactly zero, and becomes unstable if this value is very small.

According to Cornish (1939-1940), the method operates as follows:

1. Set the iteration counter "k" to zero. Estimate some reasonable values for the initial piezometric heads. Those

estimates can be as simple as linearly interpolated values between fixed head nodes (reservoirs), or each node can be given a reasonable pressure (say 20-30 m.), which, when added to the ground level, produces the initial head. Let this initial head be the vector $\underline{H}^{(k)}$, where the superscript refers to the iteration number.

2. Calculate the flows per pipe, according to the initial piezometric heads estimated before:

$$Q_{ij}^{(k)} = R_{ij} \left(H_i^{(k)} - H_j^{(k)} \right)^{1/n}$$

with R_{ij} and "n" depending on the head loss/flow relationship in use.

3. Compute the flow imbalance at each node:

$$\delta Q_i^{(k)} = \sum_j Q_{ij}^{(k)} - q_i \qquad (26)$$

4. Calculate the ratio $Q_{ij}^{(k)}/n\ h_{ij}^{(k)}$ for each pipe and add up the ratios corresponding to each node "i", obtaining:

$$\sum_j \{Q_{ij}^{(k)}/n\ h_{ij}^{(k)}\} \qquad (27)$$

5. Calculate the correction, dividing equations (26) and (27), for each node:

$$\delta H_i^{(k)} = \frac{\delta\ Q_i^{(k)}}{\sum_j \frac{Q_{ij}^{(k)}}{n\ h_{ij}^{(k)}}} \qquad (28)$$

6. Calculate the corrected piezometric heads, for every node "i", as:

$$H_i^{(k+1)} = H_i^{(k)} + \delta H_i^{(k)} \qquad (29)$$

7. The process can be stopped either if the maximum $\delta H_i^{(k)}$ is less than a pre-specified tolerance or, if the maximum nodal

imbalance δQ_i is less than a maximum limit. Otherwise, increment the iteration counter: k to k+1 and go back to step 2.

In comparison with the loop-flow method, the nodal method has the advantage that the initial solution for the heads is much easier to find than the initial balanced flow distribution required by the loop method. The main disadvantage is that the convergence can be very slow, and this is the main reason why this method was not used initially, when computers were not available.

The nodal method can handle problems with mixed networks (partly looped and partly branched) straight away, without the need to split up the looped from the branched part, as in the case of the loop method. There is no need to supply as input the definition of loops, since they are not needed in this nodal approach.

An additional advantage of the nodal method is related to the fact that we can use the Darcy-Weisbach relationship in a direct fashion (rather than the iterative one required by the loop method), thus saving some computation time. This is shown by McCormick and Bellamy (1968) and Featherstone (1983, page 114).

Dillingham (1967) reported some convergence problems with the nodal method and suggested some remedies, based on intuition and practical experience, but no guarantee of convergence could be given.

McCormick and Bellamy (1968) reported some possible sources of failure in the convergence of the nodal method, with some

possible solutions. According to them, a faster convergence can be achieved, if the head corrections (29) are not made in the sequence given by the nodes numbering, but according to the magnitude of the correction δH_i. Proceeding in that way, a number of corrections can be made in one node before another node is considered.

As pointed out by McCormick and Bellamy (1968), there are a number of situations that can result in no convergence, and it is quite a formidable task to write a computer program with convergence guaranteed. On top of that, the computer time necessary to obtain the steady state solution cannot be predicted on the basis of the network size; the resistance characteristics of the pipes and the connectivity of the network seem to have a significant impact in this respect. Manual intervention and some sound engineering thought seems to be the solution to some pathological cases of slow convergence.

Barlow and Markland (1969) reported some important reductions in the number of iterations when a quadratic expression is used to determine δH_i (instead of equation 17). Using this approach in a network with 14 nodes and 25 pipes, they reduced the number of iterations from 121 to 77. In their experience, over-relaxing the correction δH_i does not result in a significant improvement, sometimes it can even be counterproductive. For chronic ill-conditioned cases, they recommended a loop-flow method.

An inherent problem with the nodal method, which is recognised by many authors, seems to be the fact that the head correction

are carried out one node at a time, without allowing proper interaction between the nodes of the network. The loop method does allow some interaction, through the pipes common to two different loops.

Thus, this approach suffers from an internal contradiction, which is solved in the following methods, in the sense that having been developed when computers were not available, it became used only with the availability of such machines but then does not take full advantage of them, because it does not solve all the head corrections simultaneously.

2.3. Newton-Raphson-based methods.

2.3.1. Introduction.

Under this general heading, a number of different methods for the solution of the network analysis problem are described, all of them using the Newton-Raphson method to solve the corresponding systems of non-linear equations. This leads to some misunderstandings, since the Newton-Raphson method is a general-purpose algorithm. The main difference between the different network analysis methods reviewed under this general heading, will be shown to be in the way that these methods formulate the problem and assemble the equations.

For completeness, a brief review of the mathematical background of the Newton-Raphson method is included . After that, its application to the solution of the network analysis problem is reviewed, as proposed by different authors.

2.3.2. The mathematical background of the Newton-Raphson method.

Newton's method is widely accepted as an efficient algorithm for the solution of one-dimensional non-linear equations.

Let

$$f(x) = 0 \qquad (30)$$

be a non-linear function, whose solution is sought within a certain interval [a, b]. Let $x = x^{(o)}$, with $x^{(o)} \in [a, b]$, be the true solution to equation (30). Hence,

$$f(x^{(o)}) = 0 \qquad (31)$$

and $f(x) \neq 0$, for all $x \in [a, b]$, and such that $x \neq x^{(o)}$.

Newton's method is based on approximating the non-linear function locally via a linear function; starting from an approximate solution, say $x^{(1)}$, the linearized problem provides a better approximation, say $x^{(2)}$, to the true solution of the non-linear problem. Via successive linearizations, a sequence of approximations is obtained ($x^{(1)}$, $x^{(2)}$, $x^{(3)}$, ...), which gets closer and closer to the true solution.

A Taylor series expansion of the original function provides the way to linearize the originally non-linear problem. Thus, expanding the function, centred at an approximation $x^{(k)}$:

$$f(x^{(k)}+\delta x^{(k)}) = f(x^{(k)}) + f'(x^{(k)})\delta x^{(k)} + \tfrac{1}{2}f''(x^{(k)})(\delta x^{(k)})^2 + \ldots = 0 \qquad (31)$$

This means that, if $x^{(k)}$ is such that $f(x^{(k)}) \neq 0$, we are looking for a better approximation, say $x^{(k)} + \delta x^{(k)}$, where the value of the non-linear function becomes zero.

In fact, if $x^{(k)}$ is close to the true solution $x^{(o)}$, the term $(\delta x^{(k)})^2$ and its higher order terms will be very small, and they can be rejected, reducing (31) to:

$$f(x^{(k)}+\delta x^{(k)}) \approx f(x^{(k)}) + f'(x^{(k)})\ \delta x^{(k)} \qquad (32)$$

Because we aim at $f(x^{(k)}+\delta x^{(k)}) = 0$, equation (32) can be used to compute the value of the correction:

$$\delta x^{(k)} = \frac{-\ f(x^{(k)})}{f'(x^{(k)})} \qquad (33)$$

and the following recursive formula allows us to compute the sequence of x-values converging to the true solution:

$$x^{(k+1)} = x^{(k)} + \delta x^{(k)} \qquad (34)$$

We either stop the iterative procedure when two successive values are close enough, or when the function is nearly zero. This implies that some minimum accuracy must be specified.

The method converges fairly well for monotonic functions, although several cases of non-convergence and oscillatory behaviour are reported in most of the numerical analysis textbooks; the user must be aware of them, but they are not likely to occur in pipe network analysis.

The Newton-Raphson method is the direct extension of the one-dimensional Newton method to an n-dimensional space. In this context, the following non-linear system of simultaneous equations needs to be solved:

$$\left.\begin{array}{l} f_1(x_1,\ x_2,\ x_3,\ \ldots\ ,\ x_n) = 0 \\ f_2(x_1,\ x_2,\ x_3,\ \ldots\ ,\ x_n) = 0 \\ \quad\vdots \qquad\qquad\qquad\qquad\quad \vdots\ : \\ \quad\vdots \qquad\qquad\qquad\qquad\quad \vdots\ : \\ f_n(x_1,\ x_2,\ x_3,\ \ldots\ ,\ x_n) = 0 \end{array}\right| \qquad (35)$$

which can be represented in vector notation as:

$$\underline{f}(\underline{x}) = \underline{0} \tag{36}$$

Now, let us suppose we have an approximation $\underline{x}^{(k)}$ to the true solution and we need to find a better approximation, say $\underline{x}^{(k+1)} = \underline{x}^{(k)} + \delta\underline{x}^{(k)}$; then, following a similar approach as in the one-dimensional case, we expand the function (36) using a Taylor series centred at $\underline{x}^{(k)}$ and drop all the terms of second or higher order. In so doing, we get:

$$\left.\begin{array}{l}
f_1(x_1,\ldots,x_n)+ \dfrac{\partial f_1}{\partial x_1}\,\delta x_1(k)+ \dfrac{\partial f_1}{\partial x_2}\,\delta x_2(k)+\ldots+ \dfrac{\partial f_1}{\partial x_n}\,\delta x_n(k) = 0 \\
f_2(x_1,\ldots,x_n)+ \dfrac{\partial f_2}{\partial x_1}\,\delta x_1(k)+ \dfrac{\partial f_2}{\partial x_2}\,\delta x_2(k)+\ldots+ \dfrac{\partial f_2}{\partial x_n}\,\delta x_n(k) = 0 \\
\quad\vdots \qquad\qquad \vdots \qquad\qquad \vdots \qquad\qquad \vdots \qquad\quad \vdots \\
f_n(x_1,\ldots,x_n)+ \dfrac{\partial f_n}{\partial x_1}\,\delta x_1(k)+ \dfrac{\partial f_n}{\partial x_2}\,\delta x_2(k)+\ldots+ \dfrac{\partial f_n}{\partial x_n}\,\delta x_n(k) = 0
\end{array}\right| \tag{37}$$

where all the functions and derivatives are evaluated at $\underline{x} = \underline{x}^{(k)}$

This system can be represented in matrix form as follows:

$$\begin{bmatrix}
\dfrac{\partial f_1}{\partial x_1} & \dfrac{\partial f_1}{\partial x_2} & \ldots & \dfrac{\partial f_1}{\partial x_n} \\
\dfrac{\partial f_2}{\partial x_1} & \dfrac{\partial f_2}{\partial x_2} & \ldots & \dfrac{\partial f_2}{\partial x_n} \\
\vdots & \vdots & & \vdots \\
\dfrac{\partial f_n}{\partial x_1} & \dfrac{\partial f_n}{\partial x_2} & \ldots & \dfrac{\partial f_n}{\partial x_n}
\end{bmatrix} * \begin{bmatrix} \delta x_1(k) \\ \delta x_2(k) \\ \vdots \\ \delta x_n(k) \end{bmatrix} = -1 * \begin{bmatrix} f_1(x_1,\ldots,x_n) \\ f_2(x_1,\ldots,x_n) \\ \vdots \\ f_n(x_1,\ldots,x_n) \end{bmatrix} \tag{38}$$

where, again, all the expressions are evaluated at $\underline{x}=\underline{x}^{(k)}$

The system (38) is a linear system of equations in the unknown vector $\delta\underline{x}^{(k)} = (\delta x_1^{(k)}, \delta x_2^{(k)}, \ldots, \delta x_n^{(k)})^T$, the column vector of corrections.

Let us define the right-hand-side vector $\underline{f}(\underline{x}^{(k)})$ as:

$$\underline{f}(\underline{x}^{(k)}) = (f_1(x_1^{(k)}, \ldots, x_n^{(k)}), f_2(x_1^{(k)}, \ldots, x_n^{(k)}), \ldots, \ldots, f_n(x_1^{(k)}, \ldots, x_n^{(k)}))^T$$

On defining the Jacobian matrix as:

$$J^{(k)} = \left[\begin{array}{ccc} \frac{\partial f_1}{\partial x_1} & \frac{\partial f_1}{\partial x_2} & \cdots \quad \frac{\partial f_1}{\partial x_n} \\ \frac{\partial f_2}{\partial x_1} & \frac{\partial f_2}{\partial x_2} & \cdots \quad \frac{\partial f_2}{\partial x_n} \\ \vdots & \vdots & \vdots \\ \frac{\partial f_n}{\partial x_1} & \frac{\partial f_n}{\partial x_2} & \cdots \quad \frac{\partial f_n}{\partial x_n} \end{array} \right]_{\underline{x}=\underline{x}^{(k)}} \qquad (39)$$

the system (38) can be written in an even more compact way:

$$J^{(k)}\ \delta\underline{x}^{(k)} = -\underline{f}(\underline{x}^{(k)}) \qquad (40)$$

Algebraically, the unknown corrections are obtained by inverting the Jacobian matrix:

$$\delta\underline{x}^{(k)} = -[J^{(k)}]^{-1}\ \underline{f}(\underline{x}^{(k)}) \qquad (41)$$

but the numerical solution can be obtained more efficiently by Gauss elimination or any other efficient linear solver [see Appendix A].

The iterative sequence of approximations to the true solution of the non-linear system is obtained by:

$$\underline{x}^{(k+1)} = \underline{x}^{(k)} + \delta\underline{x}^{(k)} \qquad (42)$$

As in the one-dimensional Newton method, the iterative procedure is stopped when two successive solutions are close enough. In the n-dimensional case, this is when some pre-specified vector norm is smaller than a given accuracy, say ϵ:

$$| \delta \underline{X}^{(k)} | < \epsilon$$

Again, as before, the main assumption in the Newton-Raphson method is that the successive corrections are small; only in that case is it acceptable to neglect the second and higher order terms in the Taylor's expansion. This is the key factor in the success of the method, since it produces a succession of linear problems out of a non-linear one; however this may also be the origin of difficulties, especially when the algorithm is started with an initial solution too far from the true solution.

The algorithm also relies on the inversion of the Jacobian matrix [equation (41)], this implies that the Jacobian has to be a non-singular matrix, which indeed is the case in most engineering applications. Some reductions in the amount of work can be obtained, if the inverse of the Jacobian is not updated at every iteration, but at every two or three iterations.

This is the basic mathematical framework of the Newton-Raphson method. Some special properties of the method emerge when applying the method to water distribution networks, which will be explained in due course.

2.3.3. Martin and Peters formulation (1963).

Although Warga (1954) is recognised as the first author to suggest the use of the Newton-Raphson method to the solution of general networks, (gas, petroleum, power networks and also water supply), the credit for being the first to solve the water distribution analysis problem with the Newton-Raphson algorithm is attributed to Martin and Peters (1963).

In general, the application of the Newton-Raphson method for network analysis, as in the case of the Cross methods, may involve two different ways for the formulation of the equations: a loop-flow approach and a nodal (head) approach.

The solution proposed by Martin and Peters (1963) is based on the head equations (i.e. nodal approach), although in their original paper they used pressures instead of heads.

The nodal balance condition states that, in every one of the NN nodes of the network, say the i-th node, the following balance must hold:

$$\sum_j Q_{ij} - q_i = 0 \qquad (43)$$

Since, in general, the empirical head loss/flow relationship for pipes is of the form:

$$h_{ij} = H_i - H_j = K_{ij}\, Q_{ij}^{n} \qquad (44)$$

or

$$Q_{ij} = (H_i - H_j)\, \frac{|H_i - H_j|^{(1-n)/n}}{K_{ij}^{1/n}} \qquad (45)$$

then, on defining m=(1-n)/n, the nodal balance equations (43) can be written as:

$$\sum_j Q_{ij} - q_i = \sum_j (H_i - H_j) \frac{|H_i - H_j|^m}{K_{ij}^{1/n}} - q_i = 0 \qquad (46)$$

Let us call each one of these NN equations as:

$$f_i(H_1, H_2, \ldots, H_{NN}) = \sum_j (H_i - H_j) \frac{|H_i - H_j|^m}{K_{ij}^{1/n}} - q_i = 0 \qquad (47)$$

$$\text{for } i = 1, 2, \ldots, NN.$$

Since in the standard water distribution network analysis problem, the resistance characteristics K_{ij} are considered known, as well as the nodal consumptions q_i, then the following system of NN non-linear equations in NN unknowns H_i is obtained:

$$\left.\begin{aligned}
f_1(H_1, H_2, \ldots, H_{NN}) &= \sum_j (H_1 - H_j) \frac{|H_1 - H_j|^m}{K_{1j}^{1/n}} - q_1 = 0 \\
f_2(H_1, H_2, \ldots, H_{NN}) &= \sum_j (H_2 - H_j) \frac{|H_2 - H_j|^m}{K_{2j}^{1/n}} - q_2 = 0 \\
&\vdots \qquad\qquad \vdots \qquad\qquad \vdots \\
f_{NN}(H_1, H_2, \ldots, H_{NN}) &= \sum_j (H_{NN} - H_j) \frac{|H_{NN} - H_j|^m}{K_{NNj}^{1/n}} - q_{NN} = 0
\end{aligned}\right| \qquad (48)$$

which is in the familiar format of the Newton-Raphson method (section 2.3.2, equation 35).

Note that for all source nodes (reservoirs for example), the nodal balance equation (43) is redundant, and their corresponding heads are known (the reservoir water level); then, each source node can be eliminated, thus reducing the system (48) to NN-NS

equations, where NS is the number of sources. This condition is not introduced into the formulae, in order to keep the notation as simple as possible, but we have to bear it in mind.

To apply the Newton-Raphson method, the partial derivatives of the functions $f_i(H_1, H_2, \ldots, H_{NN}) = f_i(\underline{H})$ need to be computed:

$$\frac{\partial f_i(\underline{H})}{\partial H_j} = \frac{1}{n} \frac{|H_i - H_j|^m}{K_{ij}^{1/n}} \qquad \text{for } i \neq j \tag{49}$$

and

$$\frac{\partial f_i(\underline{H})}{\partial H_i} = - \sum_j \frac{\partial f_i(\underline{H})}{\partial H_j} \qquad \text{for } i = j \tag{50}$$

from equation (49), it is easy to see that:

$$\frac{\partial f_i(\underline{H})}{\partial H_j} = \frac{\partial f_j(\underline{H})}{\partial H_i} \tag{51}$$

which implies that the Jacobian is a symmetric matrix.

The Newton-Raphson algorithm can now be applied:

1. Find an initial estimate of the piezometric heads in every node. Denote the corresponding vector as:

   $$\underline{H}^{(o)} = (H_1^{(o)}, \ldots, H_{NN}^{(o)})^T.$$

2. Initialise the iteration counter k=0.
3. Evaluate the functions $f_i(\underline{h})$ at $\underline{H}=\underline{H}^{(k)}$; then:

   $$\underline{f}(\underline{H}^{(k)}) = \underline{f}(H_1^{(k)}, \ldots, H_{NN}^{(k)})$$

4. Calculate the coefficients of the Jacobian matrix using the formulae (49) and (50) for this purpose, and evaluating them at the point $\underline{H} = \underline{H}^{(k)}$ i.e.:

$$\left.\frac{\partial f_i(\underline{H})}{\partial H_j}\right]_{\underline{H}=\underline{H}^{(k)}} = \frac{1}{n} \frac{|H_i^{(k)} - H_j^{(k)}|^m}{K_{ij}^{1/n}} \qquad \text{for } i \neq j \tag{52}$$

$$\left.\frac{\partial f_i(\underline{H})}{\partial H_i}\right|_{\underline{H}=\underline{H}(k)} = -\frac{1}{n}\sum_j \frac{|H_i(k)-H_j(k)|^m}{K_{ij}^{1/n}} \qquad \text{for } i=j \qquad (53)$$

5. Assemble the linear system of equations.

6. Reduce the linear system by eliminating the rows and columns corresponding to each one of the NS sources. This leads to a system of NH=NN-NS equations, which is still symmetric.

7. Solve the reduced linear system:

$$\begin{bmatrix} \frac{\partial f_1}{\partial H_1} & \frac{\partial f_1}{\partial H_2} & \cdots & \frac{\partial f_1}{\partial H_{NH}} \\ \frac{\partial f_2}{\partial H_1} & \frac{\partial f_2}{\partial H_2} & \cdots & \frac{\partial f_2}{\partial H_{NH}} \\ \vdots & \vdots & & \vdots \\ \frac{\partial f_{NH}}{\partial H_1} & \frac{\partial f_{NH}}{\partial H_2} & \cdots & \frac{\partial f_{NH}}{\partial H_{NH}} \end{bmatrix} * \begin{bmatrix} \delta H_1(k) \\ \delta H_2(k) \\ \vdots \\ \delta H_{NH}(k) \end{bmatrix} = -1 * \begin{bmatrix} f_1(H_1, \ldots, H_{NH}) \\ f_2(H_1, \ldots, H_{NH}) \\ \vdots \\ f_{NH}(H_1, \ldots, H_{NH}) \end{bmatrix} \qquad (54)$$

where all the expressions are evaluated at $\underline{H}=\underline{H}(k)$, as shown in equations (52) and (53).

The solution of the linear system, which can be obtained by Gaussian elimination or any other method (see Appendix A for a review on linear solvers), produces the unknown vector:

$$\delta\underline{H}(k) = (\delta H_1(k),\ \delta H_2(k),\ \ldots,\ \delta H_{NH}(k))^T$$

8. Calculate the corrected heads:

$$\underline{H}(k+1) = \underline{H}(k) + \delta\underline{H}(k) \qquad (55)$$

9. If $\max.|\delta\underline{H}(k)| < \epsilon$, where ϵ is a pre-specified accuracy, stop; otherwise, increase the iteration counter (k to k+1) and go to step 3. Other convergence criteria may be used:

e.g. the maximum norm of the residuals, the maximum number of iterations, etc.

As pointed out by Martin and Peters (1963), there are in this formulation a few things that can go wrong:

a) If $H_i^{(k)}-H_j^{(k)}$ is a very small quantity, which is the case when two adjacent nodes have almost the same piezometric head, the coefficients of the Jacobian can result in extremely large numbers, overflowing the computer capacity. In these cases, Martin and Peters (1963) recommended the temporary removal of these pipes from the network model.

b) Although the corrections $\delta\underline{H}^{(k)}$ decrease quickly in magnitude, cases with oscillations were detected; the recommendation of Martin and Peters for these cases was to halve the correction $\delta\underline{H}^{(k)}$.

So far, only pipes have been considered in the network (equation 44), but it is not difficult to include any other device, provided that its head loss/flow relationship can be expressed as an analytic function. We shall return to this point later on, when dealing with more complex devices.

Additionally, Martin and Peters (1963) introduced the problem of the agreement between the mathematical model, represented by the Newton-Raphson solution of the network, and the real network. They recognised the fact that, normally, agreement will not be achieved; an adjustment of the resistances was suggested as a remedy, relying just on some intuitive knowledge of the system and guesswork.

2.3.4. Shamir and Howard nodal formulation (1968).

Shamir and Howard (1968) published a paper on the solution of the network analysis problem, acknowledging some previous work done at MIT. Also, some work carried out by Pitchai (1966) was referenced.

One of the main reasons why this paper became classical, and a compulsory reference in future works, seems to be the fact that a generalised method for the solution of the network steady state flow problem was presented.

The Shamir and Howard method is based on a head-equations formulation (nodal approach), accepting not only piezometric heads as unknowns, but also nodal consumptions and pipe resistances (i.e. either diameters or roughnesses). Furthermore, a methodology to perform a sensitivity analysis is presented, allowing the user to study the effect of changes in a single variable over the rest of the network, at a very low computational cost.

The Shamir and Howard method is based on node continuity:

$$f_i = \sum_j Q_{ij} - q_i = 0 \qquad (56)$$

for every node i=1,2, .. NN.

Following the usual procedure of expanding each one of these nodal equations, and taking just the first order terms for the extended set of unknowns:

$\underline{X}$: set of unknown piezometric heads (subset of $\underline{H}$).

$\underline{Y}$: set of unknown pipe resistances (subset of $\underline{K}$).

$\underline{Z}$: set of unknown nodal consumptions (subset of $\underline{q}$).

the following linear system of equations is obtained:

$$f_i(\underline{X},\underline{Y},\underline{Z}) + \sum_j \frac{\partial f_i}{\partial X_j} \delta X_j + \sum_j \frac{\partial f_i}{\partial Y_j} \delta Y_j + \sum_j \delta_{ij} \delta Z_j = 0 \qquad i=1,\ldots NU \qquad (57)$$

where:

NU : total number of unknowns.

δ_{ij} : Kronecker delta (δ_{ij}=1 if i=j and zero otherwise).

δX_j : correction to the unknown piezometric head in node "j". Let us assume that there are, as before, NH nodes with unknown heads.

δY_j : correction to the unknown resistance in branch "j". Let us assume that there are NR branches with unknown resistances.

δZ_j : correction to the unknown nodal consumption in node "j". Let us assume that there are NC nodes with unknown consumptions.

Note that, apart from the third and fourth terms of the left-hand-side of equation (57), the problem can be dealt with in exactly the same way as Martin and Peters (1963).

A necessary condition for the solvability of the system of equations represented by (57), is that the total number of nodes NN, must be equal to :

$$NN = NH + NR + NC \qquad (58)$$

The system of equations (57) can be written as:

$$\begin{bmatrix} \frac{\partial f_1}{\partial X_1} & \cdots & \frac{\partial f_1}{\partial X_{NH}} & \frac{\partial f_1}{\partial Y_1} & \cdots & \frac{\partial f_1}{\partial Y_{NR}} & \frac{\partial f_1}{\partial Z_1} & \cdots & \frac{\partial f_1}{\partial Z_{NC}} \\ \frac{\partial f_2}{\partial X_1} & \cdots & \frac{\partial f_2}{\partial X_{NH}} & \frac{\partial f_2}{\partial Y_1} & \cdots & \frac{\partial f_2}{\partial Y_{NR}} & \frac{\partial f_2}{\partial Z_1} & \cdots & \frac{\partial f_2}{\partial Z_{NH}} \\ \vdots & & \vdots & \vdots & & \vdots & \vdots & & \vdots \\ \frac{\partial f_{NN}}{\partial X_1} & \cdots & \frac{\partial f_{NN}}{\partial X_{NH}} & \frac{\partial f_{NN}}{\partial Y_1} & \cdots & \frac{\partial f_{NN}}{\partial Y_{NH}} & \frac{\partial f_{NN}}{\partial Z_1} & \cdots & \frac{\partial f_{NN}}{\partial Z_{NC}} \end{bmatrix} * \begin{bmatrix} \delta X_1^{(k)} \\ \vdots \\ \delta X_{NH}^{(k)} \\ \delta Y_1^{(k)} \\ \vdots \\ \delta Y_{NR}^{(k)} \\ \delta Z_1^{(k)} \\ \vdots \\ \delta Z_{NC}^{(k)} \end{bmatrix} = \begin{bmatrix} -f_1 \\ -f_2 \\ \vdots \\ \vdots \\ -f_{NN} \end{bmatrix} \qquad (59)$$

As we did in the case of the Newton-Raphson method, the iterative solution of the non-linear system requires an initial (estimated) solution, say:

$$(X_1^{(o)}, .., X_{NH}^{(o)}, Y_1^{(o)}, .., Y_{NR}^{(o)}, Z_1^{(o)}, .., Z_{NC}^{(o)})^T$$

This initial solution is improved successively until a sufficiently close approximation to the true solution is found.

The iterative procedure follows the same steps as Martin and Peters' (1963) method, and both the Jacobian coefficients and the right-hand-side vector need to be updated at each iteration.

In order to compute the coefficients of the Jacobian matrix, each partial derivative can be obtained from the nodal-balance equation. Thus, if the Hazen-Williams formula is being used, in which case the node-balance for node "i" becomes:

$$f_i = \sum_j \frac{(H_i - H_j)}{K_{ij}^{0.54} \, |H_i - H_j|^{0.46}} - q_i = 0 \qquad (60)$$

and the corresponding partial derivatives are:

$$\frac{\partial f_i(\underline{H})}{\partial X_j} = \frac{0.54}{K_{ij}^{0.54} \, |H_i - H_j|^{0.46}} = \frac{\partial f_j(\underline{H})}{\partial H_i} \quad \text{for } i \neq j \qquad (61)$$

and

$$\frac{\partial f_i(\underline{H})}{\partial X_i} = - \sum_j \frac{\partial f_i(\underline{H})}{\partial H_j} \qquad \text{for } i=j \qquad (62)$$

and

$$\frac{\partial f_i(\underline{H})}{\partial Y_k} = \frac{- 0.54 \ (H_i - H_j)}{K_{ij}^{1.54} \ |H_i - H_j|^{0.46}} \qquad (63)$$

where pipe "k" is connecting nodes "i" and "j".

and, finally:

$$\frac{\partial f_i(\underline{H})}{\partial Z_k} = - 1 \text{ if } i=k, \text{ and } 0 \text{ otherwise.} \qquad (64)$$

McCormick (1969) provided the corresponding equations for the partial derivatives when using the Darcy-Weisbach formula with the Shamir and Howard formulation.

With this proposed generalisation the Jacobian matrix is no longer symmetric, except for the case when there are neither resistances nor consumptions as unknowns.

The solution of system (59), at an intermediate step "k", gives the corrections, allowing us to updated the unknowns:

$$\left.\begin{array}{l} X_1(k+1) = X_1(k) + \delta X_1(k) \\ X_2(k+1) = X_2(k) + \delta X_2(k) \\ \vdots \qquad\quad \vdots \qquad\quad \vdots \\ X_{NH}(k+1) = X_{NH}(k) + \delta X_{NH}(k) \end{array}\right\} \; \underline{X}(k+1) = \underline{X}(k) + \delta \underline{X}(k)$$

$$\left.\begin{array}{l} Y_1(k+1) = Y_1(k) + \delta Y_1(k) \\ Y_2(k+1) = Y_2(k) + \delta Y_2(k) \\ \vdots \qquad\quad \vdots \qquad\quad \vdots \\ Y_{NR}(k+1) = Y_{NR}(k) + \delta Y_{NR}(k) \end{array}\right\} \; \underline{Y}(k+1) = \underline{Y}(k) + \delta \underline{Y}(k) \qquad (65)$$

$$\left.\begin{array}{l} Z_1(k+1) = Z_1(k) + \delta Z_1(k) \\ Z_2(k+1) = Z_2(k) + \delta Z_2(k) \\ \vdots \qquad\quad \vdots \qquad\quad \vdots \\ Z_{NC}(k+1) = Z_{NC}(k) + \delta Z_{NC}(k) \end{array}\right\} \; \underline{Z}(k+1) = \underline{Z}(k) + \delta \underline{Z}(k)$$

Because of the presence of unknown resistances and nodal consumptions, the condition that the number of nodes must be exactly the same as the number of unknowns (equation 58), is not sufficient to guarantee a solution to the non-linear system, as formulated by Shamir and Howard (1968). According to the authors, the existence of the solution will depend on the way the unknowns are selected, and their distribution within the network, since clearly if all the unknowns are concentrated in only one region of the network the set of equations (59) becomes rank-deficient; a set of rules to select the unknowns was proposed by Shamir (1973):

a) In any node, at least one of the following variables should be unknown:

- consumption at the node,
- either head at the node or the head of the adjacent nodes,
- the resistance of one pipe connected to the node .

b) A node having an unknown consumption should be connected to at least one other node with a known consumption.

c) When solving for an unknown resistance, the subsystem consisting of an unknown resistance and the two terminal nodes should not have more than one unknown in addition to the unknown resistance.

Shamir and Howard (1968) stressed the point that any device can be included in this formulation, provided that the analytic expression of the head loss/flow relationship is available. However, they warned the users, that in the event of functions with discontinuous derivatives, difficulties with the convergence of the algorithm may be expected.

2.3.5. The Newton-Cross method of Liu (1969).

K. T. Liu (1969) proposed a simplified version of the Newton-Raphson method for the analysis of water distribution networks. Liu's approach is based on a decomposition of the Jacobian matrix into two matrices, one containing the diagonal of the original Jacobian, and the other containing the off-diagonal coefficients.

Thus, the original matrix of coefficients in the system:

$$\begin{bmatrix} \frac{\partial f_1}{\partial H_1} & \frac{\partial f_1}{\partial H_2} & \cdots & \frac{\partial f_1}{\partial H_{NH}} \\ \frac{\partial f_2}{\partial H_1} & \frac{\partial f_2}{\partial H_2} & \cdots & \frac{\partial f_2}{\partial H_{NH}} \\ \vdots & \vdots & & \vdots \\ \frac{\partial f_{NH}}{\partial H_1} & \frac{\partial f_{NH}}{\partial H_2} & \cdots & \frac{\partial f_{NH}}{\partial H_{NH}} \end{bmatrix} * \begin{bmatrix} \delta H_1(k) \\ \delta H_2(k) \\ \vdots \\ \delta H_{NH}(k) \end{bmatrix} = \begin{bmatrix} -f_1(\underline{H}) \\ -f_2(\underline{H}) \\ \vdots \\ -f_{NH}(\underline{H}) \end{bmatrix} \qquad (66)$$

can be decomposed as the sum of:

$$\begin{bmatrix} \frac{\partial f_1}{\partial H_1} & 0 & \cdots & 0 \\ 0 & \frac{\partial f_2}{\partial H_2} & \cdots & 0 \\ \vdots & \vdots & & \vdots \\ 0 & 0 & \cdots & \frac{\partial f_{NH}}{\partial H_{NH}} \end{bmatrix} + \begin{bmatrix} 0 & \frac{\partial f_1}{\partial H_2} & \cdots & \frac{\partial f_1}{\partial H_{NH}} \\ \frac{\partial f_2}{\partial H_1} & 0 & \cdots & \frac{\partial f_2}{\partial H_{NH}} \\ \vdots & \vdots & & \vdots \\ \frac{\partial f_{NH}}{\partial H_1} & \frac{\partial f_{NH}}{\partial H_2} & \cdots & 0 \end{bmatrix} \qquad (67)$$

The argument of Liu is that, because, for the diagonals,

$$\frac{\partial f_i(\underline{H})}{\partial H_i} = - \sum_j \frac{\partial f_i(\underline{H})}{\partial H_j}$$

the diagonal terms are much bigger (in absolute value) than the off-diagonal terms, then the latter ones can be dropped, obtaining an approximate linear system which is much simpler to solve than the original system (66). In other words, Liu is applying the same concept behind the method of Jacobi (or simultaneous displacements method) for the iterative solution of linear systems (see Appendix A).

The new (approximated) linear system becomes:

$$\begin{bmatrix} \frac{\partial f_1}{\partial H_1} & 0 & \dots & 0 \\ 0 & \frac{\partial f_2}{\partial H_2} & \dots & 0 \\ \vdots & \vdots & & \vdots \\ 0 & 0 & \dots & \frac{\partial f_{NH}}{\partial H_{NH}} \end{bmatrix} * \begin{bmatrix} \delta H_1(k) \\ \delta H_2(k) \\ \vdots \\ \delta H_{NH}(k) \end{bmatrix} = \begin{bmatrix} - f_1(\underline{H}) \\ - f_2(\underline{H}) \\ \vdots \\ - f_{NH}(\underline{H}) \end{bmatrix} \qquad (68)$$

with all the expressions evaluated at $\underline{H}=\underline{H}(k)$

Equation (68) requires only scalar operations to find the solution vector $\delta\underline{H}(k)$:

$$\delta H_i(k) = \frac{- f_i(\underline{H}(k))}{\left[\frac{\partial f_i}{\partial H_i} \right]_{\underline{H}=\underline{H}(k)}} \qquad \forall\ i=1,2,\dots,NH \qquad (69)$$

The rest of the algorithm remains identical to the standard Newton-Raphson method. According to Liu (1969), the algorithm may diverge when starting from a poor initial solution.

It is interesting to note that Liu's method is, in essence, Cross' head-equations method. In fact, if we compare equations (69) and (25), both are completely equivalent. The point here is that the methods proposed by Cross (1936), are actually based on Newton's method, applied locally either to the loops or to the nodes.

2.3.6. Epp and Fowler loop formulation (1970).

Although the nodal approach has a simple formulation, and the initial head solution is very easy to produce, especially when compared with an initial flow solution, a number of convergence problems have been reported in the literature [Martin and Peters (1963), Shamir and Howard (1968), McCormick (1969), de Neufville and Hester (1969), etc.].

In an attempt to cope with these convergence problems, Epp and Fowler (1970) explored the possibility of using a loop formulation instead of a nodal approach. They also had in mind the fact that, normally, the number of loops is smaller than the number of nodes, producing a reduced-size system of equations; however, this point may not be relevant when adequate sparse techniques are used.

On the negative side, a loop approach needs a definition of the loops, either provided by the user or produced internally by the computer (with the associated computational cost).

Epp and Fowler (1970) gave a solution to the problem of generating automatically the loop definition, based on the

standard (minimum) connectivity data. Also, they presented a loop labelling algorithm, in order to reduce the bandwidth of the matrix of the linear system, thus reducing the storage requirements. Because the loop method needs an initial balanced flow distribution, Epp and Fowler (1970) devised an algorithm to produce it, using a minimal resistance spanning tree.

To derive the loop formulation in the Newton-Raphson format, and in order to take account of the relationship between loops, pipes and nodes, some complementary notation needs to be introduced. First of all, the establishment for each pipe of an arbitrary positive reference direction is needed, say i-j if the pipe starts in node "i" and ends in node "j"; thus a flow or head loss in the pipe i-j will be positive if it is from node "i" to "j", negative otherwise. Additionally, a positive direction has to be arbitrarily defined for moving around a loop, this is normally the clockwise direction. Thus, when moving around a loop to verify the condition $\Sigma\, h_{ij} = 0$, we shall be adding the head losses if their direction coincides with the loop rotation direction and subtracting the losses when they are in the opposite direction.

The derivation of the loop formulation is as follows: the potential continuity condition (see derivation of Cross' loop method), requires that the summation of head losses around any loop must be zero, i.e.:

$$\sum_{\text{loop}} h_{ij} = 0 \qquad (70)$$

where the summation is carried out throughout all the pipes i-j

belonging to the loop.

Introducing the usual head loss/flow relationship for pipes, equation (70) becomes:

$$\sum_{loop} K_{ij} Q_{ij}^{n} = 0 \qquad (71)$$

Starting with an initial flow distribution which fulfils the node-balance condition, say $Q_{ij}^{(o)}$, and assuming that the loop balance is not fulfilled, i.e. $\sum K_{ij} Q_{ij}^{n} \neq 0$, a loop flow additive correction can be calculated, in order to get a better approximation to the fulfilment of the loop-balance condition; this correction can be represented, at the iteration "k", as a vector $\delta\underline{Q}^{(k)}=(\delta Q_1^{(k)}, \delta Q_2^{(k)}, \ldots, \delta Q_{NL}^{(k)})^T$, where NL is the number of loops in the network. This is equivalent to what was done in the Cross' loop method, but now is done for all the NL loops simultaneously. The corrected loop balance condition can be written as:

$$\sum_{\forall i,j \in l} K_{ij} \left(\delta_{ijl} Q_{ij} + \sum_{h=1}^{NL} \delta_{ijh} \delta Q_h^{(k)}\right)^n = 0 \qquad l=1,2,\ldots,NL \qquad (72)$$

where:

$$\delta_{ijh} = \begin{cases} +1 & \text{if pipe i-j has the same direction as loop "h"} \\ -1 & \text{if pipe i-j is in the opposite direction with respect to loop "h"} \\ 0 & \text{otherwise} \end{cases}$$

Note that the second summation in (72) accounts not only for the loop flow correction in the current loop, but also for the

corrections in the neighbouring loops (for these pipes belonging to more than one loop).

Equation (72) is a system of NL non-linear simultaneous equations in NL unknowns: $\delta\underline{Q}^{(k)}=(\delta Q_1^{(k)}, \delta Q_2^{(k)}, \ldots, \delta Q_{NL}^{(k)})^T$, which can be put in the standard Newton-Raphson format:

$$\begin{aligned}
f_1(\underline{Q},\delta\underline{Q}) &= \sum_{\forall i,j\in 1} K_{ij}\,(\delta_{ij1}\,Q_{ij} + \sum_{h=1}^{NL} \delta_{ijh}\,\delta Q_h^{(k)})^n = 0 \\
f_2(\underline{Q},\delta\underline{Q}) &= \sum_{\forall i,j\in 2} K_{ij}\,(\delta_{ij2}\,Q_{ij} + \sum_{h=1}^{NL} \delta_{ijh}\,\delta Q_h^{(k)})^n = 0 \\
&\vdots \qquad\qquad \vdots \qquad\qquad \vdots \\
f_{NL}(\underline{Q},\delta\underline{Q}) &= \sum_{\forall i,j\in NL} K_{ij}\,(\delta_{ijNL}\,Q_{ij} + \sum_{h=1}^{NL} \delta_{ijh}\,\delta Q_h^{(k)})^n = 0
\end{aligned} \tag{73}$$

The Newton-Raphson solution of the non-linear system of NL equations, requires that the following linear system must be solved successively:

$$\begin{bmatrix}
\frac{\partial f_1}{\partial \delta Q_1} & \frac{\partial f_1}{\partial \delta Q_2} & \cdots & \frac{\partial f_1}{\partial \delta Q_{NL}} \\
\frac{\partial f_2}{\partial \delta Q_1} & \frac{\partial f_2}{\partial \delta Q_2} & \cdots & \frac{\partial f_2}{\partial \delta Q_{NL}} \\
\vdots & \vdots & & \vdots \\
\frac{\partial f_{NL}}{\partial \delta Q_1} & \frac{\partial f_{NL}}{\partial \delta Q_2} & \cdots & \frac{\partial f_{NL}}{\partial \delta Q_{NL}}
\end{bmatrix} * \begin{bmatrix} \delta Q_1^{(k)} \\ \delta Q_2^{(k)} \\ \vdots \\ \delta Q_{NL}^{(k)} \end{bmatrix} = \begin{bmatrix} -f_1(\underline{Q},\delta\underline{Q}) \\ -f_2(\underline{Q},\delta\underline{Q}) \\ \vdots \\ -f_{NL}(\underline{Q},\delta\underline{Q}) \end{bmatrix} \tag{74}$$

where all the functions and partial derivatives need to be evaluated at the initial conditions, where $\underline{Q}=\underline{Q}^{(k)}$ and $\delta\underline{Q}=\underline{0}$, since

the initial solution is balanced.

The partial derivatives, evaluated for the initial conditions, can be computed directly from (73):

$$\frac{\partial f_l}{\partial \delta Q_l} = + \sum_{\forall i,j \in l} n K_{ij} Q_{ij}^{n-1} \qquad \text{for } l=1,2, \ldots, NL \tag{75}$$

$$\frac{\partial f_l}{\partial \delta Q_k} = - \sum_{\substack{\forall i,j \in k \\ \forall i,j \in l}} n K_{ij} Q_{ij}^{n-1} \qquad \text{for } l \neq k \text{ and } l=1,2,\ldots NL \tag{76}$$

Note that the matrix of coefficients is symmetric.

On solving the linear system (74) for $\delta \underline{Q}^{(k)}$, a better approximation for the pipe flows can be computed by:

$$Q_{ij}^{(k+1)} = Q_{ij}^{(k)} + \sum_{h=1}^{NL} \delta_{ijh} \delta Q_h^{(k)} \tag{77}$$

If $Q_{ij}^{(k+1)}$ and $Q_{ij}^{(k)}$ are close enough, say their difference is less than ϵ, a pre-specified accuracy, or if $|\delta \underline{Q}^{(k)}| < \epsilon$, then the procedure can be stopped, otherwise the iteration counter is increased to k+1 and a new $\delta \underline{Q}^{(k)}$ is computed.

As pointed out by Epp and Fowler (1970), the introduction of more than one fixed head source can be performed via the introduction of "pseudo-loops", with a fixed head loss between two nodes. They also gave a procedure for including pumps within this formulation.

I. P. King (1970) compared the results of network analysis carried out both by the loop and nodal methods, obtaining evidence that the loop approach performs better than the nodal approach, in terms of execution time, for small and medium size

problems (less than 200 nodes); the nodal approach was apparently better for larger problems.

Epp and Fowler (1971) recognised the possibility that the loop method may perform better in some problems, while in others, the nodal approach can be the best.

2.3.7. The mesh-nodal approach of Hamam and Brameller (1971).

A rather different approach, in the context of the application of the Newton-Raphson method to network analysis, is the so called "mesh-nodal" approach of Hamam and Brameller (1971), which can be applied to any kind of network: electrical, gas, water or any other fluid.

Before describing the mesh-nodal approach, some additional notation is needed, dealing with the handling of the topology of the network. Also, some graph-theory definitions are introduced.

Following the notation introduced by Todini (1979) and Todini and Pilati (1987), three topological matrices for describing the branch-node and branch-loop connectivity are defined. The branch-to-node incidence matrix for the non-source nodes A_{12}, is a (NPx(NN-NS)) matrix, with only two non-zero elements per row:

$$A_{12}(i,j) = \begin{cases} 1 \text{ if pipe i ends at node j.} \\ -1 \text{ if pipe i starts in node j.} \\ 0 \text{ otherwise} \end{cases} \qquad (78)$$

where NP is the number of branches, NN the number of nodes and NS the number of source nodes. Thus NN-NS represents the number of unknown head nodes.

The branch-to-node incidence matrix for the source nodes A_{10}, is a (NPxNS) matrix, of similar characteristics as to A_{12}:

$$A_{10}(i,j) = \begin{cases} 1 \text{ if pipe i ends at node j.} \\ -1 \text{ if pipe i starts in node j.} \\ 0 \text{ otherwise} \end{cases} \quad (79)$$

The branch-to-loop incidence matrix A_{13} is a (NPxNL) matrix, defined as:

$$A_{13}(i,j) = \begin{cases} 1 \text{ if pipe i flows in the same direction as loop j.} \\ -1 \text{ if pipe i flows in the opposite direction as loop j.} \\ 0 \text{ if pipe i is not in loop j.} \end{cases} \quad (80)$$

where every loop has a pre-defined positive direction, normally the clockwise direction.

In general, the transpose of a topological matrix is denoted by interchanging the sub-indices in the matrices, thus:

$$A_{21} = A_{12}^T \quad (81)$$

$$A_{01} = A_{10}^T \quad (82)$$

$$A_{31} = A_{13}^T \quad (83)$$

With these topological matrices, most of the relationships used in the network analysis problem can be expressed in a simpler manner:

Nodal balance:

$$A_{21}\,\underline{Q} = \underline{q} \quad (84)$$

Pressure drop in a pipe:

$$\underline{h} = A_{12}\,\underline{H} \quad (85)$$

Loop balance:

$$A_{31}\ \underline{h} = \underline{0} \tag{86}$$

The head loss flow relationship in pipes, can also be simplified with matrix notation; thus:

$$h_{ij} = K_{ij}\ Q_{ij}^{n} \tag{87}$$

can be represented as:

$$\underline{h} = A_{11}\ \underline{Q} \tag{88}$$

where:

$$A_{11} = \text{diag}(K_i\ |Q_i|^{n-1}) \quad i=1,2,..,\ NP \tag{89}$$

with K_i and Q_i denoting the resistance and flowrate at pipe "i", respectively. Clearly, A_{11} is a (NPxNP) diagonal matrix, and is a function of the flow (i.e. it is <u>not</u> a topological matrix).

With this notation, the loop balance can re-written, by replacing (85) into (86):

$$A_{31}\ A_{12}\ \underline{H} = \underline{0} \tag{90}$$

An important conclusion can be drawn from the last equation: it is straightforward to prove that equation (90) holds for <u>any</u> piezometric head vector $\underline{H}$, because:

$$A_{31}\ A_{12} = 0 \tag{91}$$

This means, in practice, that the <u>loop balance condition is essentially a topological result</u>, rather than a physical law. Similarly, the following also holds:

$$\left.\begin{aligned} A_{31}\ A_{10} &= 0 \\ A_{21}\ A_{13} &= 0 \\ A_{01}\ A_{13} &= 0 \end{aligned}\right\} \tag{92}$$

Finally, some graph-theory concepts and notation are necessary. In an implicit way, some graph-theory notions have already been

introduced and used , e.g. the concepts of node (vertex), branch (or edge), incidence and indeed the network itself, which is a "graph", i.e. an oriented line diagram, composed of all the branches and nodes.

A "path", will be a sequence of edges which, when followed sequentially, allows us to move from one node to another.

A connected graph will be a graph such that a path exists between every pair of nodes. A subgraph is a subset (edges and vertices) of a graph, and it can be connected or disconnected.

A circuit (or loop) will formally be a subgraph such that there are exactly two different paths joining every pair of vertices in the subgraph.

The "tree" of a connected graph will be any graph fulfilling the following conditions:

a) It is a connected subgraph.

b) It contains <u>all</u> the vertices of the graph.

c) It has no circuits (loops).

As a result of the previous conditions, a tree has exactly one path joining every two vertices. Furthermore, a NN vertices graph defines a tree with only (NN-1) edges on it; this can be proved by induction.

The "co-tree" of a graph is simply the complement of the corresponding tree; thus, if NP is the number of edges and NN the number of vertices, there are NP-(NN-1) edges in the co-tree. In the graph-theory nomenclature, the edges of the tree are referred

to as "branches", and the corresponding edges of the co-tree are known as "chords". Hence, the addition of a chord to a tree produces a circuit. In water distribution networks, we may refer to the links between nodes also as "branches", meaning any kind of physical device connected between two adjacent nodes: pipe, pump, valve, etc. Fig. 2.1. helps to visualise some of the graph-theory concepts already introduced.

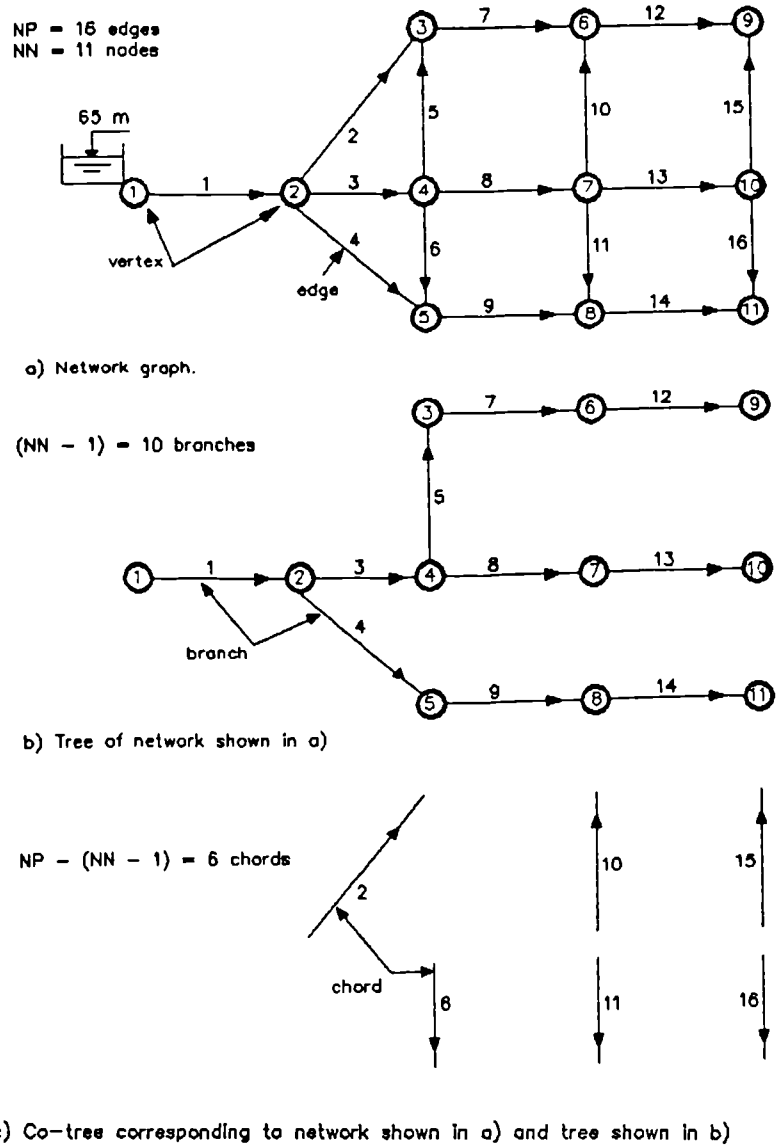

Fig. 2.1. Representation of a network graph and its tree and co-tree.

The concepts of tree and co-tree are relevant to the mesh-nodal approach of Hamam and Brameller (1971), since they allow us to separate the flows in a water network between dependent and independent flows, the independent flows being all the flows corresponding to the co-tree of a network, while the dependent flows correspond to those in the tree. It can be proved that all the dependent flows can be computed directly from the independent ones, via topological considerations only. This means that, in order to know the flow distribution in a network, we only need to specify the values of the independent flows. Thus, we can partition the flow vector $\underline{Q}$ into two sub-vectors, say $\underline{Q}_2$ and $\underline{Q}_3$, the former corresponding to the dependent flows (i.e. flows in the tree) and the latter to the independent flows (i.e. flows in the co-tree). Hence:

$$\underline{Q} = \begin{bmatrix} \underline{Q}_2 \\ \cdots \\ \underline{Q}_3 \end{bmatrix} \begin{array}{l} \text{<-- tree of dependent (NN-NS) flows} \\ \\ \text{<-- co-tree of independent NP-(NN-NS) flows} \end{array} \qquad (93)$$

With the previous definitions, the mesh-nodal approach of Hamam and Brameller (1971) is now introduced.

First of all, the computation of the dependent flows from the independent ones is presented. On introducing the partitioned flow vector (93) into the nodal balance equation (84), we get:

$$A_{21}\ \underline{Q} = A_{21} \begin{bmatrix} \underline{Q}_2 \\ \cdots \\ \underline{Q}_3 \end{bmatrix} = \underline{q} \qquad (94)$$

The matrix A_{21} can be partitioned, accordingly to the dependent/independent flow definition; thus:

$$A_{21} = \left[\begin{array}{c:c} A_{22} & A_{23} \end{array}\right] \tag{95}$$

which, when introduced into (94) gives:

$$\left[\begin{array}{c:c} A_{22} & A_{23} \end{array}\right] \left[\begin{array}{c} \underline{Q}_2 \\ \hdashline \underline{Q}_3 \end{array}\right] = \underline{q} \tag{96}$$

which, on expansion, gives:

$$A_{22}\ \underline{Q}_2 + A_{23}\ \underline{Q}_3 = \underline{q}$$

The dependent flows can be computed from the independent ones, provided that A_{22} is non-singular, as:

$$\boxed{\underline{Q}_2 = [A_{22}]^{-1}\ \underline{q} - [A_{22}]^{-1}\ A_{23}\ \underline{Q}_3} \tag{97}$$

which can be expanded back to:

$$\underline{Q} = \left[\begin{array}{c} \underline{Q}_2 \\ \hdashline \underline{Q}_3 \end{array}\right] = \left[\begin{array}{c} A_{22}^{-1}\ \underline{q} \\ \hdashline 0_3 \end{array}\right] + \left[\begin{array}{c} -A_{22}^{-1}\ A_{23} \\ \hdashline I_3 \end{array}\right] \underline{Q}_3 \tag{98}$$

or, in a more compact way:

$$\underline{Q} = \underline{Q}_a + M_{13}\ \underline{Q}_3 \tag{99}$$

where:

$$\underline{Q}_a = \left[\begin{array}{c} A_{22}^{-1}\ \underline{q} \\ \hdashline 0_3 \end{array}\right] \tag{100}$$

and

$$M_{13} = \left[\begin{array}{c} -\ A_{22}^{-1}\ A_{23} \\ \hdashline I_3 \end{array}\right] \tag{101}$$

To compute M_{13}, it is necessary to go back to the pressure drop equation (85). Noting that A_{12}, the transpose of A_{21}, can be expressed using the partition (95) as:

$$A_{12} = \left[\begin{array}{c} A_{22} \\ \hline A_{32} \end{array}\right] \tag{102}$$

equation (85) becomes:

$$A_{12}\ \underline{H} = \left[\begin{array}{c} A_{22} \\ \hline A_{32} \end{array}\right] \underline{H} = \underline{h} \tag{103}$$

By introducing the corresponding partitioning of the head loss vector, according to the dependent and independent flows:

$$\underline{h} = \left[\begin{array}{c} \underline{h}_2 \\ \hline \underline{h}_3 \end{array}\right] \tag{104}$$

equation (103) can be decomposed as:

$$A_{22}\ \underline{H} = \underline{h}_2 \tag{105}$$

and

$$A_{32}\ \underline{H} = \underline{h}_3 \tag{106}$$

From (105), it is possible to compute $\underline{H}$, provided that A_{22} is non-singular:

$$\underline{H} = A_{22}^{-1}\ \underline{h}_2 \tag{107}$$

which, when introduced into equation (106) gives:

$$A_{32}\ A_{22}^{-1}\ \underline{h}_2 = \underline{h}_3 \tag{108}$$

or, re-arranging:

$$\left[\begin{array}{c:c} -\ A_{32}\ A_{22}^{-1} & I_3 \end{array}\right] \cdot \left[\begin{array}{c} \underline{h}_2 \\ \hline \underline{h}_3 \end{array}\right] = O_3 \tag{109}$$

Equation (109) is indeed the loop equation (86), with:

$$A_{31} = \left[\begin{array}{c:c} -\ A_{32}\ A_{22}^{-1} & I_3 \end{array}\right] \tag{110}$$

Transposing the matrix A_{31} from equation (110):

$$A_{13} = \begin{bmatrix} -A_{22}^{-1} A_{23} \\ \hline I_3 \end{bmatrix} \qquad (111)$$

which shows that matrix M_{13} in equation (99) is exactly the same as A_{13}, and equation (99) can be re-written as:

$$\underline{Q} = \underline{Q}_a + A_{13}\, \underline{Q}_3 \qquad (112)$$

Now, introducing (112) and (88) into the loop equation (86), we get:

$$\boxed{[A_{31}\ A_{11}\ A_{13}]\ \underline{Q}_3 + A_{31}\ A_{11}\ \underline{Q}_a = 0} \qquad (113)$$

This is a non-linear set of equations in $\underline{Q}_3$, the independent (co-tree) NP-(NN-NS) flows, with:

$$\underline{Q}_a = \begin{bmatrix} A_{22}^{-1}\ \underline{q} \\ \hline 0_3 \end{bmatrix} \qquad (114)$$

Equation (113) can be solved iteratively with the Newton-Raphson method by:

$$\underline{Q}_3(k+1) = \underline{Q}_3(k) - J_{33}^{-1}\ \underline{f}(\underline{Q}_3(k)) \qquad (115)$$

where:

$$J_{33} = \left[\ A_{31}\ (N\ A_{11})\ A_{13}\ \right] \qquad (116)$$

with:

N = n I : diagonal matrix with the flow exponent in (87).

and:

$$\underline{f}(\underline{Q}_3(k)) = \left[\ A_{31}\ A_{11}\ A_{13}\ \right]_{\substack{\underline{Q}_3(k) \\ \underline{Q}=\underline{Q}(k)}} + \left[\ A_{31}\ A_{11}\ \underline{Q}_a\ \right]_{\underline{Q}=\underline{Q}(k)} \qquad (117)$$

Equation (115) can be solved numerically as a linear system of equations in $\delta\underline{Q}_3(k) = \underline{Q}_3(k+1) - \underline{Q}_3(k)$:

$$J_{33}\ (\underline{Q}_3(k+1) - \underline{Q}_3(k)) = -\underline{f}(\underline{Q}_3(k)) \qquad (118)$$

or

$$J_{33}\ \delta\underline{Q}_3^{(k)} = -\underline{f}(\underline{Q}_3^{(k)}) \qquad (119)$$

Upon computing $\delta\underline{Q}_3^{(k)}$, $\underline{Q}_3^{(k+1)}$ can be calculated and improved, if necessary, by re-solving (118) until convergence is achieved.

Having $\underline{Q}_3$ (the last $\underline{Q}_3^{(k+1)}$) , equation (97) allows us to compute the dependent flows $\underline{Q}_2$, and the problem is actually solved, since the head losses can be computed with (88) and the piezometric heads can be obtained by considering the head losses accumulated from the sources up to each node.

2.3.8. Other formulations.

The main approaches for the solution of the network analysis problem have been reviewed, based on the nodal and loop equations; both lead to a non-linear system of equations which is solved via the application of the Newton-Raphson algorithm. A number of variations and improvements to these main approaches have been made through the years, some of them are reviewed in the following paragraphs.

Zarghamee (1971), following a nodal approach, presented a Newton-Raphson-based formulation able to handle pumps and pressure reducing valves.

Lam and Wolla (1972a and b), based on previous work by Broyden (1965) on "quasi-Newton methods", proposed an improvement to the Newton-Raphson nodal solution of the network analysis problem, where the the Jacobian matrix (and its inverse) is not explicitly computed, but it is iteratively approximated, thus saving the

time spent in the assembly and inversion of the matrix. Another advantage of this approach, according to Lam and Wolla (1972a), is that the analytic partial derivatives are not needed, which makes things easier from the computational standpoint.

This modified Newton-Raphson method was tested by Lam and Wolla (1972b) although a case (51 branches and 32 nodes) where the method failed to converge was reported. The authors did not provide the corresponding full data set in their paper and attributed the failure to the fact that the initial values of the heads are too far from the final ones.

For the cases where the algorithm may present a low convergence rate, Lam and Wolla (1972b) included a multiplicative relaxation parameter in the correction of the unknown variables, which is computed explicitly via a one-dimensional search.

Another interesting feature of Lam and Wolla's formulation (1972a and b), is that they considered the nodal demands as a general explicit function of the nodal pressures, allowing for a more realistic modelling in this respect, since in practice the consumptions are indeed pressure-dependent.

Lemieux (1972), in applying a relaxation parameter similar to that of Lam and Wolla (1972b), claimed that convergence is always achieved.

Kesavan and Chandrashekar (1972), based on graph-theory concepts, re-formulated the nodal and loop approaches, leading to the corresponding non-linear equations, expressed as a function of topological incidence and loop matrices. Their derivation is

independent of the numerical method used to solve the non-linear systems. They did not give details on the iterative technique used to solve the non-linear equations, which is said to be based on a graph theory approach.

Donachie (1974), working with a nodal-based Newton-Raphson formulation, found that a simple way of avoiding convergence problems is to halve the correction step (i.e. a relaxation factor of 0.5), when slow convergence has been detected. Additionally, a very simple way of initialising the piezometric heads, without the risk of producing two equal heads, is presented: an arbitrary (reference) head taken as equal for all the nodes is considered, and the initial piezometric head of each node is simply this reference head minus the node number. Finally, Donachie also introduced a systematic procedure for calibrating the network model, we shall return to this in Chapter Six.

By this time, most of the developments of Newton-Raphson-based network analysis algorithms were concentrating on the search for computationally efficient numerical methods, particularly in connection with the solution of the linear system generated by the Newton-Raphson method, since it was recognised as one of the most expensive steps in the overall solution. A wide variety of methods emerged, most of them aimed at finding the numbering system for the nodes (or loops, depending on the approach in use) able to minimise the creation of non-zeros (fill-in) in the Gauss elimination process, thus reducing both the storage and computation time needed. Chandrashekar and Stewart (1975), Shamir

(1974), Chin et al. (1978), Gay et al. (1978), and others, concentrated on this subject.

In the context of efficient linear solvers, a comparison of the performance of the most efficient linear solvers is presented in Chapter Five. Appendix A includes an exhaustive review of sparse techniques, ranging from the simplest to the most sophisticated direct and iterative linear solvers, for the symmetric positive-definite case.

2.4. The linear theory method.

Under this heading, a number of network analysis methods are reviewed. This class of methods was originally devised to solve the non-linearity of the system of equations describing the steady state, without using the Newton-Raphson technique.

The linear theory method was proposed by Wood and Charles (1972), within a loop-based framework, but has evolved recently (Wood, 1981a) to a gradient-based algorithm, thus becoming closer to the Newton-Raphson based family of methods.

2.4.1. Wood and Charles formulation (1972).

The linear theory method was developed by Wood and Charles (1972) as an alternative to a looped Newton-Raphson approach, where a balanced initial flow distribution is needed and where a system of as many non-linear equations as loops has to be solved. Another objective in mind at this time was to overcome the slow convergence which had been detected in some applications of the looped Newton-Raphson method.

In the loop approach, it has been already noted that the problem is to solve the non-linear system generated by the simultaneous fulfilment of flow continuity at the nodes and potential continuity around the loops (or energy paths). This can be expressed as :

$$\sum_{j} Q_{ij} - q_i = 0 \qquad i=1,2,\ldots, \text{NN-NS} \tag{120}$$

and

$$\sum_{\text{loop}} h_{ij} = \sum_{\text{loop}} K_{ij} Q_{ij}^{n} = 0 \quad \text{loop}=1,2,\ldots, \text{NL} \tag{121}$$

The system (120) is an independent system of equations only when the source nodes are excluded, and is linear in $\underline{Q}$. Equation (121) is a non-linear system of NL equations in the flows, where NL is the number of loops (or energy paths).

Equations (120) and (121) constitute a set of NN-NS+NL non-linear equations having as unknowns the flows only. Because the number of unknown flows is exactly NN-NS+NL, the coupled system (120)+(121) is enough to determine the unknown flows. Due to the non-linearity, an iterative procedure is needed.

The main idea behind the linear theory method of Wood and Charles (1972) is remarkably simple, and it can be explained in the following terms. Let us assume that the iterative process required to determine the equilibrium flows generates the sequence of vectors :

$$\underline{Q}^{(o)}, \underline{Q}^{(1)}, \ldots, \underline{Q}^{(k)}, \underline{Q}^{(k+1)} \ldots \tag{122}$$

Then, if the flow sequence is converging, and if $\underline{Q}^{(k)}$ and $\underline{Q}^{(k+1)}$ are the flows at the iterations "k" and "k+1"

respectively, it can be assumed that both are close to the equilibrium flow vector, and that both are very similar. Hence, the non-linear term in equation (121) can be approximated by:

$$Q_{ij}^{n} \approx [Q_{ij}(k)]^{n-1} Q_{ij}(k+1) \qquad (123)$$

which is <u>linear</u> in $Q_{ij}(k+1)$.

Then, equation (121) can be re-written as:

$$\sum_{loop} K_{ij} [Q_{ij}(k)]^{(n-1)} Q_{ij}(k+1) = 0 \qquad loop=1,2,\ldots NL \qquad (124)$$

which can be simplified to:

$$\sum_{loop} K_{ij}(k)\ Q_{ij}(k+1) = 0 \qquad loop=1,2,\ldots, NL \qquad (125)$$

where:

$$K_{ij}(k) = K_{ij}\ \{Q_{ij}(k)\}^{n-1} \qquad (126)$$

Similarly, using the sequence of flow vectors (122), equation (120) can be approximated by:

$$\sum_{j} Q_{ij}(k+1) - q_i = 0 \qquad i=1,2,\ldots, NN\text{-}NS \qquad (127)$$

which, when coupled with (125), generates a system of NN-NS+NL <u>linear</u> equations in $\underline{Q}(k+1)$: the (NN-NS+NL)x1 column vector of approximate flows. Hence,

$$\boxed{\begin{array}{ll} \sum_{j} Q_{ij}(k+1) - q_i = 0 & i=1,2,\ldots, NN\text{-}NS \\ \\ \sum_{loop} K_{ij}(k)\ Q_{ij}(k+1) = 0 & loop=1,2, \ldots, NL \end{array}} \qquad (128)$$

On solving (128) for $\underline{Q}(k+1)$, we can re-compute $K_{ij}(k)$ via equation (126), and improve the approximation of $\underline{Q}$, until a certain convergence criterion is met.

At the beginning of the iterative process (k=0), any imbalanced flow solution $\underline{Q}^{(o)}$ can be used to compute $\underline{K}^{(o)}$, because the upper part of (128) ensures that the next flow approximation will always be balanced. Hence, in this method, an initial balanced flow solution is not needed, though an initial flow estimate closer to the final solution will require less iterations to reach the equilibrium conditions.

To cope with oscillations detected in some cases, Wood and Charles (1972) recommended modifying the flows, prior to the re-evaluation of the new $\underline{K}^{(k+1)}$, using an average of the last and previous flow. Thus, after computing $\underline{Q}^{(k+1)}$, and if convergence has not been achieved, increase the iteration counter k to k+1 and compute:

$$\underline{Q}^{(k)} = \tfrac{1}{2} \left(\underline{Q}^{(k-1)} + \underline{Q}^{(k-2)}\right) \qquad (129)$$

and, then, re-compute:

$$K_{ij}^{(k)} = K_{ij} \{Q_{ij}^{(k)}\}^{(n-1)} \qquad (130)$$

and solve (128) again.

The system of linear equations (128) is <u>not symmetric</u> and, as a result, it is neither possible to take advantage of that feature for storage savings nor from the stability point of view. Pivoting for stability reasons will be necessary when solving the system (128); see Appendix A for details.

It has been argued and recognised [Fietz (1973), and Wood and Charles (1973)], that one of the main disadvantages of the linear theory method is its high storage requirements, in order to store a matrix of the size NP*NP. Although this point is becoming less

important with the advent of bigger and cheaper computer memory, it is a factor to bear in mind when comparing the linear theory method with other methods.

Jeppson and Tavallaee (1975), Jeppson and Davis (1976) and Jeppson (1976), have shown how to handle pumps, multiple reservoirs and pressure reducing valves within the framework of the linear theory method.

Collins (1980) demonstrated, with a very simple example, that the linear theory method of Wood and Charles (1972) is inherently unstable when the head loss/flow relationship is exactly quadratic (n=2), where the method oscillates indefinitely between two values. Unfortunately, the head loss/flow relationship is close to quadratic for the Hazen-Williams equation (n=1.85), and exactly quadratic for the Darcy-Weisbach equation. The flow averaging procedure of equation (129) attempts to solve the stability problems, but there is no guarantee of success.

2.4.2. Nodal formulation of Isaacs and Mills (1980).

Following the initial success of the original loop-based linear theory method of Wood and Charles (1972), Isaacs and Mills (1980) presented the corresponding nodal-based version of the method.

The motivation for a nodal formulation of the linear theory method is that, when multiple fixed head sources (reservoirs) are available, an algorithm with the heads as unknowns should be more efficient. Also, a symmetrical and more storage-efficient version is highly desirable.

The rationale behind Isaacs and Mills' linear theory method is similar to that of Wood and Charles (1972). Thus, if the head loss/flow relationship for a pipe joining nodes "i" and "j" is expressed as:

$$H_i - H_j = K_{ij} |Q_{ij}|^{n-1} Q_{ij} \qquad (131)$$

and, if the node continuity equation for node "i" is written as:

$$\sum_j Q_{ij} - q_i = 0 \qquad i=1,2,\ldots, \text{NN-NS} \qquad (132)$$

and if it is assumed that the iterative procedure produces a sequence of successive flows converging to the equilibrium conditions:

$$\underline{Q}^{(o)}, \underline{Q}^{(1)}, \ldots, \underline{Q}^{(k)}, \underline{Q}^{(k+1)} \ldots \qquad (133)$$

then, near the equilibrium conditions, $\underline{Q}^{(k)}$ and $\underline{Q}^{(k+1)}$ will be very similar and, consequently, equation (131) can be approximated as:

$$Q_{ij}^{(k+1)} |Q_{ij}^{(k)}|^{n-1} = (1/K_{ij}) [H_i^{(k+1)} - H_j^{(k+1)}] \qquad (134)$$

or,

$$Q_{ij}^{(k+1)} = C_{ij}^{(k)} [H_i^{(k+1)} - H_j^{(k+1)}] \qquad (135)$$

with

$$C_{ij}^{(k)} = 1/ (K_{ij} |Q_{ij}^{(k)}|^{n-1}) \qquad (136)$$

Similarly, equation (132) can be approximated as:

$$\sum Q_{ij}^{(k+1)} - q_i = 0 \qquad i=1,2,.. \text{ NN-NS} \qquad (137)$$

Equation (135) can be introduced into the nodal balance (equation 137), obtaining:

$$\boxed{\sum_j C_{ij}^{(k)} [H_i^{(k+1)} - H_j^{(k+1)}] = q_i \quad i=1,2,\ldots \text{ NN-NS}} \qquad (138)$$

which is a system of NN-NS linear equations in the NN-NS unknown heads $\underline{H}^{(k+1)}$. The matrix of coefficients is now

symmetric, and appropriate storage handling can reduce considerably the storage requirements; from the stability viewpoint, the solution of the linear system (138) does not require pivoting.

For updating the flows at each stage, Isaacs and Mills (1980) proposed the following method:

a) Compute:

$$Q_{ij}^* = \frac{[H_i^{(k+1)} - H_j^{(k+1)}]}{K_{ij} |Q_{ij}^{(k)}|^{n-1}} \qquad (139)$$

Having computed $\underline{H}^{(k+1)}$ from (138), Q_{ij}^* should be fulfilling the nodal balance condition (137).

b) Average Q_{ij}^* with the previous flow to obtain the new updated flow:

$$Q_{ij}^{(k+1)} = \tfrac{1}{2} (Q_{ij}^* + Q_{ij}^{(k)}) \qquad (140)$$

According to Isaacs and Mills (1980) this flow updating procedure is computationally efficient and guarantees that continuity is always maintained, provided that $\underline{Q}^{(k)}$ fulfils the continuity condition .

Once $\underline{Q}^{(k+1)}$ has been obtained, a pre-established convergence criterion will stop the iterations, or else we shall need to update the iteration counter k, and go back to equation (136) and to the solution of the linear system (138). The algorithm does not need an initially balanced solution, though a sensible starting point will reduce the number of iterations required to reach the final solution.

As it can be easily seen from equations (136) and (139), the

presence of nearly zero flows will produce unbounded values, and the collapse of the algorithm. The removal of the pipes corresponding to very low flows is recommended by Isaacs and Mills (1980) as the solution for such a problem.

According to Isaacs and Mills (1980), the nodal version of the linear theory method requires less iterations than the original linear theory algorithm of Wood and Charles (1972).

Wood (1981b) points out that, from the convergence rate viewpoint, the methods based on heads are known to be less reliable than the flow-based methods, and reports that a new version of his original linear theory method [Wood and Charles (1972)], now based on a gradient approach, has much improved performance.

2.4.3. The gradient-based formulation of Wood (1981).

Wood (1981a), in an extensive comparison between different network analysis solvers, presented a modified version of his original linear theory method (Wood and Charles, 1972), the main difference being the way in which the linearization is carried out. The non-linear equations are now linearized using a gradient concept, as follows.

The non-linear head loss/flow relationship for pipes is:

$$h_{ij} = h(Q_{ij}) = K_{ij}\, Q_{ij}^{n} \qquad (141)$$

In an iterative process, for a flow $Q_{ij}^{(k)}$ at step "k", the summation of the head losses through any energy path, must be equal to the known piezometric head difference between the

initial and final nodes: δE_l. A loop is simply a path where initial and final nodes coincide (i.e. $\delta E_l = 0$).

The fact that the loop balance is not exactly met, means that:

$$\sum_{l} h(Q^{(k)}) = \sum_{l} K_{ij} [Q_{ij}^{(k)}]^n \neq \delta E_l \qquad l=1,2,\ldots, NL \tag{142}$$

where the summation is carried out over all the NL loops (or "energy paths") in the network.

The aim is to determine a pipe flow correction such that:

$$Q_{ij}^{(k+1)} = Q_{ij}^{(k)} + \delta Q_{ij}^{(k)} \tag{143}$$

or simply

$$\underline{Q}^{(k+1)} = \underline{Q}^{(k)} + \delta \underline{Q}^{(k)} \tag{144}$$

The condition to find $\delta \underline{Q}^{(k)}$ is that:

$$\sum_{l} h(\underline{Q}^{(k+1)}) = \delta E_l \qquad l=1,2,\ldots,NL \tag{145}$$

This means that to find an approximation to $\delta \underline{Q}^{(k)}$, we must expand (141) using Taylor's series and drop the second and higher order terms:

$$h(\underline{Q}^{(k+1)}) \approx h(\underline{Q}^{(k)}) + \left[\frac{\partial h}{\partial Q}\right]_{\underline{Q}=\underline{Q}^{(k)}} (\underline{Q}^{(k+1)} - \underline{Q}^{(k)}) \tag{146}$$

and, on imposing the loop-balance condition:

$$\sum_{l} h(\underline{Q}^{(k+1)}) \approx \sum_{l} h(\underline{Q}^{(k)}) + \sum_{l} \left[\frac{\partial h}{\partial Q}\right]_{\underline{Q}=\underline{Q}^{(k)}} (\underline{Q}^{(k+1)} - \underline{Q}^{(k)}) = \delta E_l \qquad l=1,2,\ldots NL \tag{147}$$

Note that in (147) the flow correction $\delta \underline{Q}^{(k)}$ is not explicitly computed and the unknown flows are calculated instead. Re-

ordering (147) leads to:

$$\sum_{1}\left[\frac{\partial h}{\partial Q}\right]_{\underline{Q}=\underline{Q}(k)} \underline{Q}^{(k+1)} = \sum_{1}\left\{\left[\frac{\partial h}{\partial Q}\right]_{\underline{Q}=\underline{Q}(k)} \underline{Q}^{(k)} - h(\underline{Q}^{(k)})\right\} + \delta E_1 \qquad (148)$$

$$1=1,2,\ldots\ NL$$

which represents a linear system of NL equations in NP unknowns.

To determine the whole set of unknown flows, the nodal balance equations need to be added:

$$\sum_{j} Q_{ij}^{(k+1)} - q_i = 0 \quad \forall i=1,2,\ldots,\ NN-NS \qquad (149)$$

which, when coupled with (148), constitutes the new linear system of equations in $\underline{Q}^{(k+1)}$:

$$\sum_{j} Q_{ij}^{(k+1)} - q_i = 0 \qquad i=1,2,\ldots,\ NN-NS$$

$$\sum_{1}\left[\frac{\partial h}{\partial Q}\right]_{\underline{Q}=\underline{Q}(k)} \underline{Q}^{(k+1)} = \sum_{1}\left\{\left[\frac{\partial h}{\partial Q}\right]_{\underline{Q}=\underline{Q}(k)} \underline{Q}^{(k)} - h(\underline{Q}^{(k)})\right\} + \delta E_1 \qquad (150)$$

$$1=1,2,\ldots\ NL$$

The linear system (150) replaces the previous linear system (128) and, due to its stability characteristics, there is no need for averaging the new flows with those of the previous stage.

Wood (1981a) pointed out that the new gradient-based method has a superior convergence rate than the original linear theory method of Wood and Charles (1972). Basically, this gradient-based algorithm is applying the Newton-Raphson method to the non-linear set of NN-NS+NL equations formed by coupling (145) and (149) and, hence, it is actually closer to the methods reviewed in the previous section 2.3.

By this time (1981), the linear theory method had a reputation as an efficient network analysis solver, mainly due to its simplicity, and the move towards the gradient-based algorithm improved its convergence.

2.5. Other approaches.

So far, we have reviewed most of the water distribution analysis methods which are relevant from the practical point of view.

Other methods have been developed as a result of the active research carried out in this field during the last decade, but they have not been widely used. Only for the sake of completeness, we shall mention some of these methods here.

2.5.1. Optimisation-based methods.

Collins et al. (1978) presented a completely different approach to the solution of the network analysis problem, formulating it within a non-linear optimisation framework. They presented two alternative formulations of the non-linear problem, one minimising a "content" function, which is in essence the expression of the power dissipation within the network, subjected to the nodal balance equations as equality constraints. The second alternative formulation consisted of minimising the "co-content", which is the dual of the "content".

The work by Collins et al. (1977, 1978 and 1979) is relevant from the theoretical point of view, since it goes back to the

fundamentals of the network analysis problem. From the practical point of view, the approach has a number of shortcomings when compared with the traditional methods; for example, it is difficult to understand for the practitioner, and it is computer intensive. We believe that this is quite a good idea to go back to the basics, but this should ultimately lead to a set of equations, or "method", easier to solve and be understood by people working in the water industry, rather than in the academic environment.

Hall (1976) presents a minimization approach to the network analysis problem, based on (generalised) geometric programming. Carpentier et al. (1985) interpret most of the network analysis methods within an optimisation approach.

2.5.2. Methods based on unsteady state analysis.

The steady state condition can be interpreted as the equilibrium reached by the unsteady state phenomenon, after a period of time. Thus, in principle, any unsteady state analysis method can be used to determine the steady state condition, provided that sufficient time is given to stabilise the flow.

Nahavandi and Catanzaro (1973), and Fox and Keech (1975), amongst others, present unsteady state methods and apply them to solve the steady state problem for pipe networks.

We believe that this is not the best way to approach the steady state network analysis problem, since the traditional methods are far more straightforward, demanding in general less computational resources. This transient approach seems to be only a by-product of the unsteady state flow analysis. It seems that this kind of

technique.. should be used only in situations where slow or fast transient phenomena are the dominant ones.

2.5.3. A method based on a finite element approach.

Collins and Johnson (1975), using an analogy between structural and pipe systems, and taking advantage of the power of existing finite element packages to solve large linear systems of equations, proposed a solution to the network analysis problem via the finite element approach. In so doing, they used a linearized flow/head loss relationship, which is updated iteratively to approximate the real non-linear equation. The linearized flow/head loss relationship is coupled with the nodal balance equations, considered as boundary conditions in the finite element terminology, and a system of linear equations is assembled and solved. Collins and Johnson (1975) compared the performance of this method with a Cross nodal algorithm, reporting a faster convergence for their method.

We are not aware of wider testing and/or use of this approach.

2.5.4. The gradient method of Todini (1979).

Todini (1979) posed the problem of finding the steady state solution flow of a water distribution network as the minimization of the power dissipated within the network, subject to the nodal balance condition as an equality constraint. This can be formally expressed, with the matrix notation already introduced in section (2.3.7), as:

$$\min P(\underline{Q}) = (A_{11}\underline{Q})^T \underline{Q} \qquad (151)$$

subject to $A_{21}\underline{Q} = \underline{q}$ (152)

where:

$$A_{11} = \begin{bmatrix} \alpha_1|Q_1|^{n-1} & & & \\ & \alpha_2|Q_2|^{n-1} & & \\ & & \ddots & \\ & & & \alpha_{NP}|Q_{NP}|^{n-1} \end{bmatrix} \quad (153)$$

with α_i equal to the pipe resistance characteristic parameter, which depends on the formula and units being used.

Upon transforming the constrained minimization problem into an unconstrained one, via the Lagrange multipliers technique, Todini (1979) found that the necessary conditions for the steady state flow in the network are represented by the simultaneous fulfilment of the nodal balance and the non-linear head loss/flow relationship for each pipe, which can be expressed in the compact form:

$$\left[\begin{array}{c:c} A_{11} & A_{12} \\ \hdashline A_{21} & 0 \end{array}\right] * \begin{bmatrix} \underline{Q} \\ \hline \underline{H} \end{bmatrix} = \begin{bmatrix} \underline{Q} \\ \hline \underline{q} \end{bmatrix} \quad (154)$$

The upper part of (154) represents the head loss/flow relationship for each one of the pipes in the network, which is clearly a non-linear function of the flows $\underline{Q}$, while the lower part of (154) represents the nodal flow balance condition. In his original formulation Todini (1979) considered one source node only, and in that case the nodal balance condition is redundant for that particular node (reference node) and its balance equation can be omitted; then, the lower part of (154) is a

system of NN-1 independent linear equations in the flows $\underline{Q}$.

Contrary to what most of the authors in network analysis have done, Todini (1979) did not attempt to reduce the dimensionality of the non-linear problem (154), and he kept the augmented vector $(\underline{Q} \mid \underline{H})^T$ as the unknown state vector.

Because of the non-linearity of (154), a direct solution is not possible and an iterative approach is needed. Todini (1979) thought of the system (154) as the non-linear system formed by two sub-systems of imbalance functions:

$$\left.\begin{array}{l} \underline{E}(\underline{Q},\underline{H}) = \underline{0} \\ \ldots\ldots\ldots\ldots \\ \underline{q}(\underline{Q},\underline{H}) = \underline{0} \end{array}\right| \qquad (155)$$

where $\underline{E}(\underline{Q},\underline{H})$ is the head loss imbalance function for each pipe [the upper part of (154)]:

$$\underline{E}(\underline{Q},\underline{H}) = A_{11}\,\underline{Q} + A_{12}\,\underline{H} = \underline{0} \qquad (156)$$

and

$$\underline{q}(\underline{Q},\underline{H}) = A_{21}\,\underline{Q} - \underline{q} = \underline{0} \qquad (157)$$

is the lower part of (154) and represents the nodal flow imbalance function.

In an iterative procedure for the solution of the non-linear system (154) or (155), at an iteration "i", the functions (156) and (157) will not be exactly zero, this means that, if $\underline{Q}^{(i)}$ and $\underline{H}^{(i)}$ are the flow and piezometric head vectors at iteration "i", then:

$$\delta\underline{E}^{(i)} = A_{11}\,\underline{Q}^{(i)} + A_{12}\,\underline{H}^{(i)} \neq \underline{0} \qquad (158)$$

and

$$\delta\underline{q}^{(i)} = A_{21}\,\underline{Q}^{(i)} - \underline{q} \neq \underline{0} \qquad (159)$$

where:

$\delta \underline{E}^{(i)}$: head loss imbalance per pipe at iteration "i".

$\delta \underline{q}^{(i)}$: nodal flow imbalance at iteration "i".

Because the analytic expressions of the imbalance functions are known [equation (156) and (157)], it is possible to compute the head loss and nodal flow imbalances via their respective total differentials, indeed, on differentiating (156) and (157):

$$d\underline{E} = n\, A_{11}\, d\underline{Q} + A_{12}\, d\underline{H} \tag{160}$$

and

$$d\underline{q} = A_{21}\, d\underline{Q} \tag{161}$$

then, on approximating $d\underline{Q}$ and $d\underline{H}$ as the finite difference between two successive flows and heads in the iterative process:

$$d\,\underline{Q} = \underline{Q}^{(i)} - \underline{Q}^{(i+1)} \tag{162}$$

and

$$d\,\underline{H} = \underline{H}^{(i)} - \underline{H}^{(i+1)} \tag{163}$$

and approximating the imbalances by the total differentials:

$$\delta \underline{E}^{(i)} \approx d\underline{E} \tag{164}$$

and

$$\delta \underline{q}^{(i)} \approx d\underline{q} \tag{165}$$

Then, starting with a certain initial augmented state vector $(\underline{Q}^{(o)}, \underline{H}^{(o)})$ the head loss and nodal flow imbalances can be computed through (158) and (159), respectively, and the new augmented state vector $(\underline{Q}^{(i+1)}, \underline{H}^{(i+1)})$ can be updated applying (160) and (161), followed by (162) and (163), recursively, until a certain convergence criterion is met.

This is the mathematical foundation of the original Todini's gradient method. To obtain the recursive numerical algorithm, Todini (1979) followed a matrix-intensive algebraic approach

which is presented below. An alternative derivation is proposed after Todini's derivation, which may be easier to follow.

a) Todini's (1979) derivation of the recursive numerical scheme:

On differentiating the non-linear system of equations (154) the equations (160) and (161) were obtained, these equations can be represented in a more compact way as:

$$\left[\begin{array}{c|c} n\ A_{11} & A_{12} \\ \hline A_{21} & 0 \end{array}\right] * \left[\begin{array}{c} d\ \underline{Q} \\ \hline d\ \underline{H} \end{array}\right] = \left[\begin{array}{c} d\ \underline{E} \\ \hline d\ \underline{q} \end{array}\right] \qquad (166)$$

where the right-hand-side vector represents the head loss and nodal flow imbalances which, in an iterative scheme, can be approximated by the equations (158) and (159), i.e.:

$$d\underline{E} = A_{11}\ \underline{Q}^{(i)} + A_{12}\ \underline{H}^{(i)} \qquad (167)$$

and

$$d\underline{q} = A_{21}\ \underline{Q}^{(i)} - \underline{q} \qquad (168)$$

The problem now consists in computing the differentials $d\underline{Q}$ and $d\underline{H}$ [in equation (166)] which, in the iterative scheme, represent the corrections to be applied to the current approximates $\underline{Q}^{(i)}$ and $\underline{H}^{(i)}$ in order to improve them towards the solution. The computation of $d\underline{Q}$ and $d\underline{H}$ is done analytically by Todini (1979):

$$\left[\begin{array}{c} d\ \underline{Q} \\ \hline d\ \underline{H} \end{array}\right] = \left[\begin{array}{c|c} n\ A_{11} & A_{12} \\ \hline A_{21} & 0 \end{array}\right]^{-1} * \left[\begin{array}{c} d\ \underline{E} \\ \hline d\ \underline{q} \end{array}\right] \qquad (169)$$

where A_{11} is computed with the current flow $\underline{Q}=\underline{Q}^{(i)}$.

The inversion of the partitioned matrix in (169) can be carried out explicitly, as another block-partitioned matrix:

$$\left[\begin{array}{c|c} n\,A_{11} & A_{12} \\ \hline A_{21} & 0 \end{array}\right]^{-1} = \left[\begin{array}{c|c} B_{11} & B_{12} \\ \hline B_{21} & B_{22} \end{array}\right] \qquad (170)$$

According to Ayres (1974), the partitioned matrices B_{ij} can be computed as shown below. Note that A_{12} and A_{21} are not square matrices.

$$\left.\begin{aligned} B_{11} &= (1/n)[A_{11}^{-1} - A_{11}^{-1}\,A_{12}\,(A_{21}\,A_{11}^{-1}\,A_{12})^{-1}\,A_{21}\,A_{11}^{-1}] \\ B_{22} &= -\,n(A_{21}\,A_{11}^{-1}\,A_{12})^{-1} \\ B_{12} &= A_{11}^{-1}\,A_{12}\,(A_{21}\,A_{11}^{-1}\,A_{12})^{-1} \\ B_{21} &= (A_{21}\,A_{11}^{-1}\,A_{12})^{-1}\,A_{21}\,A_{11}^{-1} \end{aligned}\right\} \qquad (171)$$

On introducing (171) + (170) and (167) + (168) into (169) the following is obtained:

$$d\underline{Q} = (1/n)[A_{11}^{-1} - A_{11}^{-1}A_{12}(A_{21}A_{11}^{-1}A_{12})^{-1}A_{21}A_{11}^{-1}](A_{11}\underline{Q}^{(i)} + A_{12}\underline{H}^{(i)}) + \\ + A_{11}^{-1}A_{12}(A_{21}A_{11}^{-1}A_{12})^{-1}(A_{21}\underline{Q}^{(i)} - \underline{q}) \qquad (172)$$

and

$$d\underline{H} = (A_{21}\,A_{11}^{-1}\,A_{12})^{-1}\,A_{21}\,A_{11}^{-1}(\,A_{11}\,\underline{Q}^{(i)} + A_{12}\,\underline{H}^{(i)}) - \\ - n\,(A_{21}\,A_{11}^{-1}\,A_{12})^{-1}\,(\,A_{21}\,\underline{Q}^{(i)} - \underline{q}\,) \qquad (173)$$

Assuming that a balanced flow solution $\underline{Q}^{(i)}$ is available, i.e.:

$$A_{21}\,\underline{Q}^{(i)} - \underline{q} \qquad (174)$$

then, the equations (172) and (173) simplify to:

$$d\,\underline{Q} = (1/n)[\,\underline{Q}^{(i)} - A_{11}^{-1}A_{12}\,(A_{21}\,G^{-1}A_{12}]^{-1})\,\underline{q}\,] \qquad (175)$$

and

$$d\,\underline{H} = \underline{H}^{(i)} + (A_{21}\,A_{11}^{-1}\,A_{12})^{-1}\,\underline{q}\,) \qquad (176)$$

which, when considering (162) and (163), allow us to compute the flow and head updates:

$$\boxed{\underline{H}^{(i+1)} = -[A_{21}\,A_{11}^{-1}\,A_{12}]^{-1}\,\underline{q}} \qquad (177)$$

and

$$\boxed{\underline{Q}^{(i+1)} = \{(n-1)/n\}\ \underline{Q}^{(i)} - (1/n)\ A_{11}^{-1}\ A_{12}\ \underline{H}^{(i+1)}} \qquad (178)$$

Thus, starting from some initial solution ($\underline{Q}^{(o)}$, $\underline{H}^{(o)}$), the recursive application of (177) and (178) allows us to update the augmented state vector, generating a sequence of flow and head vectors converging towards the steady state solution of the network.

Equation (177) represents a linear system of NN-1 equations in the unknown piezometric heads $\underline{H}^{(i+1)}$, which Todini (1979) solved using the conjugate gradient method.

Equation (178) allows the automatic generation of an initial flow solution. To do so, the flow exponent "n" is set to 1 in the first iteration, which leads to the following balanced flow :

$$\underline{Q}^{(o)} = -\ A_{11}^{-1}\ A_{12}\ \underline{H}^{(o)} \qquad (179)$$

<u>b) Alternative derivation of Todini's gradient algorithm</u>:

Introducing equations (162) and (163) into (160) and (161), the head loss and nodal flow imbalances can be computed as:

$$d\underline{E} = n\ A_{11}\ \underline{Q}^{(i)} - n\ A_{11}\ \underline{Q}^{(i+1)} + A_{12}\ \underline{H}^{(i)} - A_{12}\ \underline{H}^{(i+1)} \qquad (180)$$

and

$$d\underline{q} = A_{21}\ \underline{Q}^{(i)} - A_{21}\ \underline{Q}^{(i+1)} \qquad (181)$$

Replacing $\underline{H}^{(i)}$ and $\underline{Q}^{(i)}$ in (180) and (181) by their corresponding values computed from the imbalances defined by (158) and (159), and after reordering:

$$d\underline{E} = \delta\underline{E}^{(i)} - (1-n)\ A_{11}\ \underline{Q}^{(i)} - [n\ A_{11}\ \underline{Q}^{(i+1)} + A_{12}\ \underline{H}^{(i+1)}\ ] \qquad (182)$$

and

$$d\underline{q} = \delta\underline{q}^{(i)} + \underline{q} - A_{21}\,\underline{Q}^{(i+1)} \tag{183}$$

Then, on assuming (164) and (165), from (183):

$$A_{21}\,\underline{Q}^{(i+1)} = \underline{q} \tag{184}$$

which implies that the new flow is balanced.

And from (182):

$$(1-n)\,A_{11}\,\underline{Q}^{(i)} + n\,A_{11}\,\underline{Q}^{(i+1)} + A_{12}\,\underline{H}^{(i+1)} = 0 \tag{185}$$

Pre-multiplying equation (185) by $(n\,A_{11})^{-1}$:

$$\{(1-n)/n\}\,\underline{Q}^{(i)} + \underline{Q}^{(i+1)} + (n\,A_{11})^{-1}\,A_{12}\,\underline{H}^{(i+1)} = 0 \tag{186}$$

and pre-multiplying (186) by A_{21}:

$$\{(1-n)/n\}A_{21}\underline{Q}^{(i)} + A_{21}\underline{Q}^{(i+1)} + A_{21}(n\,A_{11})^{-1}A_{12}\underline{H}^{(i+1)} = 0 \tag{187}$$

Upon introducing (184) and assuming that the current flow vector is balanced (i.e. $A_{21}\,\underline{Q}^{(i)} = \underline{q}$), equation (187) simplifies to:

$$\boxed{[A_{21}\,A_{11}^{-1}\,A_{12}]\,\underline{H}^{(i+1)} = -\,\underline{q}} \tag{188}$$

which is the same as equation (177).

The flow updates are obtained from (186):

$$\boxed{\underline{Q}^{(i+1)} = \{(n-1)/n\}\,\underline{Q}^{(i)} - (n\,A_{11})^{-1}\,A_{12}\,\underline{H}^{(i+1)}} \tag{189}$$

which is the same as equation (178).

2.6. Comparison of the performance of some of the existing methods: need for a more reliable algorithm.

Despite the fact that a number of convergence problems have been reported for almost every single algorithm already reviewed, only a few attempts to compare most of these algorithms in a systematic way have been reported; these are the study carried out by Wood (1981a) and a comparison performed by Carpentier et al. (1985), which are complementary. We do not attempt here to make a full comparison, but only to review the results already published to draw some preliminary conclusions, which may allow us to narrow the search for an efficient and stable network analysis solver. A comparison between some of the most promising algorithms and our proposed gradient method is delayed until the end of the next chapter.

The comparison carried out by Wood (1981a) considered five different methods: the loop and nodal Cross' methods (single path and single node adjustment methods in Wood's terminology), the nodal and loop Newton-Raphson approaches (simultaneous node and simultaneous path adjustment methods in Wood's terminology) and the gradient version of the linear theory method.

Wood and his collaborators at the University of Kentucky prepared FORTRAN programs for all the five methods compared, so that the computer codes used were similar from the programming point of view. All the programs were designed to work with the minimum required amount of data (basic branch to node connectivity data), assembling the equations and generating the initial conditions internally within the programs. Sparse

techniques for matrix manipulation were used in all the programs.

A set of test examples was assembled, with 30 systems of under 100 pipes and 21 systems with more than 100 pipes. Changes in the data (diameter, roughness, or length) allowed the researchers to generate two extended sets of test examples of 60 and 31 cases, for networks with less and more than 100 pipes, respectively.

A detailed comparison of the performance of the different methods was carried out for all the systems with less than 100 pipes. All the cases where convergence to a pre-specified accuracy was not achieved, within a fixed number of iterations, were labelled as failures and their occurrence is summarised in Table 2.1.

The only failure found with the simultaneous path method consisted of a case where a pump operating with a steep

Table 2.1. Results of the comparison of 60 small water distribution networks (less than 100 pipes), from Wood (1981a).

Network analysis method	Failures
Single path adjustment (looped Cross method)	8
Single node adjustment (nodal Cross method)	51
Simultaneous path adjust. (looped Newton-Raphson)	1
Simultaneous node adjust. (nodal Newton-Raphson)	18
Linear theory method (gradient version)	0

characteristic curve was considered. No failure whatsoever was detected with the linear theory method.

In view of the previous results, the systematic comparison for larger networks was limited to the simultaneous path and linear theory methods only, and in all the 31 cases tested both methods managed to converge within a pre-established number of iterations. Although a systematic comparison for the single path, single node and simultaneous node adjustment methods was not carried out for the larger networks, a number of failures was found for these methods, confirming their exclusion from the systematic comparison.

The main conclusions of the Wood (1981a) study, also published by Wood and Rayes (1981), can be summarised as follows:

a) The single path, single node and simultaneous node adjustment methods failed to converge in a number of cases and, as a result, they are not recommended for water distribution network analysis, unless they are used for known well-conditioned problems. Convergence problems related to the nodal Newton-Raphson method have also been reported by de Neufville and Hester (1969).

b) Although no guarantee of convergence can be given, the simultaneous path adjustment (looped Newton-Raphson) and linear theory method (gradient version) exhibit excellent convergence behaviour. Only in one very special case did the simultaneous path adjustment method fail to converge. Both methods are recommended by Wood (1981a) for the analysis of water distribution networks.

c) The computational costs of the simultaneous path adjustment and linear theory methods are very similar. Average run-times of 5.4 and 6.9 sec. were found in the case of the larger networks, for the linear theory and simultaneous path adjustment methods, respectively. Thus, the linear theory method needs 78% of the time required by the simultaneous path method.

It should be remembered that the storage requirements of the simultaneous path adjustment method are smaller than that required by the linear theory method, since, in the former, a symmetric matrix is obtained, while, in the latter, we get a non-symmetric one. This parameter was not included in Wood's (1981a) comparison.

Focusing on the difference between the simultaneous path and linear theory method, we have to bear in mind that both methods were not starting from exactly the same initial solution. A balanced initial flow distribution was produced by the simultaneous path program, while a flow distribution computed on the basis of a uniform velocity of 4 fps. was used in the linear theory program. Hence, the results of the relative performances of the simultaneous path and the linear theory methods may be different, if both programs are started exactly at the same initial solution.

Carpentier et al. (1985) presented a numerical comparison of some of the network analysis methods: looped Cross method, looped Newton-Raphson, nodal Newton-Raphson and the hybrid mesh-nodal method of Hamam and Brameller (1971). They also looked at all these methods from a mathematical programming perspective, in

order to establish some theoretical differences.

Although the three examples of Carpentier et al. (1985) are very limited in comparison with those used in the study carried out by Wood (1981a), some interesting conclusions can be drawn, particularly in connection with the mesh-nodal method. Only three methods were found to exhibit an adequate convergence, the Cross looped method and a quasi-Newton implementation showing very low convergence. The results for those best performing methods are shown in Table 2.2.

Unfortunately, Carpentier et al. (1985) did not give any information about the initial solution (heads and flows) with which the different programs were run.

Table 2.2. Comparison of network analysis methods in terms of global and relative CPU times, and number of iterations, from Carpentier et al. (1985).

Global and relative CPU times (sec.), No. of iterations			
M E T H O D	NETWORK CHARACTERISTICS		
	46 pipes 40 nodes 10 loops	212 pipes 148 nodes 70 loops	443 pipes 297 nodes 157 loops
Looped Newton-Raphson	2.00 sec. (1.00)* 5 iter.	18.00 sec. (1.00) 7 iter.	63.90 sec. (1.00) 8 iter.
Nodal Newton-Raphson	1.15 sec. (0.58)* 10 iter.	5.70 sec. (0.32) 13 iter.	13.00 sec. (0.20) 14 iter.
Mesh-nodal	0.76 sec. (0.38)* 5 iter.	3.80 sec. (0.21) 7 iter.	8.40 sec. (0.13) 7 iter.
(*) In parenthesis is the relative performance: ratio with respect to the Looped Newton-Raphson, for the same example.			

The main conclusions that can be drawn from the comparison by Carpentier et al. (1985) are the following:

a) The mesh-nodal method of Hamam and Brameller (1971) appears to be the most efficient one in terms of global CPU time. It is also the best in terms of CPU time for initialisation (not shown in Table 2.2).

It is interesting to note that when the mesh-nodal method is compared with the looped Newton-Raphson method, as Wood (1981a) did with his linear theory method, the mesh-nodal method requires 38% of the CPU time needed for the looped Newton-Raphson for networks with less than 100 pipes (see Table 2.2), whereas the linear theory method required 78% of CPU time.
Although the programs used were not exactly the same, this appears to suggest that the mesh-nodal performs faster than the linear theory method. The results are even more favourable for the mesh-nodal method when a larger network is considered, reaching 13% for the 443 pipes example (see Table 2.2.).

b) The second conclusion of Carpentier et al. (1985) is concerned with the comparison between the nodal and loop approach. According to these authors, when analysing the continuity and differentiability of the Hessian matrix produced by the different methods (in the mathematical programming framework), the looped (flow) methods seem to be better conditioned than the nodal (head) methods; this coincides with what some authors have previously found. This conclusion is in contradiction with Table 2.2, where the nodal Newton-Raphson

clearly requires less time to converge than the looped Newton-Raphson, although the number of iterations are the other way around. Our explanation of this is as follows.

We can put the problem in simple terms, by observing the way in which the head loss/flow relationship and its derivative is handled in the nodal or looped approach:

Looped methods consider: $h_{ij} = H_i - H_j = K_{ij} Q_{ij}^n$ (190)

Nodal methods consider: $Q_{ij} = R_{ij} (H_i - H_j)^{1/n}$ (191)

Because all the Newton-Raphson methods consider (in one way or another) the derivatives of functions including either h_{ij} or Q_{ij} (looped or nodal methods, respectively), we should analyse the derivatives more carefully:

$$\text{Looped methods} : \frac{\partial h_{ij}}{\partial Q_{ij}} = n K_{ij} Q_{ij}^{n-1} \quad (192)$$

$$\text{Nodal methods} : \frac{\partial Q_{ij}}{\partial H_i} = \frac{1}{n} R_{ij} (H_i - H_j)^{(1-n)/n} \quad (193)$$

which can be re-written as:

$$\frac{\partial Q_{ij}}{\partial H_i} = \frac{R_{ij}}{n (H_i - H_j)^{(n-1)/n}} \quad (194)$$

On comparing (192) and (194), we can easily see that the derivatives needed in the looped (flow) methods are continuous for whatever flow we consider, whereas in the case of the nodal methods, equation (194) "blows up" when H_i is exactly H_j. This would explain why the nodal methods are found to be more trouble-prone than the looped or flow-based methods (see Table 2.1).

The results in terms of global CPU time in Table 2.2 can also be explained in terms of equations (194) and (192). In fact, if both methods are dealing with a convergent problem [i.e. equation (194) is not "blowing up"], the derivatives for the nodal methods [equation (194)] are, in general, "stronger" than those for the looped methods. Indeed, if we think of a typical troublesome case, with a pipe of low head loss (i.e. $H_i \approx H_j$, but not close enough to cancel), the derivatives given by (194) will be quite large and the diagonal terms of the corresponding Jacobian matrix will be even larger, increasing the well-conditioning of the linear system of equations; clearly, for such problems, a nodal-based program will converge faster than a looped program. If we consider another troublesome case, for example a pipe with high resistance (e.g. small diameter), it will produce a "small" derivative in a nodal approach [equation (194)], whilst the corresponding derivative in a looped approach [equation (192)] will tend to zero, since the flow is "small", thus spoiling the conditioning of the loop method. In the latter case, the nodal approach can still manage to converge. This shows clearly that, in some problems, one method can perform better than others, whereas, in other cases, the reverse can be true. This also suggests that, when the nodal methods do converge, they do it faster than the looped (flows) methods, as shown in Table 2.2. This has been corroborated by other authors as well [Collins et al. (1978)].

Looking at equations (194) and (192) from a strictly numerical point of view, the structure of the derivative for the nodal

methods [equation (194)] is the worst we can expect, because it is subjected to cancellation errors and also to unbounded values when the heads H_i and H_j are close enough. Expressions of this kind are normally avoided in numerical analysis [see for example Appendix C, section C.1, when preferring a recursive approach for the evaluation of B-splines, instead of the explicit formula].

In summary, from what we have seen so far in this chapter, it is clear that the methods derived by Cross (loop and nodal methods), are not reliable enough and should not be used in computer-based water distribution network analysis. The same can be said of the nodal Newton-Raphson approach which, as documented by Wood (1981a), fails to converge in a number of cases.

The looped Newton-Raphson method failed to converge in one case in the review carried out by Wood (1981a). Although this method should still be considered as a possible solution scheme, its results should be carefully analysed.

The linear theory method of Wood and Charles (1972) should <u>not</u> be used since, as shown by Collins (1980), its behaviour is inherently unstable for quadratic or nearly quadratic head loss functions. The "tricks" to overcome instabilities, like averaging flows and so on, may work for some cases, but there is no guarantee that they will work in others. Wood himself (1981a) recognised that the improved gradient-based linear theory method has much better convergence properties, although, even in that case, he insisted that no guarantee of convergence could be given.

In the limited comparison carried out by Carpentier et al. (1985), the mesh-nodal approach of Hamam and Brameller (1971) showed some impressive results with respect to the looped and nodal Newton-Raphson methods. These results suggest that the mesh-nodal method should be competitive with the gradient-based linear theory method, although further testing is needed.

As far as the non-traditional methods of network analysis are concerned, such as those based on explicit non-linear optimisation methods, unsteady flow analysis and the finite element method (section 2.5), they do not seem to be relevant from the practical point of view, particularly when the network analysis algorithm has to be linked with design or operational optimisation routines. All the traditional methods reviewed in this chapter are far more straightforward than non-traditional ones.

As a result, there is no conclusive evidence that any of the most promising methods will guarantee a solution to the analysis problem. On top of that, most of the comparisons and systematic testing of the methods have been made considering networks with pipes and pumps (at most), without including other devices like pressure reducing valves, pressure sustaining valves, etc., which will undoubtedly test the different methods to the limit. The ability of the methods to cope with extreme operational situations, like those when the network becomes disconnected, either due to the action of non-return valves or pressure regulating valves, has not been tested in the open literature reviewed so far, and we intend to do so in the following

chapters.

At this stage, there is sufficient evidence to show that the search for efficient network analysis algorithms should be extended even further. Perhaps the issue of the reliability of the methods should be at least as important as the computational efficiency, if it is planned to use the network analysis algorithm for operational or design optimisation routines.

CHAPTER THREE

GENERALISATION OF THE GRADIENT METHOD TO INCLUDE PUMPS

3.1. Introduction.

In the previous chapter most of the traditional methods for network analysis have been introduced, spanning the early work of H. Cross (1936), the application of the Newton-Raphson technique in the sixties and the development of the linear theory method in the seventies.

In this chapter we intend to review some fundamental aspects of steady state flow network analysis, and to explore an alternative formulation, adopted here which is referred to as the gradient method; we extend this method in order to include pumps, using a general head loss/flow model. In the final part of this chapter, we compare the gradient method with other similar techniques and some conclusions are drawn from that comparison.

3.2. Traditional formulation of the network analysis problem.

Most of the traditional methods for water distribution network analysis are based on the two "conditions" specified by H. Cross (1936): flow continuity and potential continuity; the former establishes mass balance at the node level, while the latter has been thought of by some authors as a loop balance condition (algebraic summation of all the head losses round a loop = 0). Other authors think of potential continuity simply as establishing that the piezometric heads at each node are unique.

Indeed, as shown in Chapter Two (Section 2.3.7., equations 90 and 91), the potential continuity condition (loop balance) can be achieved for any set of piezometric heads, and is due to the fact that the product of two topological matrices: the loop to branch matrix A_{31} and the branch to node incidence matrix A_{12} is zero, i.e.

$$A_{31}\ A_{12}\ \underline{H} = \underline{0} \qquad ,\forall\ \underline{H} \tag{1}$$

due to:

$$A_{31}\ A_{12} = 0 \tag{2}$$

Most of the methods of network analysis have been based, either explicitly or implicitly, on the acceptance of the loop balance condition and, in so doing, some of them do not seem to have been based on the fulfilment of what is presented as a physical law, but on a topological property.

As a result, it seems necessary to re-establish which are the physical laws controlling the steady state flow in a water distribution network or, in mathematical terms, which are the necessary and sufficient conditions for the steady state flow in pipe networks. Only a clear understanding of the fundamental principles can lead to the development of a more robust numerical scheme for the network analysis problem.

3.3. Minimum power dissipation formulation: necessary conditions.

Several authors have addressed the problem of establishing the fundamental principles governing the steady state flow in water distribution networks, agreeing in that, apart from the flow continuity law at each node (mass conservation law) , it is a minimum energy dissipation rate principle (minimum dissipated

power) which controls the steady state flow in a water distribution network. Basically, this means that the steady state flow stabilises in a situation wherein a minimum power is required. This "minimum effort" law is common to other physical phenomena of interest in civil engineering. By formalising the minimum power dissipation approach, we can also study the mathematical conditions for the existence and uniqueness of the steady state solution.

Collins et al. (1978, 1979), using previous results by Millar (1951), formulated the steady state flow analysis, both of pipe and channel networks, within a minimisation context. They minimised a "content" function, which is basically the power dissipated within the system, subjected to the flow continuity at each node as an equality constraint. This approach allowed Collins and collaborators to apply well-known minimisation algorithms to solve the network analysis problem.

Todini (1979) posed the network analysis problem as that of minimising a general function $E(\underline{Q}) = \underline{\alpha}^T |\underline{Q}|^{n+1}$, subjected to the nodal flow continuity as a set of linear equality constraints. Upon transforming the constrained minimisation problem into an unconstrained problem, via the Lagrange multipliers technique, and on introducing the head loss/flow relationship for each pipe, he arrived at the conclusion that the only necessary conditions for the steady state flow condition are simply the simultaneous fulfilment of the head loss/flow relationship for each pipe, and the flow continuity at each node. Based on this, Todini (1979) introduced a new iterative algorithm for network analysis,

obtained via the application of the gradient operator both to the flows and the heads. We refer to this algorithm here as the gradient method.

Subsequently, Pilati and Todini (1984) extended the original formulation of Todini (1979) to the case when laminar and turbulent flow co-exist in the same network (i.e. the flow exponent "n" in the head loss/flow relationship is variable from pipe to pipe).

Yang and Song (1979), Song and Yang (1980) and Song and Yang (1982), have applied the minimum rate of energy dissipation principle to other hydromechanical systems.

We have adopted the gradient method introduced by Todini (1979) and Pilati and Todini (1984) as the basic network analysis algorithm for the work reported in this thesis and, because it was originally limited to networks containing pipes only, we have pursued the objective of incorporating other devices into it. In the rest of this chapter, we show how to include pumps in Todini's gradient algorithm and, in the next chapter, we deal with how to model pressure regulating valves in the context of the gradient method. At the end of the present chapter, a comparison with other algorithms is carried out.

3.4. Todini's gradient method.

Todini (1979), and Pilati and Todini (1984), demonstrated mathematically that the necessary conditions for the steady state flow in water supply networks are the simultaneous fulfilment of

the nodal balance and the non-linear head loss/flow relationship for each pipe. This can be expressed in a compact format, with the notation introduced in Chapter Two (Section 2.3.7.), as:

$$\left[\begin{array}{c:c} A_{11} & A_{12} \\ \hdashline A_{21} & 0 \end{array}\right] * \left[\begin{array}{c} \underline{Q} \\ \hline \underline{H} \end{array}\right] = \left[\begin{array}{c} -A_{10}\ \underline{H}_0 \\ \hline \underline{q} \end{array}\right] \qquad (3)$$

The upper part of the system of equations (3) represents the head loss/flow relationship, whereas the lower part corresponds to the flow balance at each node. $\underline{H}_0$ corresponds to the (NS*1) vector of known piezometric heads (source nodes).

The matrix A_{11} depends on the particular head loss/flow relationship used, A_{12} is the topological matrix containing the branch to node connectivity information for the non-source nodes, and A_{10} is the equivalent branch to node matrix for the source nodes, as defined in Chapter Two (Section 2.3.7.). A_{21} is the transpose of A_{12}.

Because A_{11} depends on the flows, the upper part of (3) is a set of non-linear equations in the flows. Todini (1979), and Pilati and Todini (1984) concentrated on the solution of the non-linear system (3), applying the gradient operator to the extended vector of unknowns ($\underline{Q}$, $\underline{H}$), without attempting a reduction in the dimensionality of the problem, like other authors who dealt either with the heads or the flows. This leads to a linear system of equations in the corrections $d\underline{Q}$ and $d\underline{H}$ which, after some algebraic manipulations, can be expressed as a coupled set of equations, solved iteratively for the unknown heads and flows.

The gradient method fully recognises the fact that all the topological information, concerning the structure of the network, is contained in the branch to node incidence matrix A_{12} and, consequently, no loop information is necessary.

Because the upper part of equation (3) incorporates the head loss/flow relationship, we need to specify a function as general as possible, which is able to accommodate any kind of device normally present in a water network.

3.5. A general head loss/flow model to include pumps and valves in the gradient method.

We have already used in Chapter Two a general model to describe the non-linear behaviour of pipe flow; this model was:

$$h_{ij} = H_i - H_j = K_{ij} Q_{ij}^{n} \qquad (4)$$

where :

h_{ij} : head loss in pipe joining nodes "i" and "j"; a component of the (NPx1) head loss column vector $\underline{h}$.

NP : total number of pipes (branches, in general) in the network.

H_i : nodal piezometric head; a component of the (NNx1) piezometric head column vector $\underline{H}$.

NN : total number of nodes in the network.

K_{ij} : resistance of pipe joining nodes "i" and "j", dependent on the particular formula in use.

Q_{ij} : flow in pipe joining nodes "i" and "j"; a component of the (NPx1) flow column vector $\underline{Q}$.

n : flow exponent, dependent not only on the formula being used, but also on the hydraulic regime in which the pipe

is operating (laminar or turbulent).

Equation (4) represents a nearly quadratic function, which passes through the origin in the flow/head loss plane. The model (4) allows us to represent other kind of devices, like gate valves, butterfly valves, etc., with the condition that their characteristics remain known and fixed during the modelling. Other situations, like the introduction of minor losses due to fittings (bends, tees, reductions, etc.) can also be handled with equation (4). In these cases, all we need to know, for any particular device, is the value of "K_{ij}" and "n", which are normally supplied by the manufacturer or obtained from laboratory tests.

To introduce centrifugal pumps, other non-linear models have been proposed in the literature, relating the head gain with the flow, through quadratic or higher order polynomial functions as:

$$h_{ij} = a_o + a_1 Q_{ij} + a_2 Q_{ij}^2 \qquad (5)$$

or

$$h_{ij} = a_o + a_1 Q_{ij} + a_2 Q_{ij}^2 + a_3 Q_{ij}^3 \qquad (6)$$

or

$$h_{ij} = a_o + a_1 Q_{ij} + a_2 Q_{ij}^2 + a_3 Q_{ij}^3 + a_4 Q_{ij}^4 \qquad (7)$$

All these models allow us to take into account different types of pump characteristic curves. Also, piecewise linear representations have been used in computer models, joining known head/flow points of the characteristic curve with straight lines.

It has been argued that the higher order models (third or fourth order), would represent the characteristic curve of a pump in a more accurate way. However, other authors have put the emphasis on using accurate data on the pump characteristics,

rather than concentrating on a more mathematically sophisticated model.

Due to its simplicity, and because of other considerations which have to do with the shape of the characteristic curve of a pump, we have adopted the following model:

$$h_{ij} = \alpha_{ij} Q_{ij}^{n} + \beta_{ij} \qquad (8)$$

where the parameters α_{ij}, β_{ij} and "n" have to be determined from data on the real performance of the pump.

Upon adopting (8), we see that the model of a pipe (equation 4) is just a particular case of the model (8) (taking $\beta_{ij}=0$); hence, equation (8) can be considered a general head loss (gain)/flow model, applicable to most of the devices normally found in water distribution systems.

Another advantage considered when adopting the model (8) relates to the fact that, when modelling centrifugal pumps, equation (8) automatically avoids the inclusion in the network model, of pumps with an ascending limb in their characteristic curves. As we shall see later on, such pumps should not be included in the model for stability reasons. The computer program checks that the pump is always working with positive flows and positive head gains.

Other devices, like check valves, pressure reducing valves, pressure sustaining valves, etc. will be dealt with in the next chapter, within the framework provided by equation (8).

3.6. Extension of the gradient method to include pumps: derivation of the recursive scheme for the extended method.

Using the link to node topological matrices for non-source and source nodes (A_{12} and A_{10}, respectively), we can re-write the head-loss (or head 'gain' in the pumps case) of each link connecting two different nodes as:

$$A_{11}\,\underline{Q} + A_{12}\,\underline{H} = -A_{10}\,\underline{H}_0 \qquad (9)$$

where now

$\underline{H}$: is the ((NN-NS)x1) column vector of unknown heads.

$\underline{H}_0$: is the (NSx1) column vector of fixed (known) piezometric heads (reservoirs).

and where, upon using the general head loss (gain)/flow model (8), A_{11} can be re-defined as:

$$A_{11} = \begin{bmatrix} \alpha_1|Q_1|^{n1-1} + \beta_1/Q_1 & & & \\ & \alpha_2|Q_2|^{n2-1} + \beta_2/Q_2 & & \\ & & \ddots & \\ & & & \alpha_{NP}|Q_{NP}|^{nNP-1} + \beta_{NP}/Q_{NP} \end{bmatrix} \qquad (10)$$

On coupling equation (9) with the flow (mass) nodal balance condition, we still get equation (3), which is reproduced here:

$$\left[\begin{array}{c:c} A_{11} & A_{12} \\ \hdashline A_{21} & 0 \end{array}\right] * \left[\begin{array}{c} \underline{Q} \\ \hdashline \underline{H} \end{array}\right] = \left[\begin{array}{c} -A_{10}\,\underline{H}_0 \\ \hdashline \underline{q} \end{array}\right]$$

Because the system represented by (3) is a non-linear one, a direct solution is not possible, and an iterative procedure must be followed to determine the unknown flows and heads.

On differentiating the system of equations (3) we get:

$$\left[\begin{array}{c|c} N\ A_{11}^{*} & A_{12} \\ \hline A_{21} & 0 \end{array}\right] * \left[\begin{array}{c} d\,\underline{Q} \\ \hline d\,\underline{H} \end{array}\right] = \left[\begin{array}{c} d\,\underline{E} \\ \hline d\,\underline{q} \end{array}\right] \qquad (11)$$

where:

$d\underline{E}$: is the pipe head loss imbalance produced by a pipe flow differential $d\underline{Q}$ and to a nodal piezometric head differential $d\underline{H}$.

$d\underline{q}$: nodal flow imbalance due to a pipe flow differential $d\underline{Q}$.

$$A_{11}^{*} = \begin{bmatrix} \alpha_1|Q_1|^{n1-1} & & & \\ & \alpha_2|Q_2|^{n2-1} & & \\ & & \ddots & \\ & & & \alpha_{NP}|Q_{NP}|^{nNP-1} \end{bmatrix} = A_{11} - \begin{bmatrix} \beta_1/Q_1 & & & \\ & \beta_2/Q_2 & & \\ & & \ddots & \\ & & & \beta_{NP}/Q_{NP} \end{bmatrix} \qquad (12)$$

N = (NPxNP) diagonal matrix of the exponents "n" of the head loss-flow relationship.

At some iteration "i", when convergence has not yet been achieved, the (NPx1) vector $d\underline{E}$, representing the head loss imbalance at each branch, and the ((NN-NS)x1) vector $d\underline{q}$, representing the nodal imbalance, can be approximated as:

$$d\,\underline{E} = A_{11}^{(i)}\,\underline{Q}^{(i)} + A_{12}\,\underline{H}^{(i)} + A_{10}\,\underline{H}_0 \qquad (13)$$

and

$$d\,\underline{q} = A_{21}\,\underline{Q}^{(i)} - \underline{q} \qquad (14)$$

where $\underline{Q}^{(i)}$ and $\underline{H}^{(i)}$ represent the pipe flow and the nodal heads

at the iteration "i". $A_{11}^{(i)}$ stands for the matrix A_{11} evaluated at $\underline{Q}=\underline{Q}^{(i)}$, but from now on we drop the iteration superscript in the matrices A_{11} and A_{11}^* for the sake of notational simplicity.

The algebraic solution of (11) is:

$$\begin{bmatrix} \frac{d\,\underline{Q}}{d\,\underline{H}} \end{bmatrix} = \begin{bmatrix} N\,A_{11}^* & A_{12} \\ \hline A_{21} & 0 \end{bmatrix}^{-1} * \begin{bmatrix} \frac{d\,\underline{E}}{d\,\underline{q}} \end{bmatrix} \qquad (15)$$

where A_{11}^* is evaluated at $\underline{Q}=\underline{Q}^{(i)}$.

The inverse of the partitioned matrix in (15) can be computed as another block-partitioned matrix:

$$\begin{bmatrix} N\,A_{11}^* & A_{12} \\ \hline A_{21} & 0 \end{bmatrix}^{-1} = \begin{bmatrix} B_{11} & B_{12} \\ \hline B_{21} & B_{22} \end{bmatrix} \qquad (16)$$

On using the following notation:

$$G = N\,A_{11}^* \qquad (17)$$

We can compute the blocks of the inverse in equation (16) explicitly, according to Ayres (1974), as:

$$\left.\begin{aligned} B_{11} &= G^{-1} - G^{-1} A_{12} \left(A_{21} G^{-1} A_{12} \right)^{-1} A_{21} G^{-1} \\ B_{22} &= - \left(A_{21} G^{-1} A_{12}\right)^{-1} \\ B_{12} &= G^{-1} A_{12} \left(A_{21} G^{-1} A_{12}\right)^{-1} \\ B_{21} &= \left(A_{21} G^{-1} A_{12}\right)^{-1} A_{21} G^{-1} \end{aligned}\right\} \qquad (18)$$

With the partitioning (16), the system (15) can be re-written as:

$$\left.\begin{aligned} d\,\underline{Q} &= B_{11}\ d\underline{E} + B_{12}\ d\underline{q} \\ d\,\underline{H} &= B_{21}\ d\underline{E} + B_{22}\ d\underline{q} \end{aligned}\right\} \qquad (19)$$

On introducing equations (13) and (14), and the results of (18) into equation (19), we get:

$$d\underline{Q} = [I-G^{-1} A_{12} (A_{21}G^{-1}A_{12})^{-1} A_{21}]G^{-1} (A_{11}\underline{Q}^{(i)}+A_{12}\underline{H}^{(i)}+A_{10} \underline{H}_0) + + [G^{-1} A_{12} (A_{21} G^{-1}A_{12}]^{-1})(A_{21} \underline{Q}^{(i)}-\underline{q}) \quad (20)$$

Similarly:

$$d\underline{H} = [(A_{21} G^{-1}A_{12})^{-1}A_{21} G^{-1}](A_{11} \underline{Q}^{(i)} + A_{12} \underline{H}^{(i)} + A_{10} \underline{H}_0) - - (A_{21} G^{-1}A_{12})^{-1}(A_{21} \underline{Q}^{(i)} - \underline{q}) \quad (21)$$

The system of equations (20) and (21) can be solved for $d\underline{Q}$ and $d\underline{H}$ via an iterative procedure, on defining:

$$d\underline{Q} = \underline{Q}^{(i)} - \underline{Q}^{(i+1)} \quad (22)$$

and

$$d\underline{H} = \underline{H}^{(i)} - \underline{H}^{(i+1)} \quad (23)$$

And upon introducing (22) and (23) into (20) and (21), we obtain:

from (23):

$$\underline{H}^{(i+1)}= -[A_{21} G^{-1} A_{12}]^{-1} \{ A_{21} G^{-1} (A_{11} \underline{Q}^{(i)} + A_{10} \underline{H}_0) - - (A_{21} \underline{Q}^{(i)} - \underline{q}) \} \quad (24)$$

from (22):

$$\boxed{\underline{Q}^{(i+1)}= (I- G^{-1} A_{11}) \underline{Q}^{(i)} - G^{-1} (A_{12} \underline{H}^{(i+1)} + A_{10} \underline{H}_0)} \quad (25)$$

Equation (24) represents a linear system of (NN-NS) equations in the unknown piezometric heads, and it can be reordered into the standard format of a linear system:

$$\boxed{[A_{21} G^{-1}A_{12}] \underline{H}^{(i+1)}= - \{ A_{21} G^{-1} (A_{11} \underline{Q}^{(i)} + A_{10} \underline{H}_0) - - (A_{21} \underline{Q}^{(i)} - \underline{q}) \}} \quad (26)$$

Starting with any flow distribution, not necessarily balanced, and applying recursively the coupled system (26) and (25), the problem can be solved. Note that once a balanced solution has been obtained (second iteration and following), the right-hand-side vector of equation (26) simplifies, since the difference $(A_{21}\ \underline{Q}^{(i)} - \underline{q})$ vanishes. Equation (25) guarantees the nodal balance, as it can be proved via pre-multiplying (25) by A_{21}, which gives, after some algebra, the vector of nodal consumptions $\underline{q}$.

Figure 3.1 represents graphically the main steps of the gradient method's numerical algorithm. The main distinctive characteristic of this algorithm when compared with the rest of the existing methods, is the fact that it is based on the gradient operator being applied over both the heads and the flows, and not only to one of them, as in all the methods reviewed in the previous chapter.

The fundamental steps in the derivation of the gradient algorithm can be summarised as follows:

a) The system of non-linear equations (3) are the necessary conditions for the steady state flow in the network. The sufficient conditions are dealt with in the following section 3.7.

b) The non-linear system (3) can be linearized by applying the gradient operator to (3), in the space of the flows and heads, leading to the linear system (11), in $d\underline{Q}$ and $d\underline{H}$.

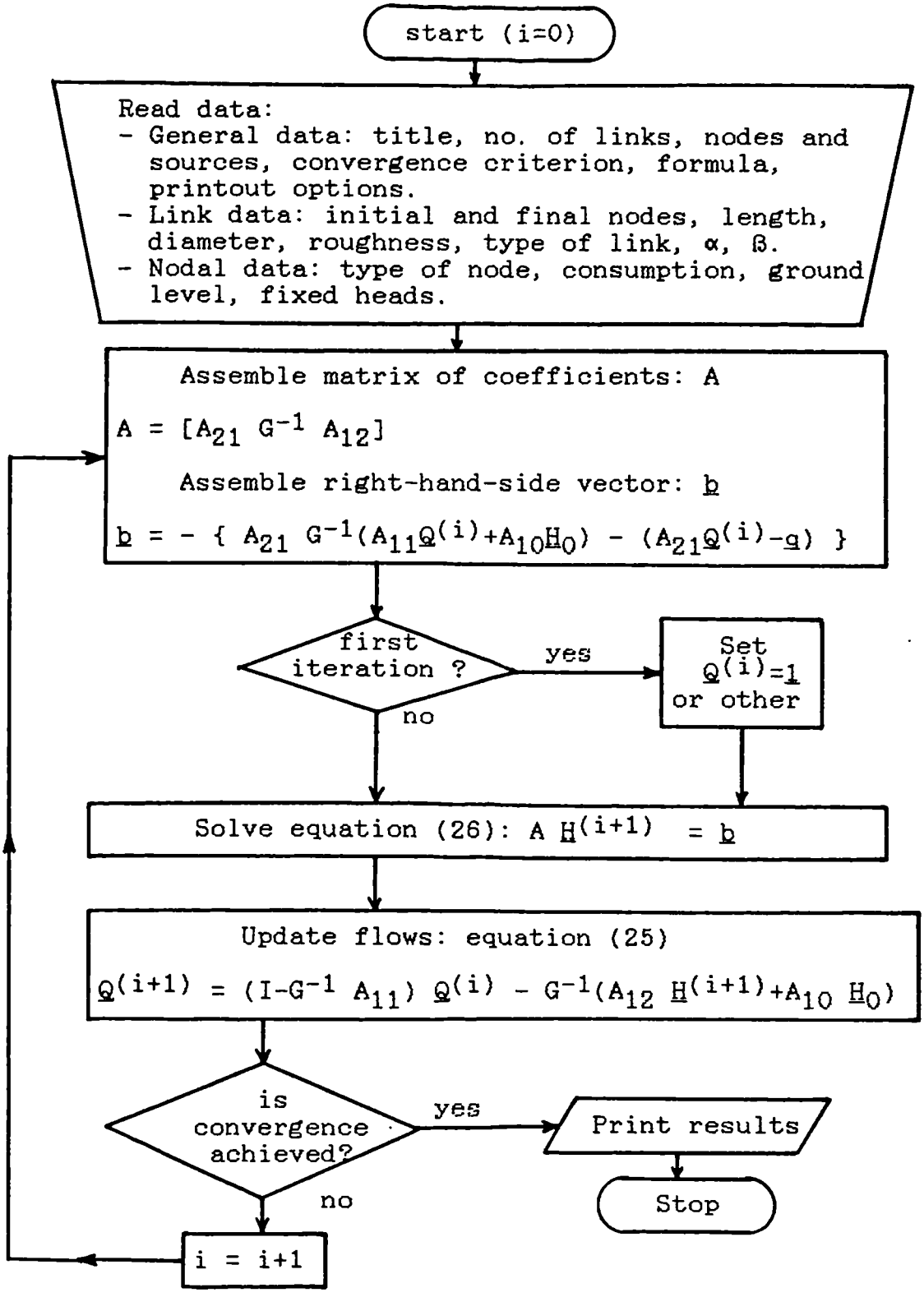

Figure 3.1. Flowchart of main steps in gradient method.

c) The system of equations (11) can be solved explicitly by inverting the partitioned matrix, producing the system (19) which, after some algebra, leads to the coupled equations (26) and (25).

d) The most computationally expensive step of the algorithm now becomes the solution of the symmetric positive definite linear system (26). Chapter Five deals with the efficient computer solution of the system (26). Equation (25) is simply the product of matrices and vectors and no linear system needs to be solved. The inversion of matrix G is straightforward, since it is a diagonal matrix.

e) Iterations: starting from any initial flow distribution, equations (26) and (25), in that order, are applied recursively until some convergence criterion is met; see Figure 3.1.

3.7. On the existence and uniqueness of the network analysis solution.

It has been said earlier that the set of non-linear equations (3), coupling the simultaneous fulfilment of nodal balance and the head loss/flow relationship for each branch, are the necessary conditions for the solution of the steady state flow in water distribution networks. The sufficient conditions for that problem remains to be defined.

Since the early stages of the study of network analysis, the question of whether the solutions provided by the different methods are unique, or whether there are multiple solutions, has been considered by different authors.

From a mathematical point of view, since the solution to the problem is in fact the solution of a set of non-linear simultaneous equations, it seemed in the past quite natural to think that the network analysis problem might have more than one solution (more than one real solution, because the presence of solutions in the complex plane can be discarded using a physical argument).

Most of the work done in this area has been adapted from work originally carried out for non-linear electrical networks, using the well-known analogy between electrical and pipe networks.

D'Auriac (1947) proved that, in the case of a network of pipes only, wherein the resistance function $h = f(Q)$ is an <u>increasing</u> function ($-\infty < Q < \infty$), the solution for the steady state flow is unique. D'Auriac suggested that this is not true when dealing with a network containing pumps.

Warga (1954), on extending previous work by Duffin, provided a set of <u>sufficient</u> conditions for the uniqueness of the solution of the set of nodal balance equations (first Kirchoff law):

$$\sum_j Q_{ij} = q_i \qquad i=1,2,\ldots,NN \tag{27}$$

where:

Q_{ij} = $f_{ij}(H_i-H_j)$: flow between nodes "i" and "j", a function of the head loss.

H_i : piezometric head at node "i".

q_i : nodal demand at node "i".

Warga's sufficient conditions can be summarised as:

a) $f_{ij}(x) = - f_{ji}(-x)$: h is symmetric with respect to the

origin.

b) $f_{ij}(x)$ is continuous, for all "x"

c) $f_{ij}(x)$ is a non-decreasing function of "x".

d) it is possible to connect each node with the reference node (which has a known piezometric head), via at least one series of branches whose characteristic function f_{ij} is strictly increasing and unrestricted (i.e. it can carry an unlimited flow).

The presence of pumps does not satisfy condition c) of Warga, since their characteristic curve is normally decreasing or, even worse, in some cases pumps have characteristic curves with partly increasing and partly decreasing limbs. Condition d) allows the presence of some decreasing and restricted branches in the network. Thus, devices such as check valves, allowing flow in just one direction, can be present in the network and uniqueness is guaranteed, provided that we can link a reference node with any other node, via strictly increasing and unrestricted branches.

Millar (1951), upon studying non-linear electrical systems, defined the concepts of "content" and "co-content" which, expressed in terms of their hydraulic analogue variables, can be written as:

$$\text{Content: } G = \int_0^{Q_{ij}} h \, dQ \tag{28}$$

$$\text{Co-content: } J = \int_0^{h_{ij}} Q_{ij} \, dh \tag{29}$$

Both the content, and its dual, the co-content, have units of power and they are actually proportional to the dissipated power. From a geometrical point of view, the content and co-content functions can be interpreted as the area underneath and above the h-Q curve. Millar (1951) demonstrated that both quantities (content and co-content) are constants when steady state flow occurs, i.e.:

$$\frac{dG}{dt} = \frac{dJ}{dt} = 0 \qquad (30)$$

These content and co-content concepts have been used later on by Collins et al. (1978, 1979), since they form the basis for establishing the necessary conditions for the steady state flow in a non-linear network.

Birkhoff and Diaz (1955-1956) proved the existence and uniqueness of the solution of the steady state flow in a non-linear network, under some particular conditions. They developed their results within a general framework, including electrical, thermodynamic and fluid flow problems. In the case of water distribution networks, where the head-loss flow relationship is expressed as:

$$Q_{ij} = R_{ij}\ \mathrm{sign}(H_i - H_j)\ |H_i - H_j|^{1/n}, \qquad (31)$$

Birkhoff and Diaz (1955-1956) proved that, if R_{ij} (the conductance function) is continuous and strictly increasing, and if some nodal heads are fixed (e.g.: reservoir levels), and when some nodal demands are also fixed (or even when they are non-increasing functions of h), then, the steady state flow problem

does have a unique solution.

In addition, Birkhoff and Diaz (1955-1956) determined that the nodal balance (first Kirchoff law) holds, if R_{ij} is continuous and strictly increasing and, if and only if the function:

$$V(h) = \Sigma \int_0^h Q(h)\, dh \qquad (32)$$

has an absolute minimum. The summation is carried out over all the links of the network. This function has again, as in the cases of the content and co-content functions, units of power and it is similar to equation (29) of Millar.

Furthermore, Birkhoff and Diaz (1955-1956) proved that in the case of exponential conductivity ,which is the case of water distribution networks, and for (1/n) = constant for all the pipes [see equation (31)], then the function V(h) is proportional to the rate of energy dissipation (or power dissipation) D, where:

$$D = \Sigma\, Q\, h \qquad (33)$$

Then, the previously mentioned results of Birkhoff and Diaz (1955-1956) are also valid if V is replaced by D.

Even though there is no proof of the existence and uniqueness of the solution when pumps are present, Millar (1951) and Birkhoff and Diaz (1955-1956) have introduced a new factor in the mathematical representation of the steady state flow in a distribution network, that is the rate of energy dissipation function or power dissipation.

In the 1960's and 1970's, the question of the existence and uniqueness of the solution remained without an explicit mathematical proof. As pointed out by Shamir and Howard (1968) and Shamir (1973), in the context of their nodal approach (Chapter Two, Section 2.3.4.), this situation happens when:

i) Some nodal consumptions and branch resistances are part of the set of unknowns of the problem.

ii) A pump with a non decreasing characteristic curve is included in the network.

Lekane (1979) also recognised the lack of mathematical proof for the uniqueness problem, except for the case of a network including pipes only. Lekane expressed the view that, in a network including pumps, check valves and pressure reducing valves (P. R. V.'s), "the experience has shown" that the network analysis problem does converge to a unique solution.

Collins et al. (1978,1979), using the results of Millar (1951), formulated the problem of determining the steady state flow as the minimization of the content function G(Q) , subject to the nodal balance equations as equality constraints. An alternative formulation based on the co-content function was also given. They used an expanded directed graph of the network, introducing an artificial one-way element to simulate two-way elements (like pipes e.g.); also they introduced fictitious one-way elements to link real reservoirs with the reference (ground) node. Then, the objective content function to be minimised is:

$$G(Q) = \sum_{(i,j)\in Ef} \left[\int_0^{Q_{ij}} \varnothing_{ij}(x)\, dx \right] - \sum_{(g,n)\in EL} H_n^* Q_{gn} + \sum_{(n,g)\in EL} H_n^* Q_{ng} \qquad (34)$$

subject to the constraints:

$$\sum_{(n,j)\in E} Q_{nj} - \sum_{(i,n)\in E} Q_{in} = q_n \qquad \text{for all nodes "n" } n=1,2,\ldots,NN \tag{35}$$

and

$$Q_{ij} \geq 0 \qquad \text{for all links and nodes } (i,j) \tag{36}$$

where:

E : is the set of all ordered pairs of nodes (i,j) of the expanded network, which is partitioned into two subsets: Ef and EL, the former corresponding to all real nodes (i.e. those connected to real elements like pipes, pumps and valves), while the latter corresponds to those nodes connected to artificial (frictionless) links, created by the expansion of the network and linking real reservoirs and ground nodes.

$\emptyset_{ij}(Q)$: is the head-loss flow relationship, $H_i - H_j = \emptyset_{ij}(Q_{ij})$

H_i : piezometric head of node "i"

H_n^* : fixed piezometric head at reservoir node "n".

Q_{ij} : flow in element connecting nodes "i" and "j"

q_n : demand on the node "n", negative if outflow.

g : subindex corresponding to the reference (ground) node.

Equation (35) is simply the nodal balance equation, and constraint (36) is compatible with the expanded directed graph where all the flows are assumed to be positive (i.e. in the prespecified direction, since, if a pipe is known to work in two ways, a second one-way pipe has been introduced).

Following Collins et al. (1978), the condition for having a unique solution in the non-linear optimisation problem

represented by equations (34), (35) and (36), is that G(Q), the content function given by equation (34), must be a strictly convex function.

Using a small example network with four pumps and one check valve, where, due to directional and flow constraints, the content function becomes a single variable function, Collins et al. (1979) showed that the content function will be strictly convex if each one of its summation terms is strictly convex and, for this purpose, the pump characteristic curves of each pumping station must be strictly monotone decreasing. Note that in the previous statement, even though a particular pump within a pumping station may not be strictly monotone decreasing, the content function will be strictly convex, provided that the rest of the pump curves of this station, make the characteristic curve of the whole station a strictly monotone decreasing function.

In networks where pumps head "gains" are the dominant factor (over pipe friction losses for example), Collins et al. (1979) showed how the information provided by the content function can be used to draw some conclusions with respect to the stability of possible multiple operation points. The conclusions formulated by Collins et al. (1979), are consistent with the well known example of a single pump, having a characteristic curve with both an ascendant and descendent limb, when two operating points can be found where the characteristic curves of the pump and that of the hydraulic system intersect.

More recently Carpentier et al. (1985), based on the content and co-content formulation of Collins et al. (1978), and using a

variational approach, provided the proof of the uniqueness when the functions $\emptyset_{ij}(x)$ in (34) are twice differentiable, strictly convex and strictly monotonically increasing. Basically, these conditions are imposing a restriction on the Hessian matrix, in the sense that it has to be invertible in order to have a unique solution. Additionally, Carpentier et al. (1985) showed that convergence problems in some network analysis algorithms (the nodal ones) are also related to singularity in the Hessian matrix.

Thus, summarising, provided that we are dealing with water distribution systems having dissipative elements, and pumps with strictly decreasing characteristics curves, the uniqueness of the solution is guaranteed. The general model adopted here for describing the head loss (gain)/flow relationship in the elements of the network model (equation 8), provides the way for automatically avoiding ill-posed problems dealing with pumps.

3.8. Other gradient formulations.

We concentrate now on some network analysis methods which have not been reviewed so far, and which also fit into the class of gradient-based methods. They are: a second mesh-nodal algorithm [the first one was that developed by Hamam and Brameller, (1971)], proposed by Stimson and Brameller (1981), and an algorithm recently published by Dupuis et al. (1987). Here, we intend to review these methods and to establish their differences from the gradient method [Todini (1979), and Pilati and Todini (1984)]. We have to remember that the improved version of the

linear theory method by Wood (1981a), can also be classified as a gradient method; this method has already been presented in Chapter Two (Section 2.4.3).

The new "integrated mesh-nodal" algorithm of Stimson and Brameller (1981) is an improvement of the previous mesh-nodal algorithm of Hamam and Brameller (1971) and, though it is based on some loop (mesh) concepts, the new algorithm has to solve a linear system of equations in the unknown piezometric heads, which has the same structure as that obtained in Todini's gradient method. There are, nevertheless, other differences, particularly in the way the flows are updated at each iteration, which make the "integrated mesh-nodal" algorithm different from the gradient method. We shall derive Stimson and Brameller's algorithm, using the notation we have already used in this chapter and in the previous one.

Stimson and Brameller (1981) recognised the fact that the loop balance condition (second Kirchoff law), is simply establishing the uniqueness of the piezometric heads at each node. Nevertheless, they use the concept of tree and co-tree to partition the set of flows into subsets of dependent and independent flows, exactly in the same way as in Hamam and Brameller (1971), the independent flows corresponding to those in the co-tree (chords) and the dependent flows corresponding to those in the tree (branches).

The basic equations, which have to be fulfilled simultaneously in the integrated mesh-nodal method, are:

Nodal (mass) balance: $$A_{21}\,\underline{Q} = \underline{q} \qquad (37)$$

Head loss per pipe: $$\underline{h} = A_{12}\,\underline{H} + A_{10}\,\underline{H}_0 \qquad (38)$$

and

Head loss/flow relationship: $$\underline{h} = A_{11}\,\underline{Q} \qquad (39)$$

Having a balanced flow solution at the iteration "i", say $\underline{Q}^{(i)}$, means that:

$$A_{21}\,\underline{Q}^{(i)} = \underline{q} \qquad (40)$$

If the rest of the basic equations are not fulfilled at iteration "i", a pipe flow correction $\delta\underline{Q}(i)$ is required, such that:

$$\underline{Q}^{(i+1)} = \underline{Q}^{(i)} + \delta\underline{Q}(i) \qquad (41)$$

and which still fulfils the nodal balance condition, i.e.:

$$A_{21}\underline{Q}^{(i+1)} = \underline{q} \qquad (42)$$

Upon introducing (40) and (41) into (42), we get:

$$\boxed{A_{21}\,\delta\underline{Q}^{(i)} = \underline{0}} \qquad (43)$$

This is simply imposing the condition that the flow changes at every node, with respect to the initially balanced condition, must be null.

The partitioning between dependent and independent flows is introduced as:

$$\underline{Q} = \begin{bmatrix} \underline{Q}_2 \\ \hline \underline{Q}_3 \end{bmatrix} \qquad (44)$$

where:

$\underline{Q}_2$: are the NN-NS dependent flows, i.e. tree flows.

$\underline{Q}_3$: are the NP-(NN-NS) independent flows, i.e. co-tree flows.

Similarly, the flow correction vector $\delta\underline{Q}$ can be partitioned as:

$$\delta\underline{Q} = \begin{bmatrix} \delta\underline{Q}_2 \\ \hline \delta\underline{Q}_3 \end{bmatrix} \tag{45}$$

The incidence matrix A_{21} can be partitioned accordingly:

$$A_{21} = \left[A_{22} \; : \; A_{23} \right] \tag{46}$$

where:

A_{22} : incidence (NN-NS)*(NN-NS) matrix corresponding to the dependent flows.

A_{23} : incidence (NN-NS)*(NP-(NN-NS)) matrix corresponding to the independent flows.

The node balance condition (43) can be written as:

$$\left[A_{22} \; : \; A_{23} \right] * \begin{bmatrix} \delta\underline{Q}_2 \\ \hline \delta\underline{Q}_3 \end{bmatrix} = \underline{0} \tag{47}$$

and the dependent component of the flow correction can be computed from (47), as a function of the independent component, provided that the sub-matrix A_{22} is non-singular:

$$\boxed{\delta\underline{Q}_2 = - A_{22}^{-1} \, A_{23} \, \delta\underline{Q}_3} \tag{48}$$

The importance of equation (48) lies in the fact that the set of unknown flow corrections ($\delta\underline{Q}$), can be reduced to the independent flow corrections ($\delta\underline{Q}_3$), the dependent flow corrections ($\delta\underline{Q}_2$) being computed from the independent flows, using just the topological information of the system. In the context of the integrated mesh-nodal approach, this is a key

issue, since (48) ensures that, starting with a balanced flow distribution, the updated flows will remain balanced, despite numerical approximations in the intermediate steps.

The only condition left is the fulfilment of the head loss/flow relationship, which is a non-linear function. In order to linearize it, the Taylor expansion is used.

If $\underline{h}(\underline{Q}) = A_{11}\,\underline{Q}$ then, at the i-th step of the iterative scheme, the head loss/flow function can be expanded as:

$$\underline{h}(\underline{Q}^{(i)} + \delta\underline{Q}^{(i)}) = \underline{h}(\underline{Q}^{(i)}) + J^{(i)}\,\delta\underline{Q}^{(i)} + E^{(i)} \qquad (49)$$

where:

$E^{(i)}$: is the summation of second and higher order terms in the Taylor's expansion.

$J^{(i)}$ is the tangent matrix $J^{(i)} = \left[\dfrac{\partial \underline{h}}{\partial \underline{Q}}\right]_{\underline{Q}=\underline{Q}^{(i)}}$ (50)

or, in our notation (see equation 17):

$$J = N\,A_{11}{}^{*} = G \qquad (51)$$

Because

$$\underline{h}^{(i)} = A_{11}\,\underline{Q}^{(i)} \qquad (52)$$

equation (49) can be introduced into the expression for the head loss (38), giving:

$$A_{12}\,\underline{H} + A_{10}\,\underline{H}_0 = A_{11}\,\underline{Q}^{(i)} + J^{(i)}\,\delta\underline{Q}^{(i)} + E^{(i)} \qquad (53)$$

where $\underline{H}$ is the "true" piezometric head vector, because we are keeping the Taylor's expansion with all its terms, including the higher order ones (in $E^{(i)}$).

Equation (53) allows us to compute the flow correction vector $\delta\underline{Q}^{(i)}$, provided that the tangent matrix is non-singular:

$$\delta\underline{Q}^{(i)} = [J^{(i)}]^{-1} \{ A_{12}\,\underline{H} + A_{10}\,H_0 - A_{11}\,\underline{Q}^{(i)} - \underline{E}^{(i)} \} \qquad (54)$$

which, when pre-multiplied by A_{21}, allows us to re-introduce the nodal balance condition (43), giving:

$$A_{21}\,[J^{(i)}]^{-1} \{ A_{12}\,\underline{H} + A_{10}\,H_0 - A_{11}\,\underline{Q}^{(i)} - \underline{E}^{(i)} \} = 0 \qquad (55)$$

Because, as a result of the Taylor's expansion, the residual $\underline{E}^{(i)}$ is not explicitly known, we can assume that its value is nearly zero when the true heads $\underline{H}$ are approximated by $\underline{H}^{(i+1)}$, hence:

$$\underline{Q}^{(i+1)} \dashrightarrow \underline{Q} \quad \text{and} \quad \underline{H}^{(i+1)} \dashrightarrow \underline{H} \quad \text{if} \quad \underline{E}^{(i)} \dashrightarrow 0 \qquad (56)$$

and equation (55) becomes:

$$A_{21}\,[J^{(i)}]^{-1} \{A_{12}\,\underline{H}^{(i+1)} + A_{10}\,H_0 - A_{11}\,\underline{Q}^{(i)} \} = 0 \qquad (57)$$

Re-ordering equation (27) gives:

$$\boxed{A_{21}[J^{(i)}]^{-1}A_{12}\,\underline{H}^{(i+1)} = A_{21}[J^{(i)}]^{-1}\,(A_{11}\,\underline{Q}^{(i)} - A_{10}\,H_0\,)} \qquad (58)$$

which is a linear system of (NN-NS) equations in $\underline{H}^{(i+1)}$.

The flows can be updated from (54) which, when introducing the assumptions (56), gives:

$$\delta\underline{Q}^{(i)} = [J^{(i)}]^{-1} \{ A_{12}\,\underline{H}^{(i+1)} + A_{10}\,H_0 - A_{11}\,\underline{Q}^{(i)} \} \qquad (59)$$

and, using (41):

$$\underline{Q}^{(i+1)} = \underline{Q}^{(i)} + [J^{(i)}]^{-1} \{ A_{12}\,\underline{H}^{(i+1)} + A_{10}\,H_0 - A_{11}\,\underline{Q}^{(i)} \} \qquad (60)$$

or, reordering:

$$\boxed{\underline{Q}^{(i+1)} = \{I - [J^{(i)}]^{-1}A_{11}\}\underline{Q}^{(i)} - [J^{(i)}]^{-1}\{A_{12}\underline{H}^{(i+1)} + A_{10}H_0\}} \qquad (61)$$

Instead of solving (61), Stimson and Brameller (1981) use the corresponding equation for the independent flows:

$$\underline{Q}_3^{(i+1)}=\{I_3-[J_3^{(i)}]^{-1}A_{33}\}\underline{Q}_3^{(i)}-[J_3^{(i)}]^{-1}\{A_{32}\underline{H}^{(i+1)}+A_{30}\underline{H}_0\} \quad (62)$$

where:

I_3 : identity matrix of order NP-(NN-NS)

J_3 : partitioned {NP-(NN-NS)}*{NP-(NN-NS)} tangent matrix corresponding to the independent flows.

A_{33}: partitioned {NP-(NN-NS)}*{NP-(NN-NS)} matrix, obtained from A_{11}, for the independent flows.

A_{30}: partitioned {NP-(NN-NS)}*{NS} matrix, obtained from A_{10}, for the independent flows.

Upon computing $\underline{Q}_3^{(i+1)}$ with (62), the dependent flows are updated using the equivalent of equation (48) for the flows:

$$\underline{Q}_2^{(i+1)} = - A_{22}^{-1} A_{23} \underline{Q}_3^{(i+1)} \quad (63)$$

As it has been said before, Stimson and Brameller (1981) use (62)+(63) to update the flows, thus avoiding the effects of round off errors in the solution of the linear system (58), where they found convergence difficulties in some networks.

In summary, Stimson and Brameller (1981) integrated mesh-nodal algorithm is as follows:

a) Initialise the iteration counter (i=1) and find a balanced flow solution: $\underline{Q}^{(1)}$. This is done via the construction of a minimal spanning tree of the network, determining dependent and independent branches, and assigning arbitrary values to the independent flows $\underline{Q}_3^{(1)}$. The dependent flows $\underline{Q}_2^{(1)}$ are computed with (63). All the matrix partitioning is done at this step, having the tree and co-tree from the spanning tree.

b) Compute the tangent matrix $J^{(i)}$ and the head loss vector: $A_{11}\ \underline{Q}^{(i)}$, using the latest flows.

c) Solve the linear system (58) for $\underline{H}^{(i+1)}$.

d) Update the independent flows using (62).

e) Update the dependent flows using (63).

f) If the latest flows satisfy the termination criterion stop, otherwise update the iteration counter and go to step b).

As it can be seen from comparing equations (58) and (26), the main structure of the linear system for the head update $\underline{H}^{(i+1)}$ in the Stimson and Brameller algorithm is fairly similar to that in the Todini algorithm; indeed apart from the difference in the sign, which is produced by the definition of $d\underline{H}$ in the gradient method (equation 23), the only difference lies in the nodal imbalance term $(A_{21}\ \underline{Q}^{(i)} - \underline{q})$.

On the other hand, for the flow updating, equations (61) and (25) are identical, although Stimson and Brameller (1981) do not use (61) for the flow updating; they use (62) which comes out directly from (61).

Thus the main difference between the integrated mesh-nodal algorithm and the gradient algorithm, is basically in the handling of the nodal balance. We have not found problems with round off in the gradient method, which allows us to drop the nodal imbalance in (26) once a balanced flow solution has been obtained in the first iteration. On dropping the imbalance in equation (26), both algorithms become equivalent in terms of the head updating stage. The difference in the flow updating remains.

The integrated mesh-nodal approach requires the generation of a minimal spanning tree, to determine the tree and co-tree of the network. It is not clear for us how the algorithm performs in cases when the topology of the network changes, for example if check valves or pressure regulating valves close completely, producing a change in the original topology of the network (26). The gradient algorithm does not require the generation of the minimal spanning tree (or loops); hence it is not affected by such topological changes. This is possible because all the topological information required by the gradient method is contained in the incidence branch to node matrix A_{12}.

The integrated mesh-nodal method is currently being used by the WATNET computer package; see Crabbe et al. (1982) and Stimson (1982a, 1982b) for more details.

Dupuis et al. (1987) presented what they called a "new method", which is based on the coupling of the nodal balance equations and the loop balance conditions (summation of head losses in a loop = 0). The resulting non-linear system is linearized via the application of a Taylor's expansion, which leads to a linear system having the flow increments as unknowns. Thus, this is basically the same as the gradient version of the linear theory method of Wood (1981a), already reviewed in Chapter Two (Section 2.4.3) and which is not referenced by Dupuis et al. (1987).

3.9. Comparison of the gradient method with some of the the existing methods of network analysis.

3.9.1. Introduction.

Our objective in this section is to compare the performance of the gradient method with those algorithms performing best in the comparison carried out by Wood (1981a) [see also Wood and Rayes (1981)], i.e. with the simultaneous loop adjustment methods (looped Newton-Raphson) and the gradient version of the linear theory method.

Since the integrated mesh-nodal model has been considered an improvement of the original mesh-nodal method of Hamam and Brameller (1971), we do not consider the latter in the comparison. The integrated mesh-nodal has not been included, because we expect similar behaviour to the gradient method, due to the fact that their structures are similar; this is also due to the fact that we do not have a source program based on the integrated mesh-nodal model, which would allow us to determine the number of iterations and the run-time for comparison purposes.

We are mainly concerned with the convergence characteristics of the algorithms, although the comparison is extended to other parameters as well.

3.9.2. The computer programs used in the comparison.

A set of network examples was assembled and run with computer programs based on the simultaneous path adjustment method, the

linear theory method and the gradient method . The computer programs used for the comparison have the following characteristics:

a) Simultaneous path adjustment method (Program LOOP)

This is a FORTRAN version of the BASIC program included in Wood (1981a); the code requires both the initial flow distribution and the definition of the energy paths (loops) to be provided by the user, as part of the input data. The linear system of equations is solved via a direct method, consisting of a Crout's LU decomposition coupled with substitution routines, as presented by Press et al. (1986). The program does not take advantage of the sparsity of the matrices.

Although other computer codes based on the same method were also used at earlier stages of this comparison, this program (LOOP) was found to have the best performance, in the sense that it was bug-free and reliable.

b) Linear Theory method (Program LT)

This code is a FORTRAN version of a BASIC program included in Wood (1981a). The algorithm used is that described in Chapter Two (Section 2.4.3). The program requires the identification of energy paths by the user, but it normally generates its own initial flows based on a velocity of 4 fps. The same direct linear system solver of program LOOP was used in this program. The program does not use sparse techniques for matrix manipulation.

Because the main objective of this comparison has been to evaluate the convergence characteristics of the methods, rather than the computer codes themselves, we do not claim that a fully fair comparison has been carried out. Indeed, the codes could have been improved by simplifying the input data required (no initial flow distributions and no identification of loops and energy paths to be provided by the user) and by using better methods for handling sparse matrices, but these improvements would not have a positive impact on the convergence characteristics of the methods on which the codes are based, only on the effective storage and run-times.

c) Gradient method (Program GRAD)

This FORTRAN program is based on the algorithm described in Section 3.6 of this chapter. The code does not need the identification of loops and the provision of an initial flow solution by the user; it uses sparse matrix manipulation and a LDL^T factorization for the direct solution of the linear system of equations, as presented by Pissanetzky (1984). (See Appendix A for details on the direct solution of linear systems). This direct linear solver was used in order to have a relatively fair comparison with the other programs, which also used a direct solver.

3.9.3. The set of test examples.

The programs were tested with a subset of 6 examples of ill-conditioned networks, all of them adapted from cases reported in the literature.

i) Example A

This is a network of 66 pipes, 41 nodes and 2 reservoirs (nodes 1 and 2 in Fig. 3.2), taken from a case presented by Chin et al.(1978) and reduced to its looped part (i.e. without the branches connected at node 25). This network incorporates small diameter pipes connected to larger diameter pipes, and its size makes it similar to real networks found in practical applications. The nodal demands have been reduced (producing velocities of under 0.2 m/s) to simulate the behaviour of the network during the night. This example network includes 2 gravitational sources and it does not include pumps.

ii) Example B

This is almost the same network as example A, except that 6 pumps with steep characteristic curves have been included; also, the branched part connected at node 25 (see Fig. 3.2) has been added which gives a total of 74 pipes, 48 nodes and 8 sources. The steep characteristic curves have been taken from data of real submersible multistage pumps with speeds in the range of 2900/3500 r.p.m..

iii) Example C

This is the same basic network as presented in example B, but now the nodal demands have been multiplied by a factor of 10, simulating extremely high daily consumptions.

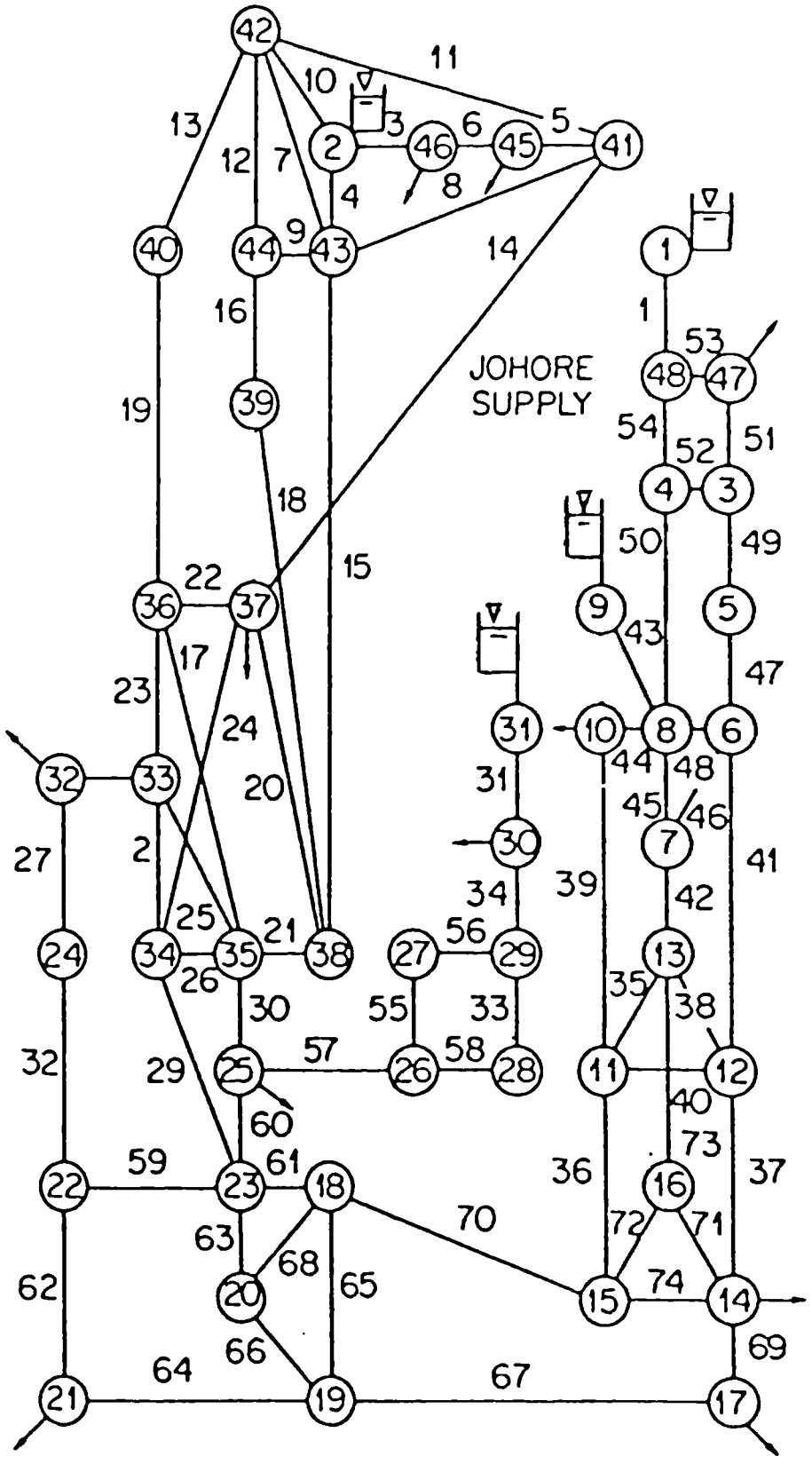

Fig. 3.2. Basic network for examples A, B, C and D, from Chin et al. (1978).

iv) Example D

The previous example C has been modified to include 2 valves (in links 67 and 70) which are completely closed in order to simulate the eventuality that a particular link ceases to carry flow (e.g. a check valve working under reverse flow or a pressure reducing valve being closed by the system downstream pressure). The valves are located in such a way that, when fully closed, the original network becomes a disconnected system, with two independent sub-networks, each one with its own sources.

v) Example E

This is a network of 16 pipes, 14 nodes and 2 sources, adapted from a case presented by de Neufville and Hester (1969), as shown in Figure 3.3. This network becomes ill-conditioned when one of its pipe diameters is reduced (pipe 10), while the remaining pipe diameters are unchanged.

vi) Example F

This is a network of 13 pipes, 10 nodes and 1 source, reported by Barlow and Markland (1969), as shown in Figure 3.4. This network becomes ill-conditioned for the particular diameter distribution used.

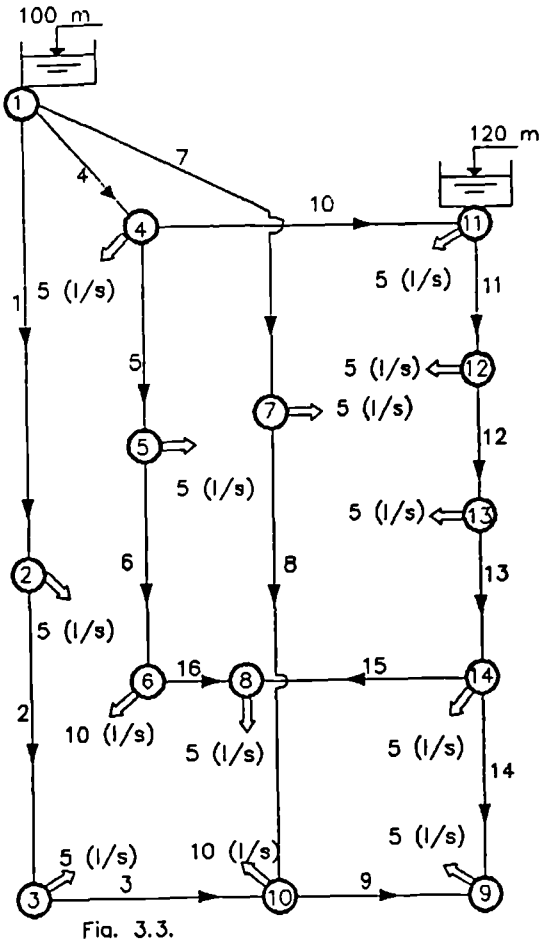

Fig. 3.3.

Fig. 3.3. Network for example E, from de Neufville and Hester (1969).

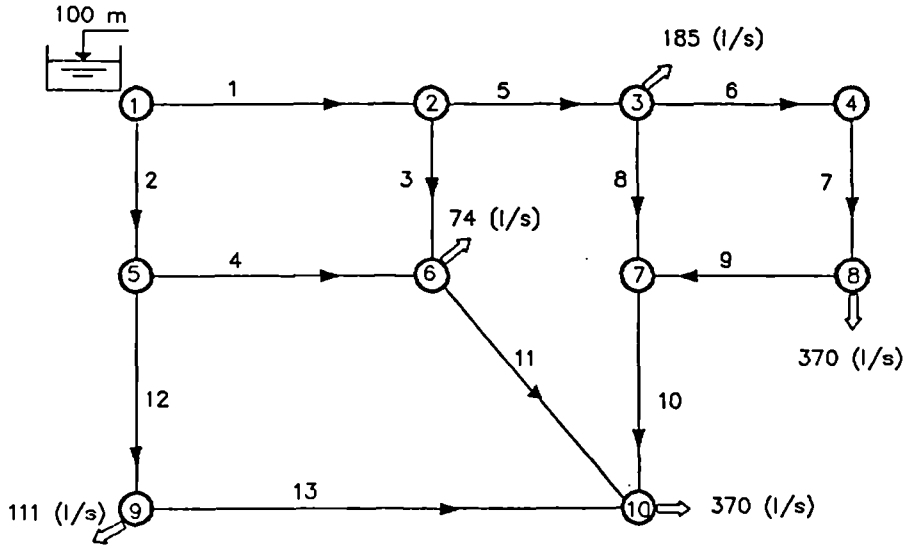

Fig. 3.4. Network for example F, from Barlow and Markland (1969).

3.9.4. Comparison of the algorithms for the simultaneous path adjustment, linear theory and gradient methods.

In order to produce a comparison of the algorithms, independent of the initial conditions, the same initial flow distribution was supplied to all the programs. In standard applications, both the linear theory and the gradient methods, do not need an initial flow solution as part of the input data. For the sake of a fair comparison, a direct solution was used for solving the linear system of equations in all the cases.

The results of running the test networks with the 3 computer programs are summarised in Table 3.1.

From the results obtained by Wood (1981a) the following are the most usual causes of convergence problems in water distribution networks:

- low resistance links connected to high resistance ones;
- the presence of pumps with steep characteristic curves.

Based on the results summarised in Table 3.1, the conclusions of Wood (1981a) are partially corroborated.

From the pipe flows point of view, the simultaneous path adjustment method (program LOOP) and the linear theory method (program LT) converged for all the examples, even under cases previously reported as ill-conditioned (examples E and F). Both programs failed to determine the piezometric heads when the network included very small diameter pipes, or nearly closed valves (examples D and E), where the high head loss (eventually

Table 3.1. Summary of the performance of the programs LOOP, LT and GRAD with test examples.

EXAMPLE	P R O G R A M		
	L O O P	L T	G R A D
A	converged iter=16 t=69.53 sec. [1]	converged iter=17 t=788.51 sec.	converged iter=16 t=29.77 sec.
B	converged iter=12 t=91.67 sec.	slow convergence iter=13 t=961.69 sec.	converged iter=10 t=34.00 sec.
C	converged iter=13 t=100.13 sec.	slow convergence iter=15 t=1109.82 sec.	converged iter=12 t=39.16 sec.
D	converged [2] iter=21 t=154.94 sec. some heads unavail.	slow convergence iter=21 [2] t=1551.76 sec. some heads unavail.	converged iter=19 t=57.28 sec.
E	converged [3] iter=12 t=4.67 sec. some approx. heads	converged iter=13 t=22.36 sec.	converged iter=12 t=5.38 sec.
F	converged iter=4 t=2.69 sec.	converged iter=8 t=9.12 sec.	converged iter=4 t=2.47 sec.

Notes:
---

[1] All the times correspond to mean execution time on an IBM-PC compatible computer (Amstrad PC1512, with co-processor 8087).

[2] Program failed to compute piezometric heads in one sector of the network.

[3] Computed heads are not exact.

[4] Only for fairness in the comparison, all the programs are starting from the same initial flow solution. For the same reason, a direct solution was used in all the programs.

of "infinite" value) produced unreliable piezometric heads in the section of the network which does not remain connected to the reference node. This is in fact a problem inherent to all loop or path-based methods, and is produced because the network is broken-up into two (or more) disconnected sub-networks and consequently the path to the reference node is lost. A solution to this problem can be produced, by re-defining the reference node, but it is not clear if this makes the program problem-dependent, because, in more complex networks, the disconnection of the system may happen anywhere (i.e. due to pressure regulating valves, maintenance work, etc.).

On the other hand, the linear theory method, in its improved form, showed slow convergence when applied to networks with steep characteristic curve pumps (examples B, C and D).

The linear theory method produces a matrix of coefficients for the linear system (see Chapter Two, equation 150), which is a non-symmetric matrix. This is another shortcoming of the linear theory method, since it makes the storage requirements critical for real networks, even when efficient sparse matrix techniques are used; in addition, pivoting is necessary in order to guarantee the stability of the linear solver, which implies an extra computational cost. The simultaneous path adjustment method, and the gradient method, produce symmetric matrices of coefficients in the linear systems of equations; as a result, their storage demands are about 34% (simultaneous path) and 41% (global gradient) of that needed for the linear theory method.

These are approximate values computed for a regular square network.

The global gradient method did not fail to converge for any of the test examples; moreover, since its development, we have not been able to find a single example of failure or unsatisfactory convergence rate. This method did not experience problems when closed valves or high resistance links where introduced into the networks. This is due to the fact that, at each stage, the algorithm computes both heads and flows; subsequently, it will converge properly provided that all the sub-networks do have a source, which is a sensible condition from the physical viewpoint. This is an important advantage of the method, since the situation described will probably occur when using this method for simulation purposes, in more complex systems having check valves and pressure regulating valves. Future implementations will include the detection of cases such as those where a sub-network does not have a source, displaying a clear warning to the user.

The proposed method requires an efficient and robust linear system solver, and we study this problem in Chapter Five.

We also ran other codes for the "simultaneous path adjustment" algorithm, using different solvers for the linear system of equations, and some of them failed to converge for some of the test examples. This suggests that some reported ill-conditioned cases are solvable, when a different linear system solver is used. This seems to be a numerical problem and not a problem of the water distribution analysis methods themselves.

3.10. Concluding remarks.

When compared with the simultaneous path adjustment method and the linear theory method, the proposed gradient method has the following advantages.

1. It can solve directly partly looped and partly branched networks, while, in the simultaneous path method, the problem needs to be transformed into an equivalent looped network, prior to the application of the iterative algorithm. This has to be done by the user (manually) or incorporated as an additional subprogram.

2. The proposed gradient method does not need a loop or path definition, as in the cases of the simultaneous path adjustment and the linear theory methods. Even though this task can also be done by the computer, it implies an additional computational cost (in the examples tested in this paper, the paths were provided as input data).

3. The proposed gradient method can solve in a straightforward way networks that during certain periods of operation can become disconnected (due to the action of check valves or pressure reducing valves, for example). The simultaneous path adjustment and the linear theory methods cannot cope with this situation, although it might be possible to implement an additional subroutine that could solve this shortcoming, although it is doubtful if an absolutely reliable algorithm can be obtained, especially when dealing with larger and more complex systems. Either way, this means an additional computational cost.

In summary, it has been shown that the gradient method for determining the steady state flow in water supply distribution networks, offers some advantages when compared with other gradient-based algorithms, such as the "simultaneous path adjustment" method and the linear theory method. The reliability of the method, in terms of its ability to converge for both the flows and the piezometric heads, under extreme cases based on ill-conditioned problems, makes it desirable for optimum design and simulation applications, where manual intervention to avoid convergence or disconnection problems is not possible.

CHAPTER FOUR

EXTENSION OF THE GRADIENT METHOD TO INCLUDE REGULATING VALVES: A NEW PHYSICALLY-BASED APPROACH

4.1. Introduction.

So far, we have studied water distribution networks having pipes, pumps and valves. The kind of valves we have been dealing with are basically gate and butterfly valves; in other words, valves with a fixed and known head loss-flow characteristic curve. These valves may be operating fully open, partly open or fully closed within the network, and the state of each valve is assumed to be known prior to the analysis of the system; in fact, the operator can alter the setting of any of these valves (by giving instructions to a field crew or via a motor-operated system), but basically the valves characteristics are known and/or are determined by the operator.

From the hydraulic point of view, gate and butterfly valves represent a local (minor) head loss whose magnitude depends on the valve type, its design and its operational status (fully open, partly open or fully closed). A short review of different types of valves and their characteristics may be found in Ruus (1981).

In the context of the gradient algorithm, we have introduced a general model in Chapter Three (Section 3.5) for the head loss/flow characteristic curve of all devices via a polynomial expression:

where:

$$h_{ij} = \alpha_{ij} Q_{ij}^{n} + \beta_{ij} \qquad (1)$$

h_{ij} : head loss (m) in the branch starting at node "i" and ending at node "j".

n : real exponent, typically 1.85-2.0, depending on the formula used.

α_{ij}, β_{ij} : characteristic parameters. Because (1) is our general model, for pipes and valves we drop the constant term (i.e. $\beta_{ij}=0$), being the head loss/flow characteristic dependent on α_{ij} only. This value is either supplied by each valve manufacturer, or is determined via laboratory or field head loss/flow measurements, for different operating conditions.

The model (1) is then able to describe any type of device with a fixed head loss/flow characteristic curve (valves, meters, fittings, etc.).

Due to the variable behaviour of water consumption, the network reacts by varying both pressures and flows, which the operator must maintain within pre-specified limits to achieve an acceptable service. Minimum and maximum pressures are required at any point in the system. Also, constant flows may be required to satisfy fixed demands. On other occasions, we may be interested in avoiding flows in certain directions. To avoid overflows when feeding a reservoir, it may be desirable to include in the network an automatic level control valve (altitude valve). Some of these requirements may even change during different periods of a day (e.g. from day to night pressures can be reduced in order

to reduce leakages).

To cope with all these requirements (and others) a wide range of pressure, flow and level control valves are available, allowing the operator to fulfil the operational constraints in an automatic way, without his permanent supervision. Since the variety of control valves is quite wide, we shall refer to the most widely used ones, namely check valves, pressure reducing valves and pressure sustaining valves. A short explanation of their physical characteristics is needed in order to understand their behaviour, and to determine an adequate mathematical representation.

4.2. Description of some control valves.

Pressure reducing valves (PRV's) and pressure sustaining valves (PSV's) belong to the same type of pressure controlling devices, but check valves (CV's) are completely different, because their design and operational behaviour is different.

4.2.1. Check valves.

The main purpose of a check valve is to allow flow in one direction only, preventing flow reversal. This situation may arise when feeding a high pressure zone of the network from a lower pressure zone, via pumps for example; in such cases, we would be interested in avoiding backflow from the higher to the lower pressure zone, when the pumping system is switched off.

The traditional hydro-mechanical design of a check valve has been based on a flap, which is forced open by the flow itself (in

one direction), but that automatically closes when the flow approaches zero, or when it is going to be in the opposite direction. Due to the undesirable side effects of this type of valve, especially from the pressure surge viewpoint, a number of modifications of the basic valve have been implemented, in order to reduce the waterhammer produced by a very fast closing of the valve. Also, some hydraulically controlled designs are available, in order to slow down the response of the valve, but we shall not describe them here.

As a result, a check valve can operate under two mutually exclusive modes:

a) Fully open: when the inlet pressure is greater than the outlet pressure.

b) Fully closed: when the outlet pressure becomes greater than the inlet pressure.

Hence, the valve has an associated direction, and its installation must be made accordingly. The valve operating mode is controlled by its outlet and inlet pressures, these being independent of the operator's commands.

Mathematically, the valve has to be described with two different head loss-flow relationships :

i) Fully open (inactive mode):

$$h_{ij} = \alpha_{ij} Q_{ij}^{n} \quad \text{when } H_i > H_j \quad (Q_{ij} > 0) \qquad (2)$$

where:

α_{ij} = constant, dependent on the valve design.

Q_{ij} = flow from node "i" to "j" (l/s)

H_i = piezometric head at node "i" (m)

ii) Fully closed (active mode):

$$h_{ij} = H_j - H_i \quad (Q_{ij} = 0) \text{ when } H_j > H_i \tag{3}$$

4.2.2. Pressure controlling devices: main features.

It is possible to identify three main components in a pressure controlling valve: main valve, relay system and connecting piping plus fittings. The main valve and the relay system are basically the same for most of the pressure control valves; they differ only in the connecting piping and fittings, which are added to the main valve to achieve its particular objectives. A more detailed description of the construction and operational characteristics of pressure reducing valves can be found in Ratcliffe (1986).

For convenience, we shall refer to Glenfield & Kennedy control valves, a leading British valve manufacturer, but most of their features are applicable to other manufacturers as well.

a) Main valve.

Although there are different design concepts for the valve body we shall refer to control valves based on globe valves.

The main valve body is a cast iron globe valve design, modified to include an upper cylindrical section, which contains a mobile element that fits into the main valve seat. Either Figures 4.1.a. or 4.2.a. can be used to follow the description of the different valve components. From the hydromechanical viewpoint, the central mobile "valve element" (component 1 in Fig. 4.1.a.) introduces a variable head loss throughout the valve, depending

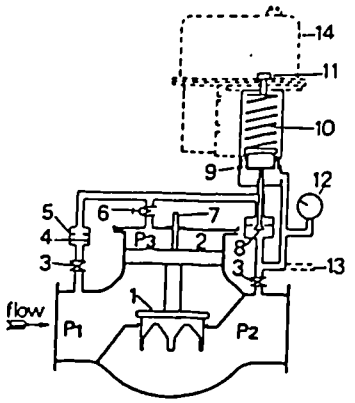

1 Valve Element
2 Upper Cylinder
3 Isolating Cocks
4 Strainer
5 Orifice
6 Needle Cock
7 Indicator
8 Relay Valve
9 Diaphragm
10 Spring
11 Adjusting Screw
12 Pressure Gauge
13 Alternative Constant Pressure Connection
14 Electric Motor

a) **Valve Nos. 1301 and 1302**
Standard and Motor Operated Valves

b) Operation

If the outlet pressure P2 becomes too high to balance the spring load, the relay valve tends to close, allowing pressure P3 to increase, causing the main valve to tend to close, thus reducing P2 to the set value.

Similarly, if P2 becomes too low to balance the spring load, the relay valve opens, P3 decreases, the main valve opens further and P2 rises again to the set value. Thus the valve continuously maintains the desired constant downstream pressure P2, which is determined only by the spring load and is entirely independent of the upstream pressure.

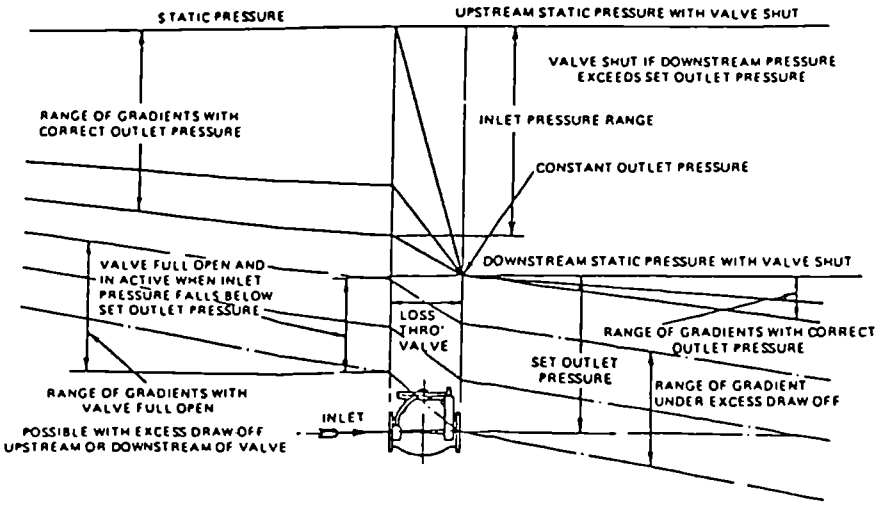

c) Hydraulic Diagram for Pressure Reducing Valves

Fig. 4.1. Pressure Reducing Valve. Design and operational features, from Glenfield & Kennedy Ltd., Pub. 215/R3.

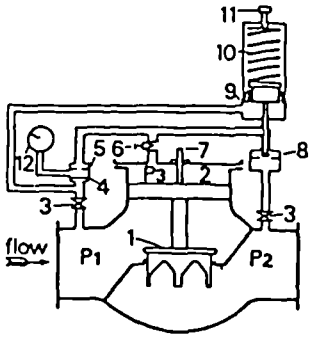

1 Valve Element
2 Upper Cylinder
3 Isolating Cocks
4 Strainer
5 Orifice
6 Needle Cock
7 Indicator
8 Relay Valve
9 Diaphragm
10 Spring
11 Adjusting Screw
12 Pressure Gauge

a) Valve No. 1310 Standard Valve with manually operated relay valves

When the inlet pressure P1 becomes too high to balance the spring load, the relay valve tends to open, allowing pressure P3 to diminish so that the main valve tends to open, thus reducing P1 to the pre-set value.

When used in the Sustaining application, if P1 becomes too low to balance the spring load, the relay valve closes, P3 increases, the main valve closes and P1 rises again to the pre-set value

b) Operation

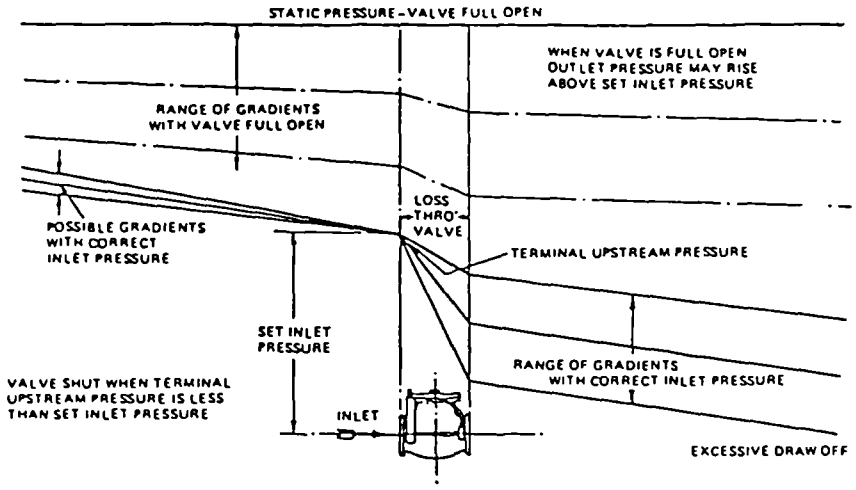

c) Valve No. 1310 Pressure Sustaining Valve Hydraulic Diagram

Fig. 4.2. Pressure Sustaining Valve. Design and operational features, from Glenfield & Kennedy Ltd., Pub. 215/R3.

on the relative values of the pressures at the inlet, outlet and upper cylinder (in Fig. 4.1.a.: P1, P2 and P3, respectively). This component (the valve element) allows the valve to move from a fully open position, with a minimum head loss (component 1 up, see Fig. 4.1.a.), to a fully closed position (component 1 down) with a maximum head loss.

b) Relay system.

The relay system allows the operator to set a pre-specified pressure to be maintained, either at the inlet or outlet of the valve (depending if we are dealing with a PSV or a PRV). This relay system consists of a small relay valve (component 8 in Fig. 4.1.a.), which is operated with a spring (component 10 of Fig. 4.1.a.), whose tension is set via an adjusting screw (component 11 in Fig. 4.1.a.). The screw can be operated by hand (local control mode) or via an electric motor (remote control mode). The force produced by the spring tension acts against the pressure being controlled (either downstream or upstream of the valve), opening or closing the relay valve when the controlled pressure differs from the pressure produced by the spring. A reinforced synthetic rubber diaphragm (component 9 in Fig. 4.1. a.) allows the controlled pressure to be applied directly against the compressed spring.

c) Connecting piping and fittings.

The inlet, outlet and upper cylinder of the valve, and the relay system, are connected by a series of small pipes and

valves. A change in their connectivity implies a change in the objective of the control valve, transforming the basic globe valve body into a PRV, a PSV, altitude valve, constant flow valve or a combination of some of them. This flexibility provided by the connecting piping system, added to the fact that the pressure settings can be adjusted on-site or by remote control, makes this type of device a very helpful piece of hardware in any efficiently operated water distribution network.

a) Pressure Reducing Valves (PRV's).

A PRV is a pressure controlling device designed to perform the following duties:

- Maintain a constant downstream pressure when the upstream pressure exceeds a pre-established pressure setting.
- Avoid reverse flow when the downstream pressure becomes higher than the pressure setting and/or when the inlet pressure becomes less than the outlet pressure .

The first objective is met via the variable head loss introduced by the "valve element", as explained before. Figure 4.1.b. explains how the PRV reacts to outlet pressure variations, different from the valve setting, adjusting the position of the valve element (component 1 in Fig. 4.1.a.), until the head losses within the valve produce the desired outlet pressure. In this operational mode, the PRV is said to be in the "active mode".

The second objective is met by the PRV being fully closed, acting in fact as a check valve and preventing backflow or backpressure. This is the "check valve mode" of operation of the

PRV. This operational mode is achieved in two situations:

i) The outlet pressure (P2, see Fig. 4.1.a.) is greater than the pressure setting; then, the difference between spring tension and outlet pressure P2 is acting upwards, closing the relay valve (component 8 in Fig. 4.1.a) and increasing the pressure in the upper cylinder (P3 in Fig. 4.1.a.). As a result of a greater P3, the valve element moves downwards, closing the valve.

ii) The outlet pressure (P2 in Fig. 4.1.a.) is lower than the setting pressure, but greater than the inlet pressure (P1 in Fig. 4.1.a.). The relay valve keeps open and $P1 < P3 < P2$, then the pressure in the upper cylinder is greater than the inlet one (P1) and the PRV closes.

A third situation arises when the inlet pressure is less than the pressure setting, but greater than the outlet pressure. In this case the PRV operates fully open in its "inactive mode", introducing a minimum head loss into the system. In this particular situation, because P2 is lower than the setting pressure, the relay valve remains open and, then, $P1 > P3 > P2$ which means that the valve element tends to stay fully open.

Figure 4.1.c. explains graphically all the possible operating modes of a PRV and shows the corresponding pressure profiles.

As a result, the head losses through the PRV are essentially variable. When the PRV is fully open, this introduces a minimum local head loss, while, when in the active mode and check valve mode, the PRV can be understood as a variable head loss device. This feature is shown in Figure 4.3.

Another way of understanding the PRV's behaviour, is by plotting both the inlet (H_i) and outlet (H_j) pressures simultaneously, as shown in Figure 4.4, for a constant positive flow through the valve.

In the operating point "1" of Fig. 4.4 ($H_i < H_{setting}$) the valve is fully open, and the difference between the inlet and outlet pressures depends only on the flow (or velocity) and the minimum head loss characteristic coefficient (α_o) of the valve. This coefficient is generally of the order of 5 to 10 velocity heads.

In the operating point "2" of Fig. 4.4 ($H_i = H_{setting} + h_1$), h_1 is equal to the local head loss produced through the valve in the inactive mode (wide open). At this point, as H_i increases, the valve starts closing, increasing its internal head loss in order to maintain a pre-specified setting.

In the operating point "3" ($H_i > H_{setting} + h_1$), H_j is maintained at $H_{setting}$ via extra head losses produced by closing the main valve.

Figure 4.4 is valid for positive constant flows only, that is to say, flows from the specified initial to final node.

A simple graphical representation of a PRV, involving the main variables H_i, H_j, Q_{ij}, $H_{setting}$ and α_{ij} has not been found in the literature. Figures 4.3 and 4.4 involve only a partial representation of the PRV's behaviour. An attempt to represent most of the variables involved is provided by Figure 4.5, in a tri-dimensional plot.

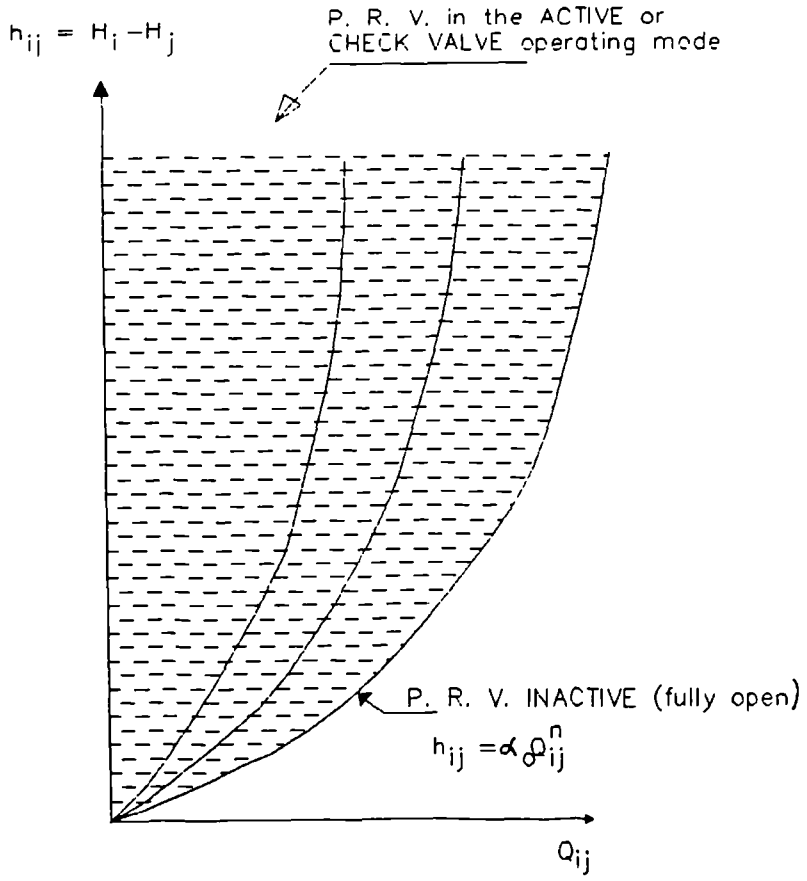

Fig. 4.3. Feasible head loss/flow region for a pressure reducing valve. (For a variable flow).

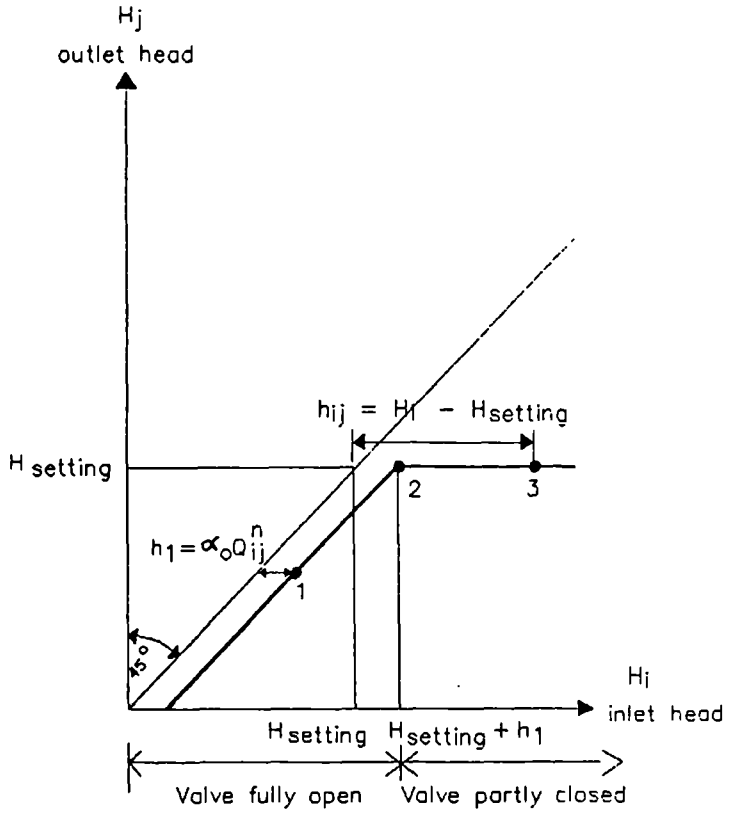

Fig. 4.4. Relationship between inlet and outlet heads in a pressure reducing valve. (For a constant flow).

Figure 4.5 is valid for positive constant flows only. In the horizontal plane, H_i versus H_j, we have the previous Figure 4.4.

When $H_i < H_{setting} + h_1$, the PRV is in the active mode (fully open), and its head loss-flow relationship is described by:

$$h_{ij} = H_i - H_j = \alpha_o Q_{ij}^n$$

where

α_o : a constant corresponding to the minimum head loss coefficient of the valve.

Q_{ij} : the flow which, for Fig. 4.5 has been held constant, then h_{ij} = constant for $H_i < H_{setting} + h_1$.

For $H_i > H_{setting} + h_1$, the valve increases its α_{ij} , i.e. we are in the active mode, and the relationship between h_{ij} and α_{ij} is linear, with a proportionality factor (slope) equal to Q_{ij}^n .

Figure 4.5 has been obtained assuming that a variable head reservoir (head variation is independent of the flow), is connected directly to the upstream node of the PRV. The flow is assumed to be constant and the setting of the PRV is also constant. This is an ideal situation, since when a PRV is inserted in a more complex real network, the upstream head H_i and the flow Q_{ij} are not independent, and the flow is not constant, because a change in the internal head loss of the PRV causes a redistribution of flows in the network.

Figure 4.6 attempts to represent the more general situation, for a <u>variable flow</u>, showing the relationship between H_i and H_j. The coefficient α_{ij} can be incorporated as a third variable, as in the case of Figure 4.5, for showing the non linear effects,

but its practical usefulness is negligible. Figure 4.6 has been obtained from a system where the reservoir is not connected directly to the valve inlet, but through a network; then, the variable inlet pressure is due to the head losses throughout the network. Starting from zero flow, we move from the point "3" (in Fig. 4.6) to the left.

The main difference between Figures 4.6 and 4.4 is that the ascending limb of the curve is no longer a straight line, since now it has to include the effect of the variation of flow.

The practical application of the previous figures is rather limited, but they help to understand the behaviour of the PRV's and also to point out their complexity.

For practical purposes, a lumped representation of the response of the network to changes in the internal resistance of the PRV's can be obtained by plotting the downstream head of the PRV versus the characteristic coefficient α_{ij} ; the result is shown in Fig. 4.7. Two possible situations are clearly differentiated, namely curve "a", where the downstream head is dependent upon the upstream conditions (i,e. dependent on the internal head loss in the PRV), whereas in curve "b", the system characteristic does not allow the downstream head to be dependent on the upstream conditions. The latter is typically the case when the downstream conditions produce heads greater than the PRV setting, and the valve tends to close; in other words, the PRV is controlled by the downstream conditions rather than the upstream ones; in this case the PRV cannot produce the desired $H_{setting}$ at its outlet and simply closes.

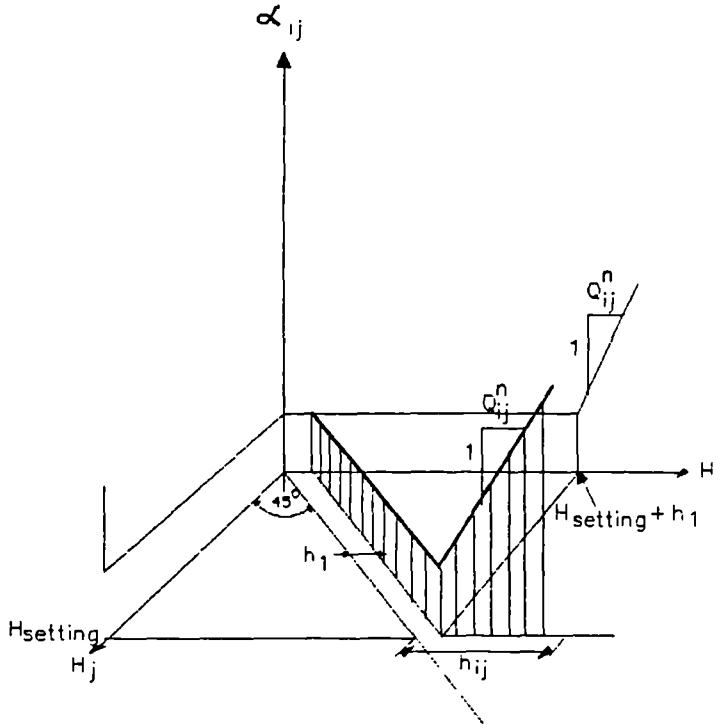

Fig. 4.5. Relationship between inlet and outlet head, and α_{ij} in a pressure reducing valve. (For constant flow).

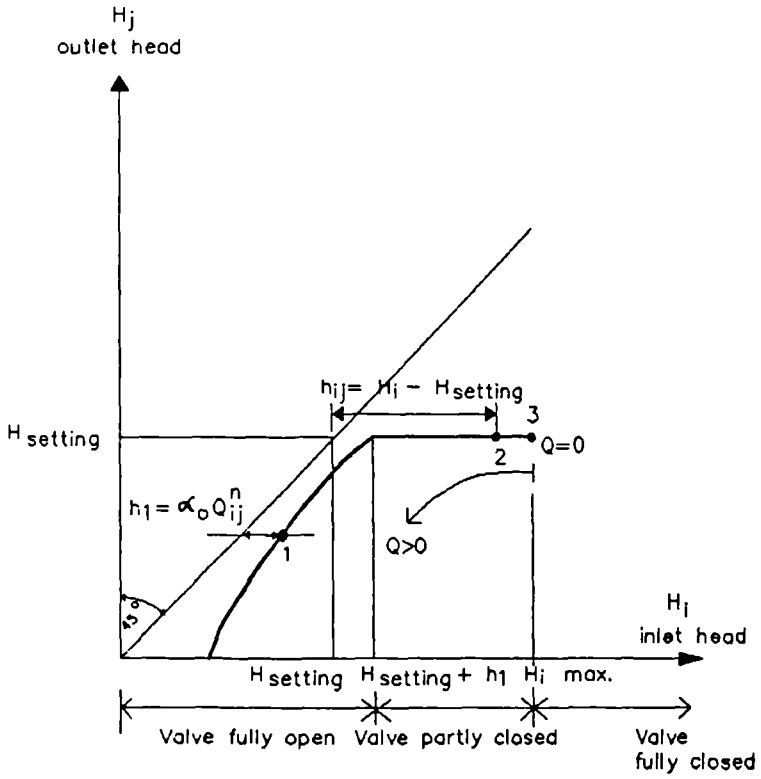

Fig. 4.6. Relationship between inlet and outlet heads in a pressure reducing valve. (For a variable flow).

In the case when the outlet pressure is dependent on the head loss through the valve, Fig. 4.7 clearly suggests how can we find the value of α_{ij}^* which produces an outlet pressure equal to $H_{setting}$.

Essentially, to include PRV's in our model, we shall be using the feature represented in Fig. 4.7 to balance the network iteratively. This procedure shall be explained in more detail in subsequent sections.

b) Pressure Sustaining Valves (PSV's).

A PSV is a pressure controlling device designed to perform the following duties:

- Maintain a constant minimum upstream pressure regardless of the downstream pressure.
- Avoid reverse flows when the upstream pressure becomes lower than the pressure setting and/or when the inlet pressure becomes less than the outlet pressure .

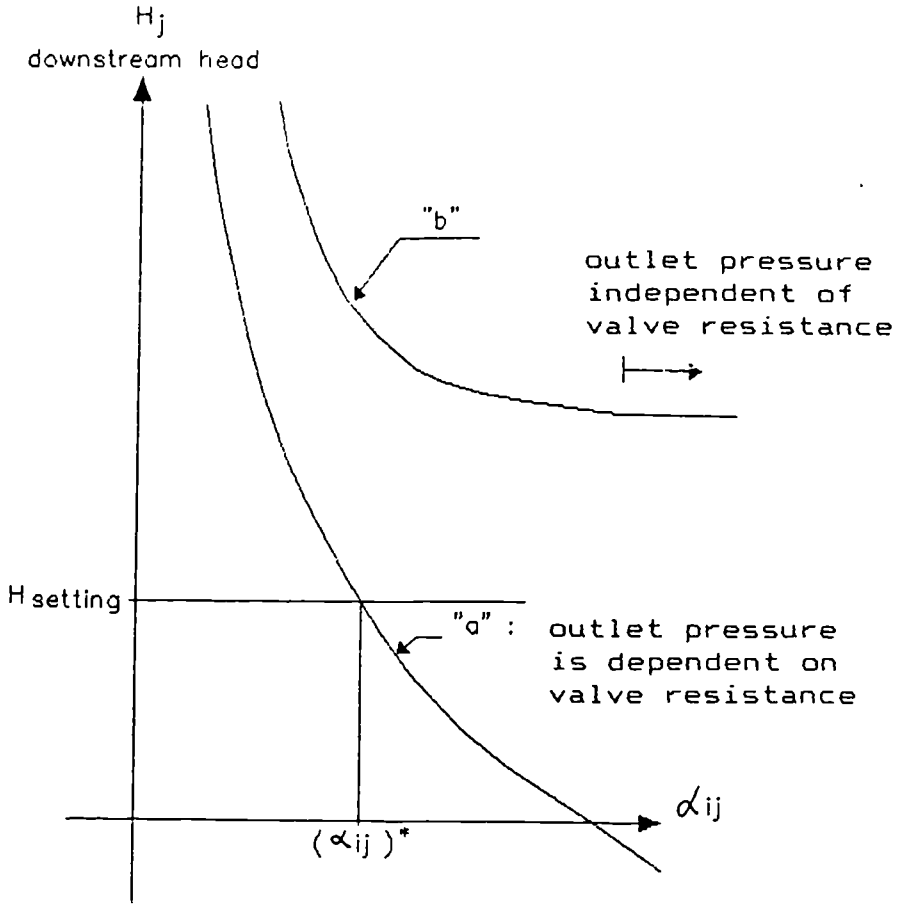

Fig. 4.7. Response of the network at the downstream end of a PRV, to variations in the resistance characteristic coefficient α_{ij}.

The first objective is met via the variable head loss introduced by the "valve element", as explained before in the case of PRV's. Figure 4.2.b. explains how the PSV reacts to outlet pressure variations, different from the valve setting, adjusting the position of the valve element (component 1 in Fig. 4.2.a.), until the head losses within the valve produce the desired inlet pressure. In this operational mode, the PSV is said to be in the "active mode".

The second objective is met by the PSV being fully closed, acting in fact as a check valve and preventing backflow .This is the "check valve mode" of operation of the PSV. This operational mode is achieved in two situations:

i) The inlet pressure (P1, see Fig. 4.2.a.) is lower than the pressure setting; then, the difference between spring tension and inlet pressure P1 is acting downwards, closing the relay valve (component 8 in Fig. 4.2.a) and increasing the pressure in the upper cylinder (P3 in Fig. 4.2.a.) and, as a result, closing the valve element downwards.

ii) The outlet pressure (P2 in Fig. 4.2.a.) is greater than the inlet pressure (P1 in Fig. 4.2.a.) and lower than the inlet pressure setting. The relay valve keeps open and P1 < P3 < P2, then the pressure in the upper cylinder is greater than the inlet one (P1) and the PSV closes.

A third situation arises when the inlet pressure is greater than the pressure setting, and greater than the outlet pressure. In this case the PSV operates fully open in its "inactive mode", introducing a minimum head loss into the system. In this particular situation, because P1 is greater than the setting pressure the relay valve remains open and, then, P1 > P3 > P2 which means that the valve element tends to stay fully open.

Figure 4.2.c. explains graphically all the possible operating modes of a PSV and shows the corresponding pressure profiles.

As a result, similar to the case of the PRV's, the head losses through the PSV are essentially variable and equally complex to

represent graphically. Figure 4.8 is the equivalent of Figure 4.4 for the case of a PSV. We shall omit the rest of the figures, corresponding with those displayed in the case of a PRV, and we shall show only the corresponding lumped schematic representing the response of the system at the inlet of the PSV versus the head loss characteristic parameter α_{ij}, which is shown in Fig. 4.9.

4.3. Existing models for pressure controlling devices.

Although it is known that many of the network analysis codes used in consultancy work are able to deal with pressure controlling devices, the open literature provides only a few references on the modelling of such devices.

In the early 1970's, Zarghamee (1971), following a nodal approach, explicitly considered the presence of PRV's. He actually modelled the set PRV plus the pipe in which the device was inserted and, for the case when the PRV is next to the upstream node "i", the model is:

$$Q_{ij} = R_{ij} (H_{setting} - H_j)^{1/n} \quad \text{when } H_i \geq H_{setting} \geq H_j \qquad (4)$$

where:

R_{ij} is the conductance of the pipe branch between the outlet of the PRV and the downstream node "j".

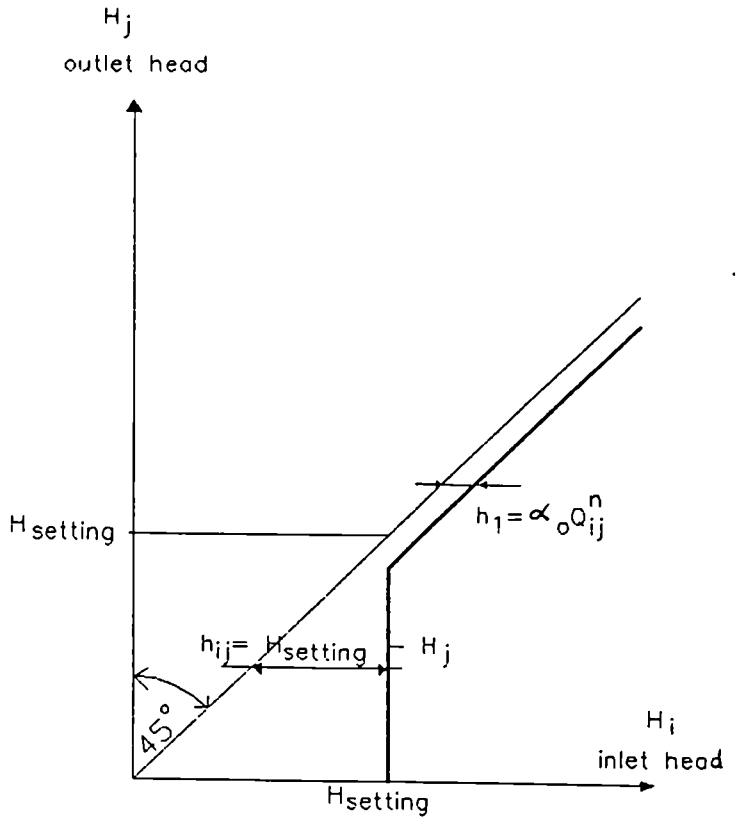

Fig. 4.8. Relationship between inlet and outlet heads in a pressure sustaining valve. (For constant flow).

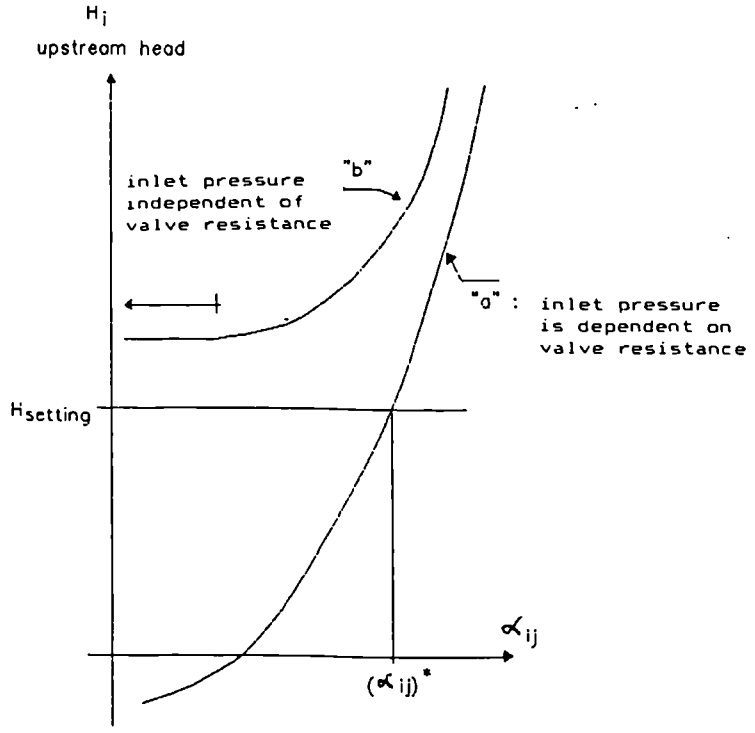

Fig. 4.9. Response of the network at the upstream end of a PSV, to variations in the resistance characteristic coefficient α_{ij}.

When $H_j < H_i < H_{setting}$, then $H_{setting}$ must be replaced by H_i in equation (1), and the same model can be used to represent the PRV's behaviour. It is implicit that the valve closes when $H_i < H_j$ or $H_j > H_{setting}$ (i.e. $Q_{ij} = 0.0$).

Zarghamee (1971) reported a successful application of his method to a water distribution system in Teheran, containing 9 PRV's and located in a steep area of the city. Although some details are not completely clear from the paper, Zarghamee did get convergence in two study cases (convergence is reported to be slower when pumps are operating). No problems were reported due to the presence of the PRV's.

Donachie (1974), within a nodal formulation, proposed a two stage process for modelling the PRV's. In the first stage of the iterative procedure, when the difference between successive heads is greater than 1 m., the outflow is computed with an upstream pressure p_i^*, such that:

$$p_i^* = \min (p_i, p_s) \qquad (5)$$

where:

p_i: is the actual upstream pressure.

p_s: is the downstream pressure setting of the PRV.

In the second stage (closer to the final solution), the PRV is considered as a fixed outlet pressure device, i.e.: with a

constant outlet pressure equal to p_s, provided that $p_i > p_s$.

Jeppson (1976) and Jeppson and Davis (1976), reviewed all the modifications needing to be introduced in the different formulations of the network analysis equations in order to include PRV's. Basically, the PRV's are modelled by splitting the branch where the PRV is, inserting a pseudo-reservoir whose head is equal to the PRV setting and imposing flow continuity over the two halves of the resulting pieces of pipe, as shown in Fig. 4.10.

As a result, the introduction of the pseudo-reservoir in the network analysis equations affects the different formulations, in a way which is summarised in Table 4.1, using the notation of Fig. 4.10 and considering the usual head loss/flow model:

$$h_{ij} = \alpha_{ij} Q_{ij}^{n} + \beta_{ij} \qquad \text{(with } \beta_{ij} = 0 \text{ for pipes)}$$

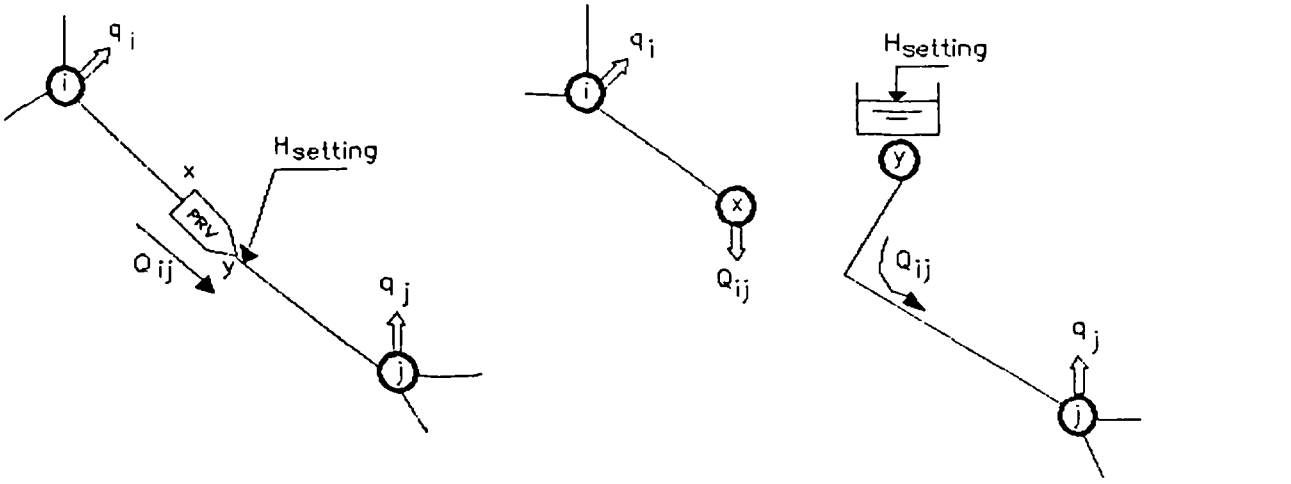

a) Real Pressure Reducing Valve. b) Pressure Reducing Valve modelled as pseudo-reservoir.

Fig. 4.10. Modelling PRV's as pseudo-reservoirs.

Table 4.1. Summary of effects of PRV's in different formulations of network analysis equations [following proposition of Jeppson (1976) and Jeppson and Davis (1976)].

Original set of equations (no PRV's)	Modified set of equations (with PRV's)
Q-equations: (NN-NS+NL eq.) a) Nodal flow continuity: $\sum_{k} Q_{ik} = q_i$ i=1,..,NN-NS b) Loop head continuity: $\sum_{l} \alpha_{ij} Q_{ij}^n = 0$ l=1,.,NL	a) Nodal flow continuity: same as in the original set b) Loop head continuity: $\sum_{l} \alpha_{ij} Q_{ij}^n = 0$ l=1,.,(NL-NPRV) (same as before) $\sum_{l"} \alpha_{ij} Q_{ij}^n = H_{setting} - H_{reservoir}$ l"=1,...,NPRV (changed, see Note 1)
H-equations: (NN-NS eq.) Nodal flow continuity: $\sum_{k} Q_{ik} = \sum_{k} ((H_i - H_k)/\alpha_{ij}))^{1/n} = q_i$ i=1,...,NN-NS	Nodal flow continuity: ($H_i > H_{setting} > H_j$) as before, except: a) Node "i": $\sum_{k} Q_{ik} = \sum_{k} ((H_i - H_k)/\alpha_{ik})^{1/n} + ((H_i - H_x)/\alpha_{ix})^{1/n} = q_i$ i=1,...,NN-NS (see Note 2+Fig. 4.10) b) Node "j": $\sum_{k} Q_{ik} = \sum_{k=i} ((H_j - H_k)/\alpha_{ik})^{1/n} + ((H_{setting} - H_j)/\alpha_{yj})^{1/n} = q_i$ j=1,...,NN-NS (see Note 3+Fig. 4.10) Additional flow continuity equation: $Q_{ix} = Q_{yj} = Q_{ij}$ i.e.: (see equ. 10) $(H_i - H_x)/\alpha_{ix} = (H_{setting} - H_j)/\alpha_{yj}$
δQ-equations: (NL eq.) Loop head continuity: $\sum_{l} \alpha_{ij}(Q_{ij} + \delta Q_l \pm \delta Q_N)^n = 0$ l=1,...,NL (see Note 4)	Loop head continuity: $\sum_{l} \alpha_{ij}(Q_{ij} + \delta Q_l \pm \delta Q_N)^n = 0$ (same as before) l=1,...,(NL-NPRV) $\sum_{l"} \alpha_{ij}(Q_{ij} + \delta Q_l \pm \delta Q_N)^n = H_{setting} - H_{reserv}$ l"=1,...,NPRV (changed)

Notes: (0) NN = total number of nodes.
NS = number of source-nodes.
NL = number of loops (or energy paths).
NPRV= number of PRV's.
(1) l" considers a pseudo-loop replacing the original loop broken-down by the introduction of the PRV and linking the pseudo-reservoir with a real reservoir .
(2) α_{ik}: α corresponding to the pipe from node "i" to "k".
α_{ix}: α corresponding to the pipe from node "i" to "x".
H_x : head at the inlet of the PRV.
(3) α_{yj}: α corresponding to the pipe from node "y" to "j".
(4) δQ_N: flow correction in neighbouring loops.

As it is clear from Table 4.1 that every PRV implies that the original pipe (from nodes "i"- "j") is split up into two parts, we need to restore one loop equation for every PRV introduced. For this purpose, it is necessary to link every PRV with some existing (real) reservoir, create a path between them, and write down the equation establishing that the head loss in this path must be equal to the difference between the pseudo-reservoir head ($H_{setting}$ corresponding to the PRV) and the head of the real reservoir.

As far as the H-equations are concerned, the model proposed by Jeppson and Davis (1976) introduces an additional unknown (the head at the inlet of the PRV: H_x) for each PRV, but also introduces an additional flow continuity equation :

$$Q_{ix} = Q_{yj} = Q_{ij} \tag{6}$$

because

$$Q_{ix} = ((H_i - H_x)/\alpha_{ix})^{1/n} \tag{7}$$

$$Q_{yj} = ((H_{setting} - H_j)/\alpha_{yj})^{1/n} \tag{8}$$

then, from equation (6):

$$[(H_i - H_x)/\alpha_{ix}]^{1/n} = [(H_{setting} - H_j)/\alpha_{yj}]^{1/n} \tag{9}$$

or

$$(H_i - H_x)/\alpha_{ix} = (H_{setting} - H_j)/\alpha_{yj} \tag{10}$$

Jeppson (1976), and Jeppson and Davis (1976) gave a number of examples on how to introduce PRV's into the networks using these procedures. We have tried to reproduce them, but we have not been able to attain the same results. This disagreement will be discussed in a subsequent section.

Lekane (1979) followed a similar approach to that proposed by Zarghamee (1971) in modelling PRV's within a nodal formulation. He also reported the results of the application of the method to a small network (18 nodes and 24 branches with 2 PRV's). Another application to a bigger network (314 nodes and 424 branches) is also mentioned.

Lekane (1979) raised the question of the uniqueness of the solution of the steady state, especially when dealing with devices like PRV's, CV's and pumps. He pointed out that, according to experience, a unique solution can be expected. Lekane also mentioned the fact that the presence of PRV's turns the symmetric Jacobian matrix into a non symmetrical one. This is relevant from the computational viewpoint.

Collins (1980), in discussing several common possible causes of difficulties in network analysis, drew attention to the uniqueness problem, especially when dealing with a network with control devices. He concluded, based on a simple example of a network with 7 nodes (3 of them reservoirs) and 6 branches (3 pumps, 2 PRV's and one gate valve), that no definitive answer has been obtained for this problem. We shall discuss this interesting case in more detail later on. Collins also questioned the validity of the usual procedure for dealing with multiple pressure controlling devices within an iterative solution, where an initial status is assumed for these devices, and a checking procedure is implemented at the end of the iterations, in order to prove that the control devices are indeed working in the assumed conditions. Collins queries if such a check should be

carried out at the beginning of the iterations or after having reached a certain degree of convergence (if so, what is the "right" degree of convergence ?); clearly, because in the first iterations, the network can be working in conditions that are very far from the final ones, the checking procedure can lead to a completely wrong solution, if it leads to any one at all (depending on the termination criteria).

Chandrashekar (1980), based on graph theory concepts, developed the models for introducing PRV's, CV's and booster pumps into the network analysis equations (nodal approach). Basically, the model for PRV's used by Chandrashekar is the same as that used by Jeppson (1976), adding a pseudo-reservoir whose head is equal to the PRV setting. This author also gave some warnings about the possibility of not finding a solution via the application of this method (and others reported in the literature); he suggested that an oscillatory behaviour and slow convergence can be expected due to numerical problems, although he did not encounter such problems . Chandrashekar also gave some examples of the application of this procedure; we agree with his results.

Gessler (1981), in a review paper, recognised the complexity added by PRV's in the network analysis, especially when dealing with a number of devices simultaneously. According to his review "at the present time there is no generally accepted procedure for handling PRV". Gessler insisted that in introducing PRV's within a nodal formulation, the symmetry of the Jacobian is lost and that, within a loop formulation, the procedure "is extremely cumbersome" due to the fact that the state of these devices

depends on the heads at the nodes, something which is determined at the end of the process in the loop approach. Consequently, Gessler recommended a nodal formulation. He also gave a couple of detailed examples on how to include PRV's; we agree with his results, as discussed in a subsequent section. Finally he addressed the problem of uniqueness, recommending a reassessment of the physical problem whenever mathematical and numerical problems are found.

In summary, from the literature reviewed, it becomes apparent that there are some common characteristics in many of the existing models for handling pressure controlling devices. All the authors reviewed, with the only exception of Gessler (1981), describe the behaviour of the PRV in conjunction with the pipe where it is inserted. Actually, in so doing, they do not describe the PRV itself but its effect on the pipe.

All the referenced authors deal only with PRV's, without even mentioning PSV's or other pressure controlling devices, like altitude valves, constant flow valves, etc. As it can be seen later on, in the section corresponding to the examples found in the literature, not a single example dealing with PSV's was reported and, more importantly, there is no example dealing with PRV's and PSV's simultaneously. The reason for this may lie in the fact that, roughly speaking, PSV's are dealt with in a similar way to PRV's, but instead of the maximum downstream pressure we are concerned with the minimum upstream pressure. No reason whatsoever can explain the lack of evidence on the behaviour of real networks having more sophisticated controlling devices.

All the authors reviewed, with the exceptions of Jeppson (1976) and Jeppson and Davis (1976), referred to a nodal formulation of the set of equations. The attempt of Jeppson and Davis is commendable, in the sense that they focused on all the possible formulations.

Gessler (1981) recommended the nodal approach as the most suitable for dealing with networks including PRV's. This seems to be implicitly accepted by most of the authors reviewed, except Jeppson and Davis (1976). This is in clear contradiction with the conclusion drawn by Wood (1981a), who recommended either the simultaneous path method (loop approach) or the linear theory method.

The question of lack of symmetry in the Jacobian matrix, when following a nodal approach, when considering the PRV in conjunction with the pipe, is relevant from the storage point of view. As far as the solution of the linear system of equations is concerned, the symmetry issue is relevant from the stability point of view, and also because it is known that an efficient method for solving symmetric linear systems of equations does not need to be as efficient when applied to a non symmetric system (if applicable at all).

Although it has not been emphasised in the literature, it is evident that all the methods proposed for dealing with PRV's need to re-assemble the structure of the matrix of the linear system, every time a device is found to be working in the wrong way. This is, for example, the case of a CV, which must be closed

because its downstream head is found to be greater than the upstream one; this implies eliminating the branch containing the CV, re-formulating the topology and re-building the corresponding Jacobian matrix. The same re-shaping of the equations is necessary in the case of the PRV's, when sometimes (in the nodal approach) an additional flow continuity equation must be added to the original set.

Also relevant are Collins (1980) worries about the risks of changing the status of a PRV at early stages within the iterative procedure, when convergence has not been fully achieved. This seems to be a common problem in existing codes, although not openly discussed in the literature.

Finally, the question of the uniqueness of the solution was raised by some authors [Lekane (1979), Collins (1980), Chandrashekar (1980) and Gessler (1981)], leaving a shadow of uncertainty over the solutions when dealing with general systems with multiple PRV's and other devices simultaneously.

All these ideas led us to a feeling of dissatisfaction about the way pressure controlling devices are handled at the present moment in the open literature, and thus motivated a search for an alternative, completely different, approach, which hopefully can cope with the disadvantages and uncertainties of the reported methods. Also, we are looking for a method able to take full advantage of the positive attributes of the gradient method.

4.4. Proposed model for pressure controlling devices.

4.4.1. Need for an alternative model.

Due to all the shortcomings affecting the modelling of pressure controlling devices in the existing methods, a new approach is needed, especially in the context of the gradient method.

Putting the existing methods in perspective, and considering the physical behaviour of the pressure controlling devices, it is clear that the fact that all these valves are variable resistance devices is not explicitly considered in the existing models. All of them are based on a post-analysis check of whether the device is working in the assumed mode or not and, as a result, the existing approaches are more combinatoric than physical, in the sense that all the possible combinations of status may have to be checked.

Also, the fact that the state of the pressure controlling devices is influenced, and indeed determined by the hydraulic system (i.e. the network as a whole), is not explicitly taken into account in the dynamics of modelling pressure controlling devices. We believe that this can lead to some misunderstandings of the way pressure controlling devices work. Clearly, the fact that we can fix the PRV setting does not necessarily mean that this is the pressure we are going to have, since in the final analysis this will depend on the system characteristics.

We shall follow what we believe is a more physically meaningful approach to modelling pressure controlling devices, aiming at a robust algorithm on which we can rely and with which a unique

solution can be obtained. We believe that because pressure controlling valves are in essence variable resistance devices, consequently dissipative devices, their steady state solution must be unique. What we shall try to do in our model is to follow, as closely as possible, what we think should be the response of the physical water distribution network.

4.4.2. Development of the computer program .

At the present moment, PRV's, PSV's and CV's have been introduced into our computer program for the gradient method. In the future new devices can be introduced using the same basic model explained in the following paragraphs. For PRV's, PSV's and CV's we define the following possible operational modes (or "STATUS" in the notation used in the program):

- Inactive mode: valve fully open, this corresponds to the valve having a minimum resistance characteristic parameter α_o. This corresponds to STATUS = 0 in the computer program.
- Active mode: this corresponds to the closed mode for a CV (this is, for CV's, STATUS = 1 in our program). For PRV's and PSV's this mode has two sub-modes:
    * Partly closed mode: the valve has a resistance characteristic parameter greater than α_o and is not completely closed, so that a flow through the valve is possible. This corresponds to STATUS = 1 in the computer program.
    * Fully closed mode: no flow can pass through the valve and its characteristic resistance parameter is set to an "infinite" value. This sub-mode corresponds

to STATUS = 2 in the program.

In addition to its use for pressure controlling valves, this STATUS index of the branches is used to introduce closed pipes, on/off pump switches, with minor changes in the data, and without having to re-define the topology of the whole network.

We also define the imbalance in each pressure controlling device, which is proportional to the force that will tend to move the valve from one operational status to another:

- For CV's this imbalance is simply defined as :

$$X = |H_j - H_i|$$

- For PRV's the imbalance may be:

$X = |H_{setting} - H_j|$ when the PRV is partly open or

$X = |H_j - H_i|$ when the PRV is fully closed.

- For PSV's the imbalance may be:

$X = |H_{setting} - H_i|$ when the PSV is partly open or

$X = |H_j - H_i|$ when the PSV is fully closed.

Our model operates in two main stages:

i) Detection stage : This aims at determining which devices are working in a status different to that originally assumed; for example, a CV with current STATUS = 0 and whose outlet head is higher than the inlet head. Also, we determine the two maximum imbalances, say X and X^*, and the indices of the devices corresponding to these imbalances, say I and I^*. On finishing the detection throughout the whole network, the index corresponding to the most imbalanced valve and its imbalance X, and also the next most imbalanced one (if any) are known. When there is only

one valve out of balance, X^* is set equal to the accuracy specified for the problem, which is the maximum head difference between the outlet head and the setting for a PRV (or inlet head in the case of a PSV). In addition, this stage identifies what is the kind of action that has to be taken in the correction stage.

ii) Correction stage : In modifying the internal resistance of the device, this part of the algorithm tries to match the controlled head (outlet head in PRV's, inlet head in PSV's, etc.) with the setting. For CV's the correction stage simply changes the characteristic resistance parameter to α_o if the valve needs to be inactive, or to "infinite" if the CV ought to be closed; the index describing the status of the CV is also changed accordingly. For PRV's and PSV's the matching procedure is based on the lumped curve presented in section 4.2 (Figure 4.7 for the PRV's and Figure 4.9 for the PSV's). This explanation will relate to the case of the PRV's only, because the case of PSV's is completely similar.

The correction stage for PRV's and PSV's operates in the following way. Let us assume that α_1 is the current resistance characteristic parameter of the PRV we are trying to correct at this stage (i.e. this is the maximum imbalanced device). Let us also represent this situation in Figure 4.11. The lumped curve suggests that, for finding α^*, the α which matches outlet head and setting, a Newton procedure can be implemented, starting at the point α_1. At this point let $X_1 = |H_1 - H_{setting}|$ be the current imbalance. Since the analytical expression of the function

represented by the lumped curve is not known, the derivative of that function must be computed numerically. To do so, we perturb α_1 by a small quantity, say $\delta\alpha$, leading to $\alpha_2=\alpha_1 + \delta\alpha$. At this point the evaluation of the outlet head for the perturbed α_2 is needed; this is done by running the program and determining the corresponding head. Let us call the new outlet head H_2, of course the imbalance at this point becomes $X_2 = |H_2-H_{setting}|$, then the derivative we are looking for can be approximated by:

$$f' \approx (H_1 - H_2)/(\alpha_1 - \alpha_2) \qquad (11)$$

Hence, the new approximation for α^* can be computed using Newton's method as:

$$\alpha_3 = \alpha_1 - [(H_1-H_{setting}) / f']. \qquad (12)$$

With this new α_3, a new evaluation of the outlet head is needed, which means that we have to run the main program again to produce a new head, say H_3, which allows us to determine the imbalance at this point $X_3=|H_3-H_{setting}|$ which must be compared with the maximum admissible tolerance. At this point of the procedure, we are faced with two main alternatives, namely carry on the Newton's iterations until H_3 is sufficiently close to $H_{setting}$, or stop the iteration when X_3 becomes smaller than X^* (the second maximum imbalance determined at the detection stage); since because there is another control valve which is more imbalanced than the current one, there is no point in carrying on the Newton iterative procedure on up to the limit. We chose the second alternative, which was found to be the most adequate, in order to avoid wasting computational resources. Actually, we should compute the current value of X^* after each change in α,

but this was not found worthwhile during the development of the program. If we find that that we have to stop the Newton iterations, we go back to the detection stage, in order to check if any other device has gone out of balance. Checking the valve status is not as computationally expensive as re-running the program.

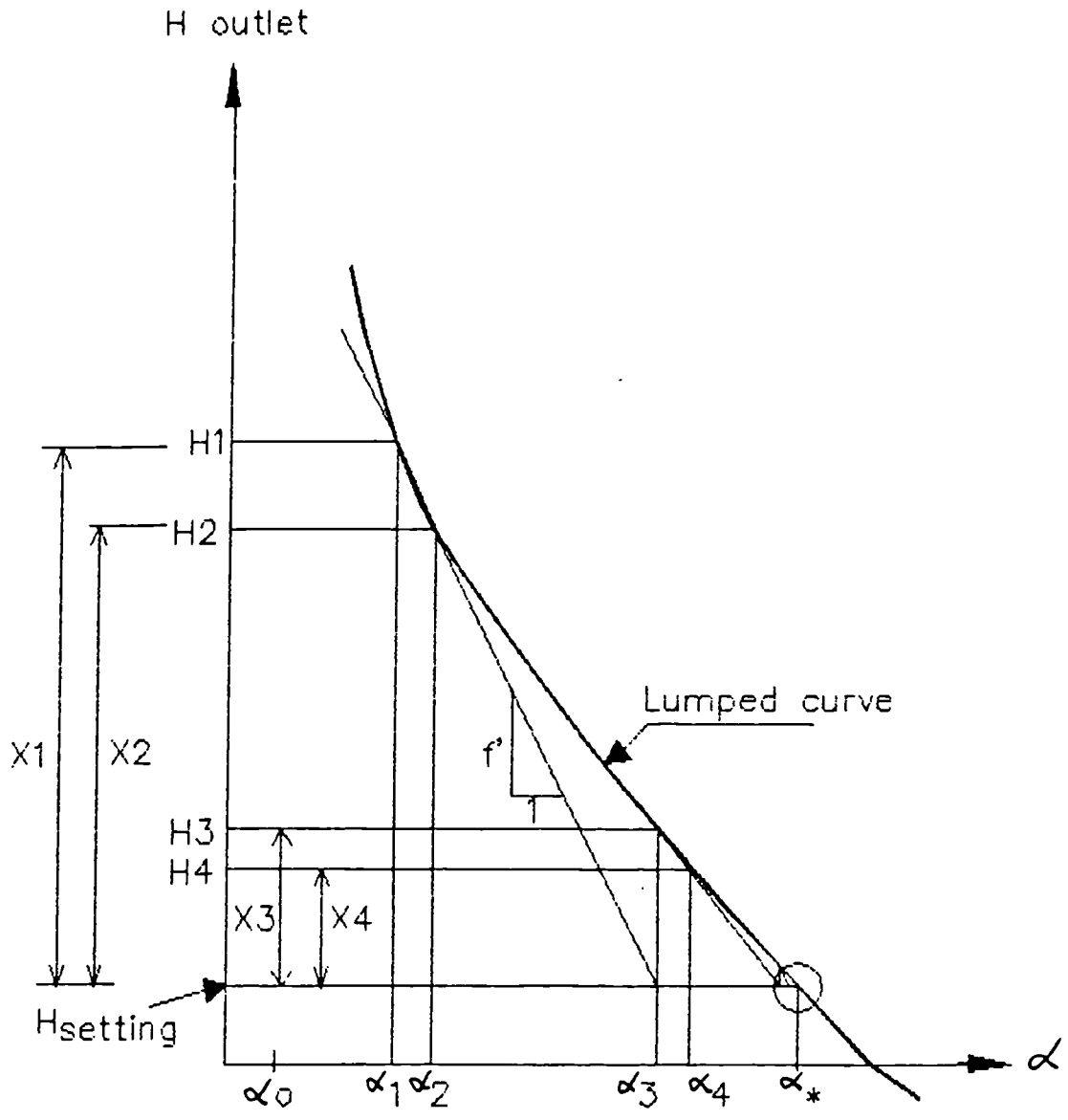

Fig. 4.11. Correction of the resistance characteristic parameter (α), for a PRV, based on the lumped curve.

In summary, the method for determining the resistance parameter α^* uses the network analysis routine intensively. As far as the network analysis program is concerned, the PRV's and PSV's are modelled as fixed head loss/flow characteristic devices, since the changes needed in the resistance (i.e. the sequence $\alpha_1, \alpha_2, \ldots, \alpha^*$) are handled outside the analysis routine, as shown in Figure 4.12.

Figure 4.12 clearly suggests that the proposed approach for modelling regulating devices can be implemented with any network analysis algorithm, since we consider the correction of the resistance parameter α as an independent process from the network analysis. This means that the proposed algorithm for modelling pressure regulating devices can be implemented with any other network analysis algorithm. From the theoretical point of view, this also means that the pressure regulating devices can be considered as any other resistive (dissipative) device, hinting that no problem with the uniqueness and existence of the solution should be expected when following this approach.

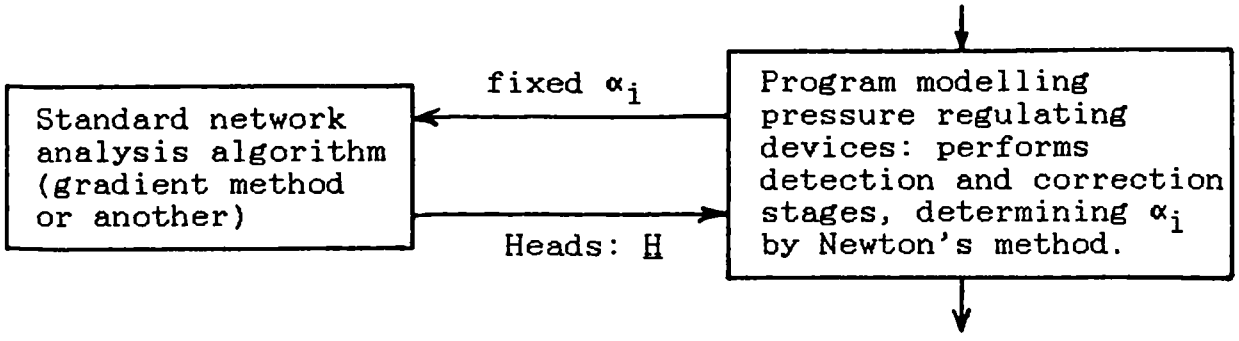

Fig. 4.12. Interaction between pressure regulating device model and the standard network analysis algorithm.

To establish the robustness of our proposed model, we have run it with a number of examples reported in the literature, and the results are detailed and analysed in the next section.

4.5. Comparison between the results given by the proposed model and some examples found in the literature.

In order to compare some of the results produced by some of the authors reviewed in previous sections, we have taken the published data and computed our own results, using a network analysis program based on the gradient method. Table 4.2 is a summary of the comparison between the published results and our results. At the end of Table 4.2. some of our own test examples are also included.

Surprisingly, we have found disagreement between our results and those reported by some authors. In this section we shall analyse in some detail these differences, in order to find out the reasons (if possible) for such discrepancies.

In the rest of this section we shall concentrate on those examples where no agreement was detected.

4.5.1. Example JEPPO, from Jeppson and Davis (1976).

The network with 15 branches and 14 nodes shown in Fig. 4.13, including one PRV, was analysed by Jeppson and Davis (1976) under two possible settings for the PRV:

a) $H_{setting}$ = 149 m

b) $H_{setting}$ = 140 m

Table 4.2. Comparison of results reported in the literature and our results for networks containing pressure control devices.

Example Name	Source (*)	Network Size: Number of Branches	Nodes	Sources	Devices CV	PRV	PSV	Comments
Jepp0	(1)	15	14	2	-	1	-	no agreement
Jepp1	(2)	10	8	2	-	1	-	no agreement
Jepp2	(2)	17	15	2	-	1	-	agreement
Jepp12	(2)	15	13	2	-	2	-	no agreement
Jepp13	(2)	15	13	2	-	2	-	no agreement
Lekane	(3)	24	18	3	1	2	-	agreement
Collins	(4)	6	7	4	-	2	-	no agreement
Chan1	(5)	12	10	1	1	1	-	agreement
Chan2	(5)	12	10	1	1	1	-	agreement
Chan3	(5)	12	10	1	1	1	-	agreement
Chan5	(5)	37	28	2	-	1	-	agreement
Gess1	(6)	14	12	1	-	3	-	agreement
Gess2	(6)	14	12	1	-	3	-	agreement
Gess3	(6)	21	17	3	1	2	-	agreement
Check	(7)	6	6	2	1	-	-	
Prv	(7)	6	6	2	-	1	-	
Psv	(7)	6	6	2	-	-	1	
Prv5	(7)	74	48	4	1	2	2	

(*) Sources:

(1) : Jeppson and Davis (1976)
(2) : Jeppson (1976), pp. 86, 88, 110 and 112
(3) : Lekane (1979)
(4) : Collins (1980)
(5) : Chandrashekar (1980)
(6) : Gessler (1981), pp. 88 for gess1 and gess2, 91 for gess3.
(7) : our test examples.

Note : In some cases, the number of branches or nodes does not coincide with the original source, because we use an initial and final node for every device.

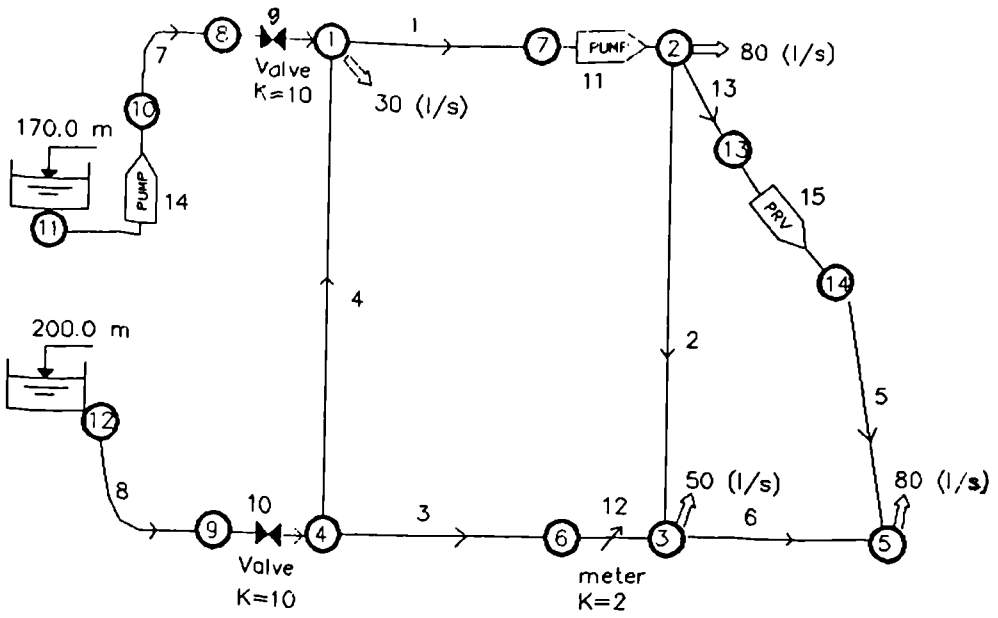

Fig. 4.13. Example JEPP0, from Jeppson and Davis (1976).

The comparison between the results presented by Jeppson and Davis and those computed with our method, corresponding to both cases a) and b), are shown in Table 4.3. Basically we differ from Jeppson and Davis in the operational mode determined for the PRV; thus, when they say that the PRV is active, we find that it is actually closed (in case a) .

According to our findings, the PRV closes for any setting under 151.34 m. This is the limit where the downstream head of the PRV is determined by the system, rather than by the PRV characteristics.

Unless there is a misprint in the data published by Jeppson and Davis (1976), we could not find a reason for the discrepancy.

Table 4.3. Comparison of results presented by Jeppson and Davis (1976) and our results, for example JEPP0.

NODE	PIEZOMETRIC HEADS (M)		
	OUR RESULTS(1)	Jeppson and Davis a)	Jeppson and Davis b)
1	176.259515	168.95	169.02
2	162.834336	153.44	153.89
3	162.200871	153.42	152.96
4	182.390276	173.81	173.76
5	151.239548	147.88	141.88
6	163.404912	(2)	
7	159.146872		
8	176.900400		
9	189.626238		
10	178.033607		
11	170.000000	170.00	170.00
12	200.000000	200.00	200.00
13	162.834336	152.88	153.89
14	151.239548 (3)	149.00	141.88

LINK	FLOWS PER BRANCH (L/S)		
	OUR RESULTS(1)	Jeppson and Davis a)	Jeppson and Davis b)
1	102.0292	108.0	107.0
2	22.0291	2.6	26.9
3	107.9708	102.0	103.0
4	76.9851	67.3	66.0
5	0.0001	25.4	0.0
6	79.9999	54.6	80.0
7	55.0441	70.7	71.0
8	184.9559	169.0	170.0
9	55.0441	70.7	71.0
10	184.9559	169.0	170.0
11	102.0292	108.0	107.0
12	107.9708	102.0	103.0
13	0.0001	25.4	0.0
14	55.0441	70.7	71.0
15	0.0001	25.4	0.0

Notes:
*****
(1) Our results are exactly the same for both cases a) and b).

(2) These values are not given by Jeppson and Davis.

(3) Node 14 corresponds to the outlet of the PRV and the settings are 149 m and 140 m, for cases a) and b), respectively. Link 15 corresponds to the PRV.

4.5.2. Example JEPP1, from Jeppson (1976).

A small network of 10 branches and 8 nodes, including one PRV, was studied to illustrate the different modes of operation of these devices. The schematic of this network is presented in Fig. 4.14 and the comparison of the results obtained here with those of Jeppson is shown in Table 4.4.

Although the numerical results seem to be in agreement, for this particular example, we have the following comments.

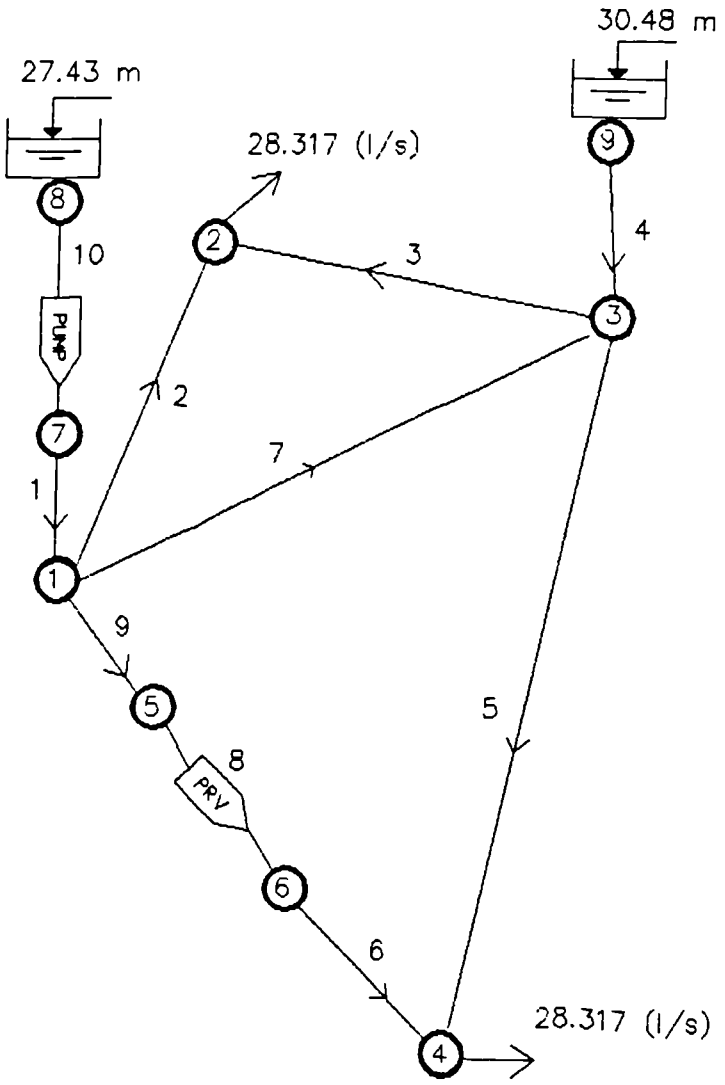

Fig. 4.14. Example JEPP1, from Jeppson (1976), page 86.

Table 4.4. Comparison of the results given by Jeppson (1976) and our results for example JEPP1.

NODE	PIEZOMETRIC HEAD (M)	
	OUR RESULTS	JEPPSON
1	35.740321	35.726
2	29.199594	29.197
3	29.201681	29.197
4	16.756944	17.672
5	35.733260	
6	16.764005 (*)	16.764
7	42.851544	
8	27.431999	27.432
9	30.480000	30.480

LINK	FLOW (L/S)	
	OUR RESULTS	JEPPSON
1	29.0793	29.167
2	27.8774	27.751
3	0.4396	0.481
4	27.5547	27.467
5	27.1839	27.184
6	1.1331	1.161
7	0.0688	0.085
8	1.1331 (**)	1.161
9	1.1331	1.161
10	29.0793	29.167

Notes:

(*) Node 6 corresponds to the outlet of the PRV, the PRV setting was 16.764 m.
(**) Link 8 corresponds to the PRV itself.

The pump characteristic curve used by Jeppson has an ascending limb, which means that we are in one of those cases when two solutions to the problem are possible, depending on the system characteristics.

According to Jeppson, the PRV in this example is working in the active mode, i.e. maintaining the head in node 6 at the preset value H_6= 16.764 m. This is corroborated, in Jeppson's words, by the fact that

"the pressure upstream from the PRV equals 117.19 ft. and downstream equals 55 ft. Consequently the assumption used in writing the final loop equation (Jeppson is referring to the pseudo-loop equation linking the outlet of the PRV with the reservoir in

node 9) above is correct. Had the solution given a negative flow rate in pipe 6, this assumption would be incorrect, since the PRV would then have acted as a check valve and allowed the elevation of the HGL downstream from the PRV to rise above 55 ft. Should this have occurred, the the flow rate in pipe 6 would no longer be unknown, but equal to zero"

In our opinion, Jeppson's statement is wrong, simply because according to his own results the head in node 4 is greater than the head in node 6, which automatically means that there should be some flow from node 4 to node 6, contradicting his assumption that the flow is in the opposite direction. Perhaps Jeppson's algorithm did not detect the situation where apparently the pseudo-reservoir is overflowing (which happens when $H_j > H_y$ in Fig. 4.10. b).

4.5.3. Example JEPP12, from Jeppson (1976).

Another example provided by Jeppson is a network consisting of 15 branches and 13 nodes, this time with 2 PRV's. The schematic of this network is shown in Fig. 4.15, and Table 4.5 presents the comparison between the results published by Jeppson and ours.

Again we differ in the operational mode for the PRV's, because where Jeppson reports a PRV closed (branch 12) we found that it is in the active mode with a flow of 117.3475 l/s.

Table 4.5. Comparison of the results given by Jeppson (1976) and our results, for example JEPP12.

NODE	PIEZOMETRIC HEAD (M)		
	OUR RESULTS		JEPPSON
1	292.385632		294.00
2	276.698475		277.79
3	264.870323		265.48
4	263.190571		263.68
5	250.442362		251.91
6	146.965080		237.54
7	248.274502		251.91
8	150.000085	(*)	237.54
9	264.870323		265.48
10	146.965080	(**)	237.54
11	284.000067		
12	300.000000		300.00
13	250.000000		250.00

LINK	FLOW (L/S)		
	OUR RESULTS		JEPPSON
1	736.1791		640.2
2	283.7416		285.7
3	183.7415		185.7
4	-83.7415		-85.7
5	249.7851		234.4
6	-253.5266		-240.2
7	117.3475		0.0
8	0.0000		0.0
9	202.6525		120.0
10	-86.1792		-190.2
11	117.3475		0.0
12	117.3475	(*)	0.0
13	0.0000	(**)	0.0
14	0.0000		0.0
15	249.7851		234.4

Notes:

(*) First PRV is in link 12, outlet node 8 and its setting is H = 150 m.
(**) Second PRV is in link 13, outlet node 10 and its setting is H = 145 m.

4.5.4. Example JEPP13, from Jeppson (1976).

In this example Jeppson presents a variation of the previous case, by changing the connectivity of branch 6, from node 4 to node 2, while maintaining the remaining characteristics of the network.

Figure 4.16 shows the schematic of the network and Table 4.6 presents the comparison between Jeppson's results and ours.

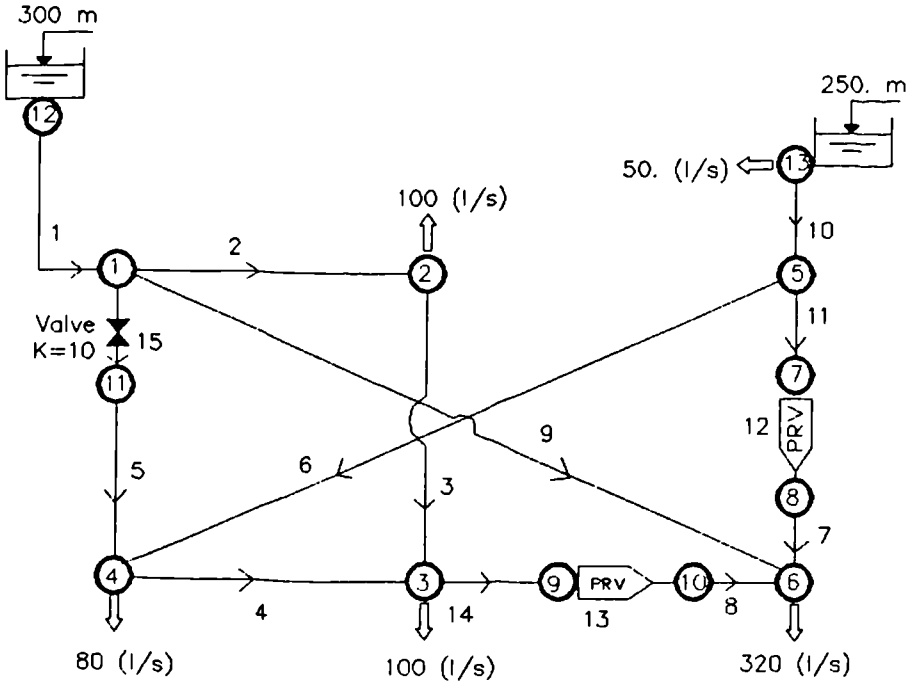

Fig. 4.15. Example JEPP12, from Jeppson (1976), page 110.

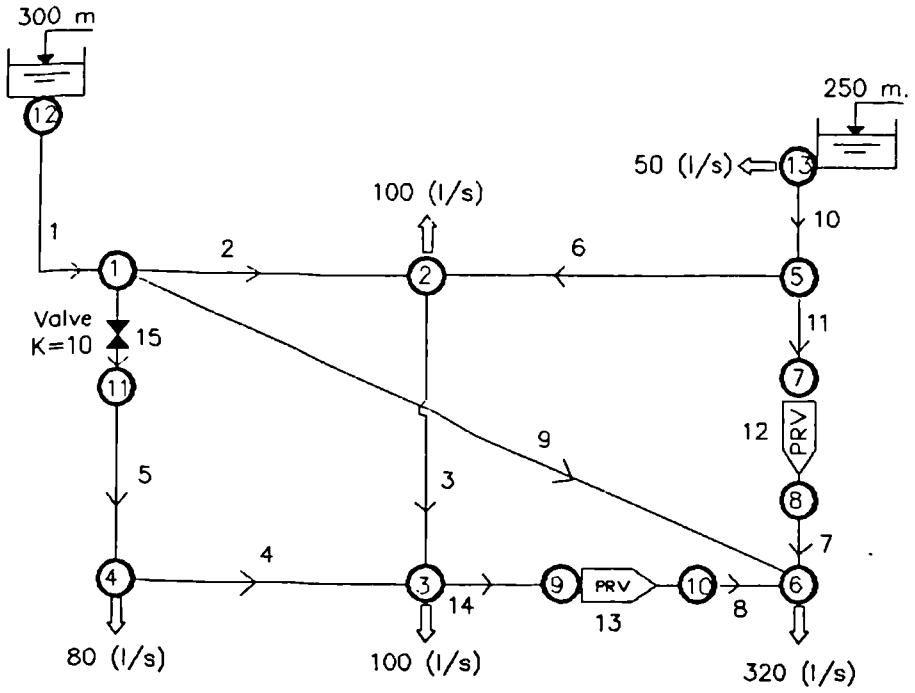

Fig. 4.16. Example JEPP13, from Jeppson (1976), page 112.

Table 4.6. Comparison of the results given by Jeppson (1976) and our results, for example JEPP13.

NODE	PIEZOMETRIC HEAD (M)		
	OUR RESULTS		JEPPSON
1	290.081524		291.745
2	258.310816		266.422
3	259.522824		266.583
4	264.547302		269.737
5	252.034725		250.718
6	146.885112		146.781
7	249.809812		248.419
8	149.999990	(*)	266.583
9	259.522824		266.583
10	146.885112	(**)	
11	282.805791		
12	300.000000		300.000
13	250.000000		250.000

LINK	FLOW (L/S)		
	OUR RESULTS		JEPPSON
1	849.3089		761.1
2	415.6674		364.0
3	-52.6691		-16.9
4	152.6691		116.9
5	232.6691		196.9
6	-368.3366		-280.9
7	119.0277		119.7
8	0.0000		0.0
9	200.9723		200.3
10	-199.3087		-111.1
11	119.0277		119.7
12	119.0277	(*)	119.7
13	0.0000	(**)	0.0
14	0.0000		0.0
15	232.6691		196.9

Notes:

(*) First PRV is in link 12, outlet node 8 and its setting is H = 150 m.
(**) Second PRV is in link 13, outlet node 10 and its setting is H = 145 m.

As before, there is disagreement, although this time the status of the PRV's is the same in both cases; however, the heads and flows do not correspond.

As a general comment on Jeppson's examples, we can say that he has been dealing with networks which are normally affected by backpressure, which is provided by some pipe connecting high pressure zones of the network with lower pressure zones (i.e. with the outlet of the PRV). This is a situation which is inconsistent with the objective of a PRV and is bound to produce problems both in the real network and in its model.

4.5.5. Example COLLINS, from Collins (1980).

On presenting a case for his statement that non-unique solutions can be found in some networks, especially when pressure controlling devices are included, Collins (1980) introduced the network of Figure 4.17, consisting of 6 branches (3 Pumps, 2 PRV's and 1 valve) and 7 nodes (4 of them reservoirs). As an additional condition Collins, established that each pump has a non-return device included, so that flow is only possible in the positive direction; also, the pumps are equipped with a device which closes when the downstream head of a pump is lower than the upstream head. According to our model, the PRV's are always acting as non-return (CV) valves; thus, the problem can be modelled without any additional feature. The results presented by Collins (1980) are summarised in Table 4.7.

Collins analyses the problem following a combinatoric approach, assuming that the operational mode of the PRV's is an independent variable of the problem; the same assumption is made for the pumps. This led Collins to assume that 16 potential operating modes are possible in the system, corresponding to all the combinations of PRV and pump states. We do not agree with this assumption, since clearly the final status of the PRV's will be determined by the system , once their settings are established by the operator. In this problem, since no automatic control is acting on the pumps, in order to start or stop them (for example according to the reservoir levels or some nodal pressures), their operating mode is controlled by the operator, i.e. it is an external (independent) variable. In this context, the 16

Table 4.7. Network solutions for example COLLINS, from Collins (1980).

MODE	Operating modes of control elements				Network solution (a)				
	PRV's status	Pumps P_1	P_2	P_3	Head (m) H_6	Flowrates (l/s) Q_{26}	Q_{46}	Q_{56}	Q_{67}
1	Passive	on	on	off	238.0476	3.5813	0.8927	0.0000	4.4739
2	Passive	on	on	on	No solution				
3	Passive	on	off	off	190.0000	2.0000	0.0000	0.0000	2.0000
4	Passive	off	on	off	No solution				
5	Passive	off	off	off	No solution				
6	Passive	off	on	on	No solution				
7	Passive	off	off	on	No solution				
8	Passive	on	off	on	No solution				
9	Active	on	on	off	No solution				
10	Active	on	off	off	No solution				
11	Active	off	on	off	No solution				
12	Active	off	off	off	No solution				
13	Active	on	off	on	No solution				
14	Active	off	on	on	No solution				
15	Active	off	off	on	No solution				
16	Active	on	on	on	245.0000	--(b)	--(b)	1.0000	4.7258

Notes: (a) $Q_{12} = Q_{26}$; $Q_{34} = Q_{46}$
(b) $Q_{26} + Q_{46} = 3.7526$

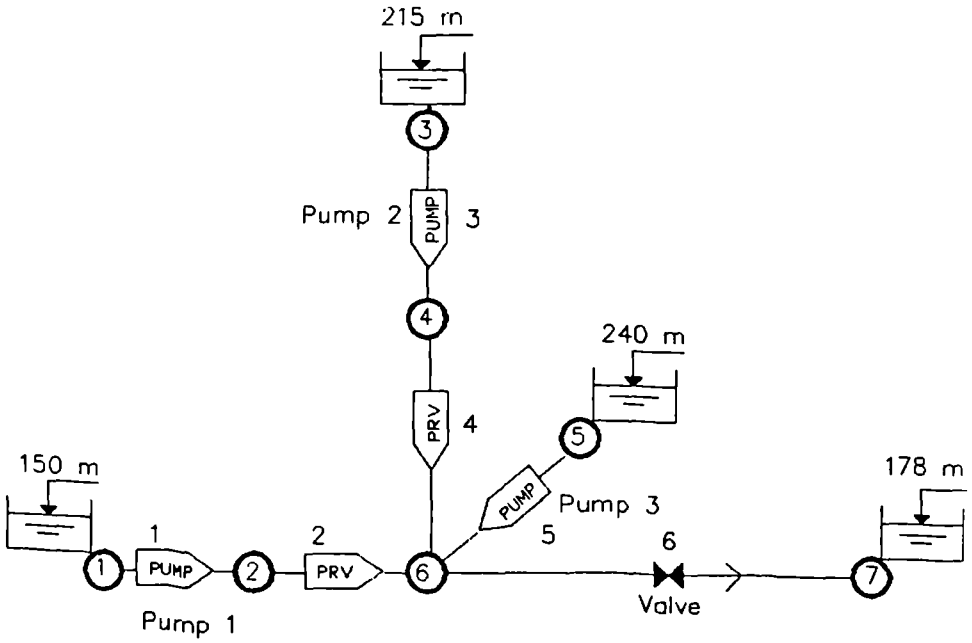

Fig. 4.17. Example COLLINS, from Collins (1980).

possible operating modes suggested by Collins are reduced to eight cases (see Table 4.8), this number being the possible combination of operational modes of the 3 pumps (with two exclusive modes: on/off).

Of course the eighth operational mode is trivial, because no flow can be possible, unless we accept that the pumps can operate as turbines, in which case some flow can be established throughout the pump in branch 5. This case is clearly outside the scope of this example.

Table 4.9 presents the results of running our program in the first seven modes defined above, assuming that the PRV's are set to a head of 245 m in their outlet (node 6).

According to Collins (1980), of the 16 possible operational modes he identified, only 3 of them are feasible and compatible with the conditions imposed to the problem. Only in his mode 16, which corresponds to our case 1, we get some similar results, although he finds that the flows between nodes 2,6 and between 4,6 admit more than one solution. In our case we found that this

Table 4.8. Operational cases for example COLLINS, based on all the possible combinations of pump operating modes.

Case	Pump 1 (link 1)	Pump 2 (link 3)	Pump 3 (link 5)
1	on	on	on
2	on	on	off
3	on	off	on
4	on	off	off
5	off	on	on
6	off	on	off
7	off	off	on
8	off	off	off

solution in also unique, the flows being controlled by the difference in the levels (available potential energy of the reservoirs connected to nodes 3 and 1, see Fig.4.17). In his mode 1, which is equivalent to our case 2, the head in node 6 was 238.0476 m, while we found that this head is the PRV's setting. In his mode 3, equivalent to our case 4, Collins found that the head in node 6 is 190.0000 while we obtained 205.000. We reproduced exactly Collins results in modes 3 and 6, provided that we change the settings of the PRV's to the heads found by Collins, but this is clearly a change in the original settings adopted for the PRV and, therefore, is another problem.

Collins (1980) did not consider as a possible operating mode the case where one PRV is active while the other is passive, which really happens in our case 5, thus confirming the weakness of his approach.

Table 4.9. Results of running our program for the operational modes possible in example COLLINS.

CASE	MODE	PRV status		Flow (l/s)				Head (m)		
		PRV_2	PRV_4	Q_{26}	Q_{46}	Q_{56}	Q_{67}	H_2	H_4	H_6
1	16	act.	act.	1.0000	2.7258	1.0000	4.7258	245.00	277.85	245.00
2	1	act.	act.	0.9982	3.7276	0.0000	4.7258	245.02	245.52	245.00
3		inac	inac	1.5709	0.0010	2.8876	4.4595	237.66	237.66	237.66
4	3	inac	inac	3.0000	0.0000	0.0000	3.0000	205.00	215.00	205.00
5		inac	act.	0.0001	3.7257	1.0000	4.7258	245.00	245.59	245.00
6		inac	inac	0.0005	4.1379	0.0005	4.1388	229.39	229.39	229.39
7		inac	inac	0.0005	0.0005	4.1224	4.1224	229.01	229.01	229.01
8				pumps off, not considered.						

Case : refers to our 8 operational cases.
Mode : refers to Collins' 16 operational modes.
Note that $Q_{12} = Q_{26}$ and $Q_{34} = Q_{46}$

In our opinion, what is happening in this example is a conceptual problem at the formulation stage, in the sense that the status of the PRV's cannot be determined a priori , but are determined by the hydraulic system under study, according to the PRV's settings.

4.6. Concluding remarks.

We have proposed a physically-based model for representing pressure regulating devices, which apparently does not have the problems detected and documented in the previous section for some traditional formulations.

Although the convergence of the model is rather slow when analysing a network from scratch, i.e. without any knowledge of the previous state of the network and its regulating devices, we believe that this apparent shortcoming is not relevant when applying this program for continuous simulation and operational purposes, when the final solution of the previous stage can be used as an initial solution for the next stage. Also, because the changes in heads and flows with respect to time are relatively slow, the changes in the operational mode of pressure regulating devices should be slow as well, which implies that, in correctly operated networks, the pressure regulating valves are not changing their status too often.

We believe that, in this section, we have proven that, when dealing with regulating devices, reliability and robustness rather than speed should be the major concern, because obviously

there is no point in having a fast program leading to the wrong solution.

Nevertheless, in order to reduce the execution time of the proposed algorithm we concentrate in the next chapter on the search for efficient fast direct linear solvers.

The main advantage of our method seems to be its robustness, as shown in Table 4.2, in detecting problems in the results given by other programs. The algorithm is able to deal with multiple pressure regulating devices simultaneously, which is something that is not clearly found in the open literature, as can be seen from Table 4.2.

We also have to emphasise the fact that the algorithm does not need a re-definition of the network topology when a regulating valve changes its status; as a result, the linear system of equations remains symmetric all the time, which is efficient from the storage and computational point of view.

We recognise the need to include other regulating devices, like flow-modulated PRV's, double relay valves (PRV's with two different settings, one for the day and the other for the night), altitude valves, constant flow valves, etc., some of them shown in Figure 4.18. This should also be done in the future to expand the capabilities of our program.

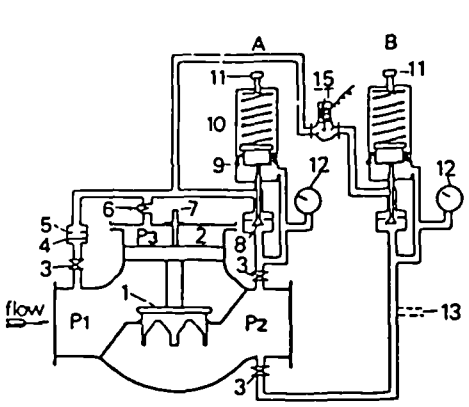

1 Valve Element
2 Upper Cylinder
3 Isolating Cocks
4 Strainer
5 Orifice
6 Needle Cock
7 Indicator
8 Relay Valve
9 Diaphragm
10 Spring
11 Adjusting Screw
12 Pressure Gauge
13 Alternative Constant Pressure Connection
14 Electric Motor
15 Solenoid operated valve

} AS FOR 1301

A. Low Pressure Relay Valve
B. High Pressure Relay Valve

a) Valve No. 1303 Valves with two relay systems

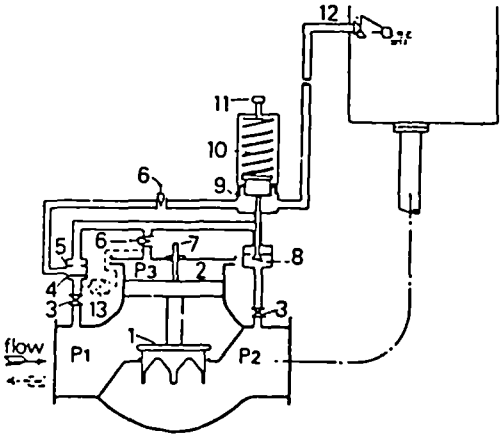

1 Valve Element
2 Upper Cylinder
3 Isolating Cocks
4 Strainer
5 Orifice
6 Needle Cocks
7 Indicator
8 Relay Valve
9 Diaphragm
10 Spring
11 Adjusting Screw
12 Ball Cock
13 Non-Return Valve

b)

Valve No. 1330 Standard Altitude Valve – Flow into tank only
Valve No. 1331 Altitude Valve allowing flow in and out of tank (Illustrated by dotted lines)

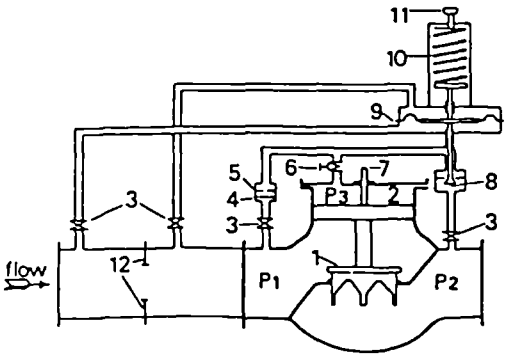

1 Valve Element
2 Upper Cylinder
3 Isolating Cocks
4 Strainer
5 Pressure Orifice
6 Needle Cock
7 Indicator
8 Relay Valve
9 Diaphragm
10 Spring
11 Adjusting Screw
12 Flow Orifice

c)

Valve No. 1340 Standard Constant Flow Valve

Fig. 4.18. Other pressure regulating valves, from Glenfield & Kennedy Ltd., Pub. 215/R3.

CHAPTER FIVE

EFFICIENT COMPUTER PROGRAM IMPLEMENTATION OF THE GRADIENT METHOD FOR WATER SUPPLY DISTRIBUTION NETWORKS

In the computer implementation of the gradient method, some issues become relevant from the computational point of view, especially if an efficient microcomputer-oriented implementation is sought. In this Chapter we are mainly concerned, for example, with the generation of an initial flow distribution and the possibility of using previous flow solutions as a starting point for a new network analysis. Another relevant issue, which perhaps is instrumental in the performance of the gradient method, is the numerical scheme for the solution of the linear system of equations generated by the gradient method. Due to the successive linearizations carried out within the gradient method, each network analysis implies the solution of a number of linear systems, typically 6-10.

In this chapter we intend to study these issues, particularly the solution of the linear system of equations, which is the most time-consuming step in the gradient method.

5.1. Automatic generation of initial flow distribution.

Unlike other network analysis algorithms reviewed in Chapter Two, the gradient method does not require an initially balanced flow distribution. In fact the algorithm itself is able to generate its own initial flows, without requiring to input the flows through the data set. This is possible because the coupled

equations which are the basis of the gradient method automatically re-balance the network at each iteration. These equations are:

Heads update:

$$\underline{H}^{(i+1)} = -[A_{21}\, G^{-1}\, A_{12}]^{-1} \{ A_{21}\, G^{-1}\, (A_{11}\, \underline{Q}^{(i)} + A_{10}\, H_0) - (A_{21}\, \underline{Q}^{(i)} - \underline{q}) \} \qquad (1)$$

Flows update:

$$\underline{Q}^{(i+1)} = (I - G^{-1}\, A_{11})\, \underline{Q}^{(i)} - G^{-1}\, (A_{12}\, \underline{H}^{(i+1)} + A_{10}\, H_0) \qquad (2)$$

Equation (1) represents a linear system of NN-NS equations in the unknown piezometric heads, and it can be reordered to the standard format of a linear system, by premultiplying equation (1) by the matrix $[A_{21}\, G^{-1} A_{12}]$, which becomes the matrix of coefficients of the linear system. For more details on the derivation of the gradient method see Chapters Two (original Todini's formulation) and Three (extended version).

Indeed, the last term of equation (1), $A_{21}\underline{Q}^{(i)}-\underline{q}$, allows us to start the first iteration with <u>any</u> flow $\underline{Q}^{(i)}$, since it accounts for the flow imbalance produced by $\underline{Q}^{(i)}$. Equation (2) guarantees that, with the heads computed via (1), the next flows $\underline{Q}^{(i+1)}$ will fulfil the nodal balance condition. This can be easily proved by premultiplying equation (2) by A_{21}, and verifying that the result is <u>always</u> the nodal demand, i.e.:

$$A_{21}\, \underline{Q}^{(i+1)} = \underline{q} \qquad (3)$$

Thus, after the first iteration, equation (2) produces a balanced flow distribution $[\underline{Q}^{(i+1)}]$ which, when used during the second iteration $[\underline{Q}^{(i)}$ in equation (1)], allows the nodal imbalance to vanish.

In the present computer implementation of the gradient method we start with $\underline{Q}$ = 1 (l/s) in the first iteration although, for large problems, a great deal of computer resources can be spared if we have stored a previous flow solution, not necessarily balanced for the new analysis conditions.

This feature of the gradient method represents the main difference with respect to the "integrated mesh-nodal" method of Stimson and Brameller (1981), which requires the generation of the tree and co-tree of the network, and the corresponding partitioning of the flow vector into dependent and independent flows. The dependent flows, computed from the independent ones, are then forced to be balanced before starting a new iteration.

These interesting properties of the gradient method allow us to reduce considerably the execution time in applications like the extended period simulation, where the flow solution of the last time-step is used as the initial (non-balanced) flow solution for the next time-step. Also, this helps us to reduce considerably the execution time in the modelling of pressure regulating devices (see Chapter Four for details), where the previous state of the system (flows and regulating valve's resistance) is used to obtain a new approximation to the equilibrium of the regulating valves.

As a result, the problems of generating an initial flow solution, and that of using an already existing flow solution to start a new analysis, can be efficiently handled within the gradient algorithm itself, without requiring additional programming.

The remaining problem from the computational standpoint is, then, the solution of the linear systems of equations generated by the gradient algorithm.

5.2. Solution of the linear system of equations generated by the gradient method.

In Appendix A we have reviewed the main approaches to the solution of linear systems of equations applicable to sparse symmetric positive definite systems. The two basic alternatives are direct and iterative methods.

5.2.1. General overview of direct sparse linear solvers.

All the direct methods for the solution of linear systems of equations are based on Gaussian elimination which, as shown in Appendix A, consists in a factorization stage followed by a substitution stage. The Cholesky factorization is the most common factorization scheme for symmetric positive definite matrices.

It is in the factorization stage where the problem of fill-in comes about, creating new non-zeros in the Cholesky factors with respect to the amount of non-zeros of the original matrix. The problem of the amount of fill-in can be handled via appropriate re-ordering of the original system; different orderings are

possible, leading to more or less efficient factorizations, ranging from a completely filled factor up to one with no fill-in at all, as shown via a small extreme example in Appendix A. Thus, the efficient handling of the fill-in problem is basically concerned with finding the most adequate re-ordering of the original system of equations. This task is eased by the introduction of graph theory concepts.

Because, in symmetric positive definite systems, the Cholesky factorization is inherently stable, we can concentrate our attention on the problem of reducing the fill-in, leaving the stability problem aside. This allows us to split up the direct solution of a linear system into a three stage process:

a) ANALYSIS stage: which searches for the re-ordering of the original system (or, equivalently, the re-labelling of the system graph), which produces the minimum fill-in. Also, at this stage, the data structures required are set up; this refers to all the auxiliary vectors and pointers required to handle the numerical parts of the algorithm.

b) FACTORIZATION stage: which carries out the numerical part of the factorization, using the ordering and data structures generated in the previous stages.

c) SOLUTION stage: which actually solves the linear system by substitution, using the Cholesky factorization produced in the previous stage, for any right-hand-side vector specified.

In Appendix A we have followed the sequence corresponding to the historical development of sparse direct linear solvers, comprising:

- Band methods.
- The envelope ("skyline") method.
- Minimum degree algorithms.
- Quotient tree algorithms.
- One-way dissection method.
- Nested dissection method.
- Frontal and multifrontal methods.

All these methods follow an increasing degree of sophistication and complexity, in parallel with an increasing degree of computational efficiency, both in terms of storage and speed.

Band and envelope methods are closely related, since both of them are based on the observation that fill-in occurs within the border lines separating the non-zeros and zeros of the matrix (see Figure 5.1). Thus, roughly speaking, the problem becomes that of interchanging the rows and columns of the original matrix, in such a way that the "area" of the non-zero region is minimized.

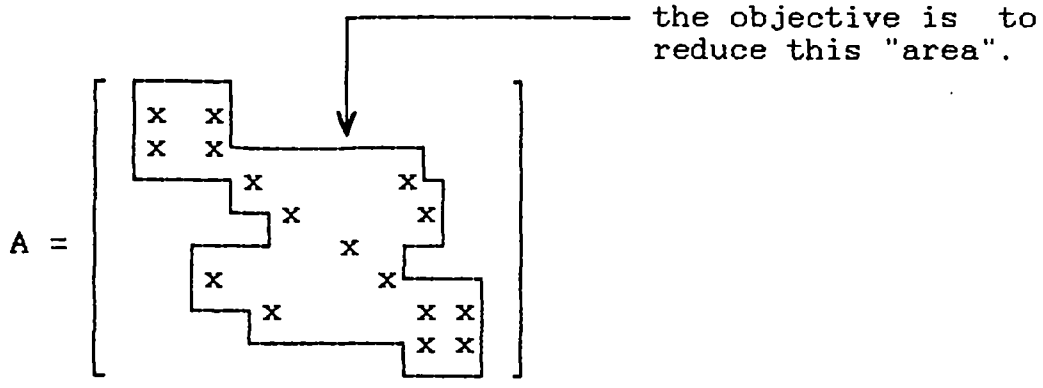

Fig. 5.1. Target "area" for band and envelope methods.

Although, for general matrices, the envelope methods are better than the band methods, the main shortcoming is concerned with the fact that the amount of fill-in is unpredictable, before actually running the numerical part of the algorithm. This means that we are constantly threatened with running out of storage, unless a large overhead is initially specified, leading to a sub-optimal storage utilisation.

As a contribution to solving the storage "predictability" problem, and to exploit even further some zeros still unexploited by the envelope methods, the minimum degree algorithm has been proposed. The minimum degree-based methods choose the next pivot, in the Gauss elimination process, from the row (or column) with the minimum number of non-zeros in it. A so-called "hybrid" implementation, due to George and Liu (1981) allows us, during the ANALYSIS stage, to determine the amount of memory required in the factorization stage, which happens to be not greater than that required to store the original matrix. Our experience with this algorithm, within the context of the gradient method, has been quite bad, particularly for networks larger than 900 nodes, where it actually failed.

Quotient tree algorithms take advantage of the fact that, on joining the neighbouring already eliminated nodes of the matrix' graph into "supernodes", a much simpler tree-like structure of "supernodes" is obtained. This "supertree" induces a partition of the original matrix, which can be efficiently handled by blocks, together with an implicit scheme, where only the diagonal blocks of the Cholesky factorization and the off-diagonal blocks of the

original matrix are explicitly needed, the rest being handled implicitly.

Dissection algorithms exploit the idea of partitioning the matrix even further. In one-way dissection the whole matrix graph is re-numbered, slicing it up via "dissectors", which are subsets of nodes running either horizontally or vertically, cutting the graph through the shorter path (i.e. in only one direction). This induces a reordered matrix structure which has low fill-in. The nested dissection algorithm exploits the dissection idea in two directions, creating a matrix which leads to very fast solutions, though requiring more storage than the one-way dissection.

The frontal method has originally been produced for finite element applications, and it takes advantage of the way the global matrix is assembled; thus, a row (node) can be eliminated as soon as all the elements connected to it have been assembled. An element numbering system, related to the order of assembling the global matrix, keeps the front-width as short as possible and, in multifrontal methods, eventually allows more than one front to be handled simultaneously, increasing the efficiency of the algorithm.

5.2.2. General overview of iterative methods for solving linear systems of equations.

Iterative methods for the solution of linear systems of equations have the common aim of constructing a sequence of vectors: $\underline{x}^{(o)}$, $\underline{x}^{(1)}$, $\underline{x}^{(2)}$,....,$\underline{x}^{(k)}$, converging to the solution of the linear problem $A\,\underline{x} = \underline{b}$.

Traditionally, iterative methods like Jacobi, Gauss-Seidel and successive over (or under) relaxation have been used to solve sparse linear systems. This is due to the fact that, in all iterative methods, sparsity is handled quite naturally and no fill-in occurs. Unless certain specific conditions are met by the matrix of coefficients (see Appendix A for details), some of these iterative methods may fail to converge, or converge slowly.

The conjugate gradient method, developed in the early 1950's by Hestenes and Stiefel (1952), and re-vitalised in the seventies by Reid (1971), has gained a reputation as an efficient linear solver. This is basically an unconstrained minimization algorithm which, when applied to the quadratic function:

$$z = \tfrac{1}{2}\, \underline{x}^T A\, \underline{x} + \underline{x}^T \underline{b} \qquad (4)$$

produces the solution of the original linear system $A\, \underline{x} = \underline{b}$.

Starting from any initial solution ($\underline{x}^{(o)}$), the method ideally converges in a fixed number of steps, though roundoff errors spoil the convergence, requiring in practice some additional iterations. Convergence is guaranteed for symmetric positive definite systems.

Acceleration of the convergence of the conjugate gradient algorithm can be achieved via a transformation, consisting of pre-multiplying the original matrix by a "pre-conditioning matrix" (L^{-1}), such that:

$$(L^{-1} A L^{-T}) (L^T \underline{x}) = L^{-1} \underline{b} \qquad (5)$$

where the new transformed matrix ($L^{-1} A L^{-T}$) is still symmetric, and is better conditioned than the original one. The

same original conjugate gradient algorithm, when applied to the transformed problem (5), is known as the preconditioned (or modified) conjugate gradient method.

In selecting a preconditioning matrix (L^{-1}), the problem of fill-in strikes back, as in the direct linear solvers, but an incomplete Cholesky factorization scheme proposed by Kershaw (1978), allows us to decompose the original matrix :

$$A \approx L\ L^T \qquad (6)$$

where L has exactly the same sparsity pattern as A. The non-zeros outside the original pattern are simply thrown away, thus solving the fill-in problem. Note that with (6), the transformed matrix ($L^{-1}\ A\ L^{-T}$) in (5) becomes nearly an identity matrix, thus being easier to invert than the original matrix A.

5.2.3. Comparison of the performance of the gradient method with different linear solvers.

In sections 5.2.1. and 5.2.2. the two main alternatives for the solution of sparse linear systems have been briefly reviewed, namely direct and iterative methods.

In the present section we intend to compare the performance of six sparse direct and one iterative linear solvers, in the context of the gradient method for water distribution network analysis. The algorithms compared are:

- The envelope ("skyline") method.
- Minimum degree algorithms.
- Quotient tree algorithms.
- One-way dissection method.

- Nested dissection method.
- Multifrontal method.
- Preconditioned conjugate gradient method.

Numerous comparisons between different algorithms have been presented in the literature , though for different kinds of problems and of limited scope (two or three methods) . George and Liu (1981) carried out an extensive comparison, geared towards finite element problems, although their comparison concentrated mostly on direct methods, excluding the frontal and multifrontal approaches.

We have taken the comparison carried out by George and Liu (1981) as a starting point, and we have extended it to include the preconditioned conjugate gradient, recognised as the best iterative algorithm available, and also a multifrontal method, which corresponds to the routine MA27 of the Harwell Library. In so doing, we are covering the widest spectrum of linear solvers possible, which is something unavailable in the literature for such problems, particularly for the case of water distribution networks.

This has led to the implementation of seven different versions of the gradient method, each one with a different linear solver. A bank of nine network examples has been set up , ranging from 48 to 4,900 nodes, and the corresponding analysis problems have been solved, keeping track of the execution time, number of iterations of the gradient method and storage required.

Table 5.1. presents the main characteristics of the examples used in the numerical comparison, while Table 5.2 presents the results, including the execution times of the tested programs in the Amdahl 5860 mainframe computer at Newcastle University; these

Table 5.1. Main data corresponding to examples used in the comparison between different linear solvers in the gradient method for pipe network analysis .

N E T W O R K D A T A							
Data file	Branches	Nodes	Sources	Equations	CV	PRV	PSV
net5.dat [1]	74	48	2	46	0	0	0
prv5.dat [2]	74	48	4	44	1	2	2
bog10.dat [3]	298	266	26	240	0	0	0
net50.dat [4]	420	225	2	223	0	0	0
net51.dat [4]	760	400	2	398	0	0	0
net52.dat [4]	1200	625	4	621	0	0	0
net53.dat [4]	1740	900	4	896	0	0	0
net54.dat [4]	4900	2500	4	2496	0	0	0
net56.dat [4]	9660	4900	4	4896	0	0	0

Notes:
=====
[1] : Data from real network, published by Chin et al. (1978), "Solution of water networks by sparse matrix methods ", Int. J. Num. Meth. Eng., 12, 1261-1277, (1978).
[2] : Based on the data of previous example, with pressure regulating devices added.
[3] : Real main network of Bogota, Colombia. Source: G. Gonzalez "The gradient method", M. Sc. Dissertation, Civil Eng. Department, University of Newcastle-upon-Tyne, 1987.
[4] : Synthetic network. Network generated as a square mesh with SQRT(Nodes) vertices per side.

Table 5.2. Comparison of execution times and number of iterations required by different linear solvers in the gradient method for pipe network analysis.

Data file	EXECUTION TIME (secs.) AND NUMBER OF ITERATIONS (*)						
	ICCG	RCM	QMD	RQT	1WD	ND	MA27
net5.dat	0.286 (7)(*)	0.112 (7)	0.106 (7)	0.166 (7)	0.442 (7)	0.113 (7)	0.115 (7)
prv5.dat	8.624 (232)	2.374 (232)	2.479 (232)	4.504 (232)	17.547 (232)	2.472 (232)	2.877 (232)
bog10.dat	18.524 (25)	2.152 (18)	2.492 (24)	2.332 (18)	3.220 (18)	1.824 (17)	1.785 (19)
net50.dat	3.698 (7)	0.924 (7)	1.812 (7)	1.121 (7)	1.452 (7)	0.907 (7)	0.884 (7)
net51.dat	12.126 (9)	2.873 (9)	10.036 (9)	3.310 (9)	3.642 (9)	2.684 (9)	2.234 (9)
net52.dat	36.428 (12)	7.670 (12)	37.677 (12)	8.658 (12)	10.965 (12)	6.836 (12)	5.269 (12)
net53.dat	63.985 (11)	13.471 (11)	(**)	14.898 (12)	14.747 (11)	11.655 (11)	8.598 (11)
net54.dat	627.275 (17)	118.850 (17)	-	130.774 (17)	116.656 (17)	95.363 (17)	55.146 (17)
net56.dat	2321.573 (17)	424.489 (17)	-	461.167 (17)	386.721 (17)	326.817 (17)	156.421 (17)

Notes:

(*) : Time is CPU-time in the Amdahl 5860 mainframe computer at Newcastle University; in rounded brackets the number of iterations required (gradient method iterations) for the solution of the water distribution network analysis problem is shown.

(**): The program failed to find a solution for the first iteration after running for 970.0 secs., the program was interrupted and cancelled. No attempt was made with the larger examples NET54.DAT and NET56.DAT.

Linear solvers:

- ICCG : modified Conjugate Gradient method, with Incomplete Choleski factorization (Kershaw factorization).
- RCM : envelope ("skyline") method with Reverse Cuthill-McKee ordering.
- QMD : Quotient Minimum Degree algorithm.
- RQT : Refined Quotient Tree algorithm.
- 1WD : one-Way Dissection method.
- ND : Nested Dissection algorithm.
- MA27 : Harwell subroutine MA27.

References:

- ICCG : based on: Ajiz and Jennings (1984) and Kershaw(1978).
- RCM, QMD, RQT, 1WD and ND : George and Liu (1981).
- MA27 : Harwell Subroutine Library, Atomic Energy Research Establishment, (AERE), U. K.

execution times are, in general, average times of at least a couple of runs and correspond to the time needed for the solution of the network (i.e. the non-linear problem) excluding the input/output of data and results. The number of (non-linear) iterations of the gradient method, for the analysis of the networks, is also presented in Table 5.2, in rounded brackets.

Table 5.3. presents the summary of the storage requirements, both in terms of main storage (that needed for the explicit handling of the non-zero values) and overhead storage, which accounts for all the extra auxiliary vectors and pointers needed to implement the algorithm.

Figures 5.2 and 5.3 show the results of the comparison, in terms of CPU execution time and total storage, respectively. The storage shown in Table 5.3 and Fig. 5.3 refers to that required by the linear solver itself; it does not include that of the non-linear solver. Thus, for comparative purposes the results are representative of the relative merits of the different algorithms for the solution of the linear systems.

Another important point in the comparison, is the fact that most of the test examples are synthetically generated networks. This is a factor which may be contributing to the good performance of the dissection methods, which have been originated for use with regular finite element meshes. This is a point that should be explored in the future, if data from larger real networks becomes available.

Table 5.3. Comparison of storage requirements (Bytes) for different linear solvers used with the gradient method for pipe network analysis.

Method [1]	Data file name and number of equations [2]								
	NET5.DAT 46	PRV5.DAT 44	BOG10.DAT 240	NET50.DAT 223	NET51.DAT 398	NET52.DAT 621	NET53.DAT 896	NET54.DAT 2496	NET55.DAT 4896
ICCG	2,576 [3]	2,464	13,440	12,488	22,288	34,776	50,176	139,776	274,176
	1,748 [4]	1,672	9,120	8,474	15,124	23,598	34,048	94,848	186,048
	4,328 [5]	4,136	22,560	20,962	37,412	58,374	84,224	234,624	460,224
RCM	1,912	1,248	15,664	22,072	50,800	95,224	161,528	715,624	1,925,944
	1,656	1,584	8,640	8,028	14,324	22,356	32,256	89,856	176,256
	3,568	2,832	24,304	30,100	65,124	117,580	193,784	805,480	2,102,200
QMD	1,760	1,752	9,072	37,336	113,392	237,496	- [6]	-	-
	3,310	3,190	17,394	18,906	37,866	60,256	-	-	-
	5,070	4,942	26,466	56,242	151,258	297,752	-	-	-
RQT	1,472	1,424	8,088	14,896	46,128	58,448	96,576	402,048	1,050,128
	3,342	3,198	17,290	16,442	32,830	45,854	66,184	184,504	362,024
	4,814	4,622	25,378	31,338	78,958	104,302	162,760	586,552	1,412,152
1WD	1,912	1,840	7,512	12,472	24,992	42,928	67,696	237,384	546,088
	2,852	2,728	15,042	14,148	25,196	39,262	56,608	157,280	307,960
	4,764	4,568	22,554	26,620	50,188	82,190	124,304	394,664	854,048
ND	1,912	1,736	8,824	17,800	37,192	62,848	97,288	327,552	720,144
	3,660	3,490	19,140	18,878	33,930	53,016	77,054	215,202	425,324
	5,572	5,226	27,964	36,678	71,122	115,864	174,342	542,754	1,145,468
MA27	1,296	1,248	5,904	17,056	33,296	57,656	95,088	336,888	728,608
	3,864	3,696	20,160	18,732	33,432	52,164	75,264	209,664	411,264
	5,160	4,944	26,064	35,788	66,728	109,820	170,352	546,552	1,139,872

Notes:

[1] : Refers to the linear solver algorithm:

ICCG : modified Conjugate Gradient method, with Incomplete Choleski factorization (Kershaw factorization).

RCM : envelope ("skyline") method with Reverse Cuthill-McKee ordering.

QMD : Quotient Minimum Degree algorithm.

RQT : Refined Quotient Tree algorithm.

1WD : one-Way Dissection method.

ND : Nested Dissection algorithm.

MA27 : Harwell subroutine MA27.

[2] : Corresponds with data sets in Table 5.1.

[3] : Upper figure corresponds to the primary storage (Bytes).

[4] : Corresponds to the overhead storage (Bytes).

[5] : Corresponds to the total storage: primary + overhead storage (Bytes).

[6] : No solution for the first iteration after 970.0 secs., program was interrupted and cancelled. No attempt was made with the larger examples NET54.DAT and NET56.DAT.

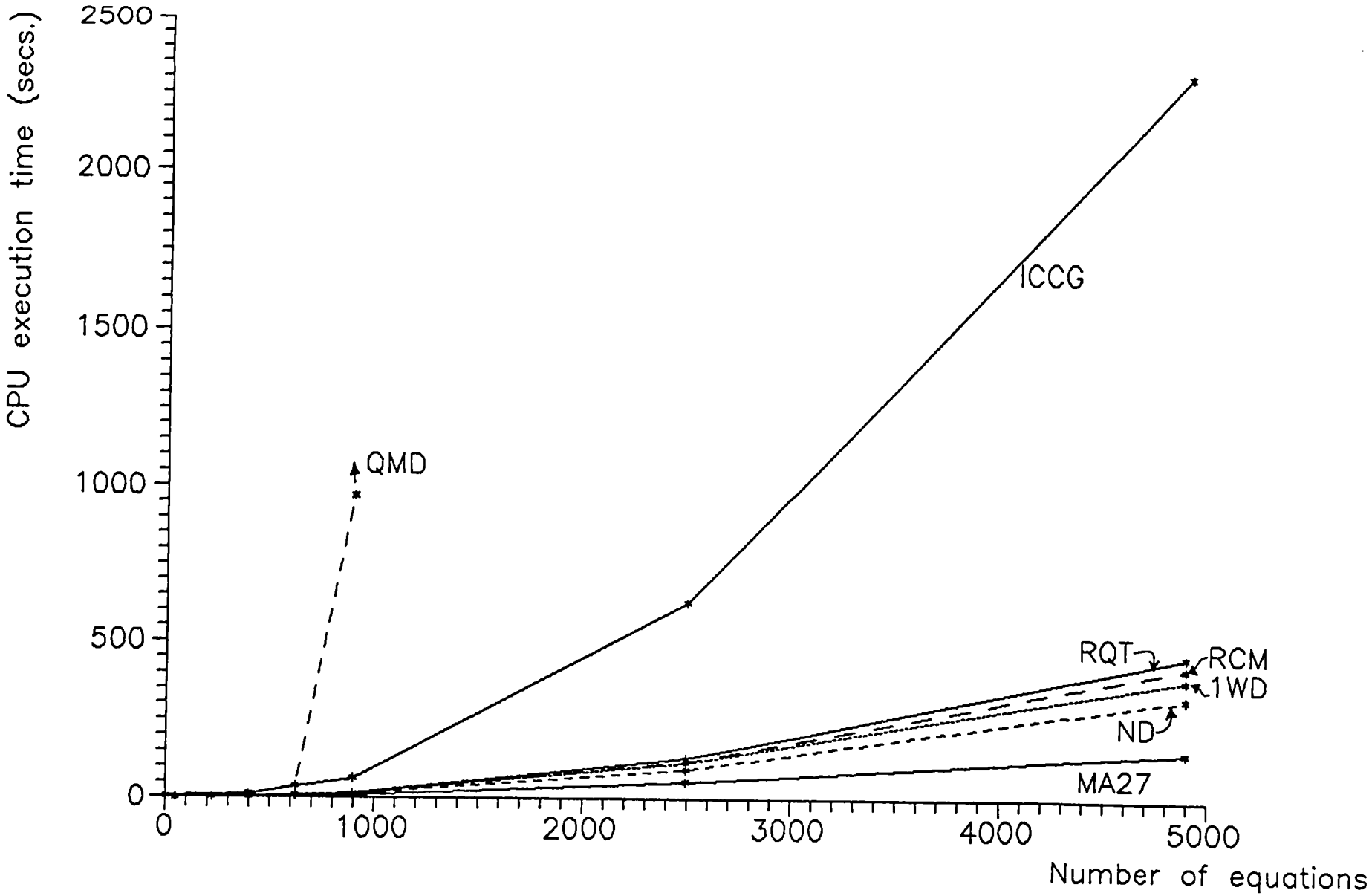

Fig. 5.2. Comparison of execution times for the gradient method, with different linear solvers.

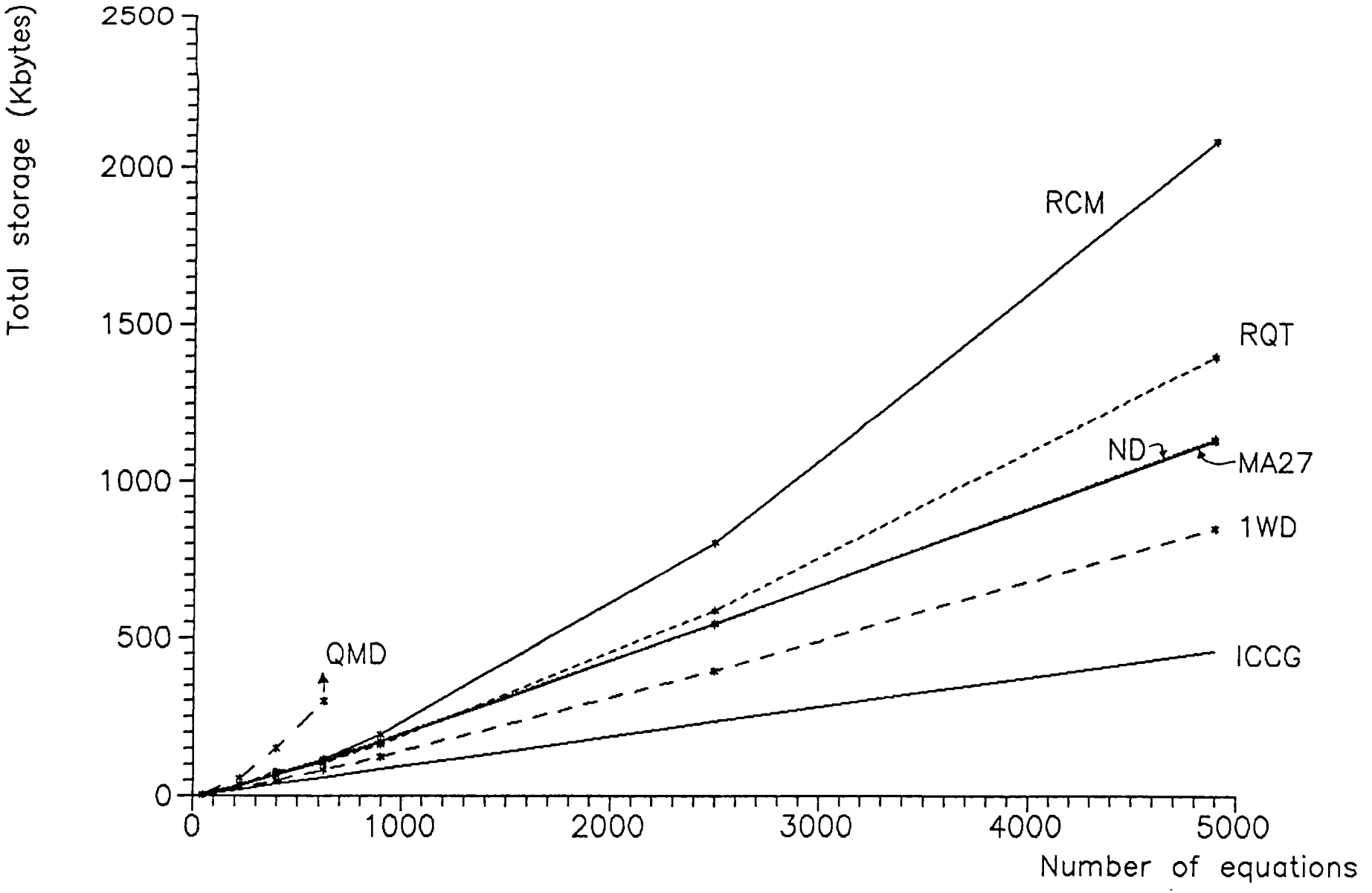

Fig.5.3. Comparison of storage requirements of the different linear solvers.

There is an additional point that is worth noting, which is that the presented execution times are not "exactly" a function of the number of nodes of the network (or the number of unknowns in the linear systems). The first four examples illustrate this point: the presence of pressure regulating valves in the data set PRV5.DAT, which is basically the same network as in NET5.DAT, produces a sharp increase in the execution time; this is due to the increase in non-linear iterations needed in order to produce the balance in the regulating devices (232 iterations). The point is also illustrated in the third and fourth examples, where a real network of 266 nodes corresponding to the main distribution system of the city of Bogotá (Colombia) requires between 1.6 to 5 times the execution time required for a similar synthetic network (the latter ratio relate to the case when the preconditioned conjugate gradient is used as the linear solver). In summary, the presence of pressure regulating devices requires the network to be solved more times than when no pressure regulating valves are present, and the hydraulic characteristics of the network (mainly represented by the distribution and connectivity of high and low resistance pipes) produces problems resulting in slower convergence.

The results in Table 5.2 show that, despite the problems mentioned in the previous paragraph, the relative difficulty of similar sized problems does not change the relative performance of the methods, i.e. "good" methods are still good when a more difficult problem has to be solved. Thus, we can rely on the synthetic data sets for determining the relative performance of

the algorithms, while the "true" performance of the algorithms in real networks is something which will depend very much on the physical characteristics of the system (i.e. presence of regulating valves, distribution of high/low resistance pipes, etc.).

5.2.4. Selection of the most efficient method.

One of the main conclusions to be drawn from the comparison carried out is in terms of the relative efficiency of direct methods when compared to the iterative algorithm (ICCG). For large problems, say of more than 200 nodes, a direct solver always produces faster results, the exception being the quotient minimum degree (QMD) algorithm. In addition, the larger the problem, the greater the relative efficiency of the best direct algorithm in comparison with the iterative scheme (the MA27 code produces a solution about 15 times faster than the preconditioned conjugate gradient algorithm, for the network of 4900 nodes).

As it can be seen form Fig. 5.2, the execution times produced with most of the direct solvers increase at a nearly linear rate with the size of the problem; the preconditioned conjugate gradient shows the strongest non-linear behaviour in this respect. The total storage (see Fig. 5.3) behaves linearly for most of the best algorithms, e.g. preconditioned conjugate gradient, dissection methods and multifrontal algorithms.

In summary, the conclusion is that when selecting a linear solver, if storage is available, a direct method is the right decision. The multifrontal method is the best choice from the

execution time viewpoint, followed by the dissection algorithms of George and Liu (1981). The nested dissection is about 100% more time-consuming for large problems than the multifrontal method, while the one-way dissection is about 120% more time-consuming than the multifrontal algorithm. From the storage point of view, the preconditioned conjugate gradient is the best choice, requiring about a half of the storage of its closest rival, the one way dissection algorithm.

Even in a limited storage environment, like in the present generation of 8 bit microcomputers, a direct solver can still be the best choice. Our current implementation of the gradient method with the one-way dissection linear solver, in a 512 Kbytes RAM microcomputer, allows us to solve networks of up to 1000 nodes in a fourth of the time required by the preconditioned conjugate gradient. Because of the reduction in the storage needed for the preconditioned conjugate gradient, networks of up to 1200 nodes can be solved in a 512 Kbytes microcomputer. The arrival of more powerful personal microcomputers, which is already taking place, makes the case for direct solvers even stronger.

5.3. Concluding remarks.

In this chapter, we have compared the performance of the gradient method for water distribution network analysis when used with a wide variety of linear solvers, including sparse direct methods and one iterative method (preconditioned conjugate gradient).

The main conclusion is that, when enough storage is available, the multifrontal approach (routine MA27 of the Harwell Library) provides the fastest solution. If storage is very limited, the preconditioned conjugate gradient is the best choice. A good compromise between storage and speed is obtained with the one-way dissection algorithm of George and Liu (1981), particularly if the maximum size of the network is between 1,000-2,000 nodes.

CHAPTER SIX

CALIBRATION OF WATER SUPPLY DISTRIBUTION SYSTEMS: A NEW COMPUTER-BASED EXPLICIT METHOD

6.1. Introduction.

Due to the inherent complexities of the mathematical model for describing the steady and unsteady state of a water distribution network, computers have been used to ease the modelling process since the early sixties, when these machines became available for practical engineering applications.

To build up the mathematical model, a number of simplifying assumptions are needed, in order to produce a mathematically tractable problem. Additionally, most of the parameters required by the mathematical model are subject to estimation errors. Consequently, we have to recognise that the mathematical model as a whole is just a rough approximation of the reality.

As a result, if we compare the predicted variables of the model with the corresponding measured variables from the real network, we shall find that agreement between both quantities is rarely reached. If the model is used to represent the reality, something has to be be done in order to improve the quality of the model results with respect to the real world.

A calibration stage is then needed before the model can be used to represent the reality for any practical purpose, the

calibration being responsible for guaranteeing that the results predicted by the model and the corresponding variables in the real network match within a reasonable degree of accuracy, for all the possible range of operating conditions in which the model is going to be applied.

The purpose of this chapter is to present a calibration procedure for water distribution networks, which can be carried out with the help of the computer, and used interactively by experienced engineers dealing with the water distribution system.

Section 6.2 deals with the identification of most of the causes of uncertainty in the modelling process, while Section 6.3 summarises the nature and accuracy of the measurements normally available in a typical water distribution network. Section 6.4 contains the problem formulation. Section 6.5 presents a review of the existing methods for calibration and Section 6.6 compares the conveniences and shortcomings of a deterministic and a probabilistic approach to the calibration problem. Section 6.7 introduces the rationale behind the proposed method, whereas Section 6.8 presents the method itself. In Section 6.9 different techniques applicable to the problem of estimating the unmeasured piezometric heads in a water distribution network are presented. Section 6.10 illustrates the application of the proposed method to some test examples, while in section 6.11 the calibration results are compared and discussed. Finally, some conclusions are drawn in Section 6.12.

6.2. Uncertainties in water distribution modelling.

First of all, we shall constrain the scope of this chapter to the steady-state flow exclusively. The unsteady state problem is a completely different problem from the mathematical viewpoint, and its modelling is usually carried out having different objectives in mind, as compared with the aims of traditional network analysis. This involves a first cause of possible error in the model, since it is more adequate to understand the real behaviour of the network as in a continuous unsteady state; this is due to the fact that demands are always changing, pumps are often switched on and off, valves are moved, etc., generating a wide range of transient phenomena, some of them with a slow response and some with a fast response as well.

In modelling the steady-state flow, some of the uncertainties and simplifications involved are concerned with :

6.2.1. Mathematical model for the flow/head loss phenomena.

It is assumed that a mathematical non-linear relationship approximates efficiently the flow-head loss phenomena in the network elements (pipes, pumps, valves, etc.). The Hazen-Williams and the Darcy-Weisbach formulae are widely accepted and both of them can be modelled as:

$$h_{ij} = \alpha_{ij} Q_{ij}^{n} + \beta_{ij} \qquad (1)$$

where h_{ij} and Q_{ij} are the head loss and flow between nodes "i" and "j", respectively; α_{ij} and β_{ij} are the characteristic parameters and n is a real exponent. All of them are formula-dependent.

The non-linear model represented by equation (1) is valid for turbulent flow (i.e. when Reynolds number is greater than 4,000-6,000). For laminar flow (i.e. Reynolds number less than 2,000), linear models in the flows (or in the velocities) like those proposed by Hagen in 1839 and Poiseuille in 1840 are recognised as a more adequate representation of the physical reality. The region with Reynolds numbers between 2,000 and 4,000 is often considered as a "transition zone", and no explicit model is available for describing the flow in that zone. Generally, either the turbulent or laminar model is applied in that transition zone, depending on the state (laminar or turbulent) prevailing prior to reaching the transition zone.

In other words, the mathematical description of the physical phenomenon itself has some degree of ambiguity, which is normally considered as non relevant for practical purposes on the grounds that, in civil engineering applications, most of the flows are turbulent, which is not always true.

The coefficients α_{ij} and β_{ij} in equation (1) are the characteristic parameters of every branch of the network. In the case of pipes $\beta_{ij}=0$ and $\alpha_{ij} = L_{ij}/(\emptyset\ C_{ij}^{1.852}\ D_{ij}^{4.87037})$ for the Hazen-Williams formula, with $\emptyset$ being a units-dependent constant. In the case of valves, $\beta_{ij}\approx 0$ and α_{ij} has to be obtained from the characteristic curve of the valve (supplied by the manufacturer or determined in a laboratory). Similarly, in the case of pumps, both α_{ij} and β_{ij} are needed.

In a real network, the characteristic coefficients α_{ij} and β_{ij} are assumed to be known. In practice, a number of factors lead us

to the uncertainty in the determination of the characteristic parameters; some of these factors are:

a) Pipe resistance:

The roughness of a pipe, represented by C_{ij} in the case of the Hazen Williams formula, is difficult to determine in practice. Field tests are needed for the estimation of the roughness of an old pipe [i.e. hydrant tests and others described by Walski (1984)]; for a new pipe, the corresponding value can be determined in a laboratory and is usually supplied by the manufacturer.

Furthermore, the pipe resistance changes slowly with time, then, in essence, we are dealing with a variable coefficient, which is assumed to be constant for practical reasons.

The older the pipe, the greater the uncertainty associated with its resistance.

b) Diameter:

Assuming that at least the nominal diameter and corresponding materials of the pipes are known (which is not always the case in the real world), different classes of pipes can be found, especially when we are studying a system of old pipes; in this case, it is usual to find different effective diameters for the same nominal diameter. In addition, deposition of mineral salts and the action of corrosion processes can reduce the effective diameter of a pipe with a known nominal diameter or change the shape of the net flow section.

c) Length:

This variable is usually determined from a map of the city under study (scales 1:5000 or 1:10000 are usual), where the pipes of the network have been drawn; as a result, the lengths are quantities subject to errors of measurement.

d) Valve settings:

The valve characteristic parameters are also subject to errors unless a periodical checking procedure is performed, which can include laboratory tests to re-determine the characteristic parameters. Furthermore, the degree of aperture of a valve in a real network is not known precisely and it is quite common to find some valves closed when a field inspection is performed. Again, we have to look at the characteristic parameters as uncertain parameters.

e) Pump characteristic values:

Similarly to the case of valves, the real values of the characteristic parameters of pumps are not precisely known, unless laboratory tests are carried out. Also, it is known that, due to the normal wear during the operation of the pumps or due to abnormal cavitation processes, the values of the characteristic parameters can change with time.

f) Minor losses:

It is an accepted practice in water supply modelling that minor losses produced by the presence of special fittings like t-joints, elbows, reductions, etc. are neglected, due to their small values in comparison with the head loss produced by friction in the pipes. This generally accepted practice can fail in some special cases when short pipe lengths and important

fittings are present. For these cases, the introduction of an equivalent extra length of pipe, which produces a head loss approximately equal to that corresponding to the fittings, is sometimes considered an acceptable solution. To cope with these cases, an adjustment of the length of the pipes should be allowed, supporting the treatment of the length as a variable subject to errors of measurement, as noted previously in c).

Consequently, it is no longer possible to consider the characteristic parameters α_{ij} and β_{ij} as deterministic, and a probabilistic model seems to be more adequate to explain their uncertainties and errors.

6.2.2. Water consumption.

The demands of water from the customers (residential houses, commerce, industries, etc.) are assumed to be concentrated in the nodes of the network model, instead of along the pipes, as happens in the real system. In addition, the spatial distribution of the consumptions is something which is difficult to establish precisely. The normal procedure for that purpose involves a sectorization of the area served, which leads to an approximation of the spatial pattern of the demand. This process involves a great deal of judgement and subjectivity, producing estimates of the demand whose accuracy is not normally known; See Crabbe et al. (1982) and Brandon (1984; chapter 6) for details.

Finally, the consumptions are subject to time variation. Within a day the consumption rate changes hour by hour, following closely the different activities of the consumers. Within a week,

there is also a daily variation, due to the fact that the consumption pattern changes from week days to the week end. In the same line, monthly variations, induced by weather changes, and yearly variations, produced by population changes, are also acknowledged.

The presence of leakages and unaccounted-for water consumptions, makes the picture of water consumption even more blurred.

In summary, both the spatial and temporal distributions of water consumption are subject to uncertainty, and the way in which this consumption is modelled (concentrated in the nodes) is a simplification required to make the problem tractable from the mathematical point of view. This means that, in practice, nodal consumptions are a fiction, created by network analysts to be able to tackle the problem; clearly, nodal demand measurements are not possible to obtain and only indirect and global measurements of consumptions are sometimes available. The practice of measuring individual consumptions on a house by house basis is common in some countries, but that information usually incorporates a great deal of uncertainty. Thus, water consumption is a parameter subject to considerable variability.

6.2.3. Effect of network reduction.

In the early stages of network analysis, when the computations were carried out manually, the real network was "skeletonized" in order to reduce the amount of pipes and nodes in the mathematical model, thus reducing the effort needed to solve the problem. The

reduction was obtained via the simple elimination from the model of those small diameter pipes which were supposed to contribute in a minor way to the flow-carrying function of the real network.

In essence, network skeletonization contributes some extra uncertainty into the network model and it will certainly lead to discrepancies between the model and the real network. As a result, skeletonization should be used carefully and a compromise should be struck when deciding which pipes are to be eliminated from the model, if any pipes have to be eliminated at all. Eventually, the convenience of skeletonization as a regular practice should be revised.

6.2.4. Influence of network pressure.

The nodal demands are generally assumed to be independent of the pressures in the network, which is clearly not true in the real world. In fact, the operators usually reduce the pressure in the network in order to lower peak demands and also to reduce the amount of leakages, especially during the night.

This factor is not considered explicitly in normal network modelling practice.

6.2.5. Other factors.

Other problems can contribute to introducing errors and uncertainty in a network model; some of them may appear at first sight as improbable but they do occur. See Crabbe et al. (1982) and Brandon (1984) for details. Some of these problems are:

* Misinterpretation of recorded data: wrong dimensions and units are reported as a common cause of error.
* Actual connections between pipes are different from those assumed in the model.

* Valves which may be operating in a completely different state, e.g. open in the real network, but closed in the model, or vice versa.
* Pipes by-passing pressure regulating valves and meters.
* Pipe obstructions, due either to the presence of debris or to untidy maintenance work, may change dramatically the resistance characteristics of the pipes.

All these factors should be checked before a formal calibration procedure is started; moreover, if some strange results are being obtained with the model, it might be necessary to go back to these possible error sources.

Clarke et al. (1981) give some examples on how meaningful (or meaningless) the results of some simple pipe hydraulics calculations can be when dealing with uncertain data. Walski (1987) stresses the sensibility of network calculations to measurement accuracy and also refers to the influence of the fact that steady state conditions are difficult to obtain in a real network, especially when pumps and pressure regulating devices are present. All these warnings are applicable to any calibration procedure.

6.3. Measurements available in a real network and their accuracy.

Accepting the previous assumptions, in standard network analysis applications we first proceed to "estimate" the physical characteristics of the network (roughnesses, diameters, lengths of pipes, characteristic parameters of pumps and valves, etc.) and the global demand and its spatial distribution for a particular time horizon. With these data, the raw model, as defined in Chapter 1, is solved and its results in terms of heads per node and flows per branch are obtained.

At this point of the modelling process, a new question arises:

How close does our model represent
the behaviour of the real network ?

To answer this question we need additional information from the real network; the required pieces of information are obtained via the field measurement of different parameters in the real network:

* pressures at selected nodes of the network.
* water levels in the reservoirs.
* flows at selected points of the system.
* demands for certain areas and users in the network.
* roughnesses of key pipes of the system (field measurements).
* characteristic coefficients of pumps and valves (laboratory or field measurements) .
* effective diameters.
* ground level elevations at certain nodes.
* meter calibration results.

To simplify the terminology, pressure and water level measurements will - from now on - be referred to as "piezometric head measurements", though pressure and level measurements need to be added to the corresponding ground level to obtain the piezometric head. Nodal piezometric heads and pipe flow measurements are generally the basic measurements in the network.

There is a wide range of measurement devices for pressures, flows and levels; for each device, different accuracies can be available and, obviously, the higher the measurement quality, the greater the reliability of the conclusions that can be obtained with these data.

Although a 1% accuracy seems to be a normal requirement for most of the flow and pressure measurement devices, we have to accept the fact that poorer measurements can be available and that it is a matter of statistical interpretation as to the quality of the results that can be obtained with such kinds of measurements. Walski (1984, 1988) presents a detailed review of the different techniques and equipment for water distribution network measurements.

Water distribution networks, unlike other public utilities, are characterised by their lack of adequate measurement systems, both from the quality and the quantity viewpoints. Normally, we should not expect to have more than 10% of the nodes of the network with pressure or level measurements. The amount of flow measurements could be even less, but generally we do have flow measurements at key points like reservoirs (inlet and outlet pipes), pumps,

important consumers (or sectors of the network), etc.

Although nowadays it is possible to find a variety of measurements devices able to record or transmit the measurements to a central command post, in many of the existing networks the presence of a human being is still required to record the measurement. A mix of telemetry with man-made measurement systems is perhaps the most common situation. The ability to handle data with different qualities, is something which seems to be indispensable if realistic comparisons between the results of network models with reality are to be carried out.

Due to meter or communication line malfunction, the measurements themselves may be subject to error and, quite possibly, some of them may become unavailable during a certain time interval. A robust calibration procedure should be able to cope with such problems and eventually reject or correct those measurements, and avoid the spreading of such errors into the modelling of the rest of the network.

6.4. Problem formulation.

Having information on the real behaviour of the network at selected points, a new question appears, since, in general, measured and modelled variables do not coincide:

What can be done to improve the agreement
between the model and the real network ?

The answer to the latter question is basically the problem referred to as "calibration" of a network. A network is said to

be calibrated when the results obtained with the model match field measurements within some pre-specified reasonable tolerance, for the different operating conditions.

In the previous definition, some key words are relevant. Firstly, what is meant to be a "reasonable tolerance" and, secondly, what do we mean by "different operating conditions" ?. In the first case, we may have different criteria for establishing a reasonable tolerance, for example we could say that we want individual measurements to be within a fixed percentage of maximum disagreement (say, 5%; thus the maximum flow and head difference should be less than 5%) or, we could ask for a certain proportion of points (say 80% of the measured points) to be within a certain percentage of disagreement (say 5%), whereas the rest (say 20%) should be within a bigger error margin (say 10%). Obviously, different criteria can lead to completely different problems and, of course, could require different data quality and quantity. There is no definite answer to this problem, but the tolerance criterion to be used should be in accordance with the objectives of the calibration. To make things worse, the establishment of a tolerance criterion is problem-dependent; thus, on some occasions, when the network is characterised by a flat piezometric plane, for example, a more stringent tolerance criterion may become crucial for a meaningful analysis

It is essential that the network should be calibrated for all possible operating conditions. Hence, high and low consumption rates should be considered, as well as all the possible

combinations of operating modes of devices like pumps, regulating valves, etc. Failure to do so may imply that a network appears to be calibrated when it is not. Of course, a model which does not match the behaviour of the real system is of little use for practical purposes and the importance of the calibration procedure becomes a key factor in the whole modelling process. This applies to all kinds of models.

The calibration problem, then, can be formulated as that of finding a corrective procedure for the different parameters involved in the network model, in order to reduce (or eventually eliminate) the discrepancies between the model and the real network, for all the possible operating conditions, using a limited amount of measurements, each one possibly with a different accuracy. This formulation is adequate for an off-line calibration procedure, when batches of data measurements are available for different operating scenarios. By a limited amount of measurements we mean the amount of measurements we normally have available in water distribution systems, where we rarely have as many measurements as parameters needing to be calibrated and, certainly, we are never in a situation where we may have redundancy of measurements, except in some very special cases, like long and important pipelines.

As far as the present work is concerned, we shall restrict ourselves to finding a solution to the calibration problem in the previous context.

In general, when a model is to be used on a real-time basis, a more demanding formulation is needed [see O'Connell (1977;

chapter 1)]. These more severe prerequisites can be expressed as:

* The model parameters should be updated whenever new data become available (adaptive model).
* The calibration procedure should be able to estimate the error associated with the corrected parameters.
* The calibration procedure should be robust, and able to operate with interrupted data sets.
* Low computational cost is desirable, in order to facilitate implementation on microcomputers.

6.5. Review of existing methods for water distribution network calibration.

We shall concentrate on full scale models of a water distribution network, these being the most widely used models for analysis and design purposes; in these models some reduction or "skeletonization" is permissible, but the model still replicates the real network both in a geometrical and a hydraulic sense.

Reduced scale models, where only 20-30 % of the original elements are included in the model are not explicitly considered here, though some of the existing techniques for full scale models are also applicable to reduced models. In reduced models, the network to be studied is no longer equivalent to the real one in the geometrical sense; this means that both the shape and the size of the model might be completely different to the real network, but the main hydraulic variables (flows at important pipes, heads at key nodes, levels at reservoirs, flows and heads

at pumping stations, etc.) are replicated by the model. Reduced models are used mainly for control purposes, especially in the cases where only the behaviour of the main network elements (reservoirs, pumping stations, etc.) is relevant; these models are necessary for computational reasons, for instance when very time consuming optimisation techniques (dynamic programming, non-linear programming, etc.) are being used. See Gilman et al. (1973), de Moyer (1973), de Moyer and Horwitz (1975) or Shimauchi et al. (1985) for details on reduced scale models

In the traditional approach to water distribution network calibration, of all the possible causes of mismatch between modelled and measured variables, two of them usually play a major role: the estimated nodal demands and the estimated resistance characteristics (pipes, valves, pumps, etc.). This has led to two different schools of thought, looking at the calibration problem either from a demand or a resistance point of view. In both cases, the way to deal with the calibration problem in the early stages of network analysis and modelling has been a trial-and-error exercise, where the network model is used as many times as possible, with different demands and/or pipe resistances until, hopefully, agreement between model results and measurements is achieved.

One of the earliest attempts to formalise and solve the calibration problem is due to Shamir and Howard (1968), where the network analysis problem (nodal formulation) has been reshaped in order to include nodal consumptions and element resistances as unknowns, as well as piezometric heads. In this context, a set of

non-linear equations is produced, now containing heads, consumptions and resistances as unknowns and, in principle, the non-linear system can be solved, provided that there are as many equations as unknowns. In practice, this is not always true, and the selection of the unknowns (specifically when dealing with consumptions and resistances) has to be done following a set of rules in order to get a "solvable" problem. Shamir and Howard (1968) enumerated some of these rules, which have subsequently been extended by Shamir (1973). However, the authors did not guarantee that even following these rules, a solution could be found.

An alternative approach has been the development of some calibration procedures based on a sensitivity analysis, where the model parameters (either demands or resistances) are studied according to their impact in the mismatch between modelled and measured variables. A correction to the most sensible parameter is computed in order to force agreement between model and real world. We shall review some of these algorithms.

Donachie (1974), following a nodal approach for the network analysis solver, presented a post-analysis calibration procedure, based on determining the impact of changes in the pipe resistances on the nodal piezometric heads. The values of the sensitivities of the nodal piezometric heads with respect to the changes in the pipe resistances are determined using the Jacobian matrix obtained in the original uncalibrated system, and these sensitivities are used to reduce the discrepancies between modelled and observed pressures. This approach leads to a set of

linear equations in the resistance corrections, which is overdetermined because there are as many equations as measurements (say M equations) and as many unknowns as pipes (say NP, with NP > M). The overdetermination is solved via a least squares fit, and the resistance to change is that which needing the smallest correction produces the largest effect in a sum of squares index. Choosing the most sensitive resistance allows us to continue the use of the original Jacobian (obtained during the network analysis solution) to carry out as many corrections as necessary, until agreement is obtained. This simplifies the procedure and reduces the computational cost. The procedure can be used under several demand conditions, thus choosing the resistance changes having in mind all the possible consumption scenarios.

Donachie (1974) also shows how the same procedure can be used to evaluate the sensitivity of the nodal piezometric heads to changes in the nodal consumptions.

The main comments that can be made in connection with Donachie's approach are:

* The method does not use the information on flow measurements (when available); calibration is carried out using the pressure measurements only.
* The selection of the pipe resistances to be adjusted is arbitrary, since the discrepancies between model and reality need not necessarily be produced by the most sensitive pipes. In practice, this means that the algorithm produces results that look like a good calibration, when this may not be the

case.

* The method considers that the pressure measurements are exact and does not allow for an explicit consideration of the quality (or error) of the measurements.
* The proposed method does not reproduce the pressure measurements, though it gets smoothed values which are close enough for practical purposes.
* The method does not give an estimate of the errors associated with the corrected values of the roughnesses.

Rahal, Sterling and Coulbeck (1980) followed a sensitivity analysis approach very similar to that of Donachie (1974), to develop a "static parameter tuning" (SPT) algorithm, since it referred to a time invariant system. This algorithm allows the characteristic parameters of pumps to be included in the calibration.

Rahal and Sterling (1981) extended the previous algorithm for dealing with the dynamics of an extended period simulation, where now the time varying nodal consumptions and reservoir levels are adjusted to match model results with the real network. The new algorithm is referred to as "dynamic parameter tuning" (DPT), to mark the difference with their previous "static parameter tuning" (SPT) method. The DPT algorithm operates in two stages:

I) Calibration of reservoir levels and reservoir inflows.

II) Calibration of nodal demands.

It is assumed that the static analysis model is exact, i.e. that the SPT algorithm has been previously used to calibrate the resistance parameters. Thus, the remaining uncertainties in the

dynamic case are the reservoir levels and the nodal consumptions.

The calibration of reservoir levels and inflows (stage I) is needed due to errors associated with the integration of the set of differential equations describing the dynamics of the system , which is done through a predictor-corrector scheme, but also because the SPT algorithm does not reproduce exactly the level measurements. Stage I is needed only once.

The second stage is based on the determination of the sensitivities of the nodal pressures and reservoir inflows to variations in the nodal consumptions; a correction for the nodal consumption is made by changing that nodal demand which, with the smallest change, produces the largest variation in the sum of squares of the errors. This needs to be carried out for one nodal consumption at a time, and as many times as is needed to keep the maximum discrepancy between the observed and modelled pressures under a pre-specified limit.

Most of the comments made for Donachie's algorithm are still valid for the SPT and DPT algorithms. In the case of the DPT, we can say that, in addition :

* The selection of which nodal demand to adjust is arbitrary, since the disagreement does not need to be produced by the most sensitive demand.
* The method is not able to reproduce exactly the level measurements and inflows in the reservoirs.

Coulbeck (1984) recognised that both the methods proposed by Donachie (1974) and Rahal et al (1980) " do not make full use of

the available information and can lead to results which disagree with practical experience". He presented a generalisation of the sensitivity-based algorithms, now including flow measurements and allowing the adjustment of most of the parameters (pipe resistance parameters, pumps control parameters, consumer demands and reservoir levels) simultaneously, rather than one at a time as previously. Coulbeck's algorithm still assumes that the measurements are exact. This leads to an overdetermined problem, since normally there are more parameters to adjust than measurements; the problem is solved via an explicit minimization of a weighted sum of squares performance index. The computer program implemented is interactive and the operator can examine the variation in the calibrated parameters, weighting factors, etc. in response to changes in the adjusting parameters.

Although Coulbeck's model removed some of the shortcomings of previous algorithms, the method is still deterministic, because no explicit handling of the measurement errors is allowed.

Gofman and Rodeh (1981), following a loop approach for the network analysis problem and looking for efficient microcomputer solutions, proposed a deterministic solution for the calibration problem. They introduced a fictitious device, which they called a "head generator", whose function is precisely to introduce extra head-losses (or gains) in order to force agreement between measured and predicted pressures. To obtain the solution, they have to add a pseudo-loop for each new pressure (head) measurement, the specification of which is arbitrary, as the

location of the "head generators"; additionally, they found that the problem is solvable only under certain conditions, otherwise the new problem either has no solution or has many solutions. Almost the same arguments as in the previous methods are applicable here, i.e. lack of capability for handling the error of the pressure measurements, no use of flow measurements, etc.

Ormsbee and Wood (1986) proposed an explicit deterministic algorithm for calibration, which is based in the well known linear theory method developed by Wood and his collaborators at the University of Kentucky. As each new pressure (head) or flow becomes available, an extra energy equation can be added to the original system, allowing for the addition of a new unknown. For calibration purposes, the algorithm proposed by Ormsbee and Wood (1986) considers that either a head loss adjustment (multiplicative) factor for the friction losses or an additive head loss factor for the minor losses are suitable variables. The user has to decide which kind of adjustment factor (or a combination of them) is to be determined. A general head loss adjustment factor is also possible (i.e. when a single measurement is available), but a combination of head loss adjustments and head loss factor (for minor losses) is preferred by the authors. This approach generates an extended non linear system of equations, one for each extra energy equation, which is solved following a similar approach as in the linear theory method. As a result, both the selection of which head loss is more relevant (friction or minor losses) and also the specific location of the pipe where that loss is to be introduced are

arbitrary and many solutions are possible, or none at all, as shown by Gofman and Rodeh (1981).

Walski (1987), in a discussion of Ormsbee and Wood's (1986) paper emphasises that errors in the pressure measurement data can lead to "unrealistic solutions", thus the accuracy of the measurements becomes a critical issue, as far as the credibility of the calibration is concerned. Also, the fact that steady state conditions are not common in a water distribution network (see section 6.2 of this chapter) has an impact on the accuracy of the measurements and in the discrepancies between modelled and measured heads. Walski's comments are applicable to all the calibration methods already reviewed.

Walski (1983, 1984, 1986), within a deterministic approach, proposed a completely different strategy for calibration. He recognised that both the pipe resistance parameters and the nodal consumptions can be the origin of the mismatch between observed and measured heads and flows. His approach is not based on re-formulating the network analysis equations. Using data (existing or especially obtained for this purpose) from fire flow testing, where a hydrant in the network is open and the pressures in the network and the level in a reference reservoir (or a PRV) are observed, Walski replaces the whole area of influence of the test, which has to be defined by the user, by an equivalent pipe and looks for multiplicative correction factors for the Hazen-Williams roughness coefficient C (say, B) and for the nodal consumptions (say, A), within the area of influence of the fire-flow test. With the information provided by the recorded

pressures in the hydrant before and during the test, plus the levels in the upstream reservoir and the flows measured at the hydrant, Walski's method leads to a system of 2 equations in the unknowns A and B, i.e. the corrective factor for the nodal demands and roughnesses, respectively; the system can be solved via an elimination process and an explicit formula for A and B can obtained. On obtaining A and B, all the previously estimated nodal demands within the area of influence are multiplied by A, while B multiplies all the Hazen-Williams roughnesses. According to Walski, the method then automatically determines whether the nodal consumptions or the roughnesses are the main factors contributing to the disagreement between observed and measured variables.

Walski's method operates over sectors of the system (which are defined based on the area of influence of the fire-flow tests), one at a time, until the whole area fed by the network is covered. The method actually is an extension of an existing practical procedure for determining the roughness of a single pipe, where now the single pipe under analysis is replaced by an equivalent (fictitious) pipe representing a sector of the network. The method is arbitrary, in the sense that the area of influence of the test is difficult to define precisely, this has an impact on the selection of the nodes affected by the test and their water demands. The method also downgrades initially well estimated demands, due to its averaging features; in fact, the original total demands may be increased or decreased by the algorithm. To apply this method, we need a network where it is easy to find a reference reservoir for a sector of the network,

which renders the method better suited for pie-shaped networks with a central reservoir feeding a nearly circular area. Another shortcoming is the difficulty of implementing the method on a computer, in order to apply it systematically. This approach is eminently practical and relies on hydrant flow tests, which forces the network to act locally under severe flow increases. Recently, Walski (1988a), based on a number of practical and real situations, expressed the view that "it will never be possible to develop a simple analytical procedure or optimisation technique that will calibrate a model"; he suggested that possibly expert systems can become helpful in this regard.

Bhave (1988), following a similar approach to Walski, but now guaranteeing that the total inflow remains constant and equal to the measured inflow (which Walski's method failed to maintain), proposed a calibration technique which adjusts pipe resistance characteristics and nodal consumptions simultaneously. Let NT be equal to the number of nodal pressure measurements plus reservoir level measurements; then, on taking a unique reference node, we can link this reference node with any of the pressure measured nodes and level measured reservoirs, thus creating NZ=NT-1 paths, each one starting at the reference node and ending at another measured node. Each measured node and associated path defines NZ zones and, for each zone "i", a demand adjustment δq_i can be made, if considered necessary by the user, such that $\Sigma\ \delta q_i = 0$ (summation over all the NZ zones is zero in order to maintain the total inflow constant) or a zonal resistance adjustment B_i can be introduced. Also, in each path, the predicted summation of head

losses and the measured total head loss between the reference and measured node must coincide. This leads to the establishment of NZ equations in NZ unknowns B_i and/or δq_i, which are to be chosen by the user; the resulting system of equations is non linear but Bhave uses a simple linearization scheme based on the fact that $B_i \approx 1$. The corrective factor B_i operates over all the pipes in a zone and the corrections in the demands per zone are distributed over the nodes, maintaining the proportions originally assumed for the nodal consumptions. An iterative procedure is followed until $B_i \rightarrow 1$ and $\delta q_i \rightarrow 0$ for all the zones.

Bhave's proposed method has most of the limitations and arbitrariness of Walski's method and according to its author "the convergence is rather slow", perhaps due to the linearization introduced in order to get a set of linear equations in the unknowns. The method is deterministic and it handles neither flow measurements nor the error inherent in the pressure measurements.

Lansey (1988) formulated the calibration problem within the framework of non linear programming, having as an objective function the sum of squared differences between measured and modelled heads (he did not consider flow measurements), though a slightly different objective function based on the ratios between measured and modelled heads is also discussed. The restrictions are basically the set of non linear equations relating head loss and flows per branch, the mass balance per node equations and additional constraints on the variation of nodal demands, roughnesses, PRV settings and valve characteristic coefficients. In order to make the problem tractable from the computational

viewpoint, Lansey does not include the set of non linear head loss/flow relationships, but replaces it in an implicit way, using the network solver in tandem with the optimisation model. Lansey provides neither examples nor performance information on this approach. The formulation presented by Lansey is able to cope with multiple loads, though it is still deterministic and uses only pressure measurements. Shimauchi et al. (1985), dealing with a reduced scale model of the network, followed a similar approach, this time including a weighting factor in the objective function to consider measurement errors and including explicitly the set of non linear head loss/flow relationships in the constraint set.

Ormsbee and Chase (1988), following a similar approach to Lansey, but now with a linear objective function minimizing the absolute value of the ratio between measured minus modelled variables and measured variables. Although the objective function is explicitly linear, in fact it is implicitly non linear in the unknowns (heads, flows, resistance parameters). The minimization problem is constrained by implicit system constraints (mass and energy equations) and also by minimum and maximum bounds for the pressures, flows, roughnesses, nodal demands and slope of the piezometric head line. As in Lansey's formulation, the solution of the non linear optimisation problem is quite expensive from the computational viewpoint and the complex method is recommended by the authors as an efficient solver, the complex method being to non linear programming as the simplex method is to linear programming. The authors applied this method to two cases in the U.S.A.; one of them corresponds to the city of Arlington (316

pipes and 197 nodes) and the other corresponds to the Federally Owned Water Main (FOWM) in Washington D.C. (64 pipes and 55 nodes); both systems link together. The authors did not present any performance- related information.

6.6. Deterministic versus stochastic approach to the solution of the calibration problem.

All the methods reviewed in the previous section for full scale water distribution network models are deterministic, in the sense that most of them are not able to handle explicitly the errors associated with the measurements and, in addition, they are not capable of producing estimates of the errors associated with the estimated parameters.

Nowadays it is recognised that data with large errors can lead to unrealistic results in the calibration process. On the other hand, due to the shortage of measurements in water supply networks, which is typical of these systems, we have to utilise all the measurement information available, even the low quality data. In addition, the availability of measurements obtained from devices of different quality is not unusual in real systems. All this leads to the need for a calibration method which can explicitly handle the errors associated with the measurements. The algorithm then must be able to "weight" the data according to their errors and finally, produce estimates not only of the calibrated variables, but also of their associated errors, since a corrected roughness of C=100±10 is very different from another of C=100±100. This is consistent with our formulation of the

problem, as presented in Section 6.4.

Only the methods based on the non linear minimization of the discrepancies between observed and modelled variables are close to this approach [Lansey (1988), Ormsbee and Chase (1988)], although they do not consider error measurements explicitly; this is something that can be added relatively easily into the objective function. Even with that modification these methods are not able to produce estimates of output errors, with the additional burden that their computational cost is very high indeed. The main problem with the non linear optimisation approach is perhaps due to the fact that it is in essence a deterministic approach, i.e. it does not truly recognise the probabilistic nature of the problem. In fact probabilistic (stochastic) estimation methods for model calibration differ from the optimisation approach in that they add some additional requirements to the problem, normally in the sense that not only must the residuals be minimized but also the variances associated with the estimates have to be explicitly minimized.

We shall adopt a stochastic approach to the calibration problem, based on some of the parameter estimation techniques already available from the statistical and control fields, which have been successfully used in other problems of water resources engineering. We believe that only in this context is it possible to handle efficiently the calibration problem, as formulated in Section 6.4; this can, eventually, lead to algorithms which can be implemented in real time at the microcomputer level. Additionally, we shall implement some deterministic calibration

techniques as well and we will compare them in order to evaluate their respective advantages and disadvantages.

6.7. The rationale of the proposed calibration method.

Although it is clear that the calibration problem has to be addressed within a dynamic framework, i.e. considering the whole range of possible operational states for the system (e.g. low demand and high demand periods), we shall follow the usual procedure of simulating the extended period operation of the system via the integration of successive static analyses. The dynamics of the extended period simulation are described via a set of differential equations which cater for the storage variation within each reservoir; the system has as many differential equations as reservoirs. In following this approach, it is reasonable to assume that the calibration process also has to be carried out in two mutually interactive stages:

* Static calibration: where it is assumed that the total demand and its spatial distribution is known at a specific time and only the pipe roughness can be considered as responsible for the mismatch between the observed and modelled variables (nodal heads and pipe flows). In this case the reservoir levels and valve and pump status are considered fixed and known.
* Dynamic calibration: now the time variation of demands and reservoir levels are assumed to be responsible for the disagreements between observed and modelled variables.

We shall concentrate mainly on the static calibration problem.

First, let us assume that we know exactly the nodal demands and their spatial distribution at a certain time instant; this assumption is based on the fact that the spatial variation of the demand has been thoroughly studied and estimated, using for example the methodology recommended by the Water Research Centre [see Brandon (1984)] for nodal demand allocation and/or using the information from meter reading at household level [see Harrison (1988)]. Additionally, we assume that the total demand is measured at any time in the system (reservoir outflows, pump discharges, etc.), so that it can be assumed that the nodal demands allocated are a correct estimate of the spatial variation and the total demand (summation of all the nodal consumptions) must match the total measured demand. A proportionality factor can be applied in order to force agreement between these total demands (measured and summation of the estimated ones).

Hence, we are faced with a calibration problem where the pipe roughnesses are meant to be the main factor contributing to the model mismatch with reality. In fact, this approach implicitly considers effective diameter and length variations, as well as minor losses, as part of the roughness to be estimated. The roughness is then the only "instrument" to be used to calibrate the model.

The rationale of the proposed static calibration method can be explained as follows: let us consider a "network" consisting of a single pipe joining node "i" and "j" then, in order to estimate the true value of the roughness at the pipe, we need to measure the difference between piezometric heads at each node and also

the flow in the pipe. With these measurements, say H_i^* - H_j^* and Q_{ij}^* , and using the known head loss/flow relationship (1), we can compute the corresponding estimate of the true resistance parameter ($\underline{\alpha}^*$) for each pipe as:

$$\alpha_{ij}^* = (H_i^* - H_j^*) / (Q_{ij}^*)^n \qquad (2)$$

Ideally, having measurements for all the head losses and flows per pipe in a larger network, the application of equation (2) would lead us to compute all the resistance parameters (i.e. the vector $\underline{\alpha}^*$). Because in practice we do not have measurements of all the nodal piezometric heads and pipe flows, we have to find the best estimates of them and use equation (2) to produce our best estimates of the resistance parameters. The calibration problem is now reduced to the estimation of nodal piezometric heads and branch flows, based on a limited amount of available measurements.

Note that if, in our single pipe system with nodes "i" and "j", Q_{ij}^* is not the true value, we would be able to find a different α_{ij}^* which could make the network look like it has been calibrated when it has not. If we analyse a network consisting of series-connected pipes, where the initial and final nodes of the series have measured piezometric heads, even when knowing the true flows per pipe, the problem of finding the resistance parameters per pipe has infinite solutions; to break up this indeterminacy we need to incorporate some additional information.

Once the α_{ij}^* have been estimated, using equation (2), the computation of the estimated pipe roughness vector ($\underline{C}^*$) is straightforward in the case of the Hazen-Williams formula, since

$\underline{C}^*$ is explicitly related to the estimated characteristic resistance parameter α_{ij}^* via the following relationship:

$$C_{ij}^* = \{ L_{ij} / [33686.36 D_{ij}^{4.87} \alpha_{ij}^*] \}^{(1/1.852)}. \quad (3)$$

When using the Darcy-Weisbach formula a similar (direct) procedure is needed to compute the friction factor. Having the friction factor, the effective roughness can also be determined directly from the Colebrook-White formula.

In practice, some control on the maximum variation allowable for C_{ij}^* is needed, in order to prevent C_{ij}^* reaching unrealistic values, especially in pipes where poor head estimation (of initial and final nodes) and poor flow estimation coincide. We allow C_{ij}^* to move within an "allowable band" around the initial roughness estimate, i.e.:

$$(1-x)C_{ij}^{(o)} \leq C_{ij}^* \leq (1+x)C_{ij}^{(o)} \quad (4)$$

where:

$C_{ij}^{(o)}$: initial roughness estimate for pipe "i-j".

x : maximum variation factor for C.

In the results presented here, the maximum variation factor "x" has been set to 0.10, thus allowing C_{ij}^* to move within 90 and 110 % of the initial roughness estimates.

In theory, when having head and flow estimates near the true values, this variation factor "x" should be left as wide as possible (i.e. C_{ij}^* is allowed to vary without constraints). In principle, with "good" head and flow estimates, the calibration algorithm should produce "good" roughness estimates, irrespective of the initial roughnesses (then there is a need for "x" to be as

large as possible).

We shall postpone further discussions on the subject of this variation factor "x" to subsequent sections of this chapter.

The calibration algorithm can be viewed in a slightly different way: let us denote the true parameters of the network by $\underline{\alpha}^t$, $\underline{H}^t$ and $\underline{Q}^t$ (i.e. resistance parameter, nodal heads and flows per pipe); then, because the head loss/flow relationship holds for every pipe joining nodes "i" and "j", we can write:

$$\alpha_{ij}{}^t = h_{ij}{}^t / (Q_{ij}{}^t)^n \qquad (5)$$

where $h_{ij}{}^t$ is the true head loss, i.e.: $h_{ij}{}^t = H_i{}^t - H_j{}^t$.

Similarly, for the estimated variables, $\underline{\alpha}^*$, $\underline{H}^*$ and $\underline{Q}^*$, the following is true (equation 2):

$$\alpha_{ij}{}^* = h_{ij}{}^* / (Q_{ij}{}^*)^n \qquad (6)$$

where $h_{ij}{}^*$ is the estimated head loss, i.e.: $h_{ij}{}^* = H_i{}^* - H_j{}^*$

Hence, dividing equations (5) and (6):

$$\frac{\alpha_{ij}{}^*}{\alpha_{ij}{}^t} = \frac{h_{ij}{}^* / (Q_{ij}{}^*)^n}{h_{ij}{}^t / (Q_{ij}{}^t)^n}$$

which can be re-arranged as:

$$\frac{\alpha_{ij}{}^*}{\alpha_{ij}{}^t} = \left[\frac{h_{ij}{}^* / h_{ij}{}^t}{\{Q_{ij}{}^* / Q_{ij}{}^t\}^n} \right] \qquad (7)$$

which can be interpreted in the sense that:

$$\left.\begin{array}{lll} & \underline{\alpha}^* \quad \text{---}> \quad \underline{\alpha}^t \\ \text{if} & \underline{h}^* \quad \text{---}> \quad \underline{h}^t \\ \text{and if} & \underline{Q}^* \quad \text{---}> \quad \underline{Q}^t \end{array}\right\} \qquad (8)$$

It is not difficult to see that equation (7) also holds for the case when:

$$E[\underline{h}^*] = K\, \underline{h}^t \qquad (9)$$

and

$$E[\underline{Q}^*] = K\, \underline{Q}^t \qquad (10)$$

where K is a constant.

The latter case implies that the estimated roughness parameters can be equal to the true parameters when both heads and flow estimates have exactly the same bias. This is only of theoretical interest, since in practice the probability of having both estimators with exactly the same bias is zero.

Clearly, (7) and (8) can be thought of as being the formal expression of the rationale of our proposed calibration algorithm.

6.8. An iterative approach for the solution of the static calibration problem.

The problem now is twofold: firstly we need to estimate the piezometric heads within the network, based on a limited amount of head (pressure and levels) measurements, which we assume are sufficient to represent the structure of the piezometric plane "floating" above the real network. The second problem will be the estimation of the pipe flows.

The problem of estimating the piezometric heads in the unmeasured nodes can be approached in various ways. We shall examine the feasibility of using a geostatistical estimation

technique known as "Kriging", which is able to explicitly handle noisy data and to produce an estimate of the error of its own estimates. We also examine the use of a data approximation technique known as bi-cubic splines, which is able to cope with noisy data as well and, finally, a simple deterministic one-dimensional interpolation technique will be described, which uses the information of the initially guessed pipe resistances to fit a broken line to the nodal head measurements.

The problem of estimating the flows is more complex, since the flow distribution is strongly dependent on the network structure. We can assume that if the flow distribution provided by the raw model is close to the true flow distribution, we can use it as an "estimate" of the true flows in the unmeasured pipes. This assumption holds if the initial roughness estimates are good in relative terms (i.e. relative to each other, rather than in terms of their absolute values), since in that case the flow distribution corresponding to the raw model will be close to the true flow distribution. Flow measurements replace the modelled flows, when available. We have found that this solution leads to pipe flow estimates in a straightforward manner and, because the assumption that the modelled flows are close to the true flows is not exact, an iterative procedure leads to the final flow estimates.

The basic structure of the proposed algorithm for static calibration of the water distribution model can be represented in the schematic shown in Fig. 6.1. The iterative algorithm converges to the true values of the roughness parameters,

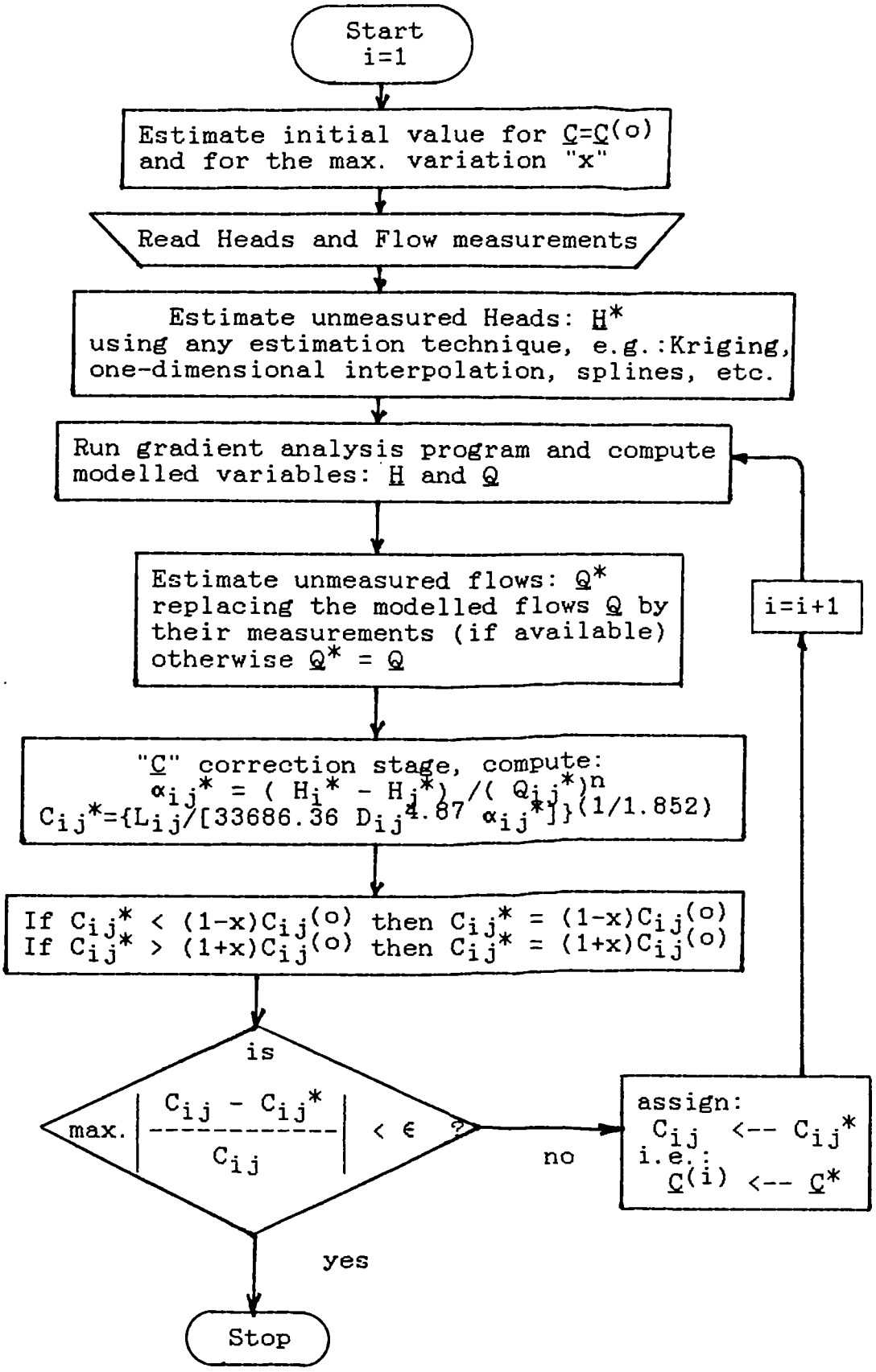

Fig. 6.1. Basic iterative static calibration procedure, computing corrected Hazen-Williams roughness vector C.

provided that we input optimal estimates of the nodal piezometric heads and pipe flows, as indicated in (8). Additionally, because the estimation processes (of heads and flows) could be carried out separately from the calibration itself, it would be possible to introduce further improvements in the estimation of heads and flows into the calibration procedure in a straightforward manner. This means that this static calibration scheme can be used as a framework for improved head and flow estimation algorithms in the future.

6.9. Estimating the piezometric heads.

6.9.1. Introduction.

There are two main approaches to estimating the piezometric heads in the unmeasured nodes of the network, namely we can either follow a probabilistic or a deterministic approach.

In a probabilistic (stochastic) approach both the measurement errors and estimation errors are explicitly handled. In this context, we have attempted to solve the problem with a standard discrete linear Kalman filter, but because of lack of measurement redundancy (which characterises these networks) the question of the observability of the system arises, rendering this approach non feasible for general distribution networks. Notwithstanding, the Kalman filter approach can be the right one in situations where the observability condition is met, like in long pipelines or in main distribution systems feeding the distribution networks of a more complex system (these main distribution systems are not

looped networks, in general). Another situation where Kalman filters have been successfully used in water distribution systems is when dealing with reduced models, like the "replication model" [see Gilman et al. (1973), de Moyer (1973) or de Moyer and Horwitz (1975)] where, because of the model reduction, the observability problem does not arise; however this is not our objective, since we are interested in full scale models. We have tried, unsuccessfully, to overcome the observability problem via the introduction of pseudo-measurements, following a similar approach to that used in power systems, but the solution via pseudo-measurements seems to be more appropriate for solving the problems of missing data and bad data replacement due to communication failure in telemetered systems, rather than overcoming the observability question. Research in this field has been quite active in recent years, which is reflected in the literature: Krumpholz et al. (1980), Alvarez and Albertos (1982), Clements et al. (1983), Lo et al. (1983), Bargiela (1985), Monticelli and Wu (1985 a,b). An alternative possible estimation technique which by-passes the observability problem is "Kriging", a geostatistical estimation technique which originated in mining engineering and is used nowadays in the water resources field (hydrology, groundwater, etc.).

Following a deterministic approach, the problem is formulated here in a one dimensional fashion, and the aim is to fit a broken line to the set of data points (measured heads) and then interpolate the unmeasured heads. This can be done either via least-square fitting techniques or interpolation methods. The main shortcoming of this approach is the fact that the errors

associated with the measurements cannot be handled and, as a result, the errors associated with the estimates cannot be produced. Nevertheless, we shall explore the effectiveness of an interpolation method, which uses the information available on pipe resistances and we shall compare its results with those produced via a probabilistic scheme.

A third alternative for head estimation, which somehow lies in between the probabilistic and the deterministic approaches is represented by the use of splines, basically a deterministic data interpolation and approximation technique which is also able to handle noisy data; this latter issue is known as the "statistical problem" in the splines literature. We shall explore the feasibility of using splines for head estimation in the final part of this Section.

6.9.2. Estimating the piezometric heads using Kriging.

6.9.2.1. Introduction.

We shall review the main assumptions underlying the application of Kriging in the estimation of the unmeasured piezometric heads in a water distribution network. We also summarise, at the end of this section, the main steps followed in the estimation of unmeasured heads using Kriging.

We assume that the piezometric heads in the network can be represented by a continuous piezometric plane "floating" above the network, at a distance from the ground level which is equivalent to the pressure at each node of the system. Recently,

Hamberg and Shamir (1988 a,b) have used the same concept for different purposes, though they extended the idea of a continuous plane to the flows as well.

The spatial variability of the piezometric plane is not random, it has an underlying structure which is a function of the distance (i.e. two head measurements close enough should give nearly the same result) and of the network characteristics. The structure of the piezometric plane is such that its higher levels are defined by the reservoir levels and then it starts to diminish towards the lower parts of the system. The piezometric plane then has a "trend" in the space, with a maximum level at the reservoirs (or source pumps, or PRV's, etc.) and a minimum level near the borders of the network. This may be valid for a whole network or a sub-network; for example: in multiple source systems, for every source we can define a sub-network, which contains all the pipes and nodes fed from this particular source. The same subdivision arises when a series of pressure regulating valves are separating the main network into different pressure zones, each pressure zone becoming a sub-network.

The piezometric plane actually exists only over the pipes, and does not exist over the rest of the space but, since we are only interested in the plane's behaviour over the pipes, there is no reason to prevent us thinking of the piezometric plane as a continuous plane. Moreover, the traditional way of modelling water distribution networks is mainly concerned with the piezometric heads above each node (including reservoir levels); thus we restrict ourselves to the values of the plane at some

particular points of the space. On the other hand, current models assume that the head loss between two connected nodes is linearly distributed; this is only because in the model the consumptions are arbitrarily concentrated in the nodes and not along the pipes, as in the real network. As a result, we get a representation of the piezometric head which is a set of straight lines, broken at the nodes. This discontinuous model may be far from the real piezometric head behaviour, since nodal consumptions are just a fiction, created to produce a mathematically tractable problem.

On top of that, the continuous plane representation of the piezometric heads in the network provides an automatic way for considering the looped nature of most water distribution networks, since a head increase in a particular node of the network (due to a booster pump, for example) will have an impact on surrounding nodes, increasing their heads in a way which is easily handled by the continuous plane approach. Another interesting feature of this way of modelling the piezometric plane is that we can, eventually, use head (pressure) measurements taken not only over the nodes, but also measurements taken at any point of the network, to estimate the head over unmeasured nodes.

Finally, we have to stress that even though we are <u>imagining</u> the piezometric head as a continuous plane, <u>we are not actually using it as such</u>, since we are constraining ourselves to the heads over the nodes only. The continuity assumption helps us to handle the underlying structure of the piezometric heads in the

network.

We are aware that Kriging might not be the best solution when dealing with networks whose piezometric plane is highly irregular, e.g. when P.R.V.'s and booster pumps are located in some pipes of the network.

We assume, for the time being, that the pressure measurements are located at key points of the network and that they are numerous enough, so that the main features of the piezometric plane are contained in the measurement set. We believe that this is <u>not</u> a very stringent requirement and, to explain it, we can take as an example the case when we need to draw a topographic map; in that case, if we fail to take measurements at key points (i.e. a hill, a hole, etc.), we shall miss them when the time comes to "reconstruct" the topography in a contour map. In other words, this means that any estimation method (for the piezometric heads in our case, or for ground levels in the topographic case) will give "bad results" if the assumption on the location and amount of measurements is not met. These concepts are dealt with in the characterisation stage of the Kriging process, something which in mining geostatistics in referred to as "structural analysis", the characterisation being a stage previous to the parameter estimation itself.

6.9.2.2. Estimation using Kriging.

For completeness, we have included in Appendix B the derivation of the Kriging estimator equations.

Following Appendix B, the main steps in estimating the unmeasured piezometric heads using Kriging can be summarised as follows:

a) Read the data corresponding to the "n" piezometric head measurements (Z_i) and their location ($\underline{x}_i$, i=1, ..., n).

b) Based on the information of the field data points, i.e. piezometric heads at certain nodes of the network (their location given by their coordinates projected on the horizontal plane), the experimental semi-variogram (or simply variogram) is constructed, via a procedure similar to that presented in Table B.1. Fig. B.1. represents an example of a resulting experimental (or estimated) variogram.

c) One of the five analytical models summarised in Table B.2. is selected as the best representation of the experimental variogram. The parameters A_o, B_o and C_o are determined. This has been done in our case on a trial-and-error basis, plotting the experimental variogram and the modelled variograms and choosing that model which follows the experimental variogram closest.

This step is critical, since the structure of the piezometric head plane is encapsulated in the semi-variogram and the quality of the estimation process will be strongly dependent on the quality of the variogram model produced at this stage.

d) With the specification, in the data set, of the points where the estimation is required (say $\underline{x}_o$), and with the analytical model fitted to the experimental variogram, the Universal Kriging linear system of equations is set up and solved for the extended

set of unknowns weights λ's and μ's in equation (62) or (63) of Appendix B, which are reproduced here as equations (11) and (12):

and

$$\boxed{\begin{aligned} &\sum_j \lambda_o^j \, K(x_i - x_j) + \sum_k \mu_k \, p^k(x_i) = K(x_i - x_o)] && i=1,\ldots,n \\ & && j=1,\ldots,n \\ &\sum_i \lambda_o^i \, p^k(x_i) = p^k(x_o)] && k=1,\ldots,m \end{aligned}} \qquad (11)$$

Equation (11) constitutes a system of (n+m) equations in (n+m) unknowns: λ_o^i i=1,...,n and μ_k k=1,...,m, which in expanded form can be seen as:

$$\begin{bmatrix} K_{11} & K_{12} & K_{13} & \cdots & K_{1n} & 1 & p_{12} & \cdots & p_{1k} \\ K_{21} & K_{22} & K_{23} & \cdots & K_{1n} & 1 & p_{22} & \cdots & p_{2k} \\ \vdots & \vdots & \vdots & & \vdots & \vdots & \vdots & \cdots & \vdots \\ K_{n1} & K_{n2} & K_{n3} & \cdots & K_{nn} & 1 & p_{n2} & \cdots & p_{nk} \\ 1 & 1 & 1 & \cdots & 1 & 0 & 0 & \cdots & 0 \\ p_{21} & p_{22} & p_{23} & \cdots & p_{2n} & 0 & 0 & \cdots & 0 \\ \vdots & \vdots & \vdots & \cdots & \vdots & \vdots & \vdots & \cdots & \vdots \\ p_{m1} & p_{m2} & p_{m3} & \cdots & p_{mn} & 0 & 0 & \cdots & 0 \end{bmatrix} * \begin{bmatrix} \lambda_o^1 \\ \lambda_o^2 \\ \vdots \\ \lambda_o^n \\ -\mu_1 \\ -\mu_2 \\ \vdots \\ -\mu_m \end{bmatrix} = \begin{bmatrix} K_{10} \\ K_{20} \\ \vdots \\ K_{n0} \\ 1 \\ p_{20} \\ \vdots \\ p_{m0} \end{bmatrix} \qquad (12)$$

where

$$K_{ij} = K(x_i - x_j)$$

and

$$p_{ij} = p^i(x_j)$$

This represents a simplification of Universal Kriging, since the generalised covariance $K(\underline{x})$ has been approximated by the analytical model determined in stage c). The computer program used for Kriging allows the specification of the order (k) of the drift polynomial $p^k(x)$ representing the trend of the piezometric plane [see equation (56) in Appendix B]; in our case we found out by successive trials that a linear drift was

adequate.

e) With the values of the unknown weights [λ's in equations (11) or (12)], the estimates of the piezometric heads at the unmeasured nodes ($\underline{x}_o$) can be computed via equation (57) in Appendix B, which is reproduced here as:

$$Z_o^* = \Sigma \lambda_o^i Z_i \qquad (13)$$

where:

Z_i represents the set of measured piezometric heads.

λ_o^i represents the unknown Kriging weights associated with the data set.

f) Having determined the values of the extended set of unknown weights [λ's and μ's in equations (11) and (12)], the Kriging variance is computed using equation (66) of Appendix B, for each point where the estimation is required ($\underline{x}_o$):

$$\sigma_o^2 = \text{var}(Z_o^* - Z_o) = K(0) + \sum_k \mu_k p^k(\underline{x}_o) - \sum_i \lambda_o^i K(\underline{x}_i - \underline{x}_o) \qquad (14)$$

The main steps of the piezometric head estimation process using Kriging are shown in Figure 6.2. This flowchart is connected with that shown in Fig. 6.1, in fact, with the exception of the input data section, Fig. 6.2 can replace the block "estimate unmeasured heads" in Fig. 6.1.

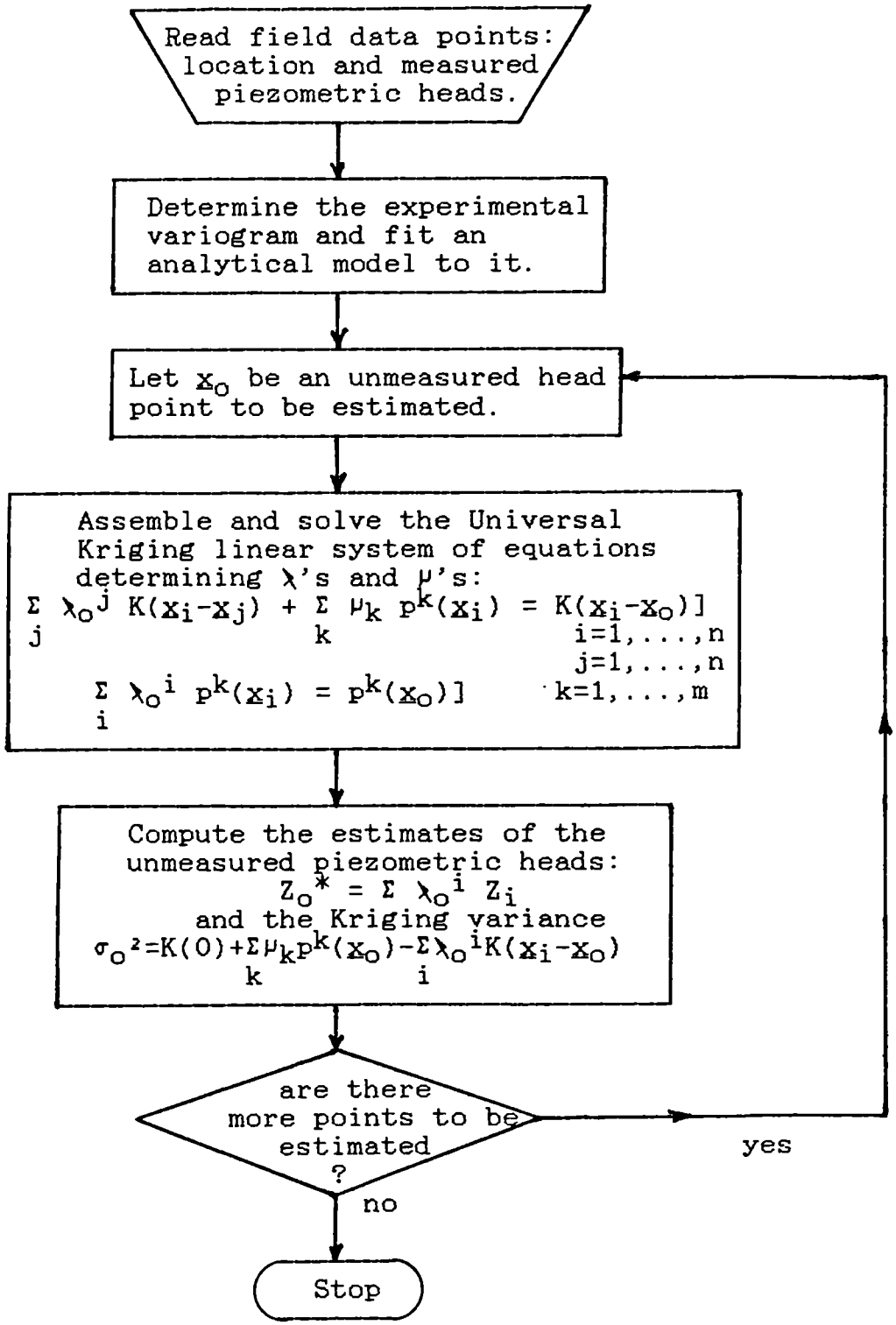

Fig. 6.2. Estimation of the piezometric heads using Kriging.

6.9.3. Estimating the piezometric heads using a deterministic one-dimensional interpolation method.

6.9.3.1. Introduction.

Prior to the calibration stage in the modelling of a water supply distribution network, a raw network model has been built by assuming the values of the resistance parameters for the pipes; these assumptions have been made based on the best information available, i.e. pipe material, age of the pipes and, eventually, some field or laboratory tests.

The information contained in the raw network model has not been explicitly used in the Kriging approach for estimating the piezometric heads, but it is clearly relevant, especially if a systematic initial roughness determination procedure has been carried out [like those described by Walski (1984, chapter 8), for example]. In so doing, we may expect local differences in the assumed roughnesses, due to unforeseeable events, with respect to the true roughnesses, but, on average, we may also expect that they do contain the main features of the roughness characteristics of the network. Consequently, we should try to use this information already contained in the raw model, together with piezometric head measurements, in order to obtain improved head estimation in the unmeasured nodes. This is precisely what we do in the deterministic one-dimensional interpolation method.

The main steps in the proposed deterministic one-dimensional interpolation procedure are:

a) Read the data corresponding to the piezometric head measurements and the initial values for the pipe roughnesses.

b) Run the raw network model (gradient method program) and determine pipe flows, nodal piezometric heads, and, particularly, pipe head losses (amount and direction). This is a standard run of the gradient method for the network analysis problem. The program is run with the initially assumed roughnesses of the pipes.

c) Determine the minimum head loss spanning trees, rooted at each reservoir (if more than one). This gives us the paths connecting each node with a reservoir, following a minimum head loss criterion. The shortest path algorithm used is Dijkstra's algorithm [see Smith (1982) or Deo (1974)], where the distance between nodes has been replaced by the head loss. The reason why the pipe head loss has been chosen as the criterion for determining the spanning tree will become apparent in the following paragraphs.

d) In the case of more than one reservoir, resolve the linkage of those nodes which are included in more than one spanning tree, maintaining their linkage only to that reservoir which leads to the minimum head loss to the node.

e) For each spanning tree, generate as many paths (one-dimensional arrangements of successive nodes), starting at a reservoir and following the spanning tree downstream, as to sweep all the nodes in that spanning tree. As we proceed downstream, the initial node of a path may be another measured node (not

necessarily a reservoir) or a previously interpolated node. When information on the accuracy of the head measurements is available, we should include the nodes with higher accuracy first, so that the lower accuracy nodes (and the unmeasured ones) are handled with the best information available, thus minimising the error of the interpolation.

The minimum head loss criterion has been used to generate the spanning tree, instead of other criteria like maximum flow or maximum head loss, because it produces paths having a flat piezometric line, thus minimizing the error in the interpolation.

f) Having the paths which cover all the nodes of the network, perform the one-dimensional interpolation in order to force coincidence at the measured nodes between modelled and measured piezometric heads, thus obtaining interpolated heads for all the unmeasured nodes. This point is explained in more detail in the next section.

The whole one-dimensional deterministic interpolation process is summarised in Fig. 6.3. This flowchart is also connected with that shown in Fig. 6.1, in fact, with the exception of the input data section and the estimation of initial roughnesses, Fig. 6.3 can replace the block corresponding to the estimation of unmeasured heads in Fig. 6.1.

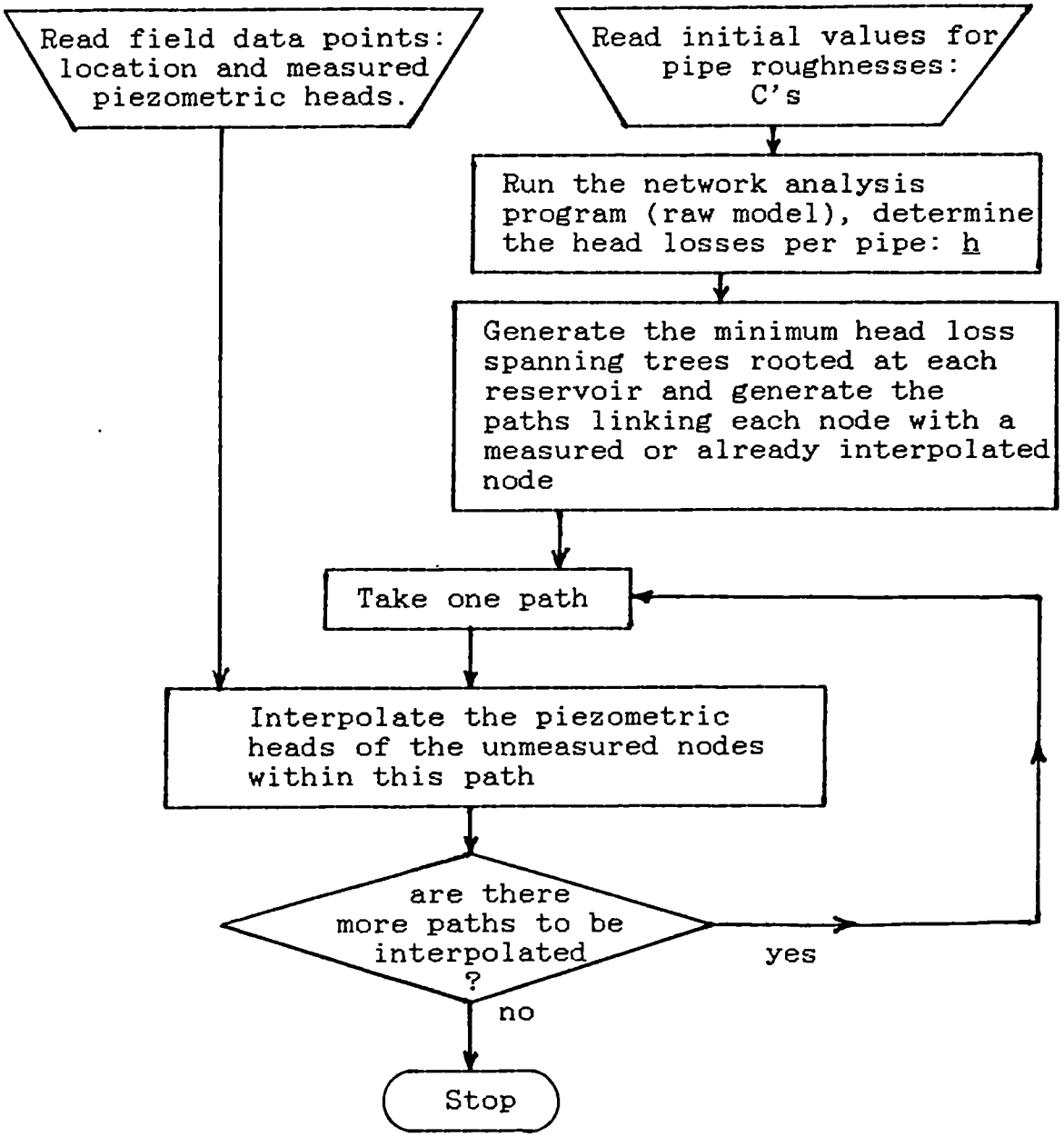

Fig. 6.3. Estimation of piezometric heads using the one-dimensional deterministic interpolation scheme.

6.9.3.2. The one-dimensional interpolation.

For the one-dimensional interpolation, we take each one of the paths (generated via the minimum head-loss spanning trees) at a time.and we compare the modelled piezometric line for every path with the corresponding head measurements. This can be represented as in Fig. 6.4.

Because each path starts in a measured node (or in an already estimated node), we search along the path for the next measured node, defining a reach between two known head nodes [see Fig. 6.4, where there are three reaches]. Having selected a reach in the path, we then compute the difference between the modelled piezometric heads corresponding to the initial and final node of the reach (DIF1 in Fig. 6.4) and also that corresponding to the observed (measured) piezometric line (DIF2 in Fig. 6.4) and we seek the coincidence of both modelled and observed piezometric lines at the measured nodes (initial and final nodes of the reach). To do so, we force the coincidence of modelled and observed piezometric lines at the initial node and spread the head difference DIF=DIF1-DIF2 along the reach in proportion to the length, so that coincidence will be achieved at the final node of the reach as well; the intermediate unmeasured (modelled) nodal heads are modified accordingly, becoming the "estimates" produced by this interpolation algorithm.

When a final measured node is not available, as in the last reach of Fig. 6.4, the modelled piezometric line of this last reach is moved parallel in order to force agreement in the initial node, since this is the only information available.

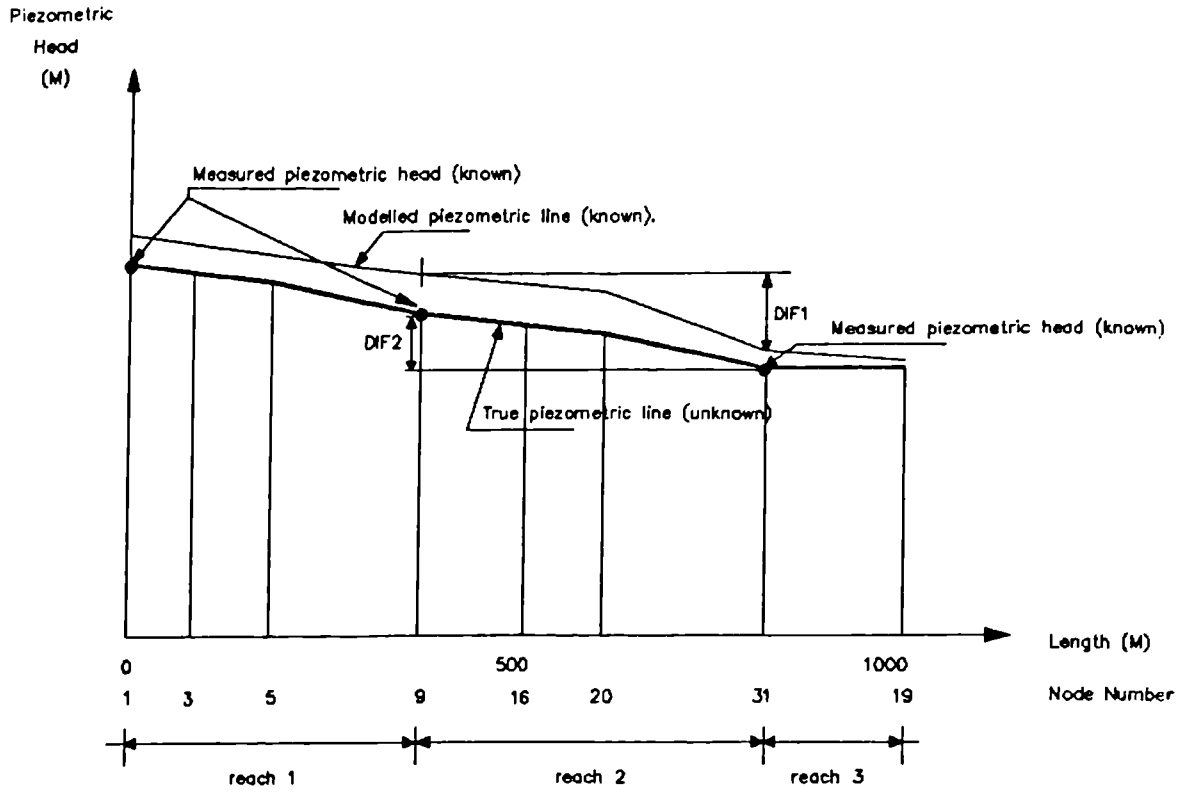

Fig. 6.4. Minimum head loss path of nodes, before the head interpolation has been carried out.

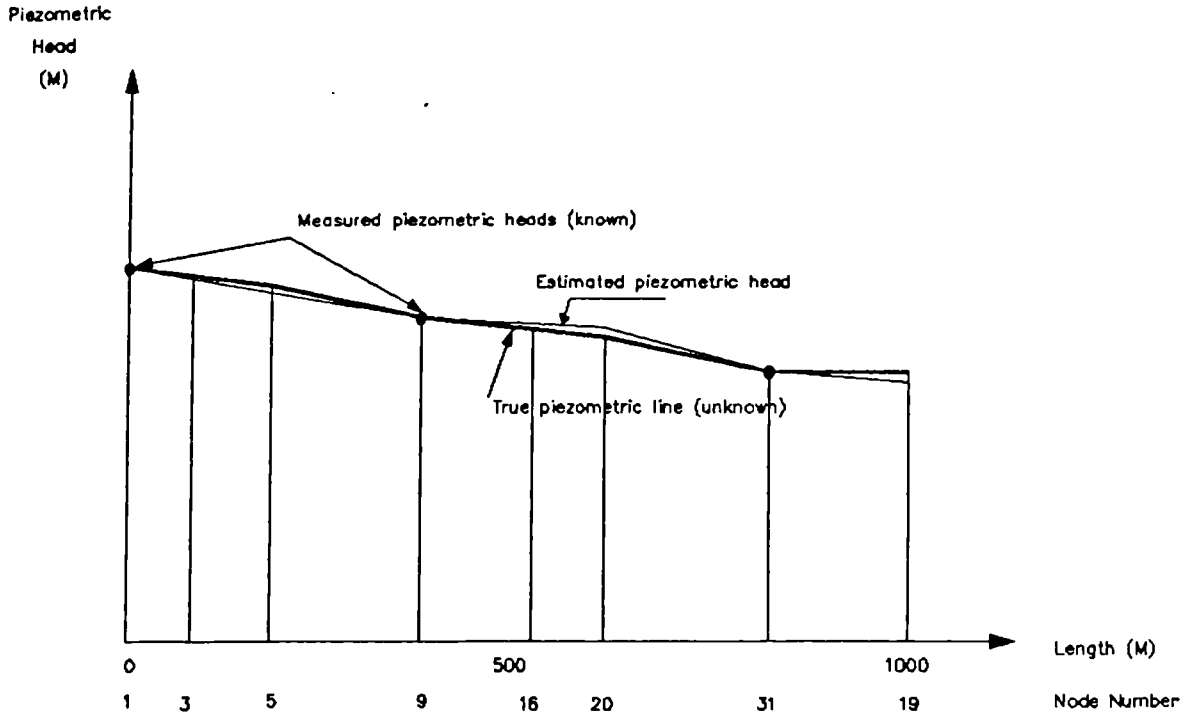

Fig. 6.5. Minimum head loss path of nodes after the head interpolation has been carried out.

The result of this one-dimensional interpolation procedure, for a particular path, after having gone through all the possible reaches, is shown in Fig. 6.5, where the adjusted modelled piezometric line coincides with the observed piezometric line at the measured nodes, while still keeping most of the information on the initially assumed roughnesses of the pipes.

The algorithm relies on the fact that the piezometric head has been measured at "key" nodes of the paths, for example:

- reservoirs (level measurements): these measurements are considered as indispensable.
- end points of the paths.
- intermediate points, between reservoirs and end points, especially if relevant changes in the piezometric line take place, due to higher consumptions or changes in the pipe characteristics.

The algorithm is deterministic, in the sense that it is not able to consider the error of the head measurements explicitly and, as a result, is not able to produce an estimate of the error in the interpolated (unmeasured) piezometric head.

6.9.4. Estimating the piezometric heads using bi-cubic splines.

6.9.4.1. Introduction.

In the previous sections we have been dealing with two different ways of estimating the piezometric heads: Kriging and a one-dimensional interpolation method. The first one is a stochastic method, which allows us to handle explicitly the errors associated with the measurements and also can give an estimate of the error associated with the estimated piezometric heads at the unmeasured nodes. The interpolation method is a deterministic approach and, as such, it does not allow us to handle the errors either in the measurements or the estimates.

In the Kriging-based method the structure of the piezometric head plane is encapsulated in the semi-variogram and the approach is valid when there is some correlation in the spatial distribution of the piezometric plane (i.e. its variation is not random).

In the interpolation method we make use of our a priori knowledge of the physical characteristics of the network. We blend this knowledge with the information provided by the head measurements, to produce an estimate of the piezometric heads in the unmeasured nodes.

The traditional way of representing the modelled piezometric heads has been through a set of broken straight lines, with the heads being computed at the nodes only and being linearly interpolated elsewhere. The one-dimensional interpolation technique already presented follows more closely this way of

representing the piezometric heads. It can be argued that, as far as the estimation of the piezometric heads is concerned, Kriging and the one-dimensional interpolation represent two completely opposite approaches. So, perhaps another approach halfway between Kriging and the one-dimensional interpolation scheme can offer a further alternative.

In the search for such an approach, and having in mind the need for an explicit handling of the errors in both the measurements and the estimates, bi-cubic splines came to our attention, particularly because of their reported ability to represent large and complex geodetic systems and terrain following problems [Anthony and Cox (1987)] , which are somehow similar to our piezometric head estimation problem, especially when pumps and regulating valves are present within the network. Splines have also been used in parameter estimation [Lainiotis and Desphante (1974)]. The possibility of obtaining the errors associated with the estimates puts the splines somewhere in between the two methods we have used so far: Kriging and the one-dimensional interpolation method.

6.9.4.2. Bi-cubic splines estimation.

Appendix C includes the derivation of the bi-cubic splines approximation equations and also includes the estimation of the error associated with the estimates. The main steps in the estimation of the piezometric heads using bi-cubic splines are the following:

a) Read the field data points representing the measured nodal piezometric heads:

$$\{x_r,\ y_r,\ f(x_r,\ y_r\}\quad r=1,\ 2,\ \ldots,\ m$$

where x_r and y_r represent the horizontal projection of the coordinates of the measured point and $f(x_r,\ y_r)$ is the corresponding value of the observed piezometric head. Also, the position of possible discontinuities in the spline polynomial or in its derivatives must be specified, within the range of the independent variables; this is done through the specification of the location of the "interior knots", both in the X and Y-directions :

X-direction knots: λ_i $i=1,2,\ \ldots,\ h$

Y-direction knots: μ_j $j=1,2,\ \ldots,\ k$

The exterior knots, needed for continuity reasons, are automatically placed by the computer program used.

b) With the data information, compute the values of the B-splines $M_i(x_r)$ and $N_j(y_r)$ using the recursive scheme represented by equations (4) and (5) in the Appendix C, set up the normal equations and solve them for the unknown vector of "weights" $\underline{\Gamma}$, i.e., from equation 14, Appendix C, solve

$$[A^T\ A]\ \underline{\Gamma} = A^T\ \underline{f} \tag{15}$$

where:

A : (mx(h+4)(k+4)) matrix obtained from the observation equations (equation 12, Appendix C):

$$\sum_{i=1}^{h+4}\ \sum_{j=1}^{k+4} \Gamma_{ij}\ M_i(x_r)\ N_j(y_r) = f(x_r,\ y_r) = f_r \qquad r = 1,2,\ \ldots,\ m \tag{16}$$

$\underline{\Gamma}$: (h+4)(k+4)x1 column vector of unknowns, with components Γ_{ij} in the previous equation.

$\underline{f}$: mx1 column vector, given by the components f_r in the observation equations.

c) For each one of the "n" pre-specified nodes where the piezometric head estimation is required:

$$(x_l, y_l) \quad l = 1, 2, \ldots, n$$

compute the B-splines $M_i(x_l)$ $N_j(y_l)$, using the recursive equations (4) and (5) of Appendix C, then introduce them into equation (11) of Appendix C to compute the splines approximates of the piezometric head at the unmeasured nodes:

$$s(x_l, y_l) = \sum_{i=1}^{h+4} \sum_{j=1}^{k+4} \Gamma_{ij} M_i(x_l) N_j(y_l) \qquad (17)$$

d) If required, compute the covariances and variances of $\underline{\Gamma}$, using equations (26) and (27) of Appendix C and use them to determine the variances of the spline estimates.

The piezometric head estimation process using bi-cubic splines is shown in Fig. 6.6. This flowchart is connected with that shown in Fig. 6.1, in fact, with the exception of the input data section, Fig. 6.6 can replace the estimation of unmeasured heads block in Fig. 6.1.

The computer software used is that contained in the NAG-Library. Step b) is carried out with the subroutine E02DAF, while step c) is performed using the subroutine E02DBF.

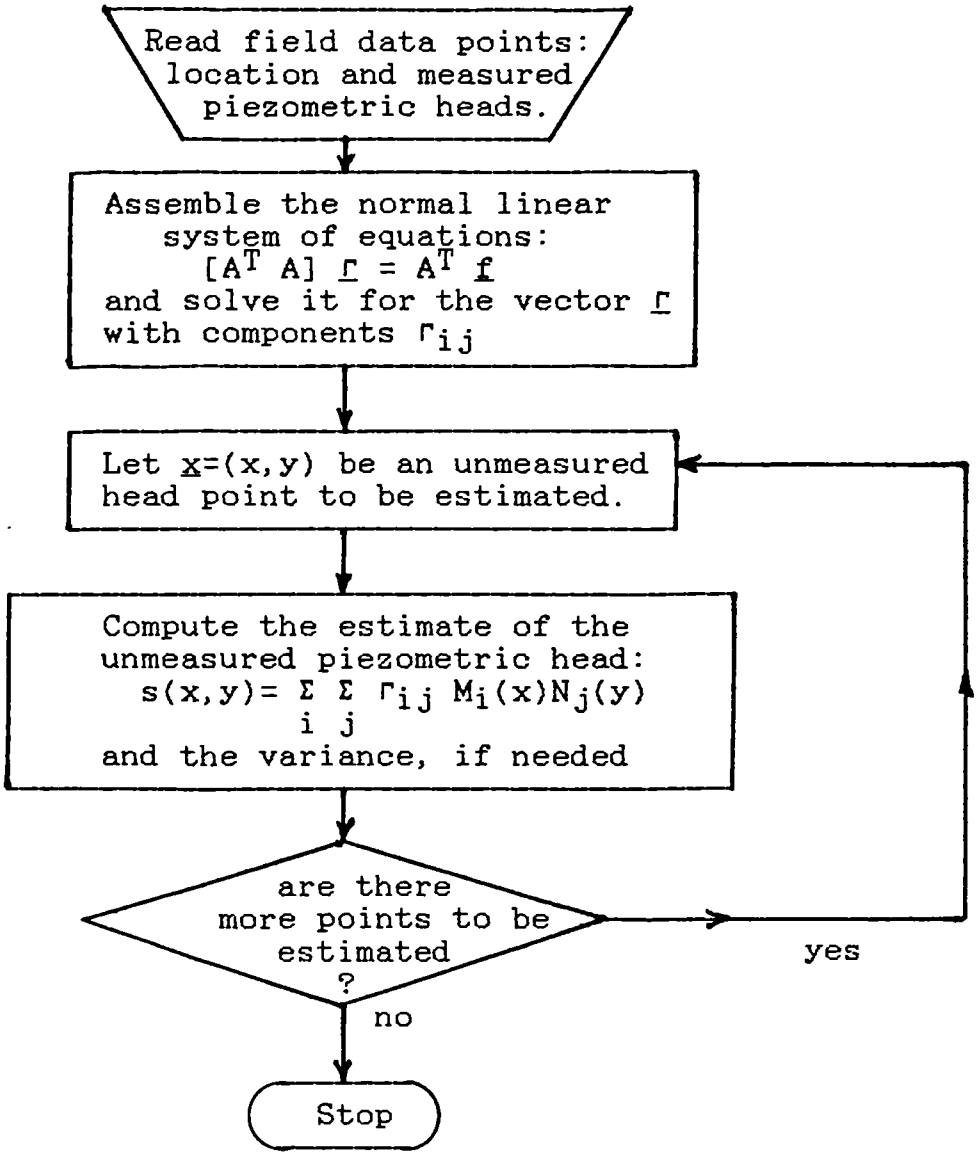

Fig. 6.6. Estimation of piezometric heads using bi-cubic splines.

6.10. Examples of applications of the proposed calibration method.

6.10.1. Description of the networks used as examples.

Six examples, based on two basic networks subjected to different operating conditions, will be used to carry out a comparison of the performance of both the proposed explicit calibration method and the different piezometric head estimation techniques.

i) Example A:

This example uses a small network, made up of 16 pipes, 11 nodes and 1 reservoir, under a low demand condition. The network structure is shown in Fig. 6.7, whereas Table 6.1 shows the corresponding numerical data. Table 6.1 a) includes the true Hazen-Williams roughness considered, both in this example and in the following two examples. Table 6.1. b) shows the nodal data. Note that the nodal consumptions for this example (example A) are the same as that for the third (example C), and that they represent a low demand condition.

ii) Example B:

The same network used in example A is subjected to higher nodal consumptions, as defined in Table 6.1. b). The objective is to study the performance of the calibration algorithm under increased demand conditions.

iii) Example C:

The same basic network used in example A will be used with a worse initial assumption for the Hazen-Williams roughness, as defined in section 6.10.4.

iv) Example D:

We use this time a 180 pipe, 100 nodes network, arranged in a square grid network of 10 nodes per side. The geometrical characteristics of this network are such that the length and the diameter of every pipe is the same (150 m. and 100 mm., respectively). As far as the nodes are concerned, the true demand is 1.0 (l/s) for all non-reservoir nodes and the ground level is 10 m. for all the nodes. This basic network, with minor changes, is used under 3 different configurations, leading to examples D, E and F.

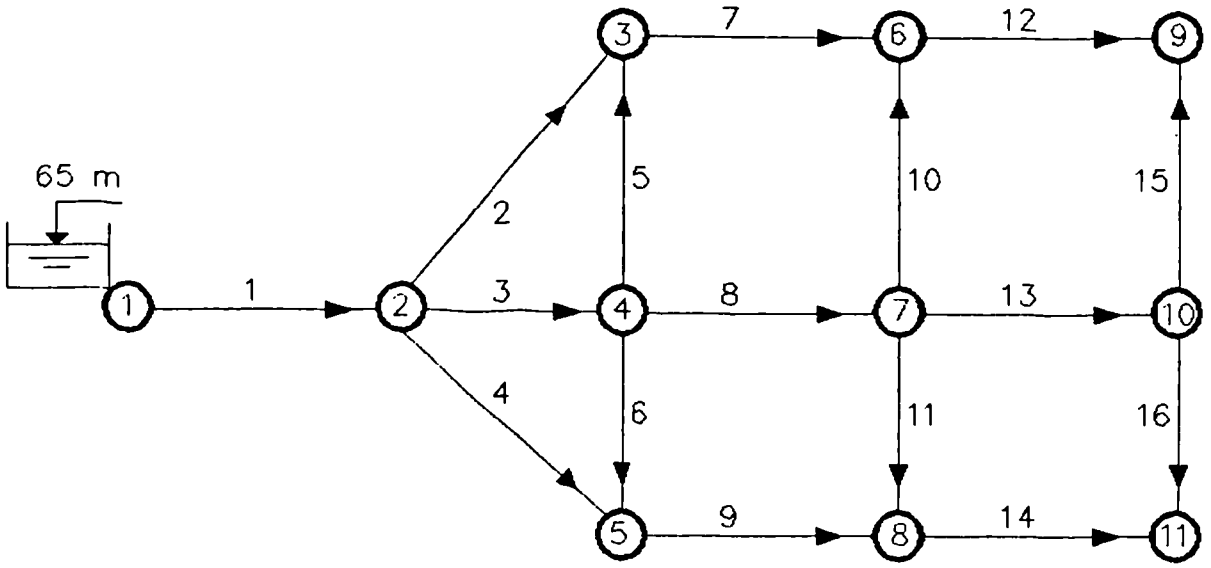

Fig. 6.7. Network for Examples A, B and C.

Table 6.1. Network data for Examples A, B and C.

a) Pipe data:

LINK NO.	INITIAL NODE	FINAL NODE	LENGTH (M)	DIAMETER (MM)	HAZEN-WILLIAMS TRUE "C'S"
1	1	2	500.0	200.0	80.0
2	2	3	650.0	150.0	85.0
3	2	4	400.0	150.0	90.0
4	2	5	575.0	150.0	95.0
5	4	3	500.0	100.0	100.0
6	4	5	400.0	100.0	105.0
7	3	6	500.0	100.0	110.0
8	4	7	500.0	100.0	115.0
9	5	8	500.0	100.0	120.0
10	7	6	500.0	100.0	125.0
11	7	8	400.0	100.0	130.0
12	6	9	500.0	100.0	135.0
13	7	10	500.0	100.0	140.0
14	8	11	500.0	100.0	145.0
15	10	9	500.0	100.0	150.0
16	10	11	400.0	100.0	155.0

b) Nodal data: only nodal demand changes between examples A, B and C.

NODE NO.	TYPE	DEMANDS (L/S) EXAMPLES A and C	DEMANDS (L/S) EXAMPLES B	GROUND LEVEL (M)	RESERVOIR LEVEL (M)
1	1	0.0	0.0	50.0	65.0
2	0	0.0	0.0	45.0	
3	0	1.5	2.0	41.0	
4	0	1.5	2.5	41.0	
5	0	1.5	2.5	41.0	
6	0	2.0	3.0	36.0	
7	0	2.0	3.0	36.0	
8	0	2.0	4.0	36.0	
9	0	1.5	4.5	31.0	
10	0	1.5	4.5	31.0	
11	0	1.5	5.0	31.0	

Note: Type = 1 for reservoirs, 0 for unknown head nodes.

In Example D only one reservoir feeds the whole network and is connected to the upper left-hand corner (node 1); the reservoir level is 100 m. The network is shown in Fig. 6.8.

v) Example E:

Using the same basic network as in example D, we now consider that four reservoirs are feeding the network and they are connected to each corner of the square (nodes 1, 10, 91 and 100); the reservoir levels are: 100.0, 90.0, 90.0 and 110.0 m., respectively. This network is presented in Fig. 6.9.

vi) Example F:

Basically the same network is employed, as in Example E, with some minor changes to introduce a line of 4 pressure reducing valves, separating the network into high and low pressure zones. The network has 178 links (4 of them pressure reducing valves, the rest are pipes), 104 nodes and 4 reservoirs (connected at nodes 1, 55, 64 and 100, with reservoir levels: 110.0, 100.0, 50.0 and 40.0 m., respectively). The node and link labelling has been changed with respect to the previous two examples, in order to get a consecutive numbering for the higher and lower pressure zones. The P.R.V.'s are located at links 175, 176, 177 and 178 and all of them have a minimum resistance parameter (α) equal to 5.0×10^{-5} (i.e. when valves are fully open) and the outlet head is set to 50.0 m. This network is shown in Fig. 6.10.

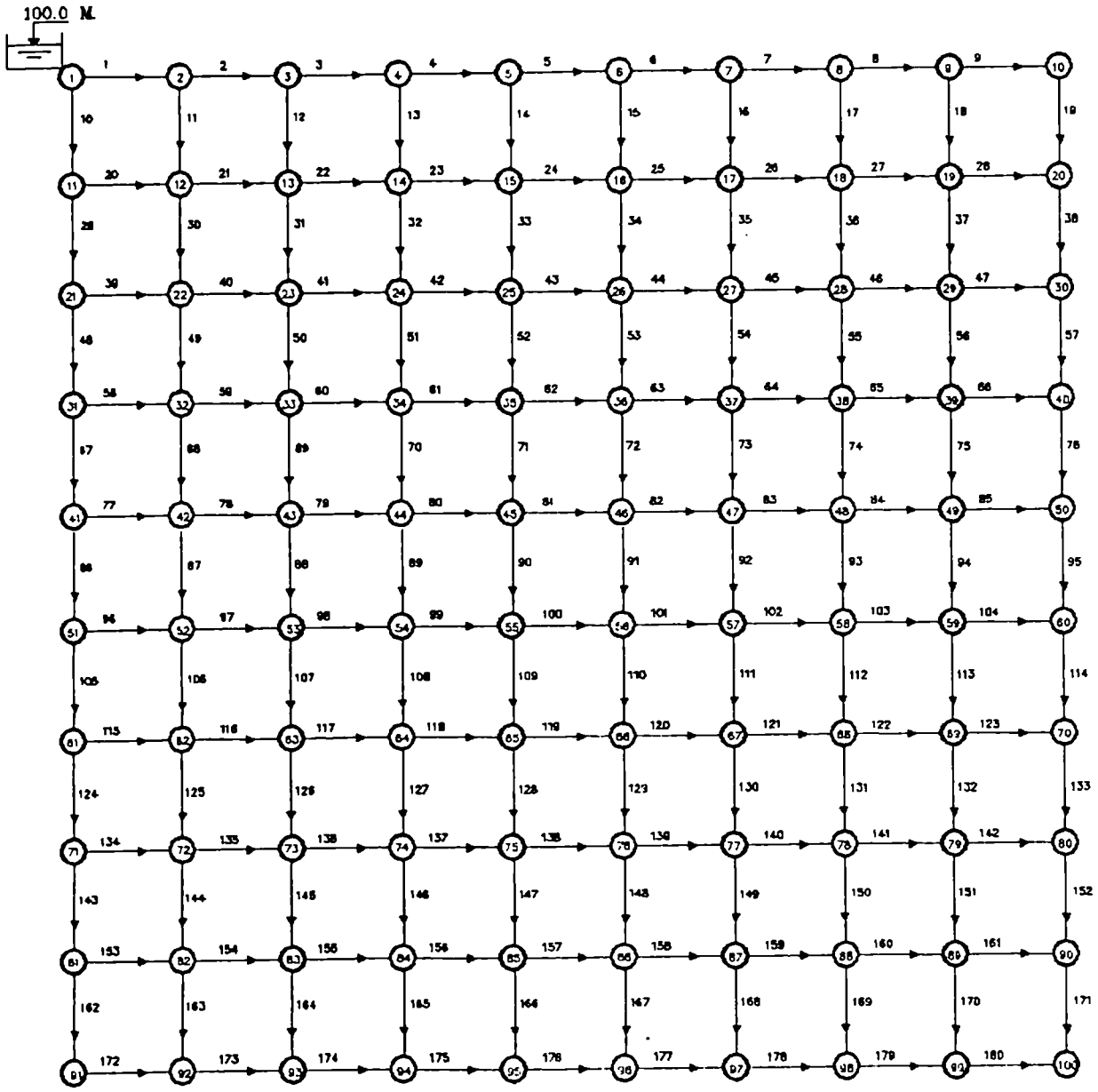

Fig. 6.8. Network for Example D.

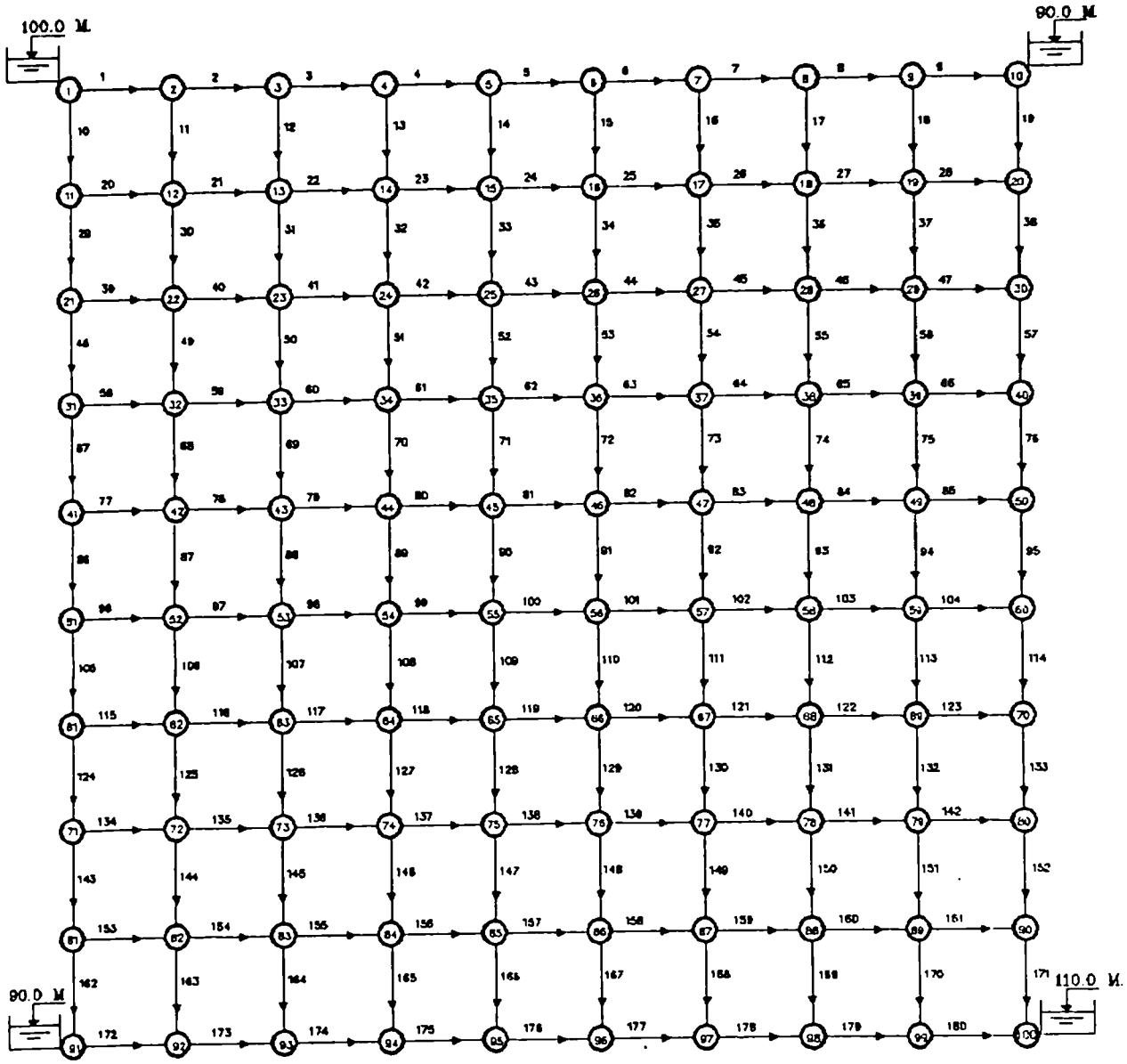

Fig. 6.9. Network for Example E.

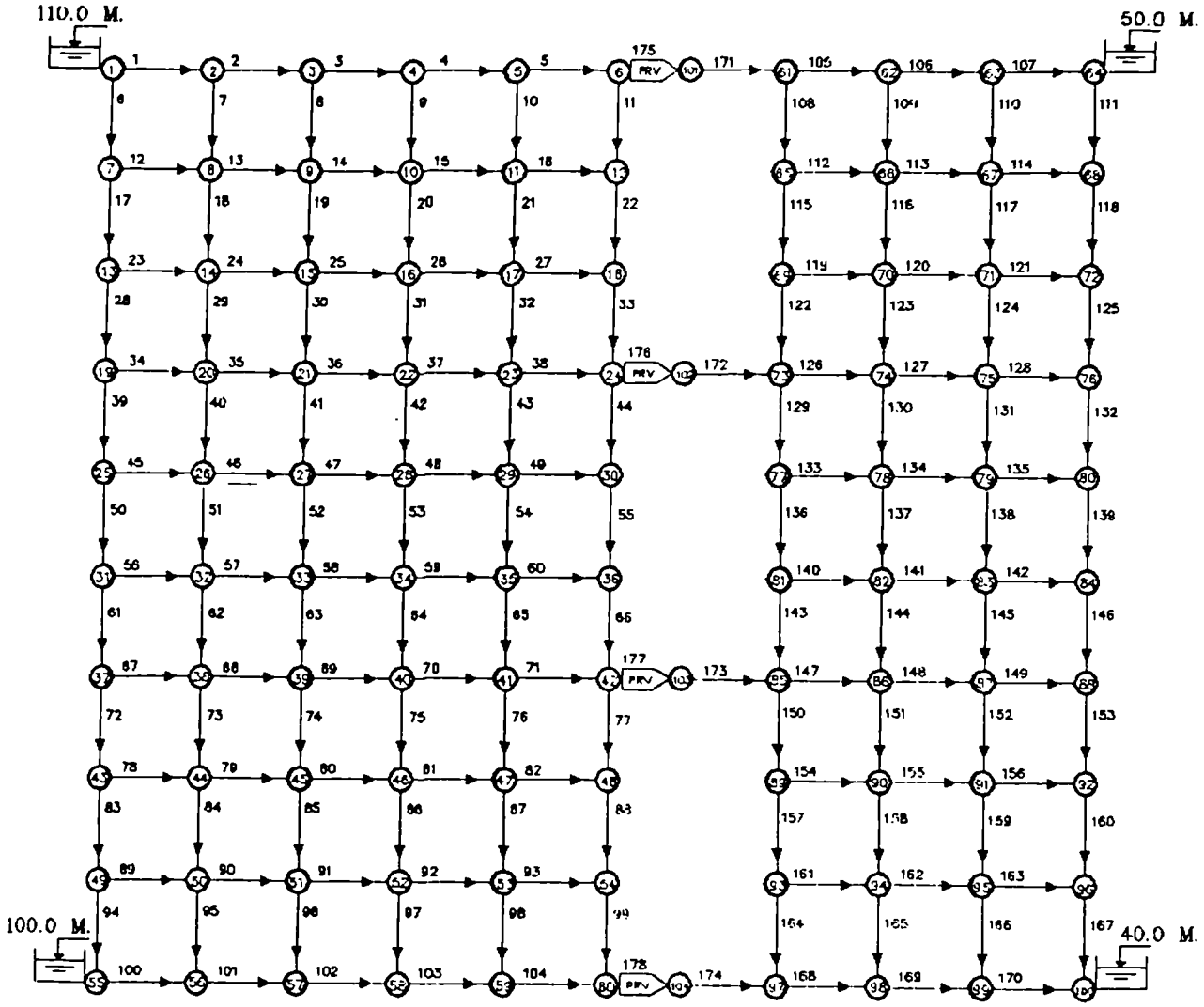

Fig. 6.10. Network for Example F.

Due to the uniformity of the data for the last 3 network examples, their numerical data are not presented in detail here.

6.10.2. Defining the "true" network characteristics.

In order to test the ability of the calibration algorithm to estimate the "true" roughnesses of the example networks, we defined a set of true roughnesses for each one of them:

a) For examples A, B and C (smaller networks) the true Hazen-Williams roughnesses were set to 80, 85, 90, ..., 160 for the 16 pipes (i.e. starting with C=80, we incremented C by 5 for each successive pipe), as shown in Table 6.1 a).
b) For examples D, E and F (bigger networks) the true Hazen-Williams roughnesses of all pipes was set to 140.

6.10.3. Defining the measurements for the network examples.

With these "true" roughnesses, and with the physical characteristics of the network defined in 6.10.1., we ran the network analysis program (gradient method) to determine the steady state flows and piezometric heads of the "true" systems. From the results of these runs we obtained our sets of "measurements", i.e. heads and flow measurements at selected nodes and pipes of the networks.

To investigate the effect of flow measurements taken in different pipes within the networks, two sets of flow measurements were produced. Table 6.2 shows the measurement data considered for Examples A B and C, while Table 6.3 corresponds to Examples D, E and F.

Table 6.2. Measurement data for Examples A, B and C.

a) Piezometric head (m) measurement data:

Example A and C		Example B	
Node	Piez. Head	Node	Piez. Head
1	65.000000	1	65.000000
4	62.818108	4	56.614697
9	60.988101	9	47.368164
11	60.988960	11	47.364705

b) Flow (l/s) measurement data:

1st set of flow measurements				2nd set of flow measurements			
Examples A and C		Example B		Examples A and C		Example B	
Pipe	Flow	Pipe	Flow	Pipe	Flow	Pipe	Flow
3	5.7045	3	11.8278	3	5.7045	3	11.8278
11	-0.1018	11	0.4583	4	4.9642	4	10.3282

Note: flowrates are considered positive when they flow from the initial into the final node of the pipe (see Table 6.1.a)

Table 6.3. Measurement data for Examples D, E and F.

a) Piezometric head (m) measurement data:

Example D		Example E		Example F	
Node	Piez. Head	Node	Piez. Head	Node	Piez. Head
1	100.000000	1	100.000000	1	110.000000
4	28.042592	4	90.087208	4	84.022801
7	21.145426	7	89.670934	6	81.718164
10	20.224128	10	90.000000	19	85.304132
31	28.042592	31	90.087208	22	83.234221
34	24.315165	34	89.797302	24	81.517016
37	20.819741	37	89.696615	37	84.756624
40	20.131486	40	89.707143	40	82.859427
56	20.665754	56	89.782311	42	80.841693
61	21.145426	61	89.670934	55	100.000000
64	20.819741	64	89.696615	58	82.891918
70	19.875863	70	90.882238	60	79.946825
78	19.876248	78	91.207603	64	50.000000
91	20.224128	91	90.000000	76	46.744788
94	20.131486	94	89.707143	88	45.060264
97	19.875863	97	90.882238	100	40.000000
100	19.770666	100	110.000000	101	50.000005
				102	49.999780
				103	50.000154
				104	49.999025

Table 6.3. Measurement data for Examples D, E and F. (Continuation).

b) Flow (l/s) measurement data:

First set of flow measurements					
Example D		Example E		Example F	
Pipe	Flow	Pipe	Flow	Pipe	Flow
1	49.5000	1	17.3758	1	28.5634
5	8.9960	5	1.7104	5	5.8167
10	49.5000	10	17.3758	6	28.3576
11	20.6499	11	7.0481	7	11.5337
20	20.6499	20	7.0481	12	11.9710
38	0.8997	38	0.9625	33	4.0455
53	3.6985	53	-0.4622	48	5.5255
79	5.5638	79	0.7851	50	1.3063
86	8.9960	86	1.7104	83	-11.6611
114	1.6112	114	-5.2377	92	6.6734
121	2.1334	121	-3.3762	118	5.2651
143	2.9574	143	-1.1708	146	4.5898
151	1.0259	151	-9.5725	147	5.0332
156	1.6824	156	-1.7850	159	5.2148

Second set of flow measurements					
Example D		Example E		Example F	
Pipe	Flow	Pipe	Flow	Pipe	Flow
1	49.5000	1	17.3758	1	28.5634
2	27.8501	10	17.3758	4	7.3102
4	12.4275	11	7.0481	6	28.3576
10	49.5000	19	3.0247	12	11.9710
13	4.4079	51	1.9283	84	-7.8444
20	20.6499	130	-3.3762	89	9.5888
47	1.3852	149	-3.1766	94	-22.2490
77	2.4315	151	-9.5725	106	-2.4649
86	8.9960	158	-4.8944	107	-7.8444
96	1.4620	170	-10.0725	151	4.4264
99	4.0688	171	-24.5171	171	7.8931
108	5.2679	172	3.0247	172	10.2300
120	2.6334	173	0.9625	173	12.6191
122	1.4826	180	-24.5171	174	13.0494

Note: flowrates are considered positive when they flow from the initial into the final node of the pipe, which is indicated by an arrow in Figures 6.8, 6.9 and 6.10. Flows are negative otherwise.

6.10.4. Defining the initially assumed roughnesses for the network examples.

In order to simulate the lack of knowledge of the true roughnesses of the pipes prior to the calibration process, we assumed that on average we knew the values of the C's and we proceeded to generate a new set of C's, with the same mean as the true values, but with some added Gaussian noise. This was done with a pseudo-random number generator program, and the corresponding values are presented in Table 6.4 (for examples A and B), for two different degrees of uncertainty in the roughnesses. Table 6.5 shows the initial roughnesses considered for example C, which have been obtained for the initially assumed C's for example A (low uncertainty) , multiplied by a factor 1.2., i.e. only in this particular example, we assume that the initial C estimates are not coinciding - on average - with the true values, but they have been over-estimated by 20%. Table 6.6. presents the initial C's assumed for examples D, E and F, for low and high degree of uncertainty in their estimates. These values have been generated by adding some Gaussian noise to the true C=140.

Table 6.4. Initial values of C (Hazen-Williams) used for testing the calibration algorithm. For Examples A and B and low and high uncertainty.

Pipe	Uncertainty in C: Low	Uncertainty in C: High
	Values of C	
1	81.4482	73.7684
2	89.6747	88.9714
3	95.4802	96.5187
4	98.6072	95.5956
5	103.7588	101.0750
6	116.2208	129.6719
7	116.7340	120.4833
8	121.4841	124.6930
9	126.4144	129.4729
10	130.4846	131.5323
11	133.3617	129.8191
12	137.0585	130.6980
13	148.0070	154.5090
14	152.2471	157.1059
15	153.0364	148.7907
16	162.2371	167.0742
Mean	122.8909	123.7362
Variance	596.1455	702.9258
For the true C's:		
Mean	122.5000	122.5000
Variance	566.6667	566.6667

Table 6.5. Initial values of C (Hazen-Williams) used for testing the calibration algorithm in Example C.

Pipe	Values of C
1	97.738
2	107.610
3	114.576
4	118.328
5	124.511
6	139.465
7	140.081
8	141.781
9	151.697
10	156.582
11	160.034
12	164.471
13	177.608
14	182.696
15	183.643
16	194.684
Mean	147.219
Variance	860.341
For the true C's:	
Mean	122.500
Variance	566.667

Table 6.6. Initial values of C (Hazen-Williams) used for testing the calibration algorithm. For Examples D, E and F, and for low and high uncertainty.

Pipe	C values * Uncertainty in C Low	High	Pipe	C values * Uncertainty in C Low	High	Pipe	C values * Uncertainty in C Low	High
1	136.777	135.4418	61	139.265	138.9603	121	143.384	144.7855
2	139.713	139.5943	62	133.002	130.1041	122	138.545	137.9428
3	140.412	140.5830	63	141.288	141.8213	123	140.936	141.3244
4	138.835	138.3520	64	139.622	139.4660	124	139.777	139.6850
5	138.987	138.5668	65	136.080	134.4567	125	141.905	142.6946
6	144.962	147.0180	66	141.210	141.7110	126	143.297	144.6623
7	141.353	141.9132	67	140.447	140.6316	127	136.971	135.7164
8	141.134	141.6030	68	142.781	143.9334	128	137.310	136.1954
9	141.058	141.4969	69	137.335	136.2316	129	139.906	139.8670
10	140.356	140.5029	70	139.742	139.6348	130	136.762	135.4204
11	138.820	138.3316	71	143.479	144.9200	131	141.459	142.0632
12	137.920	137.0585	72	141.429	142.0208	132	134.405	132.0869
13	142.089	142.9547	73	138.294	137.5873	133	141.317	141.8623
14	141.535	142.1709	74	135.402	133.4972	134	136.535	135.0998
15	138.680	138.1339	75	142.383	143.3697	135	143.593	145.0811
16	141.480	142.0926	76	140.139	140.1965	136	140.819	141.1581
17	138.061	137.2573	77	139.836	139.7682	137	136.643	135.2530
18	143.167	144.4793	78	142.321	143.2820	138	138.641	138.0779
19	138.037	137.2233	79	141.605	142.2702	139	141.706	142.4125
20	137.395	136.3165	80	137.548	136.5322	140	138.438	137.7913
21	140.941	141.3304	81	138.622	138.0510	141	131.478	127.9477
22	140.602	140.8510	82	139.878	139.8282	142	132.876	129.9255
23	136.461	134.9955	83	142.079	142.9401	143	142.037	142.8810
24	142.466	143.4878	84	141.535	142.1711	144	133.725	131.1257
25	137.879	137.0008	85	143.508	144.9613	145	140.406	140.5746
26	140.731	141.0338	86	138.512	137.8961	146	144.464	146.3133
27	145.442	147.6956	87	137.641	136.6643	147	138.508	137.8897
28	140.408	140.5774	88	142.027	142.8665	148	144.708	146.6582
29	143.092	144.3722	89	143.049	144.3116	149	138.238	137.5084
30	141.982	142.8027	90	134.054	131.5905	150	137.330	136.2236
31	137.353	136.2564	91	137.938	137.0846	151	145.478	147.7466
32	143.962	145.6036	92	142.915	144.1229	152	142.393	143.3842
33	138.493	137.8690	93	137.323	136.2145	153	141.975	142.7928
34	142.970	144.1997	94	137.420	136.3516	154	138.677	138.1289
35	140.924	141.3075	95	141.167	141.6508	155	139.800	139.7175
36	140.138	140.1959	96	141.969	142.7846	156	136.602	135.1939
37	139.260	138.9536	97	142.954	144.1778	157	134.132	131.7016
38	141.594	142.2545	98	136.841	135.5324	158	141.742	142.4635
39	141.886	142.6677	99	142.205	143.1184	159	135.740	133.9759
40	141.829	142.5865	100	136.540	135.1062	160	137.425	136.3581
41	142.539	143.5908	101	137.082	135.8732	161	139.667	139.5290
42	141.195	141.6895	102	134.688	132.4885	162	137.828	136.9281
43	143.073	144.3462	103	145.144	147.2742	163	139.878	139.8268
44	142.760	143.9030	104	140.969	141.3699	164	139.190	138.8543
45	142.281	143.2259	105	142.018	142.8537	165	141.531	142.1658

Table 6.6. Initial values of C (Hazen-Williams) used for testing the calibration algorithm. For Examples C, D and E, and for low and high uncertainty. (Continuation).

Pipe	C values * Uncertainty in C Low	High	Pipe	C values * Uncertainty in C Low	High	Pipe	C values * Uncertainty in C Low	High
46	133.313	130.5432	106	136.143	134.5457	166	138.747	138.2282
47	140.610	140.8628	107	137.139	135.9537	167	137.079	135.8693
48	138.165	137.4045	108	144.336	146.1318	168	141.363	141.9278
49	140.115	140.1627	109	139.179	138.8386	169	139.669	139.5317
50	140.800	141.1319	110	143.868	145.4707	170	138.230	137.4969
51	142.525	143.5712	111	137.100	135.8987	171	140.582	140.8232
52	143.163	144.4729	112	137.777	136.8568	172	144.035	145.7070
53	138.079	137.2839	113	142.443	143.4547	173	141.078	141.5238
54	142.135	143.0193	114	141.579	142.2325	174	140.617	140.8721
55	140.616	140.8708	115	141.920	142.7149	175	136.865	135.5667
56	138.652	138.0942	116	141.818	142.5717	176	143.407	144.8179
57	140.453	140.6406	117	139.663	139.5230	177	143.506	144.9576
58	134.676	132.4708	118	142.057	142.9091	178	137.298	136.1791
59	141.788	142.5281	119	140.220	140.3106	179	138.035	137.2212
60	140.349	140.4934	120	142.158	143.0526	180	138.745	138.2249

(*) Because example F has only 174 pipes, the first 174 values of this Table should be considered.

Summary:
****
For Examples D and E:

	Low	High
Mean	139.959	139.9418
Variance	7.499	14.9984

For example F:

	Low	High
Mean :	139.9697	139.9572
Variance :	7.4917	14.9832

For the true C's:

	Low	High
Mean	140.000	140.0000
Variance	0.000	0.0000

6.10.5. Defining a perturbed set of nodal demands.

To study the behaviour of the calibration algorithm when having an incorrect estimate of the nodal demands, we took the true nodal consumptions presented in Table 6.1. b) (for examples A, B and C) and we added some Gaussian noise, producing the sets of perturbed nodal demands presented in Table 6.7. For examples D, E and F, where the nodal consumption is 1.0 (l/s) for all the nodes, we also added some Gaussian noise to this consumption, generating the new perturbed nodal demands shown in Table 6.8

Table 6.7. Modified nodal demands (l/s), used to study the impact of bad demand estimation on the calibration algorithm. Examples A B, and C.

	Demands (l/s)	
Node	Examples A and C	Example B
1	0.0	0.0
2	0.0	0.0
3	1.2016	1.6148
4	1.4734	2.4580
5	1.5382	2.5603
6	1.8754	2.7842
7	1.8917	2.8123
8	2.5305	5.0610
9	1.6252	4.8254
10	1.6049	4.7726
11	1.5980	5.2684

Table 6.8. Modified nodal demands (l/s), used to study the impact of bad demand estimation on the calibration algorithm. Examples D, E and F.

Node	Demand	Node	Demand	Node	Demand	Node	Demand
1	0.0	26	0.8612	51	1.0524	76	1.1560
2	0.7890	27	1.0479	52	1.1653	77	1.0091
3	0.9812	28	1.3562	53	1.2071	78	0.9893
4	1.0270	29	1.0267	54	0.8743	79	1.1519
5	0.9237	30	1.2024	55	1.1398	80	1.1051
6	0.9337	31	1.1297	56	1.0403	81	0.8395
7	1.3249	32	0.8267	57	0.9118	82	0.9098
8	1.0886	33	1.2594	58	1.0297	83	0.9920
9	1.0742	34	0.9014	59	0.6515	84	1.1361
10	1.0693	35	1.1944	60	1.1170	85	1.1005
11	1.0233	36	1.0605	61	1.0228	86	1.2297
12	0.9228	37	1.0091	62	0.9519	87	0.9026
13	0.8638	38	0.9516	63	0.5419	88	0.8456
14	1.1368	39	1.1044	64	1.0843	89	1.1327
15	1.1005	40	1.1235	65	0.9753	90	1.1996
16	0.9136	41	1.1197	66	0.7434	91	0.6107
17	1.0969	42	1.1662	67	1.0792	92	0.8650
18	0.8730	43	1.0782	68	1.0292	93	1.1909
19	1.2074	44	1.2012	69	1.1821	94	0.8248
20	0.8715	45	1.1807	70	0.8256	95	0.8311
21	0.8295	46	1.1493	71	0.9831	96	1.0764
22	1.0616	47	0.5622	72	1.2278	97	1.1289
23	1.0394	48	1.0399	73	1.0935	98	1.1934
24	0.7683	49	0.8799	74	0.8883	99	0.7932
25	1.1615	50	1.0075	75	0.6990	100	1.1444

6.11. Comparison of the calibration results using different head estimation techniques.

6.11.1. Main objectives.

The main purpose of this section is to evaluate the performance of the proposed calibration algorithm under different conditions.

We also aim at establishing the advantages and disadvantages of the different head estimation techniques introduced in previous sections: Kriging, deterministic one-dimensional interpolation and bi-cubic splines. Basically, what we are trying to find out is which head estimator has a better response, in the sense of being able to provide a better estimate of the true parameters and state variables of the network. Thus, we shall compare not only the estimates of the pipe roughnesses, but also the flows per pipe and nodal piezometric heads.

6.11.2. Study cases.

To study the effect of different scenarios of measurement availability and different degrees of certainty in the initially assumed values of roughnesses and nodal consumptions, on the performance of the calibration algorithm, the following study cases have been defined:

i) Case I.

In this case we assume that all the measurement information available is provided by head measurements only. The purpose of this case is to study the response of the calibration algorithm to different levels of availability of flow measurements, this

case establishing the lowest possible level in terms of flow measurement data.

The amount of head measurements has been set to 4 in networks A, B and C (1 level measurement plus 3 pressure measurements), 15 head measurements in networks D and E and 20 head measurements in network F (4 level measurements and 16 pressure measurements, including inlet and outlet pressure measurements at the P.R.V.'s). Even though the proportion of number of measurements to number of nodes may appear high in the smaller networks (A, B and C) due to their small size (11 nodes), the proportion has been reduced to more realistic values in the case of networks D, E and F , although increasing the number of measurements, in view of the complexity of the networks under study (number of reservoirs and presence of P.R.V.'s).

The selection of the location of pressure measurements has been done having in mind that it is convenient to have them evenly distributed over the network, in order to give a representative picture of the variation of the piezometric plane. Although we recognise the importance of pressure measurement placement in the performance of any head estimation technique, we did not follow a formal measurement placement technique; this is partly justified by the fact that the networks are fairly regular both in their geometrical and physical characteristics and also in their spatial distributions of the nodal demands. In the case of Example F, with P.R.V.'s, we followed the same principle, treating each pressure zone as a regular sub-network.

ii) Case II.

To the same amount and distribution of piezometric head measurements used in Case I, we have now added 2 flow measurements for networks A, B and C, and 14 flow measurements for networks D, E and F.

The flow measurements are located in exactly the same pipes for examples A, B and C, and also for networks D, E and F. This corresponds to a first set of flow measurements, which have been placed rather arbitrarily, especially as far as examples E and F are concerned.

iii) Case III.

To study the effect of a more rational flow measurement placement, the same amount of flow measurements utilised in Case II has been redistributed , this time by studying the flow distribution patterns for each network model. Flow measurements were re-placed in order to get a better picture of the distribution of the maximum flows, particularly those leaving the reservoirs or passing through P.R.V.'s. Again, as in the case of pressure measurement placement, we did not apply a formal procedure for flow measurement placement.

iv) Case IV.

To investigate the impact of poor initial estimates of the pipes' roughnesses, we used the example networks, with the head and flow measurements as in case III, this time with worse estimates of C, as given in the previous section 6.10.4.

v) Case V.

In order to evaluate the behaviour of the calibration algorithm under perturbations in the spatial variation of the nodal demands, we used the example networks with the perturbed nodal demands given in section 6.10.5.

6.11.3. Calibration exercise.

The calibration of each example network (Examples A, B, C, D, E and F) will be performed, using the proposed algorithm, under the five different Cases already described, which represent variable degrees of knowledge of the true values of the main network characteristics.

The overall calibration process (represented in Figure 6.1.), of each network and for each one of the five Cases studied, has involved the following main stages:

a) Estimation of the unmeasured piezometric heads.

Based on the piezometric head measurements available for each example network, the unmeasured piezometric heads were estimated using Kriging and bi-cubic splines, resulting in two sets of estimated heads for each network. Since the measured and estimated heads do not depend either on the initial roughnesses assumed, or on the flow measurements, or on the quality of the nodal consumption data, these two sets of head estimates are the same for all the five Cases studied, and they depend only on the network under study. For the one-dimensional interpolation method, and because the proposed algorithm uses the information contained in the raw model, based on the a priori information

assumed to be available, the head estimates may be different from case to case. Because Cases I, II and III are based on the same initial assumptions for pipe roughnesses and nodal consumptions (i.e. same raw model), and their differences consist only in different availability of flow measurements, Cases I, II and III have the same head estimates, but those estimates are different from those for Cases IV and V, where the initial assumptions (pipe roughnesses and nodal consumptions, respectively) have changed. This difference becomes clearer in section 6.11.4.3.

The piezometric head estimation stage is carried out only <u>once</u> during the calibration process, as shown in Fig. 6.1.

b) Estimation of the unmeasured flows.

Using the initially assumed roughnesses and nodal consumptions, run the network analysis program for the raw model corresponding to each network and determine the pipe flows. If flow measurements are available at some pipes, replace the modelled flows by their corresponding measurements. This leads to a set of modelled/measured flows for each network and each study case.

c) Calibration stage.

Run the calibration program, using the set of estimated/measured heads and modelled/measured flows, and determine the calibrated roughnesses (Hazen-Williams C's).

For each example and study case, piezometric head estimates produced with Kriging, the one-dimensional interpolation method and bi-cubic splines have been used, leading to different

calibration results, corresponding to each one of the piezometric head estimation techniques used.

6.11.4. Results of the calibration.

In this section a "performance index" and a "global success" index are defined for evaluation purposes; later on, the numerical results are presented, both for the head estimation and calibration procedures, including a discussion of them.

6.11.4.1. Definition of the "performance index".

Because the calibration exercise generates a large amount of numerical information, which is impossible to display in full detail here, we have included in Appendix D a summary of the main statistics associated with such results. Even then, further condensation of the results is necessary, in order to quantify the results, particularly those concerning the performance of the calibration algorithm and the head estimation techniques. For those purposes, a performance index has been used to quantify the degree of successfulness of the calibration and estimation processes. Such a performance index is defined as follows:

$$R_x^2 = \frac{(X^t - X^i)^2 - (X^t - X)^2}{(X^t - X^i)^2} \qquad (18)$$

where:

X : represents the value of the variable being assessed (i.e. the average head, the variance of the heads, etc.).

X^t : represents the true value of that variable.

X^i : represents the initial estimate of the value of that variable.

This performance index R_X^2, which is represented in Fig. 6.11, has the following properties:

i) $R_X^2 = 0$, if no improvement results from the calibration process (i.e. when $X=X^i$).

ii) $R_X^2 = 1$, if the true value has been determined (i.e. when $X=X^t$).

iii) $R_X^2 = 0.75$, if the variable $X = 0.5*(X^t+X^i)$, i.e. if it is halfway between the initial and true values.

iv) $R_X^2 > 0$, whenever some improvement has been obtained.

v) $R_X^2 < 0$, when the calibration process has actually deteriorated the initial assumptions.

6.11.4.2. Definition of a "global success" index.

The performance index already defined allows us to quantify, in a non-dimensional way, the behaviour of a procedure with respect to a single parameter (i.e. either with respect to the average or the variance, etc.). In order to consider explicitly the ability of the procedure being assessed (Kriging, one-dimensional interpolation or bi-cubic splines) to improve both the average of the variable, its variance, the maximum residual and the variance of the residuals simultaneously, a "global success" index is defined as simply the percentage of cases when the algorithm improves all those parameters, over all the tested cases. Hence, if a procedure has a good (positive) "performance index" with respect to the average, but a negative "performance index" with respect to the variance of the residual, this procedure will not count, as far as the "global success" index is concerned.

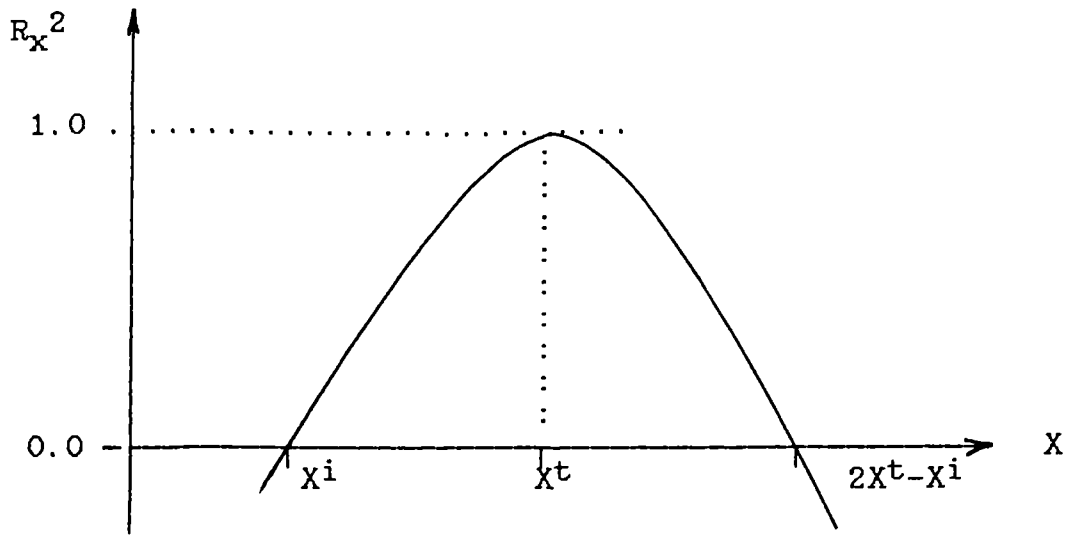

Fig. 6.11. The performance index R_X^2.

Thus, the "performance index" is associated with the improvement achieved by a certain procedure with respect to a single parameter, whereas the "global success" index is related to the consistency of the procedure.

6.11.4.3. Piezometric head estimation results.

Because the piezometric heads estimated using the one-dimensional interpolation method make use of the raw network model (based on an initial assumption of the roughnesses) for determining the minimum head loss paths, which subsequently are used in the interpolation itself, their head estimates are different according to which initial roughness estimates have been considered (i.e. they are different according to which of the five study cases we are referring to). Because Cases I, II and III are based on the same initial roughness estimate, their head estimates obtained with the one-dimensional interpolation

are exactly the same, but they differ from the head estimates for cases IV and V. This does not happen when Kriging or bi-cubic splines are used as head estimators, where the head estimates are the same for all the five study cases.

The head estimation results for example A, with the one-dimensional interpolation results corresponding to cases I, II and III, and for the three different head estimation procedures, are presented in Table 6.9., while in Figure 6.12. the residuals of the initial nodal piezometric heads (example A) are compared graphically with those produced by the one-dimensional interpolation method. Both Table 6.9. and Fig. 6.12 show how the initial residuals are reduced by the head estimation process.

Due to space constraints, the corresponding detailed results for networks B, C, D, E and F are omitted although a summary of the main statistics relating them is presented in Table 6.10.

Note that, from now on, when dealing with the residuals, we are referring to the absolute value of the residuals, as specified in the notes corresponding to the respective Table.

Table 6.11 presents a summary of the main statistics associated with the piezometric heads estimated when the one-dimensional interpolation procedure is used, for each example and under the different study cases. Table 6.11 shows that the differences in the estimated heads under different initial assumptions for pipe roughnesses and nodal consumption are not significant on average, though locally (maximum difference) they can be of the order of 1 or 2 meters (as in examples B and D, Table 6.11).

Table 6.9. Comparison between estimated piezometric heads and its residuals, for example A.

NODE [1]	TRUE	INITIAL		INTERPOLATION [2]		KRIGING		SPLINES	
	VALUES	ESTIMATES	RESIDUALS	ESTIMATES	RESIDUALS	ESTIMATES	RESIDUALS	ESTIMATES	RESIDUALS
1	65.000000	65.000000	0.000000	65.000000	0.000000	65.000000	0.000000	65.000000	0.000000
2	63.485885	63.361335	0.124550	63.432510	0.053375	63.740849	-0.254964	66.255523	-2.769638
3	62.765635	62.635732	0.129903	62.763824	0.001811	62.858039	-0.092404	23.035473	39.730162
4	62.818108	62.689977	0.128131	62.818085	0.000023	62.818108	0.000000	62.818108	0.000000
5	62.811073	62.680875	0.130198	62.756592	0.054481	62.849605	-0.038532	38.813053	23.998020
6	61.217718	61.126266	0.091452	61.213028	0.004690	61.868119	-0.650401	35.249859	25.967859
7	61.220484	61.127675	0.092809	61.210495	0.009989	61.833739	-0.613255	51.912286	9.308198
8	61.221935	61.128740	0.093195	61.208405	0.013530	61.862176	-0.640241	45.592621	15.629314
9	60.988101	60.897367	0.090734	60.988068	0.000033	60.988101	0.000000	60.988101	0.000000
10	60.988599	60.898532	0.090067	60.981339	0.007260	60.972607	0.015992	32.488891	28.499708
11	60.988960	60.899024	0.089936	60.988953	0.000007	60.988960	0.000000	60.988960	0.000000

[1] : NODES 1, 4, 9 AND 11 HAVE PIEZOMETRIC HEAD MEASUREMENTS.
[2] : THE VALUES SHOWN IN THIS TABLE CORRESPOND TO THOSE FOR CASE STUDIES I, II AND III.

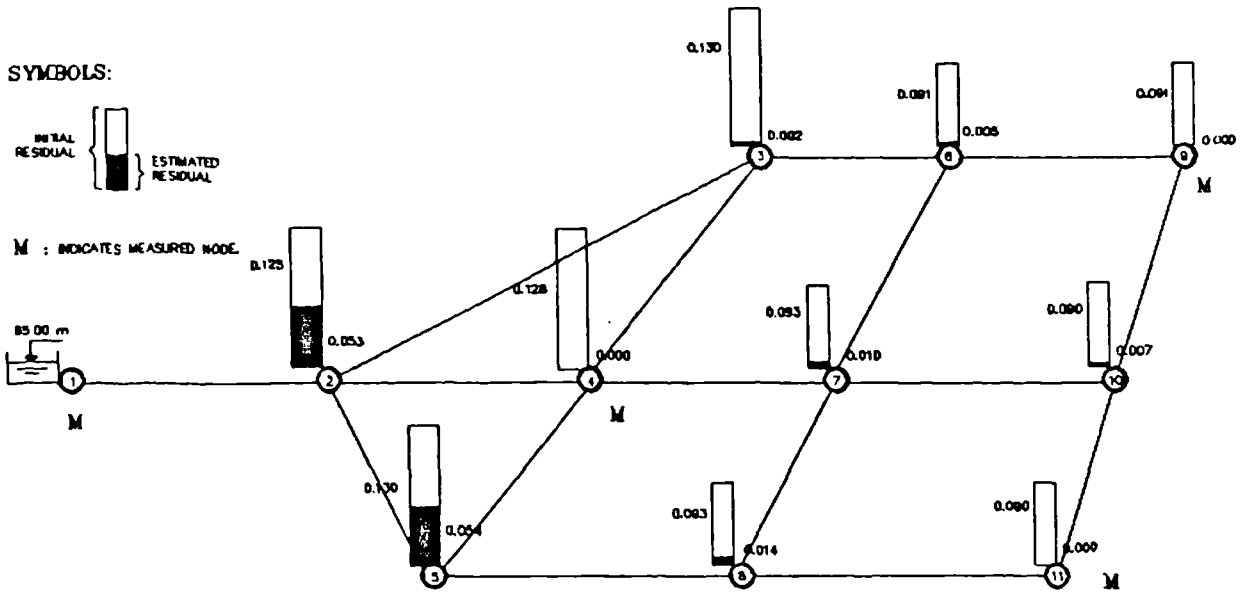

Fig. 6.12. Comparison between the initial residuals and those obtained <u>after</u> the one-dimensional interpolation procedure has been applied, for example A.

Table 6.10. Summary of the comparison between different piezometric head estimation procedures.

EXAMPLE	PROCEDURE	AVERAGE	VARIANCE	STAN.DEV.	MAXIMUM RES.[1]	AVERAGE RES.[2]	VARIANCE RES. [3]	RATIO AVERAGES EST/TRUE [4]
	TRUE	62.136954	1.780894	1.334501				
	INITIAL	62.040502	1.810364	1.345498	0.130198	0.096452	0.001502	0.998448
A	INTERPOL.	62.123754	1.766190	1.328981	0.054481	0.013200	0.000473	0.999788
	KRIGING	62.343664	1.602447	1.265878	0.650401	0.209617	0.088996	1.003327
	SPLINES	49.376625	229.028789	15.133697	39.730162	13.263900	227.144583	0.794642
	TRUE	53.068512	35.740184	5.978309				
	INITIAL	52.717053	35.932102	5.994339	0.500262	0.351459	0.023382	0.993377
B	INTERPOL.	53.068356	35.250739	5.937233	0.204610	0.046578	0.004287	0.999997
	KRIGING	53.933735	32.590245	5.708787	2.744054	0.865900	1.714367	1.016304
	SPLINES	42.850260	215.365555	14.675338	36.471455	10.671146	173.663753	0.807452
	TRUE	62.136954	1.780894	1.334501				
	INITIAL	62.878059	0.938416	0.968719	1.066052	0.741105	0.149334	1.011927
C	INTERPOL.	62.201541	1.641180	1.281085	0.243991	0.082440	0.009006	1.001039
	KRIGING	62.343664	1.602447	1.265878	0.650401	0.209617	0.088996	1.003327
	SPLINES	49.376625	229.028789	15.133697	39.730162	13.263900	227.144583	0.794642
	TRUE	23.469569	92.318030	9.608227				
	INITIAL	22.684429	93.275043	9.657901	1.141310	0.785140	0.009442	0.966546
D	INTERPOL.	23.391606	90.859916	9.532047	0.868389	0.082309	0.037531	0.996678
	KRIGING	24.378280	154.233956	12.419096	23.095598	1.389888	17.833472	1.038719
	SPLINES	23.891365	117.496713	10.839590	13.247301	0.924584	4.667879	1.017972
	TRUE	90.580945	6.435581	2.536845				
	INITIAL	90.565063	6.444084	2.538520	0.098798	0.019310	0.000276	0.999825
E	INTERPOL.	90.577184	6.438101	2.537341	0.090795	0.008939	0.000276	0.999958
	KRIGING	91.072444	10.508110	3.241622	5.765531	0.571530	1.411968	1.005426
	SPLINES	90.781541	8.434977	2.904303	3.721798	0.408525	0.429774	1.002215
	TRUE	68.544348	376.086468	19.392949				
	INITIAL	68.415341	370.880707	19.258263	0.376937	0.165889	0.014416	0.998118
F	INTERPOL.	68.528829	374.797523	19.359688	0.289966	0.041197	0.003383	0.999774
	KRIGING	69.768188	390.903668	19.771284	8.006676	1.406806	2.713941	1.017855
	SPLINES	56.852004	847.694714	29.115197	35.664425	12.608786	180.405342	0.829419

NOTES:

[1] : MAXIMUM ABSOLUTE VALUE RESIDUAL = MAX.{ABS(TRUE-ESTIMATED)}

[2] : AVERAGE OF THE RESIDUALS={SUMMATION OF ABSOLUTE VALUES OF THE RESIDUALS)/N

[3] : VARIANCE OF THE ABSOLUTE VALUE OF THE RESIDUALS = (SSAVR - N * AVR**2) / (N-2)

SSAVR : SUMMATION SQUARES ABSOLUTE VALUES RESIDUALS

AVR : AVERAGE ABSOLUTE VALUE RESIDUALS

N : NUMBER OF DATA POINTS

[4] : RATIO AVERAGE ESTIMATED VALUES/AVERAGE TRUE VALUES

[5] : ALL THE VALUES SHOWN IN THIS TABLE FOR THE ONE-DIMENSIONAL INTERPOLATION PROCEDURE CORRESPOND TO THOSE FOR CASE STUDIES I, II AND III.

Table 6.11. Estimated piezometric heads for Cases I, II, III, IV and V, using the one-dimensional interpolation procedure.

EXAMPLE	CASE	AVERAGE	VARIANCE	WITH RESPECT TO CASE I	
				RATIO AVERAGES	MAXIMUM DIFFERENCE
A	I	62.123754	1.766190		
	II	62.123754	1.766190	1.000000	0.000000
	III	62.123754	1.766190	1.000000	0.000000
	IV	62.108222	1.686334	0.999750	0.142227
	V	62.110307	1.798450	0.999784	0.103516
B	I	53.068356	35.250739		
	II	53.068356	35.250739	1.000000	0.000000
	III	53.068356	35.250739	1.000000	0.000000
	IV	53.102352	33.923882	1.000641	0.545105
	V	52.815367	36.779845	0.995233	1.221238
C	I	62.201541	1.641180		
	II	62.201541	1.641180	1.000000	0.000000
	III	62.201541	1.641180	1.000000	0.000000
	IV	62.149066	1.653343	0.999156	0.244263
	V	62.185013	1.755175	0.999734	0.243790
D	I	23.391606	90.859916		
	II	23.391606	90.859916	1.000000	0.000000
	III	23.391606	90.859916	1.000000	0.000000
	IV	23.387610	90.408397	0.999829	0.798309
	V	23.227227	89.780054	0.992973	1.732925
E	I	90.577184	6.438101		
	II	90.577184	6.438101	1.000000	0.000000
	III	90.577184	6.438101	1.000000	0.000000
	IV	90.581279	6.431283	1.000045	0.044312
	V	90.564589	6.428866	0.999861	0.108506
F	I	68.528829	374.797523		
	II	68.528829	374.797523	1.000000	0.000000
	III	68.528829	374.797523	1.000000	0.000000
	IV	69.260476	375.312015	1.010676	0.153580
	V	69.221385	373.855982	1.010106	0.258896

Figure 6.13 presents a graphical comparison of the head estimates for network E; only 4 equidistant transverse sections of the network are shown, joining nodes 1 to 10, 31 to 40, 61 to 70 and 91 to 100 (see Figure 6.9). Figure 6.13 shows how close

the one-dimensional interpolation method "follows" the true piezometric plane. Also evident from Fig. 6.13 is the oscillatory behaviour of the heads estimated using bi-cubic splines, which overestimates and underestimates the heads in different parts of the network. The heads estimated by Kriging seem to overestimate the true piezometric plane in this example.

Table 6.12. a) presents the performance indices corresponding to each head estimation procedure: deterministic one-dimensional interpolation (cases I, II and III), Kriging and bi-cubic splines. In general, we concentrate our attention on the behaviour of the estimation processes with respect to 4 parameters: the average of the piezometric head for all the nodes of the network, its variance, the maximum residual (in absolute value) and the variance of the absolute value of the residuals. In Table 6.12. b) the performance index has been averaged across the six examples, producing a unique "average index", for each one of the four parameters already mentioned. Table 6.12. c) shows the frequency in which the estimation procedure improved the initial head estimates

Tables 6.10. and 6.12. show clearly that, on the whole, the deterministic one-dimensional interpolation method effectively improves both the average and the maximum residual of the estimated heads; both parameters have been improved in 100 % of the tested cases, as shown in Table 6.12. c).

Table 6.10. shows that, as far as the average of the head estimates is concerned, this parameter is always within ± 0.4 % of the true values, for the one-dimensional interpolation

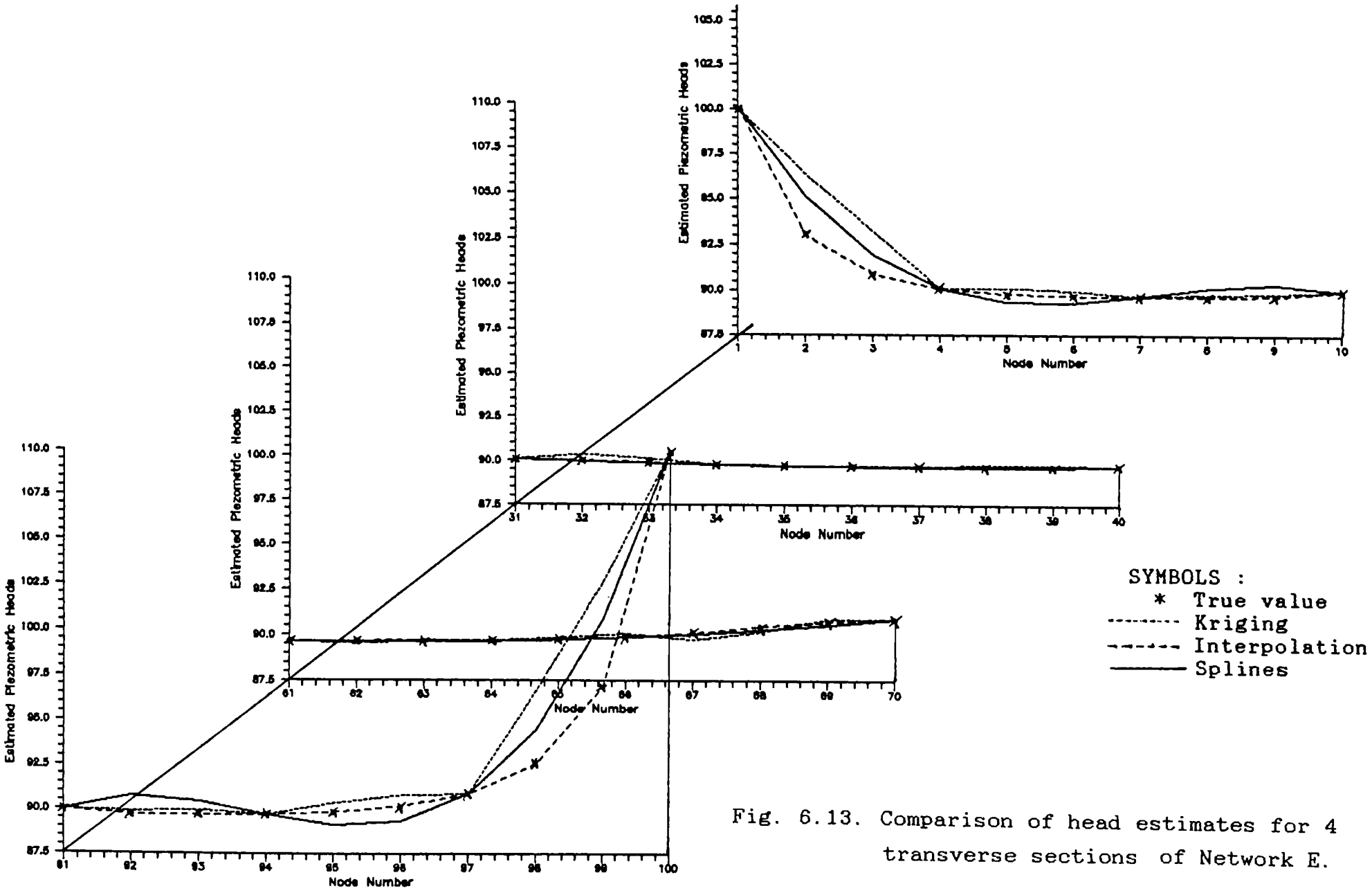

Fig. 6.13. Comparison of head estimates for 4 transverse sections of Network E.

Table 6.12. Performance indices for the different head estimation procedures, for examples A, B, C, D, E and F.

a) Performance indices.

EXAMPLE	PROCEDURE	PERFORMANCE INDEX			
		AVERAGE	VARIANCE	MAXIMUM RESID.	VARIANCE RESID.
A	INTERPOL.	0.981	0.751	0.825	0.901
	KRIGING	-3.593	-35.666	-23.955	-999.999
	SPLINES	-999.999	-999.999	-999.999	-999.999
B	INTERPOL.	1.000	-5.504	0.833	0.966
	KRIGING	-5.060	-268.385	-29.088	-999.999
	SPLINES	-844.286	-999.999	-999.999	-999.999
C	INTERPOL.	0.992	0.972	0.948	0.996
	KRIGING	0.922	0.955	0.628	0.645
	SPLINES	-295.459	-999.999	-999.999	-999.999
D	INTERPOL.	0.990	-1.321	0.421	-14.800
	KRIGING	-0.340	-999.999	-408.497	-999.999
	SPLINES	0.711	-691.198	-133.725	-999.999
E	INTERPOL.	0.944	0.912	0.155	0.000
	KRIGING	-956.712	-999.999	-999.999	-999.999
	SPLINES	-158.527	-999.999	-999.999	-999.999
F	INTERPOL.	0.986	0.939	0.408	0.945
	KRIGING	-88.996	-7.101	-450.198	-999.999
	SPLINES	-999.999	-999.999	-999.999	-999.999

NOTE: A VALUE OF -999.999 INDICATES THAT THE INDEX IS ACTUALLY LESS THAN OR EQUAL TO -999.999

b) Average indices.

PROCEDURE	AVERAGE INDEX			
	AVERAGE	VARIANCE	MAX.RES	VAR.RES
INTERPOL.	0.982	-0.542	0.598	-1.832
KRIGING	-175.630	-385.032	-318.518	-833.225
SPLINES	-549.593	-948.532	-855.620	-999.999

c) Frequency of improvement.

PROCEDURE	FREQUENCY OF IMPROVEMENT (%)			
	AVERAGE	VARIANCE	MAX.RES	VAR.RES
INTERPOL.	100.000	66.667	100.000	66.667
KRIGING	16.667	16.667	16.667	16.667
SPLINES	16.667	0.000	0.000	0.000

procedure; the worst case corresponds to example D. Table 6.12. b) shows that the average performance index (averaged across all the examples) is 0.982, which is very close to an optimal index of 1.0.

As far as the maximum residuals are concerned, their improvement when using the one-dimensional procedure is reflected in an average performance index of 0.598 (Table 6.12. b). while Table 6.10. shows that when compared with Kriging and splines, these values (produced with the one-dimensional interpolation) are at least 2.6 times smaller (for example C, 0.243991 against 0.650401 for Kriging).

Even though, by and large, the variance of the estimated piezometric head and the variance of the absolute value of the residuals deteriorated with respect to the initial estimates (those corresponding to the raw model), as shown in Table 6.12. b), both parameters actually improved in 66 % of the examples studied, when the one-dimensional interpolation method was applied. Moreover, Table 6.10 shows that, with the exception of example D, the variances of the residuals computed using the one-dimensional interpolation method are about 10 times smaller than the values obtained with Kriging (example C). Table 6.12. a) suggests that the deterioration in the variance of the heads and that of the residuals with respect to the initial conditions, occurs in networks with a steeper piezometric plane (i.e. examples B and D); the difference in the results between examples D and E is significant in this respect.

The results for the estimated heads using Kriging and the bi-cubic splines are, in general, worse than the initial estimates, although Kriging improved the initial estimates in one example (network C, Table 6.12 a).

6.11.4.4. Calibration results.

For the six networks specified in Section 6.10 and for the five cases detailed in Section 6.11.2, the calibration exercise has been carried out, and the results are tabulated in Appendix D. We refer to "initial" heads and flows as those heads and flows computed before the calibration program has been run, i.e. their values have been determined using the initial estimates for the pipe roughnesses. Similarly, we refer to "calibrated" C's, "calibrated" heads and "calibrated" flows, as the corresponding variables after the calibration program has been run, i.e. "calibrated" heads and flows refer to the values of heads and flows determined with the calibrated model, rather than with the raw model.

The results in Appendix D are ordered in the following way:

a) Calibrated heads results:

For each one of the six examples, and for each study case considered, we include a summary of the following statistics: average head, its variance and standard deviation, the maximum residual, the average absolute value of the residuals, the variance of the absolute value of the residuals and the ratio between the estimated and true averages. This represents 6 Tables (Tables D.1, D.2, D.3, D.4, D.5 and D.6). In order to quantify

the performance of the calibration algorithm, for each one of the above 6 Tables we have prepared another Table with the corresponding values of the performance index defined in section 6.11.4., for the average calibrated heads, their variance, the maximum residual and the variance of the absolute value of the residuals; this generates 6 more Tables (D.7, D.8, D.9, D.10, D.11 and D.12). Each one of the last 6 tables (with the performance index) also include an "average index", averaging across the five study cases (mid part of the tables) *and a* summary with the frequency (as a %) of the cases when the calibration algorithm actually improved the initial heads.

Figure 6.14 presents a graphical comparison of the calibrated heads for network E (case I), for 4 equidistant transverse sections, which corresponds with Fig. 6.13 already shown (comparing the estimated heads).

Tables 6.13., 6.14., 6.15. and 6.16. summarise the behaviour of the "performance index" for the five cases considered, and its variation example by example (double entry tables), for the average calibrated piezometric heads, their variance, the maximum residual and the variance of the residuals, respectively.

In Tables 6.13. to 6.16. averages have been computed across the different examples (last columns of the Tables), as well as averages corresponding to each head estimation procedure, across all the study cases (last rows of the Tables). Also, a "global average" has been computed, across all the examples and study cases, which is shown in the bottom-right corner of the Tables.

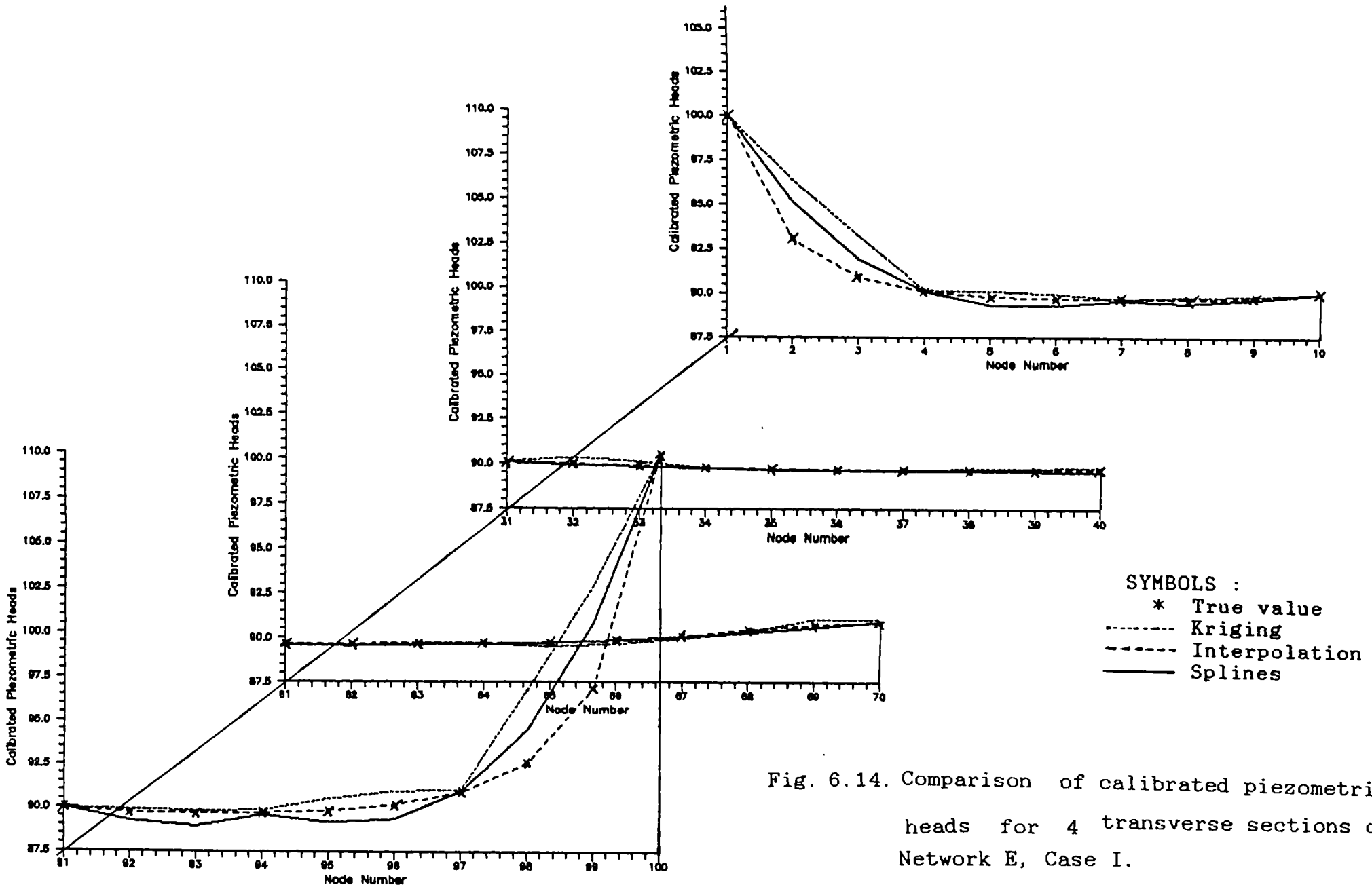

Fig. 6.14. Comparison of calibrated piezometric heads for 4 transverse sections of Network E, Case I.

Table 6.13. Summary of the comparison for the calibrated piezometric heads: average heads.

		PERFORMANCE INDEX : AVERAGE						
CASE	PROCEDURE	A	B	C	D	E	F	AVERAGE
	INTERPOL.	0.981	1.000	0.992	0.990	0.929	0.985	0.980
I	KRIGING	-3.584	-5.049	0.924	-0.144	-999.999	-77.643	-180.916
	SPLINES	-999.999	-999.999	-999.999	0.951	-13.299	-999.999	-668.724
	INTERPOL.	0.976	1.000	0.993	0.989	0.933	0.960	0.975
II	KRIGING	-4.176	-5.122	0.917	-0.195	-999.999	-78.716	-181.215
	SPLINES	-999.999	-999.999	-999.999	0.936	-10.081	-999.999	-668.190
	INTERPOL.	0.982	1.000	0.992	0.992	0.938	0.927	0.972
III	KRIGING	-4.109	-5.161	0.913	-0.155	-999.999	-80.021	-181.422
	SPLINES	-999.999	-999.999	-999.999	0.910	-52.001	-999.999	-675.181
	INTERPOL.	0.922	0.991	0.999	0.989	1.000	0.866	0.961
IV	KRIGING	-4.119	-5.065	0.856	-0.183	-999.999	-79.329	-181.307
	SPLINES	-999.999	-999.999	-999.999	0.910	-37.897	-999.999	-672.831
	INTERPOL.	0.925	0.441	0.993	0.878	-0.664	0.726	0.550
V	KRIGING	-3.413	-2.960	0.913	0.940	-999.999	-75.728	-180.041
	SPLINES	-999.999	-999.999	-999.999	0.262	-42.912	-999.999	-673.774
	INTERPOL.	0.957	0.886	0.994	0.968	0.627	0.893	0.888
AVERAGE	KRIGING	-3.880	-4.671	0.905	0.053	-999.999	-78.288	-180.980
	SPLINES	-999.999	-999.999	-999.999	0.794	-31.238	-999.999	-671.740

NOTE :
!!!!

A VALUE OF -999.999 INDICATES THAT THE INDEX IS ACTUALLY LESS THAN OR EQUAL TO -999.999

Table 6.14. Summary of the comparison for the calibrated piezometric heads: variance of the heads.

		PERFORMANCE INDEX : VARIANCE						
CASE	PROCEDURE	A	B	C	D	E	F	AVERAGE
	INTERPOL.	0.758	-5.502	0.973	-1.324	0.886	0.938	-0.545
I	KRIGING	-35.488	-267.833	0.956	-999.999	-999.999	-4.976	-384.557
	SPLINES	-999.999	-999.999	-999.999	-774.217	-999.999	-999.999	-962.369
	INTERPOL.	0.810	-5.209	0.973	-1.273	0.897	0.903	-0.483
II	KRIGING	-41.100	-271.631	0.951	-999.999	-999.999	-5.225	-386.167
	SPLINES	-999.999	-999.999	-999.999	-762.062	-999.999	-999.999	-960.343
	INTERPOL.	0.741	-5.592	0.972	-1.485	0.881	0.868	-0.602
III	KRIGING	-40.483	-273.701	0.949	-999.999	-999.999	-6.201	-386.572
	SPLINES	-999.999	-999.999	-999.999	-760.159	-999.999	-999.999	-960.026
	INTERPOL.	-9.810	-88.752	0.974	-2.944	0.758	0.821	-16.492
IV	KRIGING	-40.622	-268.612	0.946	-999.999	-999.999	-6.041	-385.721
	SPLINES	-999.999	-999.999	-999.999	-760.038	-999.999	-999.999	-960.006
	INTERPOL.	0.653	-29.432	0.998	-5.156	0.646	0.640	-5.275
V	KRIGING	-34.004	-159.964	0.951	-999.999	-999.999	-5.181	-366.366
	SPLINES	-999.999	-999.999	-999.999	-845.138	-999.999	-999.999	-974.189
	INTERPOL.	-1.370	-26.898	0.978	-2.436	0.813	0.834	-4.679
AVERAGE	KRIGING	-38.340	-248.348	0.951	-999.999	-999.999	-5.525	-381.877
	SPLINES	-999.999	-999.999	-999.999	-780.323	-999.999	-999.999	-963.387

NOTE :
****
A VALUE OF -999.999 INDICATES THAT THE INDEX IS ACTUALLY LESS THAN OR EQUAL TO -999.999

Table 6.15. Summary of the comparison for the calibrated piezometric heads: maximum residual.

		PERFORMANCE INDEX : MAXIMUM RESIDUAL						
CASE	PROCEDURE	A	B	C	D	E	F	AVERAGE
	INTERPOL.	0.829	0.833	0.948	0.420	0.145	0.407	0.597
I	KRIGING	-23.431	-29.029	0.634	-408.581	-999.999	-450.616	-318.504
	SPLINES	-999.999	-999.999	-999.999	-133.729	-999.999	-999.999	-855.621
	INTERPOL.	0.821	0.833	0.949	0.418	0.160	0.338	0.587
II	KRIGING	-24.508	-29.165	0.624	-408.782	-999.999	-452.981	-319.135
	SPLINES	-999.999	-999.999	-999.999	-133.860	-999.999	-999.999	-855.642
	INTERPOL.	0.832	0.833	0.947	0.437	0.184	0.238	0.579
III	KRIGING	-24.346	-29.244	0.619	-408.587	-999.999	-459.157	-320.119
	SPLINES	-999.999	-999.999	-999.999	-133.739	-999.999	-999.999	-855.622
	INTERPOL.	-1.257	-1.246	0.967	-0.173	-0.692	-0.491	-0.482
IV	KRIGING	-24.296	-29.057	0.479	-408.550	-999.999	-458.137	-319.927
	SPLINES	-999.999	-999.999	-999.999	-133.742	-999.999	-999.999	-855.623
	INTERPOL.	0.310	-3.819	0.939	-1.448	-0.508	-0.413	-0.823
V	KRIGING	-23.672	-24.767	0.466	-385.586	-999.999	-449.428	-313.831
	SPLINES	-999.999	-999.999	-999.999	-115.761	-999.999	-999.999	-852.626
	INTERPOL.	0.307	-0.513	0.950	-0.069	-0.142	0.016	0.092
AVERAGE	KRIGING	-24.051	-28.252	0.564	-404.017	-999.999	-454.064	-318.303
	SPLINES	-999.999	-999.999	-999.999	-130.166	-999.999	-999.999	-855.027

NOTE :

****

A VALUE OF -999.999 INDICATES THAT THE INDEX IS ACTUALLY LESS THAN OR EQUAL TO -999.999

Table 6.16. Summary of the comparison for the calibrated piezometric heads: variance of the absolute value of the residuals.

		PERFORMANCE INDEX : VARIANCE OF THE RESIDUALS						
CASE	PROCEDURE	A	B	C	D	E	F	AVERAGE
	INTERPOL.	0.915	0.966	0.996	-14.333	0.014	0.945	-1.749
I	KRIGING	-999.999	-999.999	0.660	-999.999	-999.999	-999.999	-833.222
	SPLINES	-999.999	-999.999	-999.999	-999.999	-999.999	-999.999	-999.999
	INTERPOL.	0.918	0.969	0.997	-14.135	0.007	0.943	-1.717
II	KRIGING	-999.999	-999.999	0.644	-999.999	-999.999	-999.999	-833.225
	SPLINES	-999.999	-999.999	-999.999	-999.999	-999.999	-999.999	-999.999
	INTERPOL.	0.935	0.966	0.996	-13.308	0.022	0.925	-1.577
III	KRIGING	-999.999	-999.999	0.638	-999.999	-999.999	-999.999	-833.226
	SPLINES	-999.999	-999.999	-999.999	-999.999	-999.999	-999.999	-999.999
	INTERPOL.	-12.950	-8.383	0.998	-34.845	-3.058	0.762	-9.579
IV	KRIGING	-999.999	-999.999	0.612	-999.999	-999.999	-999.999	-833.231
	SPLINES	-999.999	-999.999	-999.999	-999.999	-999.999	-999.999	-999.999
	INTERPOL.	0.019	-21.146	0.996	-382.031	-2.101	0.291	-67.329
V	KRIGING	-999.999	-999.999	0.259	-999.999	-999.999	-999.999	-833.289
	SPLINES	-999.999	-999.999	-999.999	-999.999	-999.999	-999.999	-999.999
	INTERPOL.	-2.033	-5.326	0.997	-91.730	-1.023	0.773	-16.390
AVERAGE	KRIGING	-999.999	-999.999	0.563	-999.999	-999.999	-999.999	-833.239
	SPLINES	-999.999	-999.999	-999.999	-999.999	-999.999	-999.999	-999.999

NOTE :
!!!!

A VALUE OF -999.999 INDICATES THAT THE INDEX IS ACTUALLY LESS THAN OR EQUAL TO -999.999

The results presented in Tables 6.13 to 6.16 follow the same pattern as the results corresponding to the estimated piezometric heads (see Table 6.12, for example), in the sense that the calibrated heads produced using the one-dimensional interpolation method are the best, both in the average and in the maximum residual sense. Indeed Table 6.13. shows clearly that, except in example E (case V), the calibrated heads computed using the one-dimensional interpolation scheme always improve the initial (raw model) heads; according to this Table the addition of flow measurements into the calibration process is not having a positive impact on the average of the calibrated heads (Tables 6.14., 6.15. and 6.16. show that the same holds for the head variance, maximum residual and variance of the residuals as well). We shall discuss this point later on. Table 6.13 also shows the impact of worse initial estimates of the roughnesses and nodal consumptions (Cases IV and V, respectively), the latter being the more sensitive parameter.

The calibrated heads computed using Kriging and bi-cubic splines do not improve the initial heads, except in a few examples (example C for Kriging and D for the splines, as shown in Table 6.13.).

Example C demonstrates that the calibration algorithm works well even when the average of the initial roughnesses has been overestimated (by +20 % in this example). In this particular example, the head variances, the maximum residual and the variance of the residuals are always improved when the one-dimensional interpolation or Kriging procedures are used.

Table 6.14 shows that, on average, the calibration algorithm does not reduce the initial variance of the piezometric heads (global performance average index = -4.679), although when the one-dimensional interpolation procedure is used, improvement is achieved in approximately 66 % of the cases. It is also apparent from Table 6.14 that the calibration algorithm failed to improve the initial variance in examples B and D, which are those with the steeper piezometric planes. In general, worsening the initial pipe roughnesses and the nodal consumptions (cases IV and V, respectively), makes the variance of the heads even worse; the effect of the worse initial roughnesses seems to be more important than the initial nodal consumptions. Of the three procedures tested for head estimation (one-dimensional interpolation, Kriging and splines), the one-dimensional interpolation is the procedure which performs best, as far as reducing the variance of the calibrated heads is concerned.

Table 6.15. shows that, on average, the calibration algorithm improves the initial maximum residuals when the one-dimensional interpolation procedure is used to estimate the heads, particularly when the mean initial roughness and the nodal consumptions have been well estimated (i.e. in Cases I, II and III). Example C is a different situation, since the calibration algorithm improves the maximum residuals of the heads even with worse initial roughnesses and worse nodal consumption estimates. From Table 6.15 it is also clear that the application of Kriging leads to improvements in the variance of the residuals only in example C, whereas the application of splines for head estimation

does not produce any improvement at all.

As far as variance of the residuals (absolute values) is concerned (Table 6.16), the results of the calibration algorithm are, on average, worse than the initial estimates, although the use of the one-dimensional interpolation procedure reduces the variance in almost 66 % of the cases. As before, in the case of the maximum residuals, better results are obtained when both the initial roughnesses and nodal consumptions are well estimated (cases I, II and III).

In summary, the calibration algorithm improves the initial average piezometric heads as well as the maximum residual (global average performance indices of 0.888 and 0.092, respectively). The results for the variance of the heads and the variance of the absolute value of the residuals are, by and large, negative (global average performance indices of -4.679 and -16.390, respectively), even though improvement with respect to the initial heads is achieved in 66 % of the cases, particularly when better initial estimates of the pipe roughnesses and nodal consumptions are available.

In looking at the behaviour of the calibrated heads more broadly, it is possible to find from Tables 6.13 to 6.16 that, in 15 out of 30 cases, the algorithm improved simultaneously the average heads, their variance, the maximum residual and the variance of the residuals, i.e. we have a "global success index" (as defined in section 6.11.4.2) of 50 %. This has happened for example A (Cases I, II, III, and V), example C (Cases I, II, III, IV and V), example E (Cases I, II and III) and example F (Cases

I, II and III). The corresponding "global success index" when Kriging was used is 16.67 % (5 cases out of 30) and 0.0 % for splines.

b) Calibrated flows results:

Following the same sequence as for the heads, Appendix D includes a set of 12 more tables, with the result summaries (Tables D.13 to D.18, for examples A to F, respectively) and the performance indices (Tables D.19 to D.24).

Fig. 6.15. represents the pipe flows for example E, Case I, for the same 4 transverse sections, as in Figs. 6.13 and 6.14., when the estimated and calibrated piezometric heads were compared.

Similarly to the case of the calibrated piezometric heads, four two way tables summarise the behaviour of the performance index across the five cases and six examples used for the comparison. Tables 6.17, 6.18, 6.19 and 6.20 refer to the average calibrated flows, their variance, the maximum residual and the variance of the residuals, respectively.

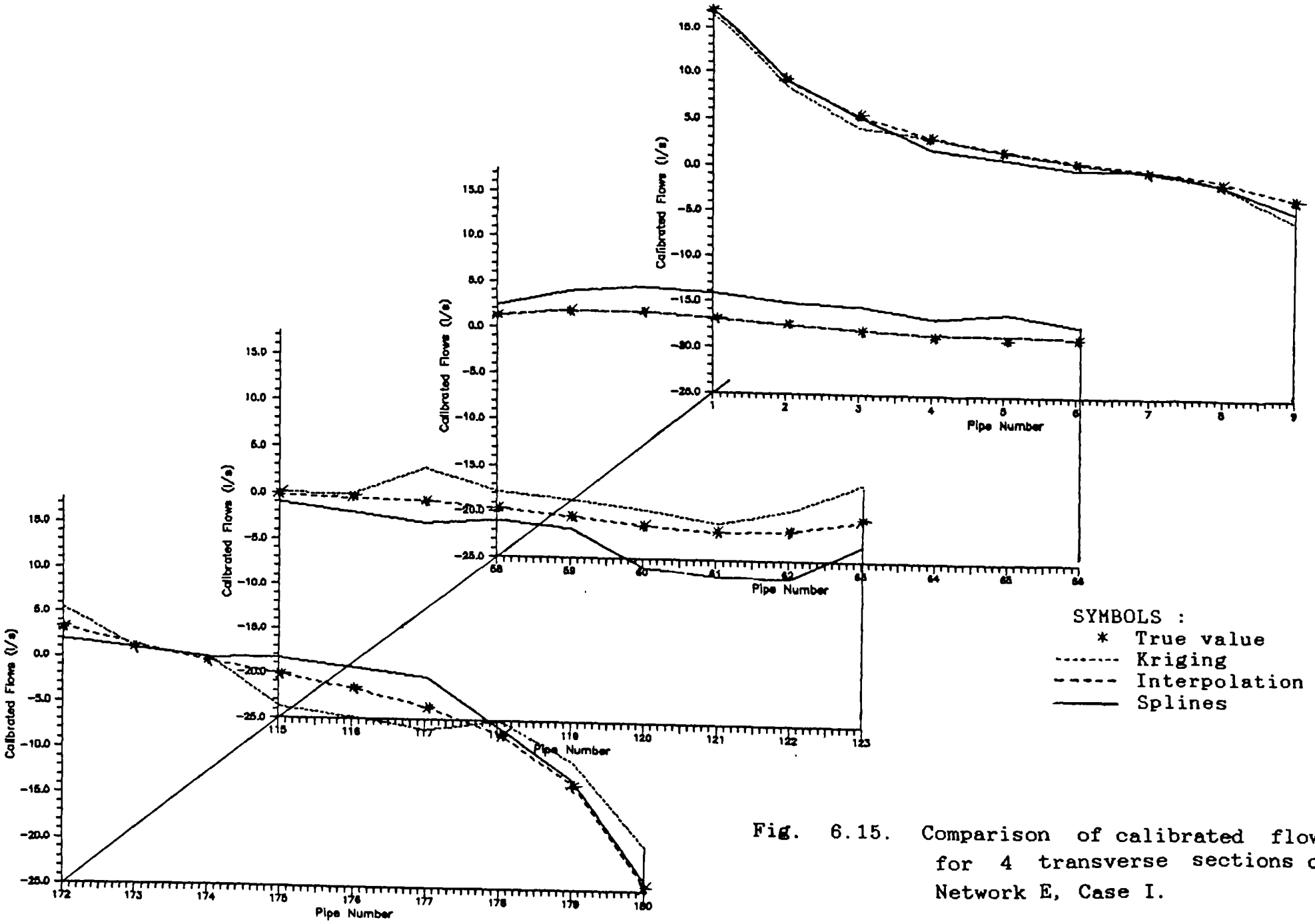

Fig. 6.15. Comparison of calibrated flows for 4 transverse sections of Network E, Case I.

Table 6.17. Summary of the comparison for the calibrated flows: average flows.

		PERFORMANCE INDEX : AVERAGE						
CASE	PROCEDURE	A	B	C	D	E	F	AVERAGE
	INTERPOL.	-0.004	0.008	-0.023	-19.250	0.453	-0.192	-3.168
I	KRIGING	-184.733	1.000	-31.332	-0.563	-999.999	0.478	-202.525
	SPLINES	-72.902	-42.610	-140.271	0.437	-459.738	-999.999	-285.847
	INTERPOL.	0.773	0.866	-12.538	-999.999	-4.690	0.958	-169.105
II	KRIGING	-2.597	0.891	-0.931	-999.999	-999.999	0.995	-333.606
	SPLINES	-29.806	-1.351	-46.695	-999.999	-333.037	-999.999	-401.815
	INTERPOL.	0.661	0.994	0.900	-999.999	1.000	0.968	-165.913
III	KRIGING	1.000	0.984	0.996	-999.999	-35.633	-0.804	-172.243
	SPLINES	-52.206	-0.861	-116.581	-999.999	-37.607	-999.999	-367.876
	INTERPOL.	0.124	0.923	0.967	-999.999	0.998	0.980	-166.001
IV	KRIGING	0.999	0.999	0.991	-999.999	-34.361	-0.858	-172.038
	SPLINES	-63.255	-7.648	-5.318	-999.999	-20.644	-999.999	-349.477
	INTERPOL.	0.937	0.548	0.988	-164.766	0.909	0.876	-26.751
V	KRIGING	-999.999	-999.999	0.342	-999.999	-83.941	-0.079	-513.946
	SPLINES	-999.999	-999.999	0.091	-999.999	-82.577	-999.999	-680.414
	INTERPOL.	0.498	0.668	-1.941	-636.803	-0.266	0.718	-106.188
AVERAGE	KRIGING	-237.066	-199.225	-5.987	-800.112	-430.787	-0.054	-278.872
	SPLINES	-243.633	-210.494	-61.755	-799.912	-186.721	-999.999	-417.086

NOTE :
!!!!
A VALUE OF -999.999 INDICATES THAT THE INDEX IS ACTUALLY LESS THAN OR EQUAL TO -999.999

Table 6.18. Summary of the comparison for the calibrated flows: variance of the flows.

		PERFORMANCE INDEX : VARIANCE						
CASE	PROCEDURE	A	B	C	D	E	F	AVERAGE
	INTERPOL.	-0.244	-0.050	0.771	-999.999	0.268	-0.127	-166.563
I	KRIGING	-177.615	0.920	-29.866	-999.999	-445.618	-999.999	-442.029
	SPLINES	-40.567	-14.722	-148.540	-999.999	-247.806	-999.999	-408.605
	INTERPOL.	0.901	0.894	-77.063	-999.999	0.694	-35.067	-184.940
II	KRIGING	-142.343	-0.129	-278.370	-999.999	-371.842	-999.999	-465.447
	SPLINES	-162.665	-117.440	-533.205	-999.999	-426.801	-999.999	-540.018
	INTERPOL.	0.877	0.940	-1.074	-999.999	1.000	-33.502	-171.960
III	KRIGING	-76.926	-0.104	-243.327	-999.999	-463.270	-999.999	-463.938
	SPLINES	-155.384	-158.095	-535.163	-999.999	-343.325	-999.999	-531.994
	INTERPOL.	0.975	0.999	1.000	-999.999	0.998	-39.651	-172.613
IV	KRIGING	-81.717	-1.145	-6.542	-999.999	-537.835	-999.999	-437.873
	SPLINES	-142.358	-472.515	-17.798	-999.999	-999.999	-999.999	-605.445
	INTERPOL.	0.978	0.956	0.994	-999.999	0.965	-37.067	-172.196
V	KRIGING	-999.999	-999.999	0.033	-999.999	-242.848	-999.999	-707.135
	SPLINES	-573.619	-999.999	0.811	-999.999	-368.592	-999.999	-656.899
	INTERPOL.	0.697	0.748	-15.074	-999.999	0.785	-29.083	-173.654
AVERAGE	KRIGING	-295.720	-200.091	-111.615	-999.999	-412.283	-999.999	-503.284
	SPLINES	-214.918	-352.554	-246.779	-999.999	-477.304	-999.999	-548.592

NOTE :

!!!!

A VALUE OF -999.999 INDICATES THAT THE INDEX IS ACTUALLY LESS THAN OR EQUAL TO -999.999

Table 6.19. Summary of the comparison for the calibrated flows: maximum residual.

		PERFORMANCE INDEX : MAXIMUM RESIDUAL						
CASE	PROCEDURE	A	B	C	D	E	F	AVERAGE
I	INTERPOL.	-0.136	0.005	-2.638	-52.814	-1.701	-0.091	-9.563
	KRIGING	-170.771	-0.154	-6.784	-936.003	-271.042	-135.710	-253.411
	SPLINES	-67.387	-26.108	-33.078	-364.938	-395.403	-999.999	-314.485
II	INTERPOL.	0.307	0.022	-2.586	-66.950	-0.834	0.037	-11.667
	KRIGING	-16.335	-0.404	-3.860	-999.999	-225.047	-178.260	-237.318
	SPLINES	-68.515	-19.608	-25.706	-346.077	-999.999	-310.745	-295.108
III	INTERPOL.	0.616	0.022	-2.870	-39.519	-1.019	-0.054	-7.138
	KRIGING	-15.565	0.376	-6.084	-999.999	-999.999	-84.489	-350.960
	SPLINES	-60.444	-22.371	-23.135	-575.257	-971.949	-467.582	-353.456
IV	INTERPOL.	-10.655	0.005	0.798	-54.663	-2.326	-0.067	-11.151
	KRIGING	-15.290	-7.038	-0.007	-999.999	-999.999	-84.659	-351.165
	SPLINES	-34.568	-69.540	-2.484	-582.368	-999.999	-467.876	-359.472
V	INTERPOL.	0.376	-16.042	0.275	-349.430	-8.595	-3.983	-62.900
	KRIGING	-108.782	-91.807	0.201	-999.999	-834.416	-87.983	-353.798
	SPLINES	-252.898	-999.999	-2.654	-575.688	-919.051	-481.720	-538.668
AVERAGE	INTERPOL.	-1.898	-3.198	-1.404	-112.675	-2.895	-0.832	-20.484
	KRIGING	-65.349	-19.805	-3.307	-987.200	-666.101	-114.220	-309.330
	SPLINES	-96.763	-227.525	-17.411	-488.865	-857.280	-545.584	-372.238

NOTE :
####

A VALUE OF -999.999 INDICATES THAT THE INDEX IS ACTUALLY LESS THAN OR EQUAL TO -999.999

Table 6.20. Summary of the comparison for the calibrated flows: variance of the absolute value of the residuals.

		PERFORMANCE INDEX : VARIANCE OF THE RESIDUALS						
CASE	PROCEDURE	A	B	C	D	E	F	AVERAGE
	INTERPOL.	0.278	-0.003	-18.641	-999.999	-2.970	-2.424	-170.627
I	KRIGING	-999.999	0.478	-73.242	-999.999	-999.999	-999.999	-678.793
	SPLINES	-999.999	-551.471	-999.999	-999.999	-999.999	-999.999	-925.244
	INTERPOL.	0.817	0.306	-15.337	-999.999	-2.373	-0.942	-169.521
II	KRIGING	-165.491	0.221	-24.126	-999.999	-999.999	-999.999	-531.565
	SPLINES	-999.999	-379.195	-999.999	-999.999	-999.999	-999.999	-896.532
	INTERPOL.	0.917	0.081	-28.460	-745.078	-1.390	-0.681	-129.102
III	KRIGING	-148.833	0.655	-50.106	-999.999	-999.999	-999.999	-533.047
	SPLINES	-999.999	-397.106	-999.999	-999.999	-999.999	-999.999	-899.517
	INTERPOL.	-84.968	0.157	0.974	-999.999	-10.028	0.014	-182.308
IV	KRIGING	-206.090	-64.831	0.109	-999.999	-999.999	-999.999	-545.135
	SPLINES	-895.254	-999.999	-7.726	-999.999	-999.999	-999.999	-817.163
	INTERPOL.	0.662	-129.818	0.605	-999.999	-59.700	-141.496	-221.624
V	KRIGING	-999.999	-999.999	-0.116	-999.999	-999.999	-999.999	-833.352
	SPLINES	-999.999	-999.999	-11.237	-999.999	-999.999	-999.999	-835.205
	INTERPOL.	-16.459	-25.855	-12.172	-949.015	-15.292	-29.110	-174.650
AVERAGE	KRIGING	-504.082	-212.695	-29.496	-999.999	-999.999	-999.999	-624.378
	SPLINES	-979.050	-665.554	-603.792	-999.999	-999.999	-999.999	-874.732

NOTE :

!!!!

A VALUE OF -999.999 INDICATES THAT THE INDEX IS ACTUALLY LESS THAN OR EQUAL TO -999.999

Contrary to what we have seen in the case of the estimated and calibrated piezometric heads, the behaviour of the calibrated flows is more variable and needs a more detailed review. Table 6.17 shows that, despite the fact that the global performance index is negative when the one-dimensional interpolation scheme is used (i.e. -106.188), most of the cause of this apparent bad performance is attributable to the example D, which will be analysed in more detail in the following paragraphs. If we remove example D, the global performance index becomes -0.0646 , indicating only a slight deterioration of the initial average flow.

As it is possible to see from looking at the averages across all the examples (last column) of Tables 6.17 to 6.20, the values of the calibrated flows computed using the one-dimensional interpolation procedure are always better than those computed using Kriging and splines.

In looking at Tables 6.17 to 6.20 as a whole, it is possible to find out that in examples A (Cases II, III and V), B (Cases II, III and IV) and C (Cases IV and V), the average flow, its variance, the maximum residual and the variance of the residuals improved simultaneously with respect to the initial estimates. This represents 7 cases out of 30, i.e. a "global success index" (as defined in section 6.11.4.2) of 26.7 % . The corresponding "global success" indices for Kriging and splines are 0.0 % in both cases.

The behaviour of the performance index for example D deserves further attention, which has to be complemented with the

corresponding Table D.16, from Appendix D. Basically, what is happening in this particular example is that the initial flows are quite close to the true values (this is a consequence of assuming that we know the mean pipe roughnesses which, by the way, is one of the reasons why we use the raw model flows as estimates of the true flows); this can be seen from Table D.16, where the true and average calibrated flows differ only by 5×10^{-6} (l/s). This implies that a calibrated flow which on average is only 3.9×10^{-5} (l/s) different with respect to the true value (as in Case I) is worse than the initial estimate, producing a large negative performance index; in practice, a difference of this magnitude is irrelevant.

On the other hand; if we review the definition of the performance index [equation(16)], it can be seen that the index "blows up" when the true and initial values of the variable being assessed are very close to each other [i.e. $X^t - X^i \approx 0$ in equation (16), and the denominator $(X^t - X^i)^2$ becomes even closer to zero]. This indicates that the "performance index" should be always checked carefully for the case where the initial and true values are too close.

In general, unless the measurement information corresponds exactly to the <u>true</u> heads and flows, any algorithm should deteriorate the initial estimates when starting too close to the true solution.

As can be seen from Table D.16 (for example D), all the calibrated flows computed either with the one-dimensional

interpolation, Kriging or splines give flows which, on average, reproduce the true values within a ± 3 % margin, although from the maximum residual and variance points of view, the one-dimensional interpolation seems to be much better than the others.

The incorporation of flow measurements, represented by cases II and III, with respect to case I (when only head measurements were considered) did not seem to produce a great impact on the calibrated flows. For example, as far as the average flows are concerned (Table 6.17), and leaving example D aside, for the reasons already explained concerning the ill-conditioning of the performance index near the true values, Examples C and E did not improve the calibrated flows when the first set of flow measurements was considered in the calibration algorithm (i.e. passing from case I to II in Table 6.17); something similar can be observed in Table 6.19 with respect to the maximum residuals. Some improvement can be detected in relation to the variance of the residuals (Table 6.20) from case I to II, though the performance index is still negative. When considering the second set of flow measurements, improvement can be noticed in all the examples (except D), for the average flows, and some smaller improvements can be detected in the flow variance and residuals. This behaviour of the calibration algorithm with respect to the availability of flow measurements perhaps reveals the need for a more systematic and rational approach for flow measurement placement, something which has not been studied here.

Thus, in summary, as far as the estimation of the true flows is concerned, which is currently done iteratively at the same time as the estimation of the roughnesses is carried out, the results given by the calibration algorithm are not as successful as in the case of the piezometric heads. This seems to suggest that perhaps a different flow estimation procedure should be implemented, instead of the iterative scheme used in the present work.

c) Calibrated Hazen-Williams roughnesses:

As before, we include in Appendix D 6 tables with the summary of the results (Tables D.25 to D.30) and another batch of 6 tables with the results corresponding to the performance indices (Tables D.31 to D.36).

Figure 6.16. presents the behaviour of the calibrated C's, for example E and case I.

Summarising the Tables presented in Appendix D, Tables 6.21, 6.22, 6.23 and 6.24 condense the results of the performance index for the average C's, their variance, the maximum residual and the variance of the absolute value of the residuals.

In Figure 6-16 a) the calibrated C's using the one-dimensional interpolation scheme are compared with the initial estimates (shown by the asterisks in Fig. 6-16) and with the true values (C=140 for all the pipes, represented by the horizontal line). The values of the roughnesses (C's) corresponding to pipes with consecutive numbering have been joined with a continuous line in order to visualise their variability; it should not be forgotten

that we are dealing with a discrete variable. Figures 6-16 b) and c) correspond to the calibrated C's obtained using Kriging and splines, respectively.

The main statistics associated with Figure 6-16 are summarised in Table D-29 (case I).

Figure 6-16 a) shows clearly that the C's produced using the one-dimensional interpolation tend to "follow" the initial estimates in some pipes. It is also clear from that Figure that the average calibrated roughnesses are close to the true values, though their dispersion (variance) is larger than that of the initial estimates.

For the C's produced using Kriging and splines Fig. 6-16 b) and c) and Table D-29 show clearly that they are, on average, underestimating the true roughnesses. What seems to be even worse with the roughnesses produced with Kriging and splines is the fact that they are "jumping" from one border to the other of the "allowable band" [determined by the maximum variation factor x=0.10, see equation (4)], but they never get close to the true values. This explains why, in general, the variances of the absolute value of the residuals are always smaller (when using Kriging and splines) than those produced using the one-dimensional interpolation; roughly speaking, the residuals (absolute value) produced by using Kriging and splines are <u>consistently</u> wrong, while those C's produced using the one-dimensional interpolation are not. In this case we have to look

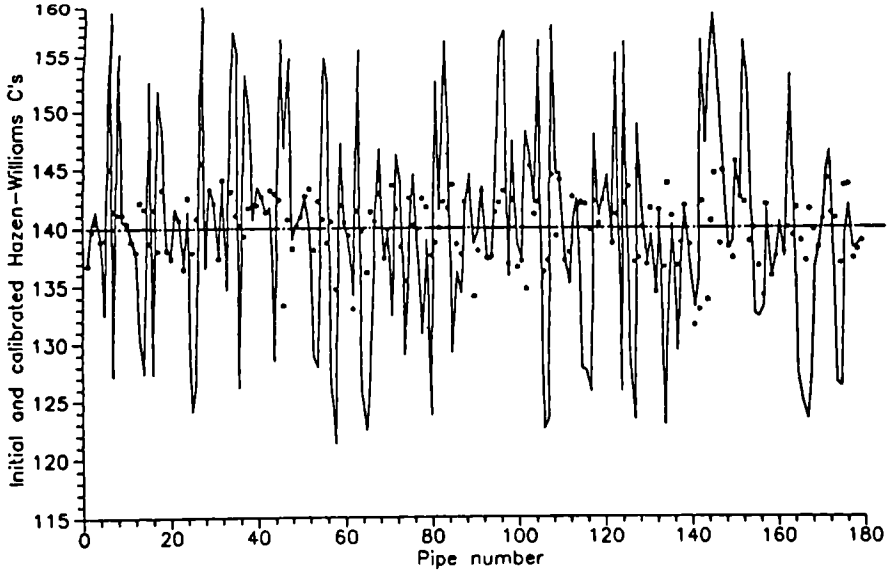

a) One-dimensional interpolation

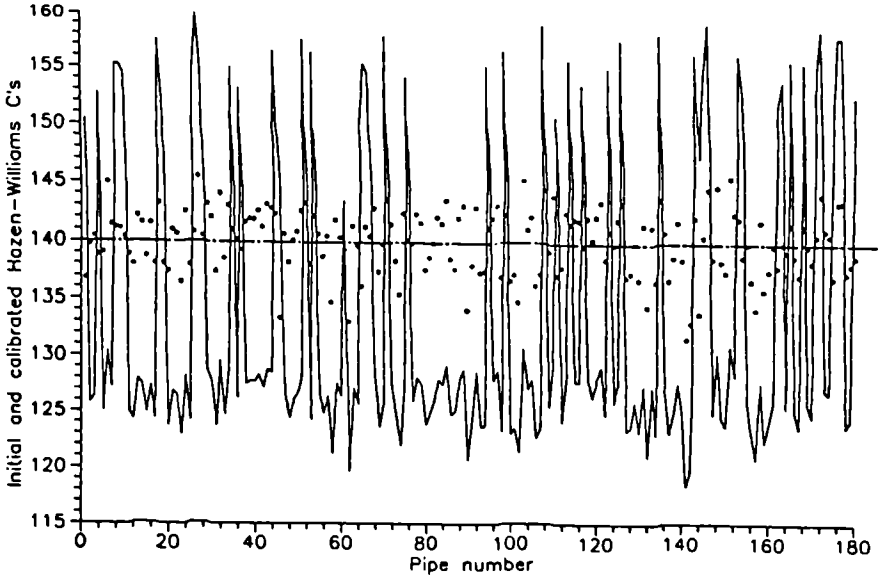

b) Kriging

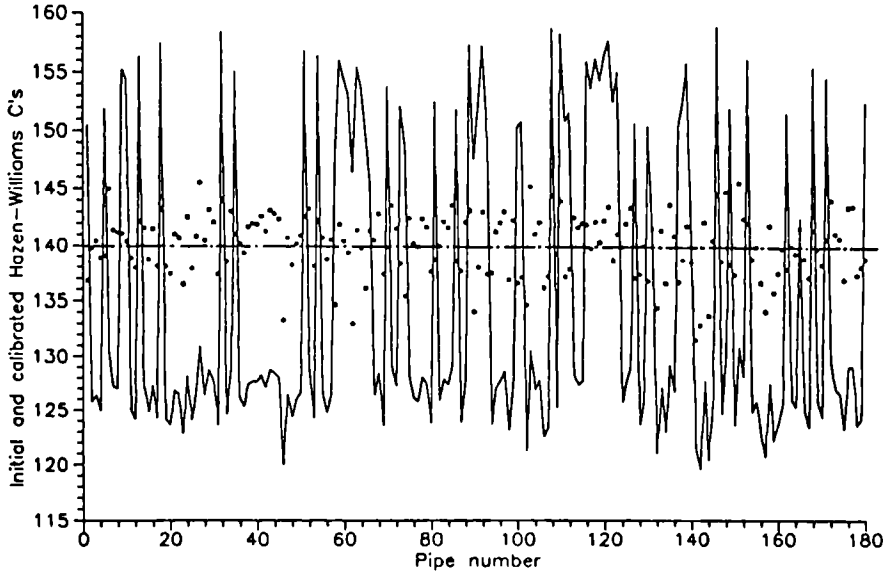

c) Splines

SYMBOLS :
* Initial estimate
—·— True value

Fig. 6.16. Comparison of calibrated C's.
Network E, Case I.

Table 6.21. Summary of the comparison for the calibrated C's: average C's.

CASE	PROCEDURE	PERFORMANCE INDEX : AVERAGE A	B	C	D	E	F	AVERAGE
	INTERPOL.	-62.709	-51.879	0.679	-384.064	0.014	-18.400	-86.060
I	KRIGING	-210.664	0.902	0.633	-999.999	-999.999	-999.999	-534.854
	SPLINES	-773.546	-564.898	0.824	-999.999	-999.999	-999.999	-722.936
	INTERPOL.	-70.898	-112.730	0.764	-594.284	0.264	-239.267	-169.359
II	KRIGING	-242.359	0.902	0.633	-999.999	-999.999	-999.999	-540.137
	SPLINES	-773.546	-564.898	0.824	-999.999	-999.999	-999.999	-722.936
	INTERPOL.	-65.936	-85.120	0.679	-33.414	-0.543	-306.269	-81.767
III	KRIGING	-242.769	0.902	0.638	-999.999	-999.999	-999.999	-540.204
	SPLINES	-773.546	-564.898	0.824	-999.999	-999.999	-999.999	-722.936
	INTERPOL.	0.916	-8.867	0.672	-351.862	-39.720	-28.531	-71.232
IV	KRIGING	-17.207	-12.650	0.634	-999.999	-999.999	-999.999	-504.870
	SPLINES	-67.284	-47.362	0.786	-999.999	-999.999	-999.999	-518.976
	INTERPOL.	-30.780	-31.573	0.604	-2.518	-999.999	-183.203	-207.912
V	KRIGING	-230.244	-19.121	0.585	-999.999	-999.999	-999.999	-541.463
	SPLINES	-773.546	-395.178	0.819	-999.999	-999.999	-999.999	-694.650
	INTERPOL.	-45.881	-58.034	0.680	-273.228	-207.997	-155.134	-123.266
AVERAGE	KRIGING	-188.649	-5.813	0.625	-999.999	-999.999	-999.999	-532.306
	SPLINES	-632.293	-427.447	0.815	-999.999	-999.999	-999.999	-676.487

NOTE :
!!!!
A VALUE OF -999.999 INDICATES THAT THE INDEX IS ACTUALLY LESS THAN OR EQUAL TO -999.999

Table 6.22. Summary of the comparison for the calibrated C's: variance of the C's.

		PERFORMANCE INDEX : VARIANCE						
CASE	PROCEDURE	A	B	C	D	E	F	AVERAGE
	INTERPOL.	-13.645	-22.196	-0.984	-131.976	-128.856	-48.132	-57.632
I	KRIGING	-14.007	-12.729	0.673	-585.184	-499.395	-247.525	-226.361
	SPLINES	-24.279	-10.740	0.892	-641.875	-494.328	-484.876	-275.868
	INTERPOL.	-12.253	-24.106	-0.099	-161.234	-122.212	-52.456	-62.060
II	KRIGING	-8.062	-12.729	0.673	-601.478	-465.098	-255.237	-223.655
	SPLINES	-24.279	-10.740	0.892	-576.977	-472.896	-468.641	-258.773
	INTERPOL.	-12.957	-18.550	-0.986	-100.423	-125.500	-44.957	-50.562
III	KRIGING	-7.990	-12.729	0.689	-604.710	-385.901	-354.426	-227.511
	SPLINES	-24.279	-10.740	0.892	-591.182	-498.385	-497.128	-270.137
	INTERPOL.	-1.648	-1.292	-0.134	-85.504	-47.949	-14.705	-25.205
IV	KRIGING	0.992	-6.325	0.727	-165.657	-107.576	-91.712	-61.592
	SPLINES	0.720	0.987	0.867	-158.133	-129.673	-137.148	-70.397
	INTERPOL.	-145.424	0.927	-3.776	-447.881	-249.762	-159.499	-167.569
V	KRIGING	-10.255	-19.584	0.580	-603.746	-413.693	-350.050	-232.791
	SPLINES	-24.279	-5.757	0.915	-595.019	-524.876	-522.272	-278.548
	INTERPOL.	-37.185	-13.043	-1.196	-185.404	-134.856	-63.950	-72.606
AVERAGE	KRIGING	-7.865	-12.819	0.668	-512.155	-374.333	-259.790	-194.382
	SPLINES	-19.279	-7.398	0.892	-512.637	-424.031	-422.013	-230.745

NOTE :

****

A VALUE OF -999.999 INDICATES THAT THE INDEX IS ACTUALLY LESS THAN OR EQUAL TO -999.999

Table 6.23. Summary of the comparison for the calibrated C's: maximum residual.

		PERFORMANCE INDEX : MAXIMUM RESIDUAL						
CASE	PROCEDURE	A	B	C	D	E	F	AVERAGE
I	INTERPOL.	-6.704	-6.704	-0.807	-3.863	-4.500	-4.737	-4.552
	KRIGING	-6.704	-7.806	-0.066	-4.737	-5.466	-5.466	-5.041
	SPLINES	-6.704	-6.704	0.800	-4.737	-4.737	-5.466	-4.591
II	INTERPOL.	-6.704	-6.704	-0.798	-4.719	-4.500	-4.737	-4.694
	KRIGING	-6.704	-7.806	-0.073	-4.737	-5.466	-5.466	-5.042
	SPLINES	-6.704	-6.704	0.800	-4.737	-4.737	-5.466	-4.591
III	INTERPOL.	-6.704	-6.704	-0.808	-3.863	-4.500	-4.737	-4.553
	KRIGING	-6.704	-7.806	-0.075	-4.737	-5.466	-5.466	-5.042
	SPLINES	-6.704	-6.704	0.800	-5.466	-5.466	-5.466	-4.834
IV	INTERPOL.	0.119	0.230	-0.062	-1.759	-1.750	-1.552	-0.796
	KRIGING	-0.293	-1.753	0.288	-2.663	-3.250	-3.250	-1.820
	SPLINES	-0.293	-0.293	0.566	-3.250	-3.250	-3.250	-1.629
V	INTERPOL.	-7.806	-7.227	-1.438	-5.466	-4.673	-4.737	-5.224
	KRIGING	-6.704	-7.806	-0.457	-4.737	-5.466	-5.466	-5.106
	SPLINES	-6.704	-6.704	0.800	-4.737	-5.466	-5.466	-4.713
AVERAGE	INTERPOL.	-5.560	-5.422	-0.782	-3.934	-3.985	-4.100	-3.964
	KRIGING	-5.422	-6.596	-0.077	-4.322	-5.023	-5.023	-4.410
	SPLINES	-5.422	-5.422	0.753	-4.585	-4.731	-5.023	-4.072

NOTE :

!!!!

A VALUE OF -999.999 INDICATES THAT THE INDEX IS ACTUALLY LESS THAN OR EQUAL TO -999.999

Table 6.24. Summary of the comparison for the calibrated C's: variance of the absolute value of the residuals.

		PERFORMANCE INDEX : VARIANCE OF THE RESIDUALS						
CASE	PROCEDURE	A	B	C	D	E	F	AVERAGE
	INTERPOL.	-273.295	-200.036	-14.342	-148.606	-195.419	-96.340	-154.673
I	KRIGING	-90.406	-42.248	-6.634	-28.590	-7.868	-23.788	-33.256
	SPLINES	-31.983	-34.296	0.931	-11.530	-14.659	-7.782	-16.553
	INTERPOL.	-261.133	-257.706	-5.482	-174.161	-204.031	-102.722	-167.539
II	KRIGING	-47.609	-42.248	-6.638	-20.929	-11.185	-28.545	-26.192
	SPLINES	-31.983	-34.296	0.931	-12.697	-8.501	-8.346	-15.815
	INTERPOL.	-268.537	-190.796	-14.355	-150.180	-200.832	-92.442	-152.857
III	KRIGING	-47.169	-42.248	-6.104	-17.321	-9.159	-22.785	-24.131
	SPLINES	-31.983	-34.296	0.931	-11.248	-17.220	-10.806	-17.437
	INTERPOL.	-0.770	-0.801	-0.278	-31.279	-50.605	-22.705	-17.740
IV	KRIGING	-1.719	-7.621	-0.354	-11.312	-8.416	-12.585	-7.002
	SPLINES	-1.047	-1.318	0.755	-9.002	-9.477	-7.886	-4.663
	INTERPOL.	-282.156	-139.664	-27.710	-127.279	-218.845	-174.175	-161.638
V	KRIGING	-64.730	-42.482	-12.893	-18.142	-12.487	-21.099	-28.639
	SPLINES	-31.983	-35.257	0.933	-14.938	-12.089	-8.499	-16.972
	INTERPOL.	-217.178	-157.801	-12.433	-126.301	-173.947	-97.677	-130.889
AVERAGE	KRIGING	-50.327	-35.369	-6.525	-19.259	-9.823	-21.760	-23.844
	SPLINES	-25.796	-27.893	0.896	-11.883	-12.389	-8.664	-14.288

NOTE :

****

A VALUE OF -999.999 INDICATES THAT THE INDEX IS ACTUALLY LESS THAN OR EQUAL TO -999.999

at the average residuals, which in the case of the one-dimensional interpolation are about one half of those for the cases of Kriging and splines. When the variance of the residuals is computed (not that of their absolute values) the situation reverses, in sense that the minimum variance is obtained when the one-dimensional interpolation is used. We have used the absolute value of the residuals (instead of just the residual) because it implies a more stringent test.

Tables 6.21 to 6.24 show that, with the exception of the example C, the calibration algorithm, in general, does not improve the initially assumed pipe roughnesses. The "global success" index is now zero (0 %) when the one-dimensional interpolation and Kriging have been used to estimate the heads, and 16.7 % when the bi-cubic splines have been used for that purpose, thus conflicting with previous results in favour of the one-dimensional interpolation.

As in the case of the calibrated flows, a closer look to the detailed results is needed, and also a review of the way in which the whole calibration exercise was planned is required.

In carrying out the calibration exercise, it was assumed that the initial estimation of pipe roughnesses, considering the pipe material, pipe age, laboratory data, etc., was good enough to capture the true average roughness of the network, and we were expecting only "local" differences in the roughnesses. This means that, in general, the average initial estimates of the pipe roughnesses are nearly the same as the true values; the only exception to this is example C, where the initial C's were

overestimated by 20% with respect to the true values. This can be seen from Tables D.25 to D.30, where the ratio between estimated and true averages of the C's are shown in the last column of those Tables; on averaging those values across the different study cases (I to V), we obtain Table 6.25.

Table 6.25 shows that the initial roughness estimates, except example C, are always within 0.46 % of the true values. This implies that again, as in the case of example D for the calibrated flows, we may find ill-conditioned behaviour in the performance index (although this time it does not seem to be as bad as in the case of the flows). On the other hand, as already noted, the way to improve initial estimates too close to the true values is by using better estimates and/or more measurements (in this case both of the heads and the flows, since the calibrated roughnesses are computed from these two variables), which is not the present case, specially from the flows point of view. As a result, some deterioration of the initial C's is not a surprise, although, on average, Table 6.25 is showing that the calibrated C's produced when using the one-dimensional interpolation procedure are better than the originally estimated ones, including example C (i.e. 1.0115 against 1.0354, last row of Table 6.25).

Example C illustrates that, on average, the proposed calibration algorithm improves the initial roughness estimates of C when starting from poor initial estimates. Table 6.21, for example C, shows that improvement was obtained when <u>any</u> of the head estimation procedures was used.

Table 6.25. Summary of the ratios between average calibrated roughnesses and average true roughnesses.

	Ratio averages calibrated/true roughnesses			
Example	Initial	Interpolation	Kriging	Splines
A	1.0046	0.9885	0.9525	0.9123
B	1.0046	0.9726	1.0109	0.9277
C	1.2039	1.1150	1.1249	1.0876
D	0.9997	0.9987	0.9740	0.9749
E	0.9997	0.9955	0.9485	0.9613
F	0.9998	0.9986	0.9495	0.9565
Average	1.0354	1.0115	0.9934	0.9700

Table 6.24 shows that the splines-based results produce the least variance of the absolute value of the residuals, but this should be considered similarly to the analysis made of the results shown in Fig. 6-16, in the sense that a least variance of the residuals estimate is not decisive when the average, the variance and the maximum residuals of the estimate are the worst.

The results obtained for example C help us to review the discussion on the "maximum variation factor" for C [see equation (4)], used to control the change in the calibrated C's. Indeed, because the variation factor "x" used in the calibration exercise was x=0.10 (i.e. 10 % of variation), and because the initial roughnesses for example C were overestimated by + 20 %, the algorithm is performing the best it can, within the specified constraints (i.e. ± 10 %) thus, the average estimates are always halfway between the initial and true roughnesses.

To study the effect of the "maximum variation factor" on the results of the calibration exercise for example C, we ran the calibration program again, this time allowing a ± 30 % of variation for C [i.e. x=0.30 in equation (4)] and the results can be summarised as follows:

- As far as the calibrated piezometric heads are concerned, the results are nearly the same as with x=0.10, though a little bit worse.

- The new calibrated flows are much worse than when x=0.10.

- The calibrated roughnesses using the one-dimensional interpolation procedure are much better from the average C point of view, although from the variance, maximum residual and from the variance of the residuals standpoint they are worse.

The value x=0.10 used in the calibration exercise was determined by successive trials. We found that, in so doing, the initial estimates lead, by and large, to reasonable calibrated roughnesses, although this value of x depends on the quality of the initial roughness estimates; poorer initial estimates would need a larger x than better initial estimates. Because the quality of the initial roughness estimates is not known, a trial and error solution might be necessary to determine "x".

On the other hand, the factor "x" can be used to spot pipes or zones of the network where problems with the quality of the estimators exist. In fact, when the calibration algorithm gives a C^* equal either to the minimum or maximum allowable (the computer

program displays a message in that case), it means, unless there is some physical evidence to the contrary, that either the initial C, or the head or flow estimates are wrong, requiring a closer look at the pipe or zone of the network. This clearly deserves more attention in the future.

Another alternative to control the variation of C is not through the initial roughness estimates ($\underline{C}^{(o)}$), as in equation (4), but as a function of the "current" C within the iterative calibration procedure.

Eventually, the calibration process should be carried out in stages, with a variable "maximum variation factor" (x), starting with a small value and relaxing it as soon as values of C lying in the border of the allowable band are produced and provided that the there is some additional evidence to support the new roughnesses. Some way of linking the value of "x" to the quality of the estimates (not available at the moment) should be devised.

In summary, we believe that the results for the calibrated C's are highly dependent on the flow estimation, an aspect that deserves more attention in the near future. On the other hand, the way in which the calibration exercise was planned, means that the performance index for the calibrated C's tends to give a rather disappointing picture, perhaps worse than the real one. Example C has been included to show the behaviour of the calibration algorithm when the calibration exercise is carried out in another way.

6.11.5. Summary of the results.

We summarise the results in terms of the main variables involved in the whole calibration process: piezometric head estimates, calibrated nodal piezometric heads, calibrated pipe flows and calibrated C's.

As a summary of the discussion presented in section 6.11.4, Table 6.26 recapitulates the results for the "global success" index, for the different head estimation procedures tested.

a) Piezometric head estimation.

According to the results obtained using different methods for estimating the unmeasured heads (see Tables 6.10 and 6.12) the best approach seems to be the deterministic one-dimensional interpolation method. All the evidence available strongly suggests that the deterministic one-dimensional interpolation method should be used for head estimation purposes, instead of Kriging and splines.

Table 6.26. Summary of the "global success" index.

Variable	Global success index (%)		
	1-D interpolation	Kriging	Splines
Calibrated heads	50.0	16.7	0.0
Calibrated flows	26.7	0.0	0.0
Calibrated C's	0.0	0.0	16.7

The main reasons for the success of the one-dimensional interpolation scheme, seems to be attributable to the fact that it is the only method which explicitly considers the initially assumed shape of the piezometric plane. Kriging and splines-based estimation algorithms seem to be smoothing the estimated piezometric plane, whereas the interpolation method has the ability to keep the main structure of the initial piezometric plane (raw model) throughout the whole estimation procedure.

There is an additional advantage of the interpolation method over Kriging and splines, which is not clearly apparent from the examples tested. The one-dimensional interpolation method seems to be more appropriate for handling the head estimation problem when sharp and local variations of the piezometric plane take place; this is the case when booster pumps, high minor losses, or special regulating valves are installed in the network. In these cases the smoothing effect of both Kriging and splines should lead to a poorer performance of those methods.

The head interpolation method relies not only on the piezometric head measurements, as do the other methods, but also on the initial estimates of the pipe roughness characteristics, since it uses the raw model to determine the minimum head loss spanning tree, which allows us to generate the paths used in the one-dimensional interpolation procedure. This emphasises the need and the importance of a systematic study of the network resistance characteristics (according to pipe material, age, etc.), prior to the head estimation, if a successful network calibration is to be achieved; this study should be able to

determine accurately at least the relative value of the roughnesses of the different pipes.

As a result of this calibration exercise, it is believed that the one-dimensional interpolation procedure for the estimation of the unmeasured heads could be improved a bit further. The improvement could be achieved by re-estimating the heads once a first run of the calibration program has been made; the new head estimates being computed with the pipe head losses of the calibrated model, not with those of the raw model. The calibrated model may have a flow (and head loss) distribution slightly different from that of the raw model, in certain pipes or zones of the network. Perhaps this can help to reduce both the variance of the head estimates and that of the residuals.

b) Calibrated piezometric heads.

As expected from what has been noted in section 6.7, and from the results presented in section 6.11.4, the calibrated piezometric heads follow closely the estimated piezometric heads (compare Figures 6.13 and 6.14). Indeed, the use of the one-dimensional interpolation head estimation method again leads to the best results, as confirmed in the summary of Table 6.26.

As can be seen from Tables 6.13 to 6.16, the results using Kriging and splines are clearly unacceptable.

Further improvements should be achieved, as a by-product of the improvement suggested for the head estimation procedure already mentioned but, in general, the proposed calibration algorithm seems to be satisfactory with respect to the piezometric heads.

c) Calibrated pipe flows.

It has been already noted that the performance of the calibration algorithm must be assessed in terms of the agreement between the true and calibrated roughnesses; however, the assessment should also extend to the pipe discharges, since flows, together with piezometric heads, are the main state variables of the networks.

In general, as far as the calibrated flows are concerned, the calibration algorithm performs better when using the deterministic one-dimensional interpolation procedure, as shown in Table 6.26. This re-affirms previous conclusions concerning the superiority of the deterministic one-dimensional interpolation method over Kriging and splines.

As shown in Table 6.26, the "global success" index with respect to the flows (26.6 %) is about one half of that corresponding to the heads, and this is not good enough for our purposes, especially because the flows are subsequently used to estimate the roughnesses. Consequently, it is our belief that the weak point within the proposed calibration procedure is precisely the estimation of the unmeasured flows, which is currently done iteratively, using the information contained in the raw model. Whilst performing this calibration exercise, an alternative approach has emerged, which avoids the use of the raw model by estimating the unmeasured flows from the topology of the network. The basic idea is to relate the flow measurements with the co-tree "chords" of the network (i.e. the independent set of flows,

as defined in Chapter Two, section 2.3.7, Fig. 2.1), and to compute the rest of the flows (i.e. the dependent ones) directly from the flow measurements. However, this has yet to be tested

d) Calibrated Hazen-Williams roughnesses.

As summarised in Table 6.26 the success of the proposed calibration algorithm with respect to the roughnesses is relatively small, specially in comparison with the success in the piezometric heads.

We believe that, due to the rationale behind the proposed calibration algorithm (section 6.7 of this chapter), the best way to improve the calibrated roughnesses is by previously improving the estimation of the unmeasured flows. In theory, if we include more flow measurements, the performance of the calibration algorithm improves; in the extreme, if the estimation of heads and flows provides all the true nodal heads and pipe flows, the calibration algorithm is able to compute all the true pipe roughnesses. This holds irrespective of the initial roughnesses assumed in the raw model.

Additionally, and due to the fact that the head and flow estimation are carried out as independent processes, some consistency check should be implemented in the future, in order to detect situations where both estimates (heads and flows) are not reasonable for some pipes. For example, if for pipe joining nodes "i" and "j", the head estimator $H_i > H_j$ and the flow estimator gives a flow from node "j" to "i". A decision on which estimate to adopt could be based on the quality of the estimates

(when available). Undoubtedly, this should improve the performance of the calibration algorithm.

6.12. Concluding remarks.

A new computer-based water distribution network static calibration algorithm has been proposed, which is based on the estimation of unmeasured nodal piezometric heads and on the estimation of unmeasured pipe flows.

Three different piezometric head estimation techniques have been proposed and tested: a geostatistical interpolation procedure known as Kriging, a deterministic one-dimensional interpolation scheme and a third procedure based on a bi-cubic splines fitting.

For the flow estimation, the raw network model, obtained with initial estimates of the roughnesses, provides the estimates of the flows for the unmeasured pipes. Because those estimates, when merged with the flow measurements, are neither balanced nor compatible with head estimates, an iterative algorithm approximates those flow estimates to the true ones (as shown in Fig. 6.1.), also giving the estimates of the C's.

The results of systematic testing of the calibration algorithm, with a set of six examples, subjected to five different conditions, show that:

i) The best piezometric head estimator is the deterministic one-dimensional interpolation procedure.

ii) Following on from i), the calibration algorithm produces calibrated piezometric heads which follow closely the estimated head results, and which are superior to those produced using Kriging and bi-cubic splines.

iii) The calibrated flow results produced using the one-dimensional interpolation procedure for the estimation of unmeasured piezometric heads are better than those using Kriging and splines, but not good enough, and an alternative new approach for unmeasured pipe flow estimation has been suggested for future implementation.

In the case that with an alternative pipe flow estimation procedure an iterative calibration algorithm is still needed, like the one proposed in this work, the possibility of updating only the flows (by-passing the updating of the heads) in the gradient method should be explored. This could save considerable computer resources, since the head updating is the most computationally expensive step of the gradient algorithm.

iv) The calibrated roughnesses produced by the calibration algorithm do not seem to be fully satisfactory. This can be explained partly because the pipe flow estimation procedure produces flow estimates which are, in general, not fully satisfactory. The improvements suggested both for the nodal piezometric heads and pipe flow estimators should have a positive impact on the calibrated roughnesses.

To summarise, we believe that the proposed calibration algorithm has shown to be the adequate framework for solving the the water distribution static calibration problem, but clearly extra efforts should be made in the future to improve it. The deterministic one-dimensional interpolation procedure for unmeasured piezometric head estimation has been identified as the best piezometric head estimator. An alternative approach for pipe flow estimation is required for improving both the calibrated flows and roughnesses.

In our opinion, one of the main advantages of the proposed calibration algorithm, with the one-dimensional interpolation head interpolator, lies in the fact that it allows us to incorporate the physical and engineering knowledge of the network, existing prior to the calibration, thus breaking up the inherent ill-definition of the calibration problem. The ill-definition comes from the fact that, normally, there is insufficient measurement information to estimate reliably all the parameters.

Further intensive testing of the proposed algorithm and the suggested improvements should be carried out, with data from real networks.

Some effort should be made to estimate the estimation errors associated with the head estimates produced by the one-dimensional interpolation scheme, as well as errors in the flow estimates, in order to be able to produce an estimate of the error in the calibrated C's.

Some way of testing the quality of head and flow estimates, prior to the calibration process, should be devised, since there is no point in carrying on with the calibration when the head and flow estimates are not satisfactory.

The problem of the design of the piezometric head and flow measurement system has not been studied here, but the need for a rational measurement placement algorithm has became clear, as a pre-requisite for a successful calibration.

Also, the problems of bad data detection and replacement need to be addressed, particularly if the algorithm were to be used in telemetered networks in the future.

CHAPTER SEVEN

FURTHER EXTENSIONS OF THE GRADIENT METHOD

7.1. Introduction.

In this chapter we deal with some additional extensions to the gradient method, particularly an extended period simulation version of the program, which is useful, for example, in determining the best operating policy from a set of alternatives.

We also introduce in this chapter the latest extension of the gradient algorithm, which consists of modelling the nodal consumptions as a linear function of the pressures, thus providing a more realistic model for the demands. We re-derive the gradient algorithm for the new conditions, and we briefly discuss the implications that this approach can have for extended period simulation and calibration purposes

7.2. Extended period simulation version of the gradient method.

As a natural development of the gradient method, an extended period simulation algorithm has been implemented, which allows us to simulate the behaviour of a water distribution system over a period of 24-48 hours, for example.

As far as the simulation algorithm is concerned, the approach followed is fairly standard, since it follows approximately the same pattern as other simulation algorithms [Stephenson (1985), Coulbeck and Orr (1983), Rao and Bree (1977)]. The main objective

has been the study of the performance of the gradient method in such applications, particularly with some of the implementation features discussed in Chapter Five.

The program makes use of the output of a demand forecasting routine, with the total demand of the system discretised hour by hour, or in shorter periods if necessary. Demand forecasting has not been covered in the present work. The program computes the nodal demand, using the standard demand profiles (residential, commercial, industrial demands, etc.), and demand allocation data, which must be supplied by the user, together with the physical and topological data on the network.

The inflows at the reservoirs are also needed as input, with the corresponding geometrical data of each reservoir: level/volume relationship parameters, maximum and minimum levels, initial water levels, etc. The inflows can be input either as flows per hour or through profile curves associated with a reference maximum flow; thus, for gravitational sources (constant flow) only one flow is needed, while for pumped sources an on/off diagram with the maximum flow is enough.

Starting from a known initial state, represented by some nodal consumptions and reservoir levels, the problem is to model the variation of reservoir levels (or storage) with respect to time, due to the differences between network consumptions and inflows.

This is done by considering that, for each reservoir "i", the volume variation (denoted by the differential d Vol_i) in a time interval "dt" is equal to the difference between inflow (QIN_i)

and the outflow (Q_i), i.e.:

$$\frac{d\ Vol_i}{dt} = QIN_i - Q_i \qquad (1)$$

or

$$\frac{d\ h_i}{dt} = \frac{QIN_i - Q_i}{(d\ Vol_i / d\ h_i)} \qquad (2)$$

where h_i : is the water level at the reservoir "i".

On knowing the geometry of each reservoir, we can relate the volume with the water level, through a polynomial function as:

$$Vol_i = a_i\ h_i^2 + b_i\ h_i + c_i \qquad (3)$$

where a_i, b_i and c_i : are constants, dependent on the geometrical characteristics of the reservoir .

Hence, from (3), we get:

$$\frac{d\ Vol_i}{d\ h_i} = 2\ a_i\ h_i + b_i \qquad (4)$$

and the water level variation (2) is given by:

$$\frac{d\ h_i}{dt} = \frac{QIN_i - Q_i}{2a_i\ h_i + b_i} = f_i(t,\ h_i) \qquad (5)$$

For the particular case of a prismatic reservoir (cylindrical, rectangular, etc.) the coefficient $a_i = 0$ and b_i represents the transversal section, thus:

$$Vol_i = b_i\ h_i + c_i \qquad (6)$$

and

$$\frac{d\ Vol_i}{d\ h_i} = b_i \qquad (7)$$

which, when introduced into (2), gives:

$$\frac{d\,h_i}{dt} = \frac{QIN_i - Q_i}{b_i} = f_i(t,\ h_i) \qquad (8)$$

The problem now reduces to integrating equation (5), or equivalently, equation (8) for the case of prismatic reservoirs. Because (5) holds for each reservoir, the problem is actually to integrate a set of NS differential equations like (5).

On introducing the superscript "k" for identifying the time step, the water level variation in a finite time interval δt can be approximated as:

$$\frac{h_i(k+1) - h_i(k)}{\delta t} \approx f_i(t,\ h_i(k)) \qquad (9)$$

where the approximation holds because the right hand side should correspond to an average value of the function between time steps "k" and "k+1".

This approximation allows us to implement a simple integration scheme corresponding to Euler's integration method, which is, from (9), as follows:

$$h_i(k+1) \approx h_i(k) + \delta t\ f_i(t,\ h_i(k)) \qquad (10)$$

Because the analytic expression of the functions $f_i(t,h)$ are not known, the network analysis program is used to compute the reservoir outflows Q_i, thus allowing the values of the functions to be obtained.

The error in the approximation is relatively small, due to the fact that the function "f" depends on $QIN_i - Q_i$ and, as a result, oscillates between positive and negative values, thus allowing for error cancellation. In a small example with two reservoirs,

the error accumulated during a 24 hours simulation has been computed as 5.8 m^3, in a total inflow of 12,960 m^3, for a simulation with a time step of one hour. The error was defined as the difference between the total inflow, on the one hand, and the summation of the total consumption plus the storage variation, on the other hand. This shows that the error due to the simple integration scheme is not relevant for most practical purposes, though it can be reduced even further either by reducing the time step, or by including some more sophisticated integration scheme.

The main flow chart corresponding to the extended period simulation program is shown in Figure 7.1.

The present extended period simulation implementation should be taken as a first step towards a more complete simulation program, able to provide additional facilities such as: graphical output of user specified variables, variable time step, a more flexible nodal demand allocation scheme (possibly including the pressure-sensitive algorithm presented in the next section), different kinds of switches (pressure, water level and time switches). etc.

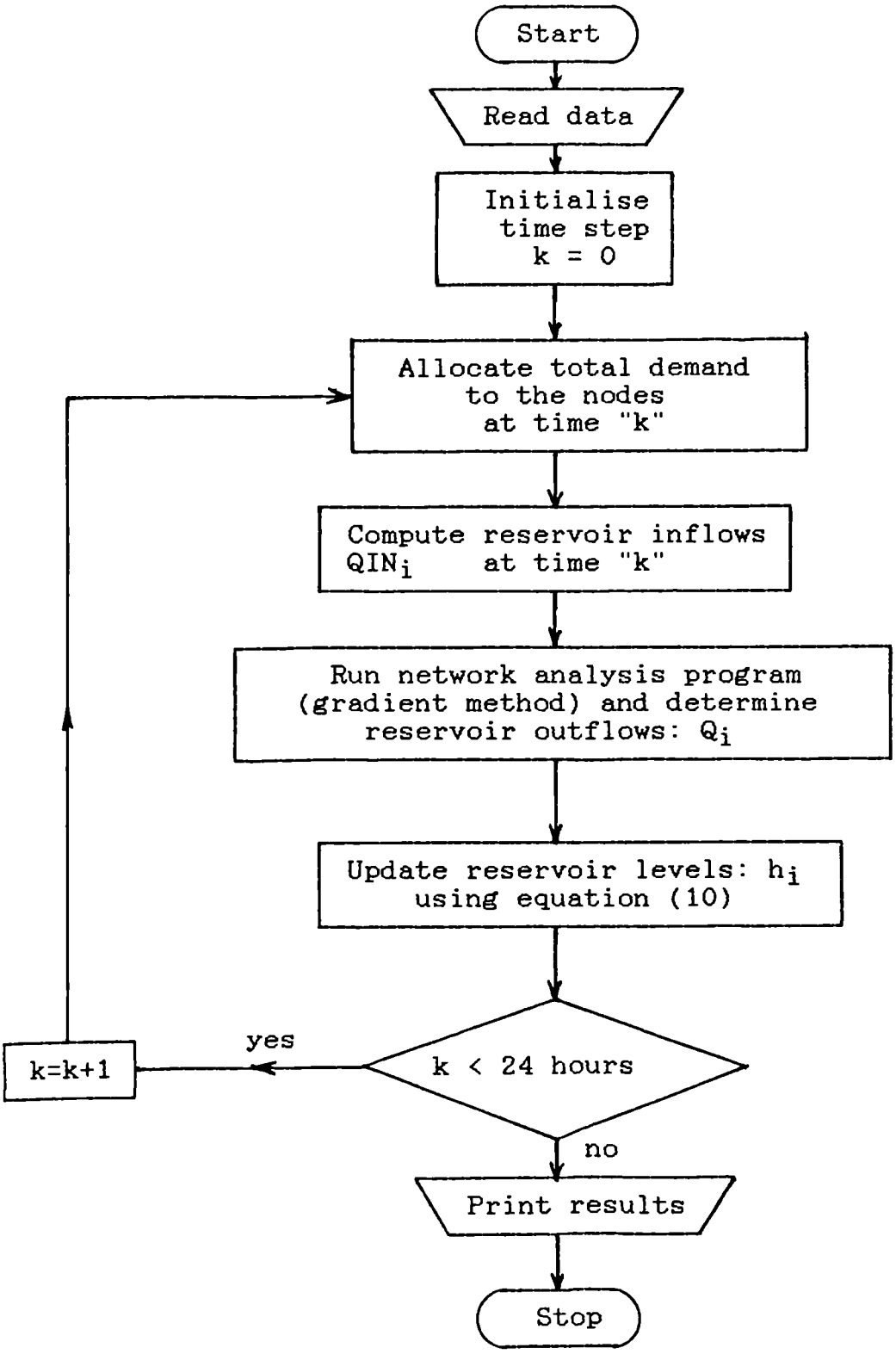

Fig. 7.1. Main flow chart of extended period simulation program.

7.3. Extending the gradient method for pressure-dependent nodal demands.

Practically all the authors in networks analysis, with the exceptions of Lam and Wolla (1972 a and b) and Bhave (1981), consider the nodal demands as independent of the pressure at the node. Thus, the nodal demands remain the same regardless of whether or not the pressure is very low or very high. It is a well known fact that the actual consumptions in the network are pressure-dependent. Indeed, most network operators reduce the pressures in order to cope with extreme demands. One of these cases is clearly the reduction of nocturnal pressures to reduce leakages.

Thus, we have to understand the traditional way of modelling the network demands as valid for a certain pressure range (i.e. around a nominal service pressure). For design purposes this assumption may be reasonable, because in that case we are interested in the behaviour of the system at a certain time horizon, where we have to assume that the pressure is at least at the nominal service level. Nevertheless, it seems that the assumption of a constant demand is not fully valid when studying the behaviour of the network during a period of, say, 24 hours, where the pressures at the nodes change over a wide range. The same might be true for calibration purposes, where we try to match the performance of the network model with that of the real network, under at least two extreme situations: very high and very low flows (i.e.: very low and very high pressures), to cover the widest spectrum of operational scenarios.

Lam and Wolla (1972 b) proposed a general model to include the influence of the pressures on the nodal demands:

$$q_i = a_i + b_i H_i^c \qquad (11)$$

where q_i : consumption at node "i".

H_i : piezometric heads at node "i".

a_i, b_i and c_i : appropriate constants.

Lam and Wolla's approach is close to the pressure/discharge relationship for irrigation emitters [see Karmeli et al. (1985)]:

$$q_i = k_i P_i^x \qquad (12)$$

where

P_i : emitter operating pressure.

k_i : characteristic coefficient of the emitter, dependent on the nozzle physical dimensions and form.

x : discharge exponent, dependent on the flow regime and pressure/discharge relationship of the emitter, with typical values of 0.4-0.6.

In general, all the parameters a_i, b_i and c_i in Lam and Wolla's relationship, and k_i and x in the emitter's case, have to be determined either by field testing or from manufacturers' data (emitters).

Bhave (1981) followed a completely different approach, establishing a discrete relationship between nodal demands and heads, and satisfying the demands if the heads are greater or equal to a minimum, the nodal outflow being zero otherwise. Bhave posed the problem in a constrained non-linear optimisation format, maximising the outflow. To solve the non-linearity, a

recurrent algorithm is used, based on the repetitive solution of a standard network analysis algorithm, verifying if the head at each node allows a given consumption to be satisfied.

We believe that the right way to approach the problem is through an explicit demand/head relationship, similar to that proposed by Lam and Wolla (1972 b), allowing the system itself to find the equilibrium point between the actual nodal outflow and pressure.

We are aware that this implies a completely different approach to the traditional network analysis problem, but it seems a much more realistic approach, in the sense that it is closer to what actually happens in a real network. Because of that, we expect that the results of using this approach in extended period simulation, or for calibration purposes, would be worthwhile, though this is something that should be fully investigated in the near future, using data from real networks.

The importance of pressure variations on the demands is fully recognised by Lonsdale (1985) who, upon using information published by the National Water Council (1980), showed that, instead of a theoretical relationship depending on the square root of the pressure (like in the irrigation emitter case) the discharges actually follow a slightly quadratic relationship, as shown in Figure 7.2, which may be well represented as a piecewise linear function, or via a simple linear relationship in the range of working pressures (say, between 25-60 m). As correctly pointed out by Lonsdale (1985), the difference is due to various reasons; first of all, in the case of leakages an increase in pressure

produces an increase in the size of the leaking cracks or holes, then the square-rooted model is no longer valid. The second reason deals with a more conceptual topic, connected with the way water consumption is actually carried out by the customers. There appears to be two different ways in which consumption occurs: first, on a volumetric basis, i.e.: we may need to fill a cup of tea or a bath, which produces a demand that is independent of pressure (the pressure only affecting the timing, or peak flow, but not the volume); the second consumption is on a time basis, i.e.: if we are taking a shower or washing a car, we consume more water if a high pressure is available in the system. Clearly, for the whole system, the water consumption increases with pressure.

We shall assume that a linear relationship between pressure and consumption is enough to describe the real demand/pressure behaviour of the system around the service pressure region. This relationship is shown in Figure 7.3, and is such that:

$$\underline{q} = \underline{q}_S - A_{22} \, (\, \underline{p} - \underline{p}_S \,) \qquad (13)$$

where

$\underline{q}$: pressure-dependent nodal demand, a (NN-NS)x1 column vector.

$\underline{q}_S$: demand at the service pressure ($\underline{p}_S$), a (NN-NS)x1 column vector. See Figure 7.3. This is equal to the demand when nodal consumption is assumed to be independent of pressure.

A_{22} : a diagonal (NN-NS)x(NN-NS) matrix of the sensitivities of the nodal demands with respect to changes in the pressures:

$$A_{22} = \text{diag} \, (-\partial q_i / \partial p_i) \quad , \; i=1,2,\ldots,NN-NS \qquad (14)$$

$\underline{p}$: pressure (NN-NS)x1 column vector, which is computed as:

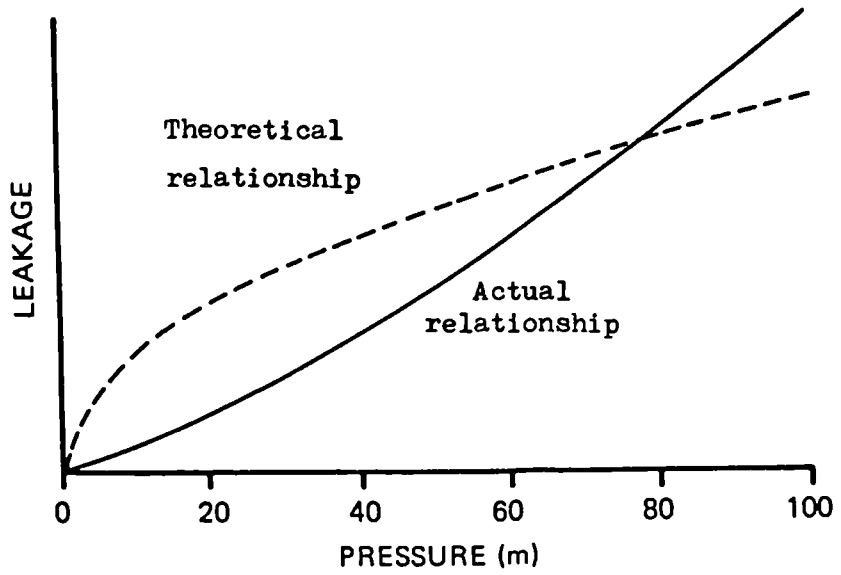

Fig. 7.2. The effect of pressure on leakages. From: National Water Council (1980).

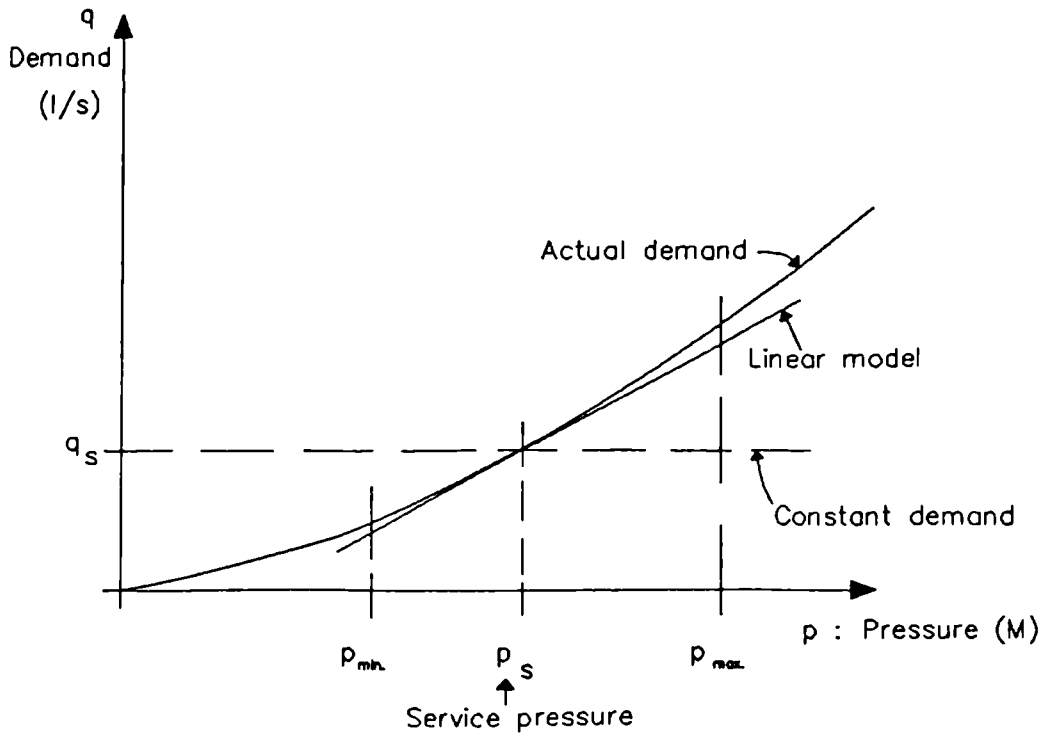

Fig. 7.3. Relationship between actual demand, pressure, adopted linear model and constant demand.

$$\underline{p} = \underline{H} - \underline{z} \qquad (15)$$

where:

$\underline{H}$: piezometric head (NN-NS)x1 column vector.

$\underline{z}$: ground level (NN-NS)x1 column vector, which is known from the topography of the system.

Note that, with this demand/pressure model, $\underline{q} = \underline{q}_S$ either when $A_{22}=0$ (demands are not dependent on pressure) or when the pressure is equal to the service pressure.

Upon introducing (15) into (13) we get:

$$\underline{q} = \underline{q}_S - A_{22}\,\underline{H} + A_{22}\,\underline{z} + A_{22}\,\underline{p}_S \qquad (16)$$

or

$$\underline{q} = \underline{q}_o - A_{22}\,\underline{H} \qquad (17)$$

with

$$\underline{q}_o = \underline{q}_S + A_{22}\,\underline{z} + A_{22}\,\underline{p}_S \qquad (18)$$

Other demand/pressure linear models are also possible, but all of them lead to a relationship like (17), only with a different definition for $\underline{q}_o$ (equation 18).

Then, recalling that the necessary conditions for the steady state flow in the network [see Chapter Three, equation (3)], for the constant demand case, are:

$$\left[\begin{array}{c:c} A_{11} & A_{12} \\ \hdashline A_{21} & 0 \end{array}\right] * \left[\begin{array}{c} \underline{Q} \\ \hline \underline{H} \end{array}\right] = \left[\begin{array}{c} -A_{10}\,\underline{H}_0 \\ \hline \underline{q} \end{array}\right]$$

and introducing the pressure-dependent nodal demands from (17), we get:

$$\left[\begin{array}{c:c} A_{11} & A_{12} \\ \hdashline A_{21} & A_{22} \end{array}\right] * \left[\begin{array}{c} \underline{Q} \\ \hline \underline{H} \end{array}\right] = \left[\begin{array}{c} -A_{10}\ \underline{H}_0 \\ \hline \underline{q}_0 \end{array}\right] \qquad (19)$$

We can now re-derive the gradient algorithm for the new conditions. In fact, on differentiating (19) and assuming that A_{22} does not depend either on the flows or on the heads, we get:

$$\left[\begin{array}{c:c} N\ A_{11}^* & A_{12} \\ \hdashline A_{21} & A_{22} \end{array}\right] * \left[\begin{array}{c} d\ \underline{Q} \\ \hline d\ \underline{H} \end{array}\right] = \left[\begin{array}{c} d\ \underline{E} \\ \hline d\ \underline{q} \end{array}\right] \qquad (20)$$

where, as before in the constant demand case:

$$A_{11}^* = \begin{bmatrix} \alpha_1 |Q_1|^{n1-1} & & & \\ & \alpha_2 |Q_2|^{n2-1} & & \\ & & \ddots & \\ & & & \alpha_{NP} |Q_{NP}|^{nNP-1} \end{bmatrix} = A_{11} - \begin{bmatrix} \beta_1/Q_1 & & & \\ & \beta_2/Q_2 & & \\ & & \ddots & \\ & & & \beta_{NP}/Q_{NP} \end{bmatrix}$$

where N = (NPxNP) diagonal matrix of the exponents "n" of the head loss-flow relationship.

In the right hand side of (20), $d\underline{E}$ represents the head imbalance at each branch, and the ((NN-NS)x1) vector $d\underline{q}$, represents the nodal imbalance which, at an iteration "i" when convergence has not yet been achieved , can be expressed as:

$$d\ \underline{E} = A_{11}^{(i)}\ \underline{Q}^{(i)} + A_{12}\ \underline{H}^{(i)} + A_{10}\ \underline{H}_0 \qquad (21)$$

and

$$d\ \underline{q} = A_{21}\ \underline{Q}^{(i)} + A_{22}\ \underline{H}^{(i)} - \underline{q}_0 \qquad (22)$$

The solution of (20), for the flow and head increments, can be obtained as:

$$\begin{bmatrix} d\,\underline{Q} \\ \hline d\,\underline{H} \end{bmatrix} = \left[\begin{array}{c|c} N\,A_{11}^{*} & A_{12} \\ \hline A_{21} & A_{22} \end{array}\right]^{-1} * \begin{bmatrix} d\,\underline{E} \\ \hline d\,\underline{q} \end{bmatrix} \qquad (23)$$

where A_{11}^{*} is evaluated at $\underline{Q}=\underline{Q}^{(i)}$.

The inverse of the partitioned matrix in (23) can be computed as another block-partitioned matrix:

$$\left[\begin{array}{c|c} N\,A_{11}^{*} & A_{12} \\ \hline A_{21} & A_{22} \end{array}\right]^{-1} = \left[\begin{array}{c|c} B_{11} & B_{12} \\ \hline B_{21} & B_{22} \end{array}\right] \qquad (24)$$

On defining:

$$G = N\,A_{11}^{*} \qquad (25)$$

the blocks of the inverse can be computed explicitly, according to Ayres (1974), we get:

$$\left.\begin{aligned} B_{11} &= G^{-1} + G^{-1}\,A_{12}\,(\,A_{22} - A_{21}\,G^{-1}\,A_{12}\,)^{-1}\,A_{21}\,G^{-1} \\ B_{22} &= (A_{22} - A_{21}\,G^{-1}\,A_{12})^{-1} \\ B_{12} &= -\,G^{-1}\,A_{12}\,(A_{22} - A_{21}\,G^{-1}\,A_{12})^{-1} \\ B_{21} &= -\,(A_{22} - A_{21}\,G^{-1}\,A_{12})^{-1}\,A_{21}\,G^{-1} \end{aligned}\right\} \qquad (26)$$

With the partitioning (24), the system (23) becomes:

$$\left.\begin{aligned} d\,\underline{Q} &= B_{11}\;d\underline{E} + B_{12}\;d\underline{q} \\ d\,\underline{H} &= B_{21}\;d\underline{E} + B_{22}\;d\underline{q} \end{aligned}\right\} \qquad (27)$$

which, when introducing equations (21) and (22), becomes:

$$d\,\underline{Q} = B_{11}[A_{11}\underline{Q}^{(i)}+A_{12}\underline{H}^{(i)}+A_{10}\underline{H}_0] + B_{12}[A_{21}\underline{Q}^{(i)}+A_{22}\underline{H}^{(i)}-\underline{q}_o] \qquad (28)$$

and

$$d\,\underline{H} = B_{21}[A_{11}\underline{Q}^{(i)}+A_{12}\underline{H}^{(i)}+A_{10}\underline{H}_0] + B_{22}[A_{21}\underline{Q}(i)+A_{22}\underline{H}(i)-\underline{q}_o] \quad (29)$$

introducing (26) into (29) and considering:

$$d\,\underline{Q} = \underline{Q}^{(i)} - \underline{Q}^{(i+1)} \quad (30)$$

and

$$d\,\underline{H} = \underline{H}^{(i)} - \underline{H}^{(i+1)} \quad (31)$$

we obtain, after some algebra:

$$\underline{H}^{(i+1)} = [A_{22} - A_{21}\,G^{-1}\,A_{12}]^{-1}\,\{\,A_{21}\,G^{-1}\,(A_{11}\,\underline{Q}^{(i)} + A_{10}\,\underline{H}_0) - (A_{21}\,\underline{Q}^{(i)} - \underline{q}_o)\,\} \quad (32)$$

and from (28):

$$\boxed{\underline{Q}^{(i+1)} = (I - G^{-1}\,A_{11})\,\underline{Q}^{(i)} - G^{-1}\,(\,A_{12}\,\underline{H}^{(i+1)} + A_{10}\,\underline{H}_0)} \quad (33)$$

Equation (32) can be re-ordered into the traditional format of a linear system of NN-NS equations in the unknown piezometric heads:

$$\boxed{[A_{21}\,G^{-1}A_{12}-A_{22}]\,\underline{H}^{(i+1)} = -\,\{\,A_{21}\,G^{-1}\,(A_{11}\,\underline{Q}^{(i)} + A_{10}\,\underline{H}_0) - (A_{21}\,\underline{Q}^{(i)} - \underline{q}_o)\,\}} \quad (34)$$

As in the case of the gradient method with constant demands [Chapter Three], equations (34) and (33) have to be solved recursively, in that order. The structure of the equations is nearly the same as before, except that now the matrix of coefficients of the linear system in $\underline{H}$ has its diagonal modified by A_{22} (the consumption sensitivity matrix) while in the right hand side the previous nodal demands $\underline{q}$ are now replaced by $\underline{q}_o$, as defined in equation (18) of the present chapter. Of course, when $A_{22}=0$, $\underline{q}_o = \underline{q}_s$ and we are in the previous case of demands being independent from the network pressures.

At the present time the computer implementation of this extended algorithm is under way, and its application for extended period simulation and calibration purposes has to be studied in the near future. In order to assess the real advantages of this approach, data from real systems will be required. The actual sensitivity of the demands with respect to pressure has to be determined through field tests, either at the level of the whole network (total demand versus average pressure) or by grouping nodes on a geographical basis.

CHAPTER EIGHT

SUMMARY, CONCLUSIONS AND FURTHER WORK

8.1. Summary.

The present work has been mainly concerned with the development and testing of a steady state network analysis algorithm, known as the gradient method, and with the development of a new automatic calibration procedure.

The gradient method, due to Todini (1979), has been extended in the present work to include pumps and pressure reducing and sustaining valves. Those pressure regulating devices have been modelled using an original physically-based method, which can be used as a framework for modelling other regulating valves in the future. Also, a generalised version of the gradient algorithm which considers the nodal demands as a linear function of the pressures has been introduced. An extended period simulation version of the gradient method has also been developed.

An extensive investigation has been carried out to find the best solver of the linear systems of equations generated by the gradient method, including direct and iterative methods.

An automatic calibration algorithm has been proposed which estimates the true pipe resistance parameters, based on estimates of the unmeasured nodal piezometric heads and unmeasured pipe flows. For estimating the unmeasured piezometric heads, three different methods have been proposed and compared: one based on

Kriging, another based on bi-cubic splines and a third based on an original deterministic one-dimensional interpolation procedure. For the estimation of the unmeasured flows, the raw (non-calibrated) network model has been used, based on initial estimates of the pipe roughnesses. The calibration algorithm has been tested with a set of 6 examples, subjected to five different measurement availability scenarios.

8.2. Conclusions.

As far as the development of the gradient method is concerned, the main conclusions are the following:

a) The original gradient method [Todini (1979), Pilati and Todini (1984)], has been extended to include pumps and pressure regulating valves. The extended algorithm is now able to handle most of the devices normally found in water distribution systems. A comparison with some of the best existing algorithms shows that the extended version of the gradient method is stable and efficient, and it can be recommended for modelling water distribution systems under the most demanding circumstances: for example, when the network becomes disconnected, when multiple pressure regulating valves are working simultaneously, in ill-conditioned examples, etc.

b) An original physically-based algorithm for modelling pressure regulating valves has been proposed, implemented and tested with several examples. The algorithm follows closely the physical behaviour of the regulating valves, modelling them as variable-resistance devices, thus being completely different in

comparison with most of the existing methods. A comparison with some examples found in the literature demonstrates that the proposed method is robust and, indeed, has allowed the detection of problems in the results published by other authors. The proposed approach for modelling regulating valves provides the appropriate framework for including other regulating devices in the near future. Other advantages of the algorithm are such that neither topological changes within the model nor re-assembly of the system of equations are needed, as in other existing methods. The matrix of coefficients of the linear system of equations remains symmetric, retaining the advantages of such matrices from the storage and stability point of view.

c) In order to improve the efficiency of the gradient method, which relies heavily on the successive solution of symmetric positive-definite linear systems of equations, an extensive investigation of its computational performance has been carried out, using seven of the most efficient linear solvers. A multifrontal linear solver has been identified as the fastest method when enough computer memory is available (routine MA27 of the Harwell Library); if storage is limited, a preconditioned (modified) conjugate gradient method is the recommended linear solver. A good compromise between memory and speed is represented by the one-way dissection method of George and Liu (1981). The current microcomputer implementation of the gradient method, using a 512 Kbytes RAM computer, allows the analysis of networks of up to 1,200 nodes with the preconditioned conjugate gradient linear solver, whereas the one-way dissection solver allows a

maximum of 1,000 nodes, though is four times faster than the version with the preconditioned conjugate gradient.

d) As a natural development, an extended period simulation version of the gradient method has been implemented, providing a framework for further work in this direction.

e) Finally, an attempt has been made to overcome one of the main limitations of present network analysis techniques, in the sense that most of them consider a constant nodal demand, irrespective of the pressures within the system. Indeed, a generalised version of the gradient method algorithm has been proposed, which incorporates explicitly the sensitivity of the nodal consumptions with respect to the pressures, the constant demand case being a particular case of this more general formulation.

As far as the development of an automatic calibration algorithm is concerned, the main conclusions are as follows:

a) A new automatic calibration procedure has been proposed and tested using synthetically generated data. The method relies on piezometric head and flow estimates to compute the pipe resistance parameters. The proposed calibration algorithm is such that it allows the incorporation of alternative piezometric head and flow estimators.

b) Three new alternative methods for estimating the unmeasured piezometric heads in the network have been proposed, implemented and compared. These methods are based on the application of Kriging, bi-cubic splines and an original one-dimensional

deterministic interpolation method. The results of such a comparison indicate that the deterministic one-dimensional interpolation method is the most appropriate one.

c) The iterative method proposed to estimate the unmeasured pipe flows does not give results which are as good as the head estimator and, as a consequence, the calibrated roughnesses obtained are far from the true ones, indicating that further work is needed. An alternative direct method, using the topological concepts of tree and co-tree, has been identified as a possible solution.

8.3. Further work.

The present work has meant the development of a number of algorithms and computer programs, covering the areas of network analysis, simulation and calibration. As is common in the development stages, and because the programs have been developed practically from scratch, there is an immediate need to re-write all of them having in mind their integration into a single water distribution network modelling program, using a modular structure both for programs and data files. Also, future developments in areas like optimum design, unsteady state flow and optimum operation should be borne in mind.

We also feel that an effort should be made in order to describe the basis and main features of the gradient method in the simplest possible terms, thus widening the spectrum of potential users, particularly engineers in the water industry. It is a

well-known fact that many engineers are not very keen on highly sophisticated mathematical developments and, unfortunately, this may be the case for the gradient method and its related techniques. It is quite natural for the users to avoid the application of methods which they cannot understand, and a bridge should be built between the present work and future potential users.

From the particular point of view of each application, the following work is envisaged in the near future:

8.2.1. Gradient method for network analysis.

a) Re-write the existing software in modular fashion, so that any other application can make use of it via a simple subroutine call. Although the arrival of new powerful microcomputers makes the memory requirements a less important issue, an effort should still be made in order to allow the integration of the gradient method with other applications by using the computational resources in the most efficient way. A single precision version of the program should be developed in order to reduce the memory requirements even further.

b) The generalised version of the gradient method, which allows the inter-dependence between nodal consumption and pressures to be considered explicitly, should be fully implemented and tested. Its convenience for extended period simulation and calibration should be fully investigated and assessed, ideally with data from real water distribution systems.

8.2.2 Calibration.

a) The calibration program should be integrated in the single network modelling program we have already referred to. At the moment the head estimator (the deterministic interpolation algorithm) is not integrated with the calibration program, and they should also be linked in the near future.

b) So far, we have relied on the network model itself to estimate unmeasured flows. This implies that the calibration procedure has to be carried out iteratively. An explicit flow estimation procedure would improve both the quality and the performance of the calibration procedure. One alternative, which has not been developed in the present work, is to use the graph-theory concepts of tree and co-tree of the network (see section 2.3.7., chapter 2, Figure 2.1), and to identify the flow measurements with the co-tree, so that the unmeasured flows (in the tree) can be determined explicitly, following a similar approach as that of Hamam and Brameller (1971), though with a different purpose. This might improve the quality of both flow and roughness estimates.

c) Further improvement in the performance of the piezometric head estimator (the deterministic one-dimensional interpolator) is possible. An iterative scheme, which involves re-computing the head estimates after the calibration algorithm has been run was suggested in Chapter 6 and should be implemented and tested in the future.

d) One of the assumptions made in the proposed calibration method is that the nodal consumptions are known. This hypothesis should be reviewed, particularly if the gradient algorithm incorporating pressure-sensitive demands proves to be relevant for calibration purposes. Eventually, some practical computer-assisted procedure for demand estimation and allocation should be developed. The possibility of an on-line demand estimation procedure should also be kept in mind.

e) We have suggested that techniques used for piezometric head estimation should be able to quantify the errors associated with the estimates. In this context, only Kriging and splines are able to produce this statistical information. Some way of handling this within the one-dimensional interpolation method should be devised. The same should be required for the flow estimates, thus allowing us to estimate the error in the estimated pipe resistance parameters.

f) Some validation procedure for the head and flow estimates should be devised, in order to decide whether the estimates are good enough to be used in the roughness calibration process, prior to the calibration itself. Also, some consistency check should be implemented, to avoid conflict between head and flow estimates.

g) The subject of the design of the measurement system (heads and flows) has not been explicitly tackled here. This subject is relevant, since in fact it is a pre-requisite for a successful calibration, therefore it has an impact on our final product, which is a calibrated model of the water distribution system.

Thus, it seems that something should be done in the future in this respect. Kriging provides a neat way of determining the benefit of an additional measurement within the system ,since the standard error of an estimate at any ungaged point in the domain is given, but further research is needed on this aspect.

REFERENCES

AJIZ M. A. AND JENNINGS A.: (1984), "A robust incomplete Choleski conjugate gradient algorithm", International Journal for Numerical Methods in Engineering, Vol. 20, pp. 949-966.

ALVAREZ C. AND ALBERTOS P.: (1982), " On-line observability determination as a further result of state estimation algorithms". IEEE Transactions on Power Apparatus and Systems, Vol. PAS-101, No.4,April.

ANTHONY G. T. AND COX M. G.: (1987a), "The fitting of extremely large data sets by bivariate splines", in Mason J.C. and Cox M.G. (Editors): (1987), "Algorithms for approximation", Clarendon Press, Oxford, 1987, pp. 5-20. Also NPL Report DITC 84/86.

ANTHONY G. T. AND COX M. G.: (1987b), "The National Physical Laboratory's data approximation subroutine library", in Mason J.C. and Cox M.G. (Editors): (1987), "Algorithms for approximation", Clarendon Press, Oxford, 1987, pp. 669-687. Also NPL Report DITC 71/86.

ARMSTRONG M. : (1984), "Improving the estimation and modelling of the variogram", in Verly G. et al. (Editors), "Geostatistics for natural resources characterization", Part 1, 1-19, 1984 by D. Reidel Pub. Co.

D'AURIAC A. (1947), "A propos de l'unicité de solution dans les problèmes de reseaux maillés", La Houille Blanche, Mai-Juin 1947, pp. 209-211.

AYRES F.: (1974), "Matrices", Schaum's outline series, McGraw Hill Book Co.

BARGIELA A.: (1985), "An algorithm for observability determination in water-system state estimation". IEE proceedings, Vol.132,Pt. D,No. 6, November, 1985.

BARLOW J. F. AND MARKLAND E.: (1969), "Computer analysis of pipe networks", Proc. Inst. Civ. Eng., 43, May-Aug 1969, pp. 249-259.

BARNETT S.: (1979), "Matrix methods for engineers and scientists", McGraw-Hill, London.

BARKER V. A. (Editor): (1977), "Sparse matrix techniques", Advanced course held at the Technical University of Denmark, Copenhagen, August 9-12,1976, Lecture Notes in Mathematics 572, Springer-Verlag, New York.

BATHE K. J.: (1982), "Finite elements procedures in engineering analysis", Prentice Hall

BHAVE P. R.: (1981), "Node flow analysis of water distribution systems", Transportation Engineering Journal, ASCE, Vol. 107, No. TE4, pp. 457-467.

BHAVE P. R.: (1988), "Calibrating water distribution network models", Journal of Environmental Engineering, ASCE, Vol. 114, No. 1,pp 120-136, February 1988.

BIRKHOFF G. and DIAZ J. B. (1955-1956), "Non-linear network problems", Quarterly of Applied Mathematics, 13, pp. 431-443.

de BOOR C.: (1978), "A practical guide to splines", Springer Verlag, New York.

BRANDON T. W. (Editor): (1984), "Water distribution systems", Water practice manuals, Vol. 4, compiled and published by the Institution of Water Engineers and Scientists, London, U. K.

BROUSSOLLE F.: (1978), "State estimation in power systems: detecting bad data through the sparse inverse matrix method", IEEE Transactions on Power Apparatus and Systems, Vol. PAS-97, No. 3.

BROYDEN C. G.: (1965), "A class of methods for solving non-linear simultaneous equations", Math. of Computations, pp. 577-593.

CARPENTIER P., COHEN G. AND HAMAM Y.: (1985), "Water network equilibrium. Variational approach and comparison of numerical algorithms", 7th Congress on Operational Research, Bologna, Italy.

CHANDRASHEKAR M. (1980): "Extended set of components in pipe networks", Journal of the Hydraulics Division, ASCE, Vol. 106, No. HY1, January 1980, pp. 133-152.

CHANDRASHEKAR M. AND STEWART K. H.: (1975), "Sparsity oriented analysis of large pipe networks", Journal of the Hydraulics Division, ASCE, Vol. 101, No. HY4, pp. 341-355.

CHAUDHRY M. H. AND YEVJEVICH V. (Editors), (1981): "Closed-conduit flow", Water Resources Publications, Colorado, USA.

CHEN D-Q. AND TEWARSON R. P.: (1986), "Use of incomplete decomposition of the coefficient matrix in solving linear equations", International Journal for Numerical Methods in Engineering, Vol. 23, pp. 199-208.

CHIN K. K., GAY R. K. L., CHINA S. H., CHAN C.H. AND YO S.Y.: (1978), "Solution of water networks by sparse matrix method", International Journal for Numerical Methods in Engineering, Vol. 12, pp. 1261-1277.

CLARKE D. A., MCBEAN E. A. AND AL-NASSRI S. A.: (1981), "Uncertainties in water distribution systems", Journal of Hydraulics Division, ASCE, Vol. 107, No. HY10, pp. 1263-1267.

CLEMENTS K.A., KRUMPHOLZ G.R. AND DAVIS P.W.: (1983), "Power system state estimation with measurement deficiency: an observability/measurement placement algorithm", IEEE Transactions on Power Apparatus and Systems, Vol. PAS-102,No. 7, July,1983.

COLLINS M. A.: (1980), "Pitfalls in pipe network analysis techniques", Transportation Engineering Journal, ASCE, Vol. 106, No. TE5, pp.507-521.

COLLINS M. A., COOPER L. AND KENNINGTON J. L.: (1977), "Analysis of hydraulic networks using minimization principles", Proc. 17th Congress International Association for Hydraulic Research, Baden-Baden, Vol. 5, pp. 241-248.

COLLINS M. A., COOPER L., HELGASON R., KENNINGTON J. AND LE BLANC 1. (1978), "Solving the pipe network analysis problem using optimization techniques", Management Science, 24, 7, pp. 747-760.

COLLINS M. A., COOPER L. AND KENNINGTON J. L. (1979), "Multiple operating points in complex pump networks", Journal of the Hydraulics Division, ASCE, Vol. 105, No. HY3, pp. 229-244.

COLLINS A. G. AND JOHNSON R. L.: (1975), "Finite-element method for water-distribution networks", Journal American Water Works Association, July 1975, pp. 385-389.

CORNISH R. J.: (1939-1940), "The analysis of flow in networks of pipes", Journal of the Institution of Civil Engineers, 13, pp. 147-154.

COULBECK B.: (1984), "A computer program for calibration of water distribution systems", Journal Institution of Water Engineers and Scientists, Vol. 38,NO.1,February 1984.

COULBECK B. AND ORR C. H.: (1983), " A network analysis and simulation program for water distribution systems", Research Report No. 31, Computer Control of Water Supply, Leicester Polytechnic.

COX M. G. : (1972), "The numerical evaluation of B-splines", J. Inst. Maths Applics (1972), 10, pp. 134-149.

COX M. G. : (1982a), "Direct versus iterative methods of solution for multivariate spline-fitting problems", IMA Journal of Numerical Analysis (1982), 2, pp. 73-81. Also NPL Report DNACS 37/80, October 1980.

COX M. G. : (1982b), "Practical spline approximation", NPL Report DITC 1/82, February 1982.

COX M. G. : (1986), "Data approximation and surface fitting", in Johnson M.W. (Editor): "Workshop on neutron scattering data analysis", Rutherford Appleton Laboratory, Chilton, 13-14

March, 1986, Institute of Physics Conference Series Number 81, Bristol, IOP Publishing Ltd., pp. 103-125. Also NPL Report DITC 81/86.

COX M. G. : (1987a), "Data approximation by splines in one and two independent variables", in Iserles A. and Powell M.J.D. (Editors): "The state of the art in Numerical Analysis", Oxford University Press, 1987. Also NPL Report DITC 77/86, October 1986.

COX M. G. : (1987b), "The NPL data approximation subroutine library: current and planned facilities", NPL Report DITC 104/87, November 1987.

COX M. G., HARRIS P. M. AND JONES H. M. : (1987), "Strategies for knot placement in least squares data fitting by splines", NPL Report DITC 101/87, September, 1987.

COX M. G. AND HAYES J. G.: (1973), "Curve fitting: a guide and suite of algorithms for the non-specialist user", NPL Report NAC 26, December 1973.

CRABBE R., CREASEY J. D., FIELD D. B., LACEY R. F. AND STIMSON K. : (1982), "A guide to water network analysis and the WRC computer program WATNET, Part I", Technical Report TR 177, Water Research Centre (WRC), WRC Engineering Centre, Swindon, U. K.

CROSS H. (1936), "Analysis of flow in networks of conduits or conductors", Bulletin No. 286, University of Illinois, Engineering Experimental Station, Urbana, Illinois.

DELFINER P. AND DELHOMME J.P. : (1973), "Optimum interpolation by Kriging", in Davis J.C. and McCullagh M.J. (Editors): "Display and analysis of spatial data", NATO ASI, Nottingham 1973, published by John Wiley and Sons, 1975.

DELFINER P. : (1976), "Linear estimation of nonstationary spatial phenomena", in Guarascio M., David M. and Huijbregts C. (Editors): "Advanced geostatistics in the mining industry", pp. 49-68, D. Reidel, Hingham, Mass., 1976.

DELHOMME J. P. : (1978), "Kriging in the hydrosciences", Advances in water resources, Vol. 1, No. 5, 1978

DELHOMME J. P. : (1979), "Spatial variability and uncertainty in groundwater flow parameters: a geostatistical approach", Water Resources Research, Vol. 5, No. 2, pp. 269-280, April, 1979.

DEO N.: (1974), "Graph theory with applications to engineering and computer science", Prentice Hall.

DILLINGHAM J. H.: (1967), Computer analysis of water distribution systems, part 2", Water and Sewage Works, 114, 2, pp. 43-45

DONACHIE R. P.: (1974), "Digital program for water network analysis", Journal of the Hydraulics Division, ASCE, Vol. 100, No. HY3.

DUBIN Ch.: (1947), "Le calcul des réseaux maillés. Contribution à l'application pratique de la Méthode Hardy Cross", La Houille Blanche, Mai-Juin 1947, pp. 213-227.

DUFF I. S.: (1980), "Recent developments in the solution of large sparse linear equations", Report No. CSS 80, Computer Science and Systems Division, AERE Harwell, Oxfordshire.

DUFF I. S. (Editor): (1981), "Sparse matrices and their uses", Academic Press.

DUFF I. S.: (1983), "Direct methods for solving sparse systems of linear equations", Report No. CSS 131, Computer Science and Systems Division, AERE Harwell, Oxfordshire.

DUFF I. S.: (1985), "Comments on the solution of sparse linear equations", Report No. CSS 190, Computer Science and Systems Division, AERE Harwell, Oxfordshire.

DUFF I. S., GOULD N. I. M., LESCRENIER M. AND REID J. K. : (1987), "The multifrontal method in a parallel environment", Report No. CSS 211, Computer Science and Systems Division, AERE Harwell Laboratory, Oxfordshire.

DUFF I. S. AND REID J. K.: (1976), "A comparison of some methods for the solution of sparse overdetermined systems of linear equations", Journal IMA, 17, pp. 276-280.

DUFF I. AND REID J. K.: (1978), "Algorithm 529. Permutation to block triangular form", ACM Transactions Mathematical Software, 4, pp. 189-192.

DUFF I. S. AND REID J. K.: (1982 a), "The multifrontal solution of indefinite sparse symmetric linear systems", Report No. CSS 122, Computer Science and Systems Division", AERE Harwell Laboratory, Oxfordshire.

DUFF I. S. AND REID J. K.: (1982 b), "MA 27 - A set of Fortran subroutines for solving sparse symmetric sets of linear equations", Report No. R-10533, AERE Harwell Laboratory, Oxfordshire.

DUFF I., ERISMAN A. M. AND REID J. K. : (1986), "Direct methods for sparse matrices", Oxford University Press, London.

DUPUIS P., ROBERT J. L. AND OUELLET Y.: (1987), "A modified method for pipe network analysis", Journal of Hydraulic Research, Vol. 25, No.1, pp. 27-40.

EISENSTAT S. C., GURSKY M. C., SCHULTZ M. H. AND SHERMAN A. H.: (1982), "Yale sparse matrix package. 1: The symmetric codes", International Journal of Numerical Methods in Engineering, 18,

pp. 1145-1151.

EPP R. AND FOWLER A. G.: (1970),"Efficient code for steady-state flows in networks", Journal of the Hydraulics Division, ASCE, Vol. 96, No. HY1, pp. 43-56.

EPP R. AND FOWLER A. G.: (1971),closure of discussions to Epp and Fowler: (1970),"Efficient code for steady-state flows in networks", Journal of the Hydraulics Division, ASCE, Vol. 97, No. HY7, p. 1131.

EVANS D. J. (Editor): (1983), "Preconditioning methods: theory and applications", Gordon and Breach, New York.

EVANS D. J. (Editor): (1985), "Sparsity and its applications", Cambridge University Press.

FEATHERSTONE R. E. : (1983), "Computational methods in the analysis and design of closed conduit hydraulic systems", in Novak P. (Editor): "Developments in Hydraulic Engineering-1", Elsevier Applied Science Publisher.

FIETZ T. R.: (1973), discussion to Wood and Charles (1972): "Hydraulic network analysis using linear theory", Journal of the Hydraulics Division, ASCE, Vol. 99, No. HY5, pp. 855-857.

FOX J. A. AND KEECH A. E.: (1975), "Pipe network analysis-A novel steady state technique", Journal of the Institution of Water Engineers and Scientists, 29, pp. 183-194.

GAMBOLATTI G. : (1980), "Fast solution to finite element flow equations by Newton iteration and modified conjugate gradient method", International Journal for Numerical Methods in Engineering, Vol. 15, pp. 661-675.

GAMBOLATTI G. AND PERDON A.: (1984), "The conjugate gradients in subsurface flow and land subsidence modelling" pp. 955-984 in Bear and Corapcioglu (Editors): "Fundamentals of transport phenomena in porous media", Martinus Nijhoff Pub., 1984. NATO ASI Series E, No. 82.

GAY R. K. L.,CHIN K. K., CHUA S. H., CHAN C. H. AND HO S. Y.: (1978), "Node reordering algorithms for water network analysis", International Journal of Numerical Methods in Engineering, Vol. 12, pp. 1241-1259.

GELB A. (Editor) : (1974), "Applied optimal estimation", MIT Press.

GEORGE A.: (1981), "Direct solution of sparse positive definite systems: some basic ideas and open problems", in Duff I. S. (Editor), "Sparse matrices and their uses", Academic Press.

GEORGE A., HEATH M. T. AND NG E.: (1984), "Solution of a sparse underdetermined system of linear equations", SIAM J. Sci. & Stat. Comput., Vol. 5, No. 4, pp. 988-997.

GEORGE A. AND LIU J. W-H.: (1981), "Computer solution of large sparse positive definite systems", Prentice Hall.

GESSLER J. (1981): "Analysis of pipe networks", Chapter 4 in Chaudhry and Yevjevich (1981).

GILMAN H. D., GOODMAN M. Y. AND de MOYER R. : (1973), "Replication modeling for water distribution control", Journal American Water Works Association, April 1973, pp. 255-260.

GLENFIELD & KENNEDY LTD.: "Pressure and flow control valves", Publication No. 215/R3.

GOLUB G. H. AND VAN LOAN C. F.: (1983), "Matrix computations", North Oxford Academic Pub. Co. Ltd., U. K., (The Johns Hopkins University Press).

HALL M. A.: (1976), "Hydraulic network analysis using (generalized) geometric programming", Networks, Vol. 6, pp. 105-130.

HAMAM Y. M. AND BRAMELLER A.: (1971), "Hybrid method for the solution of piping networks", Proceedings Institution of Electrical Engineers, Vol. 118, No. 11.

HAMBERG D. AND SHAMIR U. : (1988 a), "Schematic models for distribution systems design. I: Combination concept", Journal of Water Resources Planning and Management, ASCE, Vol. 114, No. 2, pp. 129-140, March 1988 .

HAMBERG D. AND SHAMIR U. : (1988 b), "Schematic models for distribution systems design. II: Continuum approach", Journal of Water Resources Planning and Management, ASCE, Vol. 114, No. 2, pp. 141-162, March 1988 .

HARARY F.: (1972), "Graph Theory", Addison Wesley, Third Edition.

HARRIS B. (Editor): (1970), "Graph theory and its applications", Academic Press.

HARRISON C. : (1988), "Water system demand estimates based on meter book subtotals", International Symposium on Computer Modeling of Water Distribution Systems, University of Kentucky, Lexington, May 12-13, 1988.

HAYES J. G. AND HALLIDAY J.: (1974), "The least-squares fitting of cubic spline surfaces to general data sets", J. Inst. Maths Applics (1974), 14, pp. 89-103.

HESTENES M. R. AND STIEFEL E.: (1952), "Methods of conjugate gradients for solving linear systems", National Bureau of Standards J. Res., 49, (1952), 409-436.

HOEKSEMA R. J. AND KITANIDIS P. K. : (1984), "An application of

the geostatistical approach to the inverse problem in two-dimensional groundwater modeling ", Water Resources Research, Vol. 20, No. 7, pp. 1003-1020, July 1984.

HOEKSEMA R. J. AND KITANIDIS P. K. : (1985), "Analysis of the spatial structure of properties of selected aquifers ", Water Resources Research, Vol. 21, No. 4, pp. 563-572, April 1985.

HUGHES J. P. AND LETTENMAIER D. P. : (1981), "Data requirements for Kriging: Estimation and network design", Water Resources Research, Vol. 17, No. 6., pp. 1641-1650, December 1981.

HUIJBREGTS C.J. : (1973), "Regionalized variables and quantitative analysis of spatial data", in Davis J.C. and McCullagh M.J. (Editors): "Display and analysis of spatial data", NATO ASI, Nottingham 1973, published by John Wiley and Sons, 1975.

IDA N. AND LORD W. : (1984), "Solution of linear equations for small computer systems", International Journal of Numerical Methods in Engineering, Vol. 20, pp.625-641.

IRONS B. M.: (1970) , "A frontal solution program for finite element analysis", International Journal for Numerical Methods in Engineering, Vol. 2, pp. 5-32.

ISAACS L. T. AND MILLS K. G.: (1980), "Linear theory methods for pipe networks", Journal of the Hydraulics Division, ASCE, Vol. 106, No. HY1.

JACKSON C. P. AND ROBINSON P. C. : (1985), "A numerical study of various algorithms related to the preconditioned conjugate gradient method", International Journal for Numerical Methods in Engineering, Vol. 21, pp. 1315-1338.

JENNINGS A. : (1977), "Matrix computations for engineers and scientists", John Wiley and Sons Ltd.

JENNINGS A.: (1971), "Accelerating the convergence of matrix iterative processes", J. Inst. Math. Appln., 8, 99-110.

JENNINGS A. AND MALIK G. M.: (1978), "The solution of sparse linear equations by the conjugate gradient method". International Journal for Numerical Methods in Engineering, Vol. 12, pp. 141-158.

JEPPSON R. W.: (1976), "Analysis of flow in pipe networks", Ann Arbor Science Pub.

JEPPSON R. W. AND DAVIS A. L. (1976): "Pressure reducing valves in pipe network analysis", Journal of the Hydraulics Division, ASCE, Vol. 102, No. HY7, July 1976, pp. 987-1001.

JEPPSON R. W. AND TAVALLAEE A.: (1975), "Pumps and reservoirs in networks by linear theory", Technical Note, Journal of the Hydraulics Division, ASCE, Vol.101, No. HY3, pp. 576-580.

KARMELI D., PERI G. AND TODES M.: (1985), "Irrigation systems design and operation", Oxford University Press, Cape Town.

KERSHAW D.: (1978), "The incomplete Cholesky-Conjugate gradient method for the iterative solution of systems of linear equations", Journal of Computational Physics, 26, pp. 43-65.

KESAVAN H. K. AND CHANDRASHEKAR M.: (1972), "Graph-theoretic models for pipe network analysis", Journal of the Hydraulics Division, ASCE, Vol. 98, No. HY2, pp. 345-364.

KING I. O.: (1970), discussion to Epp and Fowler: (1970),"Efficient code for steady-state flows in networks", Journal of the Hydraulics Division, ASCE, Vol. 96, No. HY11, pp. 2379-2380.

KITANIDIS P. K. AND VOMVORIS E. G. : (1983), "A geostatistical approach to the inverse problem in groundwater modeling (steady state) and one-dimensional simulations", Water Resources Research, Vol. 19, No. 3, pp. 677-690, June 1983.

KRUMPHOLZ G.R., CLEMENTS K.A. AND DAVIS P.W.: (1980), "Power system observability: a practical algorithm using network topology", IEEE transactions on Power Apparatus and Systems, Vol. PAS-99, No. 4, July/August 1980.

LAINIOTIS D. G. AND DESPHANTE J. G.: (1974), "Parameter estimation using splines", in Lainiotis D. G. (Editor): "Estimation theory", American Elsevier, pp. 101-125.

LAM C. F. AND WOLLA M. L.: (1972a), "Computer analysis of water distribution systems: Part I - Formulation of equations", Journal of the Hydraulics Division, ASCE, Vol. 98, No. HY2, pp. 335-344.

LAM C. F. AND WOLLA M. L.: (1972b), "Computer analysis of water distribution systems: Part II - Numerical solution", Journal of the Hydraulics Division, ASCE, Vol. 98, No. HY3, pp. 447-460.

LANSEY K. E.: (1988), " A procedure for water distribution network calibration considering multiple loading conditions", International Symposium on Computer Modeling of Water Distribution Systems, University of Kentucky, Lexington, May 12-13, 1988.

LEKANE TH. (1979): "Modèle de calcul de l'écoulement en régime permanent dans un réseau d'eau maillé", Journal of Hydraulic Research, 17, (1979), No. 2, pp. 149-163.

LEMIEUX P.: (1972), "Efficient algorithm for distribution networks", Journal of the Hydraulics Division, ASCE, Vol. 98, No. HY11, p. 1911.

LEWIS J. G. : (1977), "Algorithms for sparse matrix eigenvalue problems", Computer Science Department, Stanford University Report STAN-CS-77-595.

LIU K. T. H.: (1969). "The numerical analysis of water supply networks by digital computers", Proc. 13-th Congress of IAHR, Vol. 1, Subject A, pp. 25-42.

LIVESLEY R. K. : (1983), "Finite elements: an introduction for engineers", Cambridge University Press, Cambridge.

LO K.L., ONG P.S., McCOLL R.D., MOFFATT A.M. AND SULLEY J.L.: (1983 a), "Development of a static state estimator. Part I: Estimation and bad data suppression", IEEE Transactions on Power Apparatus and Systems, Vol. PAS-102, No. 8,pp. 2486-2491, August, 1983.

LO K.L., ONG P.S., McCOLL R.D., MOFFATT A.M. AND SULLEY J.L.: (1983 b), "Development of a static state estimator. Part II: Bad data replacement and generation of pseudomeasurements", IEEE Transactions on Power Apparatus and Systems, Vol. PAS-102, No. 8, pp. 2492-2500, August, 1983.

LONSDALE P. B.: (1985), "Automatic control of pressure in distribution systems", The Water Officers' Journal, January, pp. 34-44.

MARKOWITZ H. M. (1957), "The elimination form of the inverse and its application to linear programming", Management Science, 3, pp. 255-269.

de MARSILY G. : (1986), "Quantitative hydrogeology. Groundwater hydrology for engineers", Academic Press, 1986. Enlarged and translated from the original french edition entitled "Hydrogéologie quantitative", Masson, Paris, 1981.

MARTIN D. W. AND PETERS G.: (1963), "The application of Newton's method to network analysis by digital computer", Journal Institution of Water Engineers and Scientists, p. 115.

McCORMICK M.: (1969), discussion to Shamir and Howard (1968): "Water distribution system analysis", Journal of the Hydraulics Division, ASCE, Vol. 95, No. HY1, pp.481-483.

McCORMICK M. AND BELLAMY B. E.: (1968), "A computer program for the analysis of networks of pipes and pumps", J. Instn. Engrs. Aust., 38, 3, pp. 51-58.

MEIJERINK J. A. AND VAN DER VORST H. A. : (1977), "An iterative solution method for linear systems of which the coefficient matrix is symmetric M-matrix", Math. Comp., pp. 148-162.

MILLAR W. (1951), "Some general theorems for non-linear systems possessing resistance", Phil. Mag. (Ser. 7), Vol. 42, pp.1150-1160.

MONTICELLI A. AND WU F.F.: (1985), "Network observability: identification of observable islands and measurement placement". IEEE transactions on Power Apparatus and Systems, Vol. PAS-104, No. 5, May 1985.

MONTICELLI A. AND WU F.F.: (1985), "Network observability : Theory". IEEE transactions on Power Apparatus and Systems, Vol. PAS-104, No.5, May 1985.

de MOYER R.: (1973), "A statistical approach to modeling and control of water distribution systems", Ph.D. Dissertation, Polytechnic Institute of New York, Brooklin,N.Y.,1973.

de MOYER R. AND HORWITZ L. B.: (1975), "A system approach to water distribution modeling and control", Lexington Books.

MUNKSGAARD N. : (1980), "Solving sparse symmetric sets of linear equations by preconditioned conjugate gradients", ACM Transactions on Mathematical Software, Vol. 6, No. 2, pp. 206-219.

NAHAVANDI A. N. AND CATANZARO G. V.: (1973), "Matrix methods for the analysis of hydraulic networks", Journal of the Hydraulics Division, ASCE, Vol. 99, No. HY1, pp. 47-63.

NATIONAL WATER COUNCIL (1980), "Leakage control policy and practice", Department of Environment Standing Technical Committee, Report 26, reprinted by the Water Authorities Association, London, 1985.

de NEUFVILLE R. AND HESTER J.: (1969), Discussion of " Water distribution system analysis" of Shamir and Howard (1968), Journal of the Hydraulics Division, ASCE, Vol. 95, No. HY1.

NIESSNER H. AND REICHERT K.: (1983), "On computing the inverse of a sparse matrix", International Journal for Numerical Methods in Engineering, Vol. 19, No. 10, pp. 1513-1526.

O'CONNELL P. E. (Editor): (1977), "Real Time Forecasting and Control", Proceedings of the First International Workshop held at the Institute of Hydrology, July 4-29, 1977, Wallinford, England.

O'NEIL P. V. : (1983), "Advanced engineering mathematics", Woodsworth Pub. Co.

OGBUOBIRI E. C.: (1970), "Dynamic storage and retrieval in sparsity programming", IEEE Trans. on Power Apparatus and Systems, Vol. PAS-89, NO. 1, pp. 150-155

OGBUOBIRI E. C., TINNEY W. F. AND WALKER J. W. : (1970), "Sparsity directed decomposition for Gaussian elimination on matrices", IEEE Trans. on Power Apparatus and Systems, Vol. PAS-89, NO. 1, pp. 141-150.

ORMSBEE L.E. AND WOOD D.J.: (1986), "Explicit pipe network calibration", Journal of Water Resources Planning and Management, ASCE, Vol.112, No. 2, April 1986. pp 166-182.

ORMSBEE L. E. AND CHASE D. V.: (1988), "Hydraulic network calibration using nonlinear programming", International Symposium on Computer Modeling of Water Distribution Systems, University of Kentucky, Lexington, May 12-13, 1988.

ORTEGA J. M. AND POOLE W. G.: (1981), "An introduction to numerical methods for differential equations", Pitman.

OSTERBY O. AND ZLATEV Z. : (1983), "Direct methods for sparse matrices", Lecture notes in computer science, 157, Springer-Verlag.

PARLETT B. N.: (1980), "A new look at the Lanczos algorithm for solving symmetric systems of linear equations", Linear Algebra and its Applications, 29, pp. 323-346.

PENROSE R.: (1955), "A generalized inverse for matrices", Proc. Cambridge Philosophical Society, 51, 406-413 (1955).

PILATI S. and TODINI E . (1984), "La verifica delle reti idrauliche in pressione", Istituto di Costruzioni Idrauliche, Facolta D'Ingegneria dell'Universita di Bologna. (in italian).

PISSANETZKY S. : (1984), "Sparse matrix technology", Academic Press.

PITCHAI R.: (1966), "A model for designing water distribution pipe networks", Ph. D. Thesis Harvard University, Cambridge, Mass.

PRESS W. H., FLANNERY B. P., TEUKOLSKY S. A. AND VETTERLING W. T.: (1986), "Numerical Recipes. The art of scientific computing", Cambridge University Press.

RAHAL C.M., STERLING M.J.H. : (1981), "Dynamic parameter tunning for water distribution network models in an extended period simulation". Proc. Instn. Civ. Engrs.,71,2,March, 1981,pp 151-164.

RAHAL C.M., STERLING M.J.H. AND COULBECK B.: (1980), "Parameter tunning for simulation models of water distribution networks", Proc. Instn. Civ. Engrs., September 1980, pp 751-762.

RAO C. R. : (1962), "A note on a generalized inverse of a matrix with applications to problems in mathematical statistics", Journal Royal Statistical Society, Series B, Vol. 24, No. 1, pp. 152-158.

RAO H. S. AND BREE D. W.: (1977), "Extended period simulation of water systems - Part A", Journal of the Hydraulics Division, ASCE, Vol. 103, No. HY2, pp. 97-108.

RATCLIFFE B.: (1986), "The performance and selection of pressure reducing valves", Technical Report TR 238, WRC Engineering Centre.

REID J. K.(Editor) : (1971), "Large sparse sets of linear equations", Academic Press

REID J. K. : (1971), "On the method of conjugate gradients for the solution of large sparse systems of linear equations", in Reid J. K. (Ed.): "Large sparse sets of linear equations", Academic Press

REID J. K. : (1981), "Frontal methods for solving finite-element systems of linear equations", in Duff I. S. (Editor): "Sparse matrices and their uses" , Academic Press.

REID J. K.: (1976), "Sparse matrices",in Jacobs D. (Editor), "The state of the art in Numerical Analysis", Proc. of the Conference on the State of the Art in Numerical Analysis, held at the Univ. of York, 12- 15 April 1976, Academic Press,1977.

REID J. K.: (1986), "Sparse matrices", Report No. CSS 201, Computer Science and Systems Division, Harwell Laboratory, Oxfordshire.

RUHE A. : (1977), "Computation of eigenvalues and eigenvectors", in Barker V. A. (Editor): "Sparse matrix techniques".

RUUS E. (1981): "Head losses", Chapter 2 in Chaudhry and Yevjevich (1981).

SAMUELSSON A., WIBERG N. E. AND BERNSPANG L.: (1986), "A study of the efficiency of iterative methods for linear problems in structural mechanics", International Journal for Numerical Methods in Engineering, Vol. 22, pp. 209-218.

SARTORETTO F.: (1984), "A modified conjugate gradient method for the solution of sparse linear systems on microcomputers", Engineering Software for microcomputers. Proc. of the first International Conference, Venice, Italy, 2-5 April 1984, pp. 325-333. Riveridge Press, Swansea.

SCOTT D. S. : (1981), "The Lanczos algorithm", in Duff I. S. (Editor): "Sparse matrices and their applications".

SHAMIR U.: (1973), "Water distribution system analysis", IBM Research Report RC 4389, Yorktown Heights, N. Y., June 1973.

SHAMIR U.: (1974), "Optimal design and operation of water distribution systems", Water Resources Research, 10:1:27-36

SHAMIR U. AND HOWARD C. D. D.: (1968), "Water distribution systems analysis", Journal of the Hydraulics Division, ASCE, Vol. 94, No. HY1, pp. 219-234.

SHERMAN A. H.: (1975), "On the efficient solution of sparse linear and non-linear equations", Report 46, Ph. D. Thesis, Department of Computer Science, Yale University.

SHIMAUCHI S., TABATA A. AND SHINOMIYA F.: (1985), "Distribution network control for water supply systems", Instrumentation and control of water and wastewater treatment and transport systems, Proc. 4th IAWPRC Workshop, Houston, Denver USA, 1985.

SMITH D. K.: (1982), "Network optimisation practice: a computational guide", Ellis Horwood, Chichester, England.

SONG C.C.S. AND YANG C.T. (1980), "Minimum stream power: theory", Journal of the Hydraulics Division, ASCE, Vol. 106, No. HY9, pp. 1477-1487.

SONG C.C.S. AND YANG C.T. (1982), "Minimum energy and energy dissipation rate", Journal of the Hydraulics Division, ASCE, Vol. 108, No. HY5, pp. 690-706.

STEPHENSON D. (1985), "Continuous simulation of flow in pipe networks", Aqua, No. 5, pp. 258-262.

STEWART G. W.: (1973), "Introduction to matrix computations", Academic Press.

STIMSON K. : (1982a), "A guide to water network analysis and the WRC computer program WATNET. Part 2 -The interactive version", Technical Report TR 177 Part 2, WRC Engineering Centre.

STIMSON K. : (1982b), "A guide to water network analysis and the WRC computer program WATNET. Part 3 - The interactive graphics version", Technical Report TR 177 Part 3, WRC Engineering Centre.

STIMSON K. AND BRAMELLER A.: (1981), "An integrated mesh-modal method for steady state water distribution network analysis", Journal of the Institution of Water Engineers and Scientists, 35, 2, p. 186. (full text paper).

STOER J. AND BULIRSH R. : (1980), "Introduction to Numerical Analysis", Springer Verlag, New York.

TEWARSON R. P. : (1973), "Sparse matrix", Academic Press.

THOMAS P. D. AND BROWN R. A. : (1987), "LU decomposition of matrices with augmented dense constraints", International Journal for Numerical Methods in Engineering, Vol. 24, pp. 1451-1459.

TINNEY W. F. AND WALKER J. W. : (1967), "Direct solutions of sparse network equations by optimally ordered triangular factorization", Proc. IEEE, Vol. 55, pp. 1801-1809, November 1967.

TODINI E. (1979), "Un metodo del gradiente per la verifica delle

reti idrauliche", Bolletino degli Ingegneri della Toscana, No. 11 , pp. 11-14 (in italian).

TODINI E. AND PILATI S. : (1987), "A gradient algorithm for the analysis of pipe networks", Proceedings International Conference on Computer Applications for Water Supply and Distribution, Leicester Polytechnic, 8-10 September.

VAN DER VORST H. A. : (1981), "Iterative solution methods for certain sparse linear system with a non-symmetric matrix arising from PDE-problems", J. Comp. Phys., 44, pp. 1-19.

VARGA R. S. : (1962), "Matrix iterative analysis", Prentice Hall.

VOYLES C. F. AND WILKE H. R.: (1962), "Selection of circuit arrangements for distribution network analysis by the Hardy Cross method", Journal of the American Water Works Association, March 1962, pp.285-290.

WALSKI T.: (1983), "Technique for calibrating network models", Journal of Water Resources Planning and Management, ASCE, Vol. 109, No.4, October, 1983. pp 360-372.

WALSKI T.: (1984), "Analysis of water distribution systems", Van Nostrand Reinhold.

WALSKI T.: (1986), "Case study: pipe network model calibration issues", Journal Water Resources Planning and Management, ASCE, Vol.112, No. 2, April, 1986, pp. 238-249.

WALSKI T. : (1987), discussion to "Explicit pipe network calibration" by Ormsbee and Wood (1986), Journal Water Resources and Management, ASCE, Vol. 113, No. 4, July, 1987, pp. 591-593.

WALSKI T. : (1988a), "Model calibration in Austin, Texas or Sherlock Olmes meets Hardy Cross", International Symposium on Computer Modeling of Water Distribution Systems, University of Kentucky, Lexington, May 12-13, 1988.

WALSKI T.: (1988b), "Equipment needs for field data collection in support of modeling", International Symposium on Computer Modeling of Water Distribution Systems, University of Kentucky, Lexington, May 12-13, 1988.

WARGA J. (1954), "Determination of steady-state flows and currents in a network", Instrument Society of America, Vol. 9,Pt. 5, Paper 54-43-4.

WILLIAMS G. N.: (1973), "Enhancements of convergence of pipe network solutions", Journal of the Hydraulics Division, ASCE, Vol. 99, No. HY7, pp.1057-1067.

WILSON R. J. : (1985), "Introduction to Graph Theory", Longman.

WOOD D. J.: (1981a), "Algorithms for pipe network analysis and

their reliability", Research Report No. 127, Water Resources Research Institute, University of Kentucky.

WOOD D. J.: (1981b), discussion to Isaacs and Mills (1980): "Linear theory methods for pipe network analysis", Journal of the Hydraulics Division, ASCE, March 1981, pp. 384-385.

WOOD D. J. AND CHARLES C. O. A.: (1972), "Hydraulic network analysis using linear theory", Journal of the Hydraulics Division, ASCE, Vol. 98, No. HY7, pp. 1157-1170.

WOOD D. J. AND CHARLES C. O. A.: (1973), closure to discussions to Wood and Charles (1972): "Hydraulic network analysis using linear theory", Journal of the Hydraulics Division, ASCE, Vol. 99, No. HY11, p. 2129.

WOOD D.J. AND RAYES A. G.: (1981), "Reliability of algorithms for pipe network analysis", Journal Hydraulics Division, ASCE, Vol. 107, No. HY10, pp. 1145-1161.

YANG C.T. AND SONG C.C.S. (1979), "Theory of minimum rate of energy dissipation", Journal of the Hydraulics Division, ASCE, Vol. 105, No. HY7. .ls2

ZARGHAMEE M. S. : (1971), "Mathematical model for water distribution systems", Journal of the Hydraulics Division, ASCE, Vol. 97, No. HY1.

ZISSERMAN A.: (1984), "Program F Matinv for the solution of the sparse linear system A x = b ", Adv. Eng. Software (G.B.), Vol.6, No. 1, pp. 2-8.

ZOLLENKOPF K.: (1970), "Bi-factorization: Basic Computational Algorithm and programming techniques", in Reid J. K. (Editor): "Large sparse sets of linear equations", Conference on large sets of linear equations, Institute of Mathematics and its Applications, Oxford, April, 1970.